

**COMPUTATIONAL STUDY OF THE REACTION MECHANISMS OF IODINE  
MOLECULE WITH SOME HYDRAZINES AND BIOMOLECULES**

**BY**

**GIDEON ADAMU SHALLANGWA**

**DEPARTMENT OF CHEMISTRY  
AHMADU BELLO UNIVERSITY, ZARIA,  
NIGERIA**

**SEPTEMBER, 2015**

**COMPUTATIONAL STUDY OF THE REACTION MECHANISMS OF IODINE  
MOLECULE WITH SOME HYDRAZINES AND BIOMOLECULES**

**BY**

**Gideon Adamu SHALLANGWA, B. Tech (Hons) (ATBU) 1990, M.Sc. (ABU) 2005.  
Ph.D/SCIE/58720/2005-2006**

**A THESIS SUBMITTED TO THE SCHOOL OF POSTGRADUATE STUDIES,  
AHMADU BELLO UNIVERSITY, ZARIA,  
IN PARTIAL FULFILLMENT OF THE REQUIREMENTS FOR THE AWARD  
OF A  
DOCTOR OF PHILOSOPHY DEGREE IN PHYSICAL CHEMISTRY**

**DEPARTMENT OF CHEMISTRY,  
AHMADU BELLO UNIVERSITY,  
ZARIA, NIGERIA**

**SEPTEMBER, 2015**

## **Declaration**

I hereby declare that the work in this Thesis titled “**Computational Study of the Reaction Mechanisms of Iodine with some Hydrazines and Biomolecules**” has been carried by me in the Department of Chemistry, Ahmadu Bello University, Zaria. The information derived from literature has been duly acknowledged in the text and a list of references provided. No part of this work has been presented for another degree or diploma at this or any other institution

**Gideon AdamuSHALLANGWA**

---

**Signature**

---

**Date**

## Certification

This Thesis titled “**COMPUTATIONAL STUDY OF THE REACTION MECHANISMS OF IODINE MOLECULE WITH SOME HYDRAZINES AND BIOMOLECULES**” by Gideon Adamu SHALLANGWA, meets the regulations governing the award of the Degree of Doctor of Philosophy of Ahmadu Bello University, and is approved for its contribution to knowledge and literary presentation.

**Prof. A. Uzairu**

\_\_\_\_\_  
Chairman, Supervisory Committee

\_\_\_\_\_  
Signature

\_\_\_\_\_  
Date

**Prof. V. O. Ajibola**

\_\_\_\_\_  
Member, Supervisory Committee

\_\_\_\_\_  
Signature

\_\_\_\_\_  
Date

**Dr. H. Abba**

\_\_\_\_\_  
Member, Supervisory Committee

\_\_\_\_\_  
Signature

\_\_\_\_\_  
Date

**Prof. V. O. Ajibola**

\_\_\_\_\_  
Head of Department

\_\_\_\_\_  
Signature

\_\_\_\_\_  
Date

**Prof. K. Bala**

\_\_\_\_\_  
Dean, School of Postgraduate Studies

\_\_\_\_\_  
Signature

\_\_\_\_\_  
Date

## **Dedication**

I dedicate this research work to the Self-Existent One, Jehovah; the Ancient of Days; The One Who Is, Was and lives forever. The God Who inhabits eternity. The One who is highly exalted, the Sovereign Lord and Most lofty in Majesty – for His Grace and Sustenance over my Life through all; And to my wife, Binta; my children, Nehemiah, Hannatu, Ezra, Josiah; and my younger brother, Sharon - for their love, support and personal sacrifices.

## Acknowledgements

I would like to acknowledge God Almighty as my source of strength in all things. (“I have strength for all things in Christ who empowers me,” Philippians 4:13). Furthermore, I would like to give my heart-felt thanks to the “three wise men for this research”, my current supervisors: Prof A. Uzairu, my friend and academic mentor, whose open-door, yet hands-off approach gave me room to spread my wings to the wind and fly, my mentor and Head of Department, Prof. V. O. Ajibola and my friend, Dr. H. Abba. You guys have been wonderful, I would not ask for more. I say, a million thanks and more, Sirs, for all the things I cannot pen down here.

I also want to thank my former supervisors, late Prof. G.F.S. Harrison, late Prof. J.F. Iyun and late Prof. J.A. Kagbu, who challenged and moulded me into the academic that I am today. It’s a pity we could not all see the end of that which we started. Your memories are still fresh in my mind. I also want to acknowledge the professors of Chemistry Department, Prof. J. A. Amupitan, Prof A.O. Oyewale, Prof. E.B. Agbaji, Prof. I.G. Ndukwe, Prof. C.E. Gimba and my PG Coordinator, Dr. S.O. Idris for their encouragement.

I wish to thank my colleagues in the Theoretical and Computational Chemistry Group during the course of the study: Mr. Abdul Hamidu, Mr. Sani Kwalwa, Mr. Hamza Umar and Mr. Abdulfatai Siyaka, for constantly challenging me with questions about computational chemistry and, in so doing, kept my knowledge of the subject up to par. I also want to thank my colleagues in Chemistry Department, Mr. Dallatu Ali Yakubu, Dr. J. O. Ocholi, Dr. P. A. Ekwumemgbo, Dr. S. E. Abechi, Dr. Hamisu Ibrahim, Mr. A. B. Aliyu, Dr. Sani Uba, Dr. N. C. Nwokem, Mrs. S. A. Hamza, Dr. A. A. Nuhu, Dr. E. D. Paul, Dr. P. A. A. P Mamza, Dr. F. G. Okibe, Dr. M. S. Sallau, Mr. S. Y. Na’adunguwa, and all other Staff of the Department. All of you guys have been wonderful; many thanks.

I also want to thank my external examiner, Prof. J. Na’aliya; my internal examiners, Prof. E. B. Agbaji, Dr. S. O. Idris and Prof. M. K. Anigo; and all the fellows who graced the viva. You all made the day memorable.

Finally, but equally importantly, the love, care, support, and encouragement of my dear wife and best friend, Binta; my wonderful children, Nehemiah, Hannatu, Ezra and Josiah; my brother, Sharon, and my dear friends, Prof. B. D. Tarfa, Mr. Maina W. Tarfa, and Mr. Abbas I. Banu have been paramount for me during my research period.

Once again, I raised my hands in praise to the all sufficient God, Who was and is, the beginning and the end, the Alpha and the Omega, for His grace throughout the research and writing. It wouldn’t have been without you, dear God! Were the pages of this thesis to have mouth, they would never cease to sing your praise through all the ages.

## Abstract

The oxidation of hydrazine, hydrazinium ion, 1,2-diphenylhydrazine, L-tyrosine, D-ascorbic acid and D-fructose, by molecular iodine was studied using semi-empirical and density functional theory (DFT) methods, respectively. The computational method used for calculating geometries in this work is termed a “cascade method” because of its use of molecular mechanics to remove strain energies followed by semi-empirical methods as precursors for more accurate DFT methods. The semi-empirical studies were carried out at either the modified neglect of diatomic overlap (MNDO) or parameterization method 3 (PM3) levels while all the DFT studies were carried out using 6-311+G\*\* basis set of the density functional theory (DFT) method at the Becke 3 term, Lee Yang, Parr (B3LYP) level of computation. For each system studied, molecular information such as net charges, values of frontier orbital energies, composition, proportions and bonding contribution were determined and analysed. Thus, through these means, possible reactive sites of molecules or reacting species were searched and obtained. Postulated transition states, intermediates and products were also searched and computed using the PM3 and DFT methods. Based on the results of the computation for the different systems studied, different possible reaction mechanisms for the various systems were proposed. For the 1,2-diphenylhydrazine – iodine reaction system, two possible reaction mechanisms were proposed, for the L-tyrosine – iodine reaction system, previously published reaction mechanism was modified based on the most favourable energetics of the transition states, for the L-ascorbic acid – iodine reaction system, two possible reaction mechanisms were proposed, for the D-fructose – iodine reaction system, one reaction mechanism was proposed, while for the hydrazine / hydrazinium ion – iodine reaction system, four reaction mechanisms were proposed. For each system investigated, out of the various plausible mechanisms postulated, comparisons of the enthalpies of reactions of the various pathways as well as the activation barriers of the respective rate determining steps were made. The computed enthalpies of the oxidation reactions

were carried out at standard conditions of 298.15K and 1 atmosphere for the PM3 and DFT calculations. For each system, the pathway with the least activation barriers and enthalpy of reactions were chosen as the most probable mechanism of reaction for the system. Other thermodynamic parameters such as  $\Delta G^\circ$  and  $\Delta S^\circ$  for reacting species, especially transition states and intermediates which were used to support the validity of the postulated mechanisms were also computed. The activation parameters for the most energetically favourable pathway for the respective reaction systems were calculated and given. The data obtained for the limiting step of the 1,2-diphenylhydrazine – iodine reaction system are:  $\Delta^\ddagger G = -7.11 \times 10^3$  kJ/mol,  $\Delta^\ddagger S = 2.71 \times 10^1$  kJ/mol and  $E_a = 44.40$  kJ/mol. For the L-tyrosine – iodine reaction system,  $\Delta^\ddagger G = -1.10 \times 10^5$  kJ/mol,  $\Delta^\ddagger S = 1.28 \times 10^5$  kJ/mol and  $E_a = 3.52 \times 10^3$  kJ/mol. For the limiting step for the D-ascorbic acid – iodine reaction system,  $\Delta^\ddagger G = -2.93 \times 10^4$  kJ/mol,  $\Delta^\ddagger S = 1.28 \times 10^5$  kJ/mol and  $E_a = 3.14 \times 10^3$  kJ/mol. For the limiting step for the D- fructose – iodine reaction system,  $\Delta^\ddagger G = -6.78 \times 10^4$  kJ/mol,  $\Delta^\ddagger S = 6.74 \times 10^4$  kJ/mol and  $E_a = 3.82 \times 10^3$  kJ/mol. While for the hydrazine / hydrazinium ion – iodine reaction system, activation parameters for the limiting step of the most energetically favourable pathway were determined as,  $\Delta^\ddagger G = -8.01 \times 10^4$  kJ/mol,  $\Delta^\ddagger S = -1.24 \times 10^6$  kJ/mol and  $E_a = 6.86 \times 10^3$  kJ/mol.

## Table of Contents

|  |           |
|--|-----------|
| Cover page                                   | i         |
| Title page                                   | ii        |
| Declaration                                  | iii       |
| Certification                                | iv        |
| Dedication                                   | v         |
| Acknowledgements                             | vi        |
| Abstract                                     | vii       |
| Table of Contents                            | ix        |
| List of Tables                               | xvii      |
| List of Figures                              | xix       |
| List of Schemes                              | xxii      |
| Appendices                                   | xxiii     |
| List of Abbreviations                        | xxiv      |
| CHAPTER ONE                                  | 1         |
| <b>1.0 INTRODUCTION</b>                      | <b>1</b>  |
| <b>1.1 Iodine</b>                            | <b>1</b>  |
| <b>1.2 Hydrazine and Its Derivatives</b>     | <b>3</b>  |
| <b>1.3 L-Tyrosine</b>                        | <b>5</b>  |
| <b>1.4 L-Ascorbic Acid</b>                   | <b>6</b>  |
| <b>1.5 Reducing Sugars</b>                   | <b>8</b>  |
| <b>1.6 Statement of the Research Problem</b> | <b>10</b> |
| <b>1.7 Justification of the Research</b>     | <b>11</b> |
| <b>1.8 The Research Questions</b>            | <b>13</b> |

|             |  |           |
|-------------|--|-----------|
| <b>1.9</b>  | <b>The Research Hypotheses</b>   | <b>14</b> |
| <b>1.10</b> | <b>Conceptual Framework</b>  | <b>14</b> |
| <b>1.11</b> | <b>Theoretical Framework</b>   | <b>16</b> |
| <b>1.12</b> | <b>Aim and Objectives</b>  | <b>17</b> |
| CHAPTER TWO |  | 18        |
| <b>2.0</b>  | <b>LITERATURE REVIEW</b>   | <b>18</b> |
| <b>2.1</b>  | <b>Computational Approaches for Investigation of the Reaction Mechanisms</b> | <b>18</b> |
| <b>2.2</b>  | <b>Computational Chemistry</b>   | <b>24</b> |
| <b>2.3</b>  | <b><i>Ab initio</i> (Quantum Mechanics)</b>                                  | <b>25</b> |
| 2.3.1       | The Born-Oppenheimer approximation   | 28        |
| 2.3.2       | Potential energy surface   | 29        |
| 2.3.2.1     | Hessian index  | 31        |
| 2.3.3       | Geometry optimization  | 31        |
| 2.3.4       | Hartree-Fock self-consistent field method                                    | 32        |
| 2.3.5       | Post-Hartree-Fock methods  | 32        |
| <b>2.4</b>  | <b>Semi-Empirical Calculations</b>   | <b>34</b> |
| 2.4.1       | Modified neglect of diatomic overlap   | 35        |
| 2.4.2       | Austin model 1   | 35        |
| 2.4.3       | Parameterization method 3  | 36        |
| 2.4.4       | Partial retention of diatomic differential overlap                           | 37        |
| 2.4.5       | Parameterization method 3 with extension for transition metals               | 38        |
| <b>2.5</b>  | <b>Density Functional (Theory) Calculations</b>                              | <b>38</b> |
| 2.5.1       | Basis sets   | 39        |
| 2.5.1.1     | Basis set superposition error  | 44        |

|               |  |           |
|---------------|--|-----------|
| 2.5.1.2       | Temperature  | 45        |
| 2.5.1.3       | Performance  | 45        |
| <b>2.6</b>    | <b>Molecular Mechanics</b>   | <b>46</b> |
| 2.6.1         | Force field parameterization   | 48        |
| 2.6.2         | Atomic charges   | 49        |
| 2.6.3         | Polarizable force fields   | 51        |
| <b>2.7</b>    | <b>Simulations</b>   | <b>52</b> |
| 2.7.1         | Free energy perturbations  | 55        |
| <b>2.8</b>    | <b>Molecular dynamics calculations</b>   | <b>57</b> |
| <b>2.9</b>    | <b>Computational Chemistry and Experiment</b>  | <b>57</b> |
| CHAPTER THREE |  | 58        |
| <b>3.0</b>    | <b>MATERIALS AND METHODS</b>   | <b>58</b> |
| <b>3.1</b>    | <b>Materials</b>   | <b>58</b> |
| <b>3.2</b>    | <b>Methodology</b>   | <b>59</b> |
| <b>3.3</b>    | <b>Details of the Computation Procedures</b>   | <b>60</b> |
| 3.3.1         | Geometry optimization of reactants, activated complexes, intermediates and products using semi-empirical methods       | 61        |
| 3.3.1.1       | Geometry optimization of reactants, activated complexes, intermediates and products using dft methods                  | 62        |
| 3.3.2         | Calculation of HOMO and LUMO of optimized molecules  | 63        |
| 3.3.3         | Determination of chemical reactivity of optimized molecules: mapping of HOMO and LUMO densities of optimized molecules | 63        |
| 3.3.4         | Calculation of thermodynamics, molecular and other physicochemical properties of reacting species and products         | 64        |
| 3.3.5         | Construction of potential energy surface diagrams  | 64        |
| 3.3.6         | Enthalpy of reaction and rate constant calculations  | 65        |
| <b>3.4</b>    | <b>Post Computation Processing</b>   | <b>67</b> |

|  |           |
|--|-----------|
| CHAPTER FOUR   | 68        |
| <b>4.0 RESULTS</b>   | <b>68</b> |
| <b>4.1 Structure Optimization of Reactants, Transition States, Intermediates and Products</b>  | <b>68</b> |
| 4.1.1 Optimized geometries of 1,2-diphenylhydrazine – iodine reaction system   | 68        |
| 4.1.2 Optimized geometries of l-tyrosine – iodine reaction system  | 70        |
| 4.1.3 Optimized geometries of l-ascorbic acid – iodine reaction system   | 71        |
| 4.1.4 Optimized geometries of d-fructose – iodine reaction system  | 72        |
| 4.1.5 Optimized geometries of hydrazine/hydrazinium ion – iodine reaction system   | 73        |
| 4.1.6 Mapping and calculation of HOMO and LUMO of reactants  | 74        |
| <b>4.3 Searches for Transition States and Intermediates</b>  | <b>80</b> |
| 4.3.1 Transition states and intermediates for 1,2-diphenylhydrazine – iodine reaction system   | 80        |
| 4.3.2 Transition states and intermediates for L-tyrosine – iodine reaction system  | 81        |
| 4.3.3 Transition states and intermediates for L-ascorbic acid – iodine reaction system   | 82        |
| 4.3.4 Transition states and intermediates for D-fructose– iodine reaction system   | 83        |
| 4.3.5 Transition states and intermediates for hydrazine/hydrazinium ion – iodine reaction system   | 84        |
| <b>4.4 Calculation of Thermodynamics, Molecular and other Physicochemical Properties of Reacting Species and Products</b>  | <b>85</b> |
| 4.4.1 Computation of heat of formation, total electronic energy and other thermodynamic parameters of reacting species and products for 1,2-diphenylhydrazine – iodine reaction system | 85        |
| 4.4.1.1 Charge distribution and exposed surface study of 1,2-diphenylhydrazine   | 85        |
| 4.4.2 Computation of heat of formation, total electronic energy and other activation parameters of reacting species and products for L-tyrosine – iodine reaction system               | 85        |
| 4.4.2.1 Charge distribution and exposed surface study of L-tyrosine  | 86        |
| 4.4.3 Computation of heat of formation, total electronic energy and other activation parameters of reacting species and products for L-ascorbic – iodine reaction                      |           |

|            |  |            |
|------------|--|------------|
|            | system   | 86         |
| 4.4.3.1    | Charge distribution and exposed surface study of L-ascorbic acid   | 87         |
| 4.4.4      | Computation of heat of formation, total electronic energy and other activation parameters of reacting species and products for D-fructose – iodine reaction system                     | 87         |
| 4.4.4.1    | Charge Distribution and Exposed Surface Study of D-Fructose  | 88         |
| 4.4.5      | Computation of heat of formation, total electronic energy and other thermodynamic parameters of reacting species and products for hydrazine / hydrazinium ion – iodine reaction system | 88         |
| 4.4.5.1    | Charge distribution and exposed surface study of hydrazine / hydrazinium ion   | 89         |
| <b>4.5</b> | <b>Construction of Potential Energy Surface Diagrams</b>   | <b>89</b>  |
| 4.5.1      | Potential energy surface diagrams of reaction of 1,2-diphenylhydrazine - iodine reaction system according to the chain multi-step and cyclic mechanism                                 | 89         |
| 4.5.2      | Potential energy surface diagrams of reactions of l-tyrosine – iodine reaction system according to the PM3 and DFT methods, respectively   | 125        |
| 4.5.3      | Potential energy surface diagrams of reaction of L ascorbic acid -iodine reaction system according to the DFT and PM3 studies  | 125        |
| 4.5.4      | Potential energy surface diagrams of reaction of D-fructose – iodine reaction system for the respective DFT and PM3 studies  | 125        |
| 4.5.5      | Potential energy surface diagrams of reactions of hydrazine / hydrazinium ion – iodine reaction system according to the DFT methods for routes i-iv, respectively                      | 126        |
| <b>4.6</b> | <b>Proposal of More Plausible Mechanisms for the Biomolecules – Iodine Reaction Systems</b>  | <b>144</b> |
| 4.6.1      | More plausible mechanisms for reaction of 1,2 diphenylhydrazine – iodine reaction system according to the chain multi step and cyclic mechanism  | 144        |
| 4.6.2      | More plausible mechanisms for reactions of L-tyrosine – iodine reaction system   | 146        |
| 4.6.3      | More plausible mechanisms for reaction of L-ascorbic acid – iodine reaction system   | 147        |
| 4.6.4      | More plausible mechanisms for reaction of d-fructose – iodine reaction system  | 149        |
| 4.6.5      | More plausible mechanisms for reactions of hydrazine / hydrazinium ion – iodine reaction system according to the dft methods for routes i - iv,  |            |

|  |            |
|--|------------|
| respectively   | 150        |
| CHAPTER FIVE   | 154        |
| <b>5.0    DISCUSSION</b>   | <b>154</b> |
| <b>5.1    Geometry Optimization of Reactants, Activated Complexes, Intermediates and Products</b>                            | <b>154</b> |
| <b>5.2    Mapped and Calculated HOMO and LUMO of Reactants</b>   | <b>154</b> |
| <b>5.3    Searched Transition States and Intermediates</b>   | <b>158</b> |
| 5.3.1    Transition states and intermediates for 1,2-diphenylhydrazine – iodine reaction system                              | 159        |
| 5.3.2    Transition states and intermediates for L-Tyrosine – iodine reaction system   | 159        |
| 5.3.3    Transition states and intermediates for L-ascorbic acid – iodine reaction system                                    | 160        |
| 5.3.4    Transition states and intermediates for D-fructose– iodine reaction system  | 161        |
| 5.3.5    Transition states and intermediates for hydrazine/hydrazinium ion – iodine reaction system                          | 161        |
| <b>5.4    Calculation of Thermodynamics, Molecular and other Physicochemical Properties of Reacting Species and Products</b> | <b>162</b> |
| 5.4.1    1,2-diphenylhydrazine – iodine system   | 162        |
| 5.4.1.1    Charge distribution, bond length and exposed surface area of 1,2-diphenylhydrazine                                | 163        |
| 5.4.2    L-tyrosine – iodine system  | 164        |
| 5.4.2.1    Charge distribution, bond length and exposed surface area of L-tyrosine   | 165        |
| 5.4.3    L-ascorbic acid – iodine system   | 166        |
| 5.4.3.1    Charge distribution, bond length and exposed surface area of L-ascorbic acid                                      | 166        |
| 5.4.4    D-fructose – iodine system  | 167        |
| 5.4.4.1    Charge distribution, bond length and exposed surface area of D-fructose   | 167        |
| 5.4.5    Hydrazine/hydrazinium ion – iodine system   | 168        |
| 5.4.5.1    Charge distribution, bond length and exposed surface area of hydrazine / hydrazinium ion                          | 169        |
| <b>5.5    Construction of Potential Energy Surface Diagrams</b>  | <b>170</b> |

|            |   |            |
|------------|---|------------|
| <b>5.6</b> | <b>Proposal of More Plausible Mechanisms for the Biomolecules -Iodine Reaction Systems</b>                | <b>172</b> |
| 5.6.1      | 1,2-diphenylhydrazine – iodine reaction system  | 175        |
| 5.6.2      | L-tyrosine – iodine reaction system   | 177        |
| 5.6.3      | L-ascorbic acid – iodine reaction system  | 179        |
| 5.6.3.1    | Route I   | 180        |
| 5.6.3.2    | Route II  | 180        |
| 5.6.3.3    | DFT studies   | 181        |
| 5.6.3.4    | Semi-empirical PM3 studies  | 181        |
| 5.6.4      | D-fructose – iodine reaction system   | 182        |
| 5.6.4.1    | Step 1  | 183        |
| 5.6.4.2    | Step 2  | 183        |
| 5.6.4.3    | Step 3  | 183        |
| 5.6.5      | Hydrazine / hydrazinium ion – iodine reaction system  | 184        |
| 5.6.5.1    | Route I   | 185        |
| 5.6.5.2    | Route II  | 185        |
| 5.6.5.3    | Route III   | 186        |
| 5.6.5.4    | Route IV  | 186        |
| <b>5.7</b> | <b>Enthalpy of Reaction and Rate Constant Calculations for the Biomolecules - Iodine Reaction Systems</b> | <b>187</b> |
| 5.7.1      | 1,2-diphenylhydrazine – iodine reaction system  | 189        |
| 5.7.2      | L-tyrosine – iodine reaction system   | 191        |
| 5.7.3      | L-ascorbic acid – iodine reaction system  | 191        |
| 5.7.4      | D-fructose – iodine reaction system   | 193        |
| 5.7.5      | Hydrazine / hydrazinium ion – iodine reaction system  | 194        |
| <b>5.8</b> | <b>Rate Laws for the Proposed Mechanisms of Reactions</b>   | <b>195</b> |

|                   |  |            |
|-------------------|--|------------|
| 5.8.1             | Rate laws for 1,2-diphenylhydrazine – iodine reaction system | 195        |
| 5.8.1.1           | The chain multi-step mechanism                               | 195        |
| 5.8.1.2           | The one-step cyclic activated complex mechanism              | 196        |
| 5.8.2             | L-tyrosine – iodine reaction system                          | 196        |
| 5.8.3             | L-ascorbic acid – iodine reaction system                     | 197        |
| 5.8.3.1           | The one-step cyclic activated complex mechanism              | 197        |
| 5.8.3.2           | The two-steps mechanism                                      | 198        |
| 5.8.4             | D-fructose – iodine reaction system                          | 198        |
| 5.8.5             | Hydrazine / hydrazinium ion – iodine reaction system         | 200        |
| 5.8.5.1           | Route I  | 200        |
| 5.8.5.2           | Route II   | 201        |
| 5.8.5.3           | Route III  | 202        |
| 5.8.5.4           | Route IV   | 202        |
| <b>5.9</b>        | <b>Comparison of Rate Constants</b>                          | <b>203</b> |
| CHAPTER SIX       |  | 206        |
| <b>6.0</b>        | <b>SUMMARY, CONCLUSION AND RECOMMENDATION</b>                | <b>206</b> |
| <b>6.1</b>        | <b>Summary</b>   | <b>206</b> |
| <b>6.2</b>        | <b>Conclusion</b>  | <b>207</b> |
| <b>6.2</b>        | <b>Recommendation</b>  | <b>208</b> |
| <b>REFERENCES</b> |  | <b>210</b> |

## List of Tables

|            |   |     |
|------------|---|-----|
| Table 4.1  | Total electronic energy, heat of formation and other thermodynamic parameters of reacting species and products of 1,2-diphenylhydrazine – iodine reaction system  | 90  |
| Table 4.2  | Heat of formation and other activation parameters of reacting species 1,2-diphenylhydrazine – iodine reaction system for route 1 and route according to MNDO calculations                                 | 91  |
| Table 4.3  | Bond length and exposed surface area of 1,2-diphenylhydrazine molecule  | 93  |
| Table 4.4: | Total electronic energy, heat of formation and other thermodynamic parameters of reacting species and products for L-tyrosine-iodine reaction system  | 94  |
| Table 4.5  | Heat of formation, total electronic energy and other activation parameters of reacting species and products for L-tyrosine-iodine reaction system for the most favored pathway                            | 95  |
| Table 4.6  | Net atomic charges and exposed surface area of L- tyrosine molecule   | 97  |
| Table 4.7  | Bond lengths of the reactive sites of the transition states L-tyrosine system   | 98  |
| Table 4.8  | Total electronic energy and other thermodynamic parameter at standard condition of 1 atmosphere and 298.15K of reacting species and products of L-ascorbic acid system for DFT studies route I            | 99  |
| Table 4.9  | Total electronic energy and other thermodynamic parameters at standard condition of 1 atmosphere and 298.15K of reacting species and products of L-ascorbic acid system for DFT studies route II          | 100 |
| Table 4.10 | Total electronic energy and other activation parameters at standard condition of 1 atmosphere and 298.15K of reacting species and products of L-ascorbic acid system for DFT studies route I and route II | 101 |
| Table 4.11 | Heat of formation and other thermodynamic parameters at standard condition of 1 atmosphere and 298.15K of reacting species and products of L-ascorbic acid system for PM3 studies                         | 102 |
| Table 4.12 | Heat of formation and other activation parameter at standard condition of 1 atmosphere and 298.15K of reacting species of L-ascorbic acid system for PM3 studies  | 103 |
| Table 4.13 | Molecular information of the optimized ascorbic acid molecule   | 105 |
| Table 4.14 | Total electronic energy and other thermodynamic parameters of reacting species and products according to the DFT method for D-fructose system   | 106 |
| Table 4.15 | Total electronic energy and other activation parameters of reacting species and   |     |

|             |   |     |
|-------------|---|-----|
|             | products according to the DFT method for D-fructose system  | 108 |
| Table 4.16  | Heat of formation and other thermodynamic parameters of reacting species according to the PM3 method for D-fructose system  | 109 |
| Table 4.17  | Heat of formation and other activation parameters of reacting species according to the PM3 method for D-fructose system   | 110 |
| Table 4.18  | Net atomic charges and exposed surface area of D- fructose molecule   | 112 |
| Table 4.19  | Total electronic energy and other thermodynamic parameters at standard condition of 1 atmosphere and 298.15K of reacting species and products for route I for hydrazine / hydrazinium ion – iodine reaction system        | 113 |
| Table 4.20  | Total electronic energy and other thermodynamic parameters at standard condition of 1 atmosphere and 298.15K of reacting species and products for route II for hydrazine / hydrazinium ion – iodine reaction system       | 115 |
| Table 4.21  | Total electronic energy and other thermodynamic parameters at standard condition of 1 atmosphere and 298.15K of reacting species and products for route III for hydrazine / hydrazinium ion – iodine reaction system      | 116 |
| Table 4.22  | Total electronic energy and other thermodynamic parameters at standard condition of 1 atmosphere and 298.15K of reacting species and products for route IV for hydrazine / hydrazinium ion – iodine system                | 117 |
| Table 4.23  | Total electronic energy and other activation parameters at standard condition of 1 atmosphere and 298.15K of reacting species for routes I and II for hydrazine / hydrazinium ion – iodine reaction system                | 119 |
| Table 4.24  | Total electronic energy and other activation parameters at standard condition of 1 atmosphere and 298.15K of reacting species and products for routes III and IV for hydrazine / hydrazinium ion – iodine reaction system | 121 |
| Table 4.25: | Bond lengths and exposed surface areas of hydrazine molecule and hydrazinium ion  | 124 |

## List of Figures

|             |   |    |
|-------------|---|----|
| Figure 1.1  | The research conceptual framework   | 15 |
| Figure 4.1  | Optimized geometries of the reactants, intermediates, transition states and products for 1,2-diphenylhydrazine – iodine reaction system       | 69 |
| Figure 4.2  | Optimized geometries of the reactants, intermediates, transition states and products for L-tyrosine – iodine reaction system                  | 70 |
| Figure 4.3  | Optimized geometries of the reactants, intermediates, transition states and products for L-Ascorbic Acid – iodine reaction system             | 71 |
| Figure 4.4  | Optimized geometries of the reactants, intermediates, transition states and products for D-Fructose – iodine reaction system                  | 72 |
| Figure 4.5  | Optimized geometries of the reactants, intermediates, transition states and products for hydrazine / hydrazinium ion – iodine reaction system | 73 |
| Figure 4.6a | Solid model of HOMO and LUMO for 1,2-diphenylhydrazine – iodine reaction system   | 74 |
| Figure 4.6b | Transparent model of HOMO and LUMO for 1,2-diphenylhydrazine – iodine reaction system   | 75 |
| Figure 4.7  | Solid and transparent models of HOMO and LUMO for L-tyrosine  | 76 |
| Figure 4.8  | Solid and transparent models of HOMO and LUMO for L-ascorbic acid   | 77 |
| Figure 4.9  | Solid and transparent models of HOMO and LUMO for D-fructose  | 78 |
| Figure 4.10 | Solid and transparent models of HOMO and LUMO for hydrazine / hydrazinium ion   | 79 |
| Figure 4.11 | Transition states for 1,2-diphenylhydrazine –iodine reaction system   | 80 |
| Figure 4.12 | Transition states and intermediates for L-tyrosine – iodine reaction system   | 81 |
| Figure 4.13 | Transition states and intermediates for D-ascorbic acid – iodine reaction system  | 82 |
| Figure 4.14 | Transition states and intermediates for D-fructose – iodine reaction system   | 83 |
| Figure 4.15 | Transition states and intermediates for hydrazine/hydrazinium ion – iodine reaction system  | 84 |
| Figure 4.16 | Labelled structure of 1,2-diphenylhydrazine   | 92 |

|             |   |     |
|-------------|---|-----|
| Figure 4.17 | Labelled structure of L-tyrosine  | 96  |
| Figure 4.18 | Labelled structure of L-ascorbic acid   | 104 |
| Figure 4.19 | Labelled structure of D-fructose  | 111 |
| Figure 4.20 | Labelled structures of hydrazine molecule and hydrazinium ion   | 123 |
| Figure 4.21 | Energy profile of the oxidation of 1,2-diphenylhydrazine by iodine as per the DFT calculations  | 127 |
| Figure 4.22 | Energy profile of the oxidation of 1,2-diphenylhydrazine by iodine as per the MNDO calculations   | 128 |
| Figure 4.23 | Energy profile of the oxidation of 1,2-diphenylhydrazine by iodine via the cyclic activated complex for the DFT calculations                        | 129 |
| Figure 4.24 | Energy profile of the oxidation of 1,2-diphenylhydrazine by iodine via the cyclic activated complex for the MNDO calculations                       | 130 |
| Figure 4.25 | Energy profile of the oxidation of L- tyrosine by iodine according to the PM3 calculations  | 131 |
| Figure 4.26 | Energy profile of the oxidation of L- tyrosine by iodine according to the DFT calculations  | 132 |
| Figure 4.27 | Energy profile of the oxidation of L- tyrosine by iodine according to the most favored route showing the position of the optimized reacting species | 133 |
| Figure 4.28 | Energy profile of the oxidation of L-ascorbic acid by iodine according to the DFT studies route I proposed mechanism                                | 134 |
| Figure 4.29 | Energy profile of the oxidation of L- ascorbic acid by iodine according to the DFT studies route II proposed mechanisms                             | 135 |
| Figure 4.30 | Energy profile of the oxidation of L-ascorbic acid by iodine according to the PM3 studies route I proposed mechanism                                | 136 |
| Figure 4.31 | Energy profile of the oxidation of L-ascorbic acid by iodine according to the PM3 studies route II proposed mechanism                               | 137 |
| Figure 4.32 | Energy profile of the oxidation of D-fructose by iodine according to the DFT studies proposed mechanism   | 138 |
| Figure 4.33 | Energy profile of the oxidation of D-fructose by iodine according to the PM3 studies proposed mechanism   | 139 |
| Figure 4.34 | Energy profile of the oxidation of hydrazine / hydrazinium ion by iodine according to the route I proposed mechanism                                | 140 |

|             |   |     |
|-------------|---|-----|
| Figure 4.35 | Energy profile of the oxidation of hydrazine / hydrazinium ion by iodine according to the route II proposed mechanisms  | 141 |
| Figure 4.36 | Energy profile of the oxidation of hydrazine / hydrazinium ion by iodine according to the route III proposed mechanisms | 142 |
| Figure 4.37 | Energy profile of the oxidation of hydrazine / hydrazinium ion by iodine according to the route IV proposed mechanism   | 143 |

## List of Schemes

|             |   |     |
|-------------|---|-----|
| Scheme 4.1  | Proposed multi-step mechanism for the 1,2-diphenylhydrazine reaction with iodine  | 144 |
| Scheme 4.2  | The one-step mechanism with cyclic activated complex for the 1,2-diphenylhydrazine reaction with iodine                                 | 145 |
| Scheme 4.3  | The reaction mechanism of L-tyrosine as modified by this study  | 146 |
| Scheme 4.4  | The one-step reaction mechanism via the cyclic activated complex for the L-ascorbic acid reaction with iodine                           | 147 |
| Scheme 4.5  | The two-steps reaction mechanism for the L-ascorbic acid reaction with iodine   | 148 |
| Scheme 4.6  | Proposed reaction mechanism for the oxidation of D-fructose with iodine   | 149 |
| Scheme 4.7  | The first proposed mechanism for the hydrazine / hydrazinium ion reaction with iodine (Route I)   | 150 |
| Scheme 4.8  | The second proposed mechanism for the hydrazine / hydrazinium ion reaction with iodine (Route II)                                       | 151 |
| Scheme 4.9  | The third proposed mechanism for the hydrazine / hydrazinium ion reaction with iodine (Route III)                                       | 152 |
| Scheme 4.10 | The fourth proposed mechanism for the hydrazine / hydrazinium ion reaction with iodine (Route IV)                                       | 153 |
| Scheme 5.1  | Published multi-step mechanism for the 1,2- diphenylhydrazine reaction with iodine  | 172 |
| Scheme 5.2  | The published one-step mechanism with cyclic activated complex for the 1,2- diphenylhydrazine reaction with iodine                      | 173 |
| Scheme 5.3  | The reaction mechanism as proposed by Aghaie <i>et al.</i> (2008)   | 178 |
| Scheme 5.4  | The reaction mechanism of L-ascorbic acid as proposed by several groups (Morelli, 1976; Rahmawati and Bundjali, 2009; Canterbury, 2014) | 179 |
| Scheme 5.5  | The reaction mechanism as proposed by Mshelia <i>et al.</i> (2010)  | 184 |

## APPENDICES

The appendices consist of list of published or accepted papers from this work.

- I. Shallangwa, G.A., Uzairu, A., Ajibola, V.O., Abba, H., (2014). MNDO and DFT Computational Study on the Mechanism of the Oxidation of 1,2-Diphenylhydrazine by Iodine, *ISRN Physical Chemistry*, Vol. 2014, Article ID 592850, 8 pages. <http://dx.doi.org/10.1155/2014/592850>
- II. Shallangwa, G.A., Uzairu, A., Ajibola, V.O., Abba, H., (2014). Computational study of the mechanism of the oxidation of ascorbic acid by iodine in the gas phase, *Biointerface research in applied chemistry*, **4(2)**, 712-720.
- III. Shallangwa, G.A., Uzairu, A., Ajibola, V.O., Abba, H., (2014). DFT and PM3 Computational Study of the Reaction Mechanism of the Oxidation of L-Tyrosine by Iodine in the Gas Phase, *Aceh International Journal of Science and Technology*, **3(2)**: 106-116; [Doi: 10.13170/AIJST.0302.06](https://doi.org/10.13170/AIJST.0302.06)
- IV. Shallangwa, G.A., Uzairu, A., Ajibola, V.O., Abba, H., (2014). Theoretical Study of the Plausible Routes of the Oxidation of Ascorbic Acid by Iodine in the Gas Phase, *International Journal of Modern Chemistry*, **6(2)**: 96-109
- V. Shallangwa, G.A., Uzairu, A., Ajibola, V.O., Abba, H., (2014). A Computational Study on the Mechanism of the Oxidation of Hydrazobenzene by Iodine, *World Journal of Computational Sciences- Accepted*
- VI. Shallangwa, G.A., Uzairu, A., Ajibola, V.O., Abba, H., (2015). Computational Study of the Reaction Mechanism of the Oxidation of Hydrazine / hydrazinium ion by Iodine in the Gas Phase, *International Journal of Computational and Theoretical Chemistry*, **3(2)**: 6-18. [DOI: 10.11648/j.ijctc.20150302.11](https://doi.org/10.11648/j.ijctc.20150302.11)
- VII. Shallangwa, G.A., Uzairu, A., Ajibola, V.O., Abba, H., (2015). A Preliminary Computational Study of the Mechanism of Oxidation of D-Fructose by Iodine in Gas Phase, *Journal of Modern Chemistry and Chemical Technology*, **6(2)**: 41-49. [www.stmjournals.com](http://www.stmjournals.com)

## List of Abbreviations

|                 |  |
|-----------------|--|
| A               | Azobenzene (trans-1,2-diphenyldiazene)                                     |
| Å               | Ångström   |
| AA              | Ascorbic acid  |
| AH              | 1,2-diphenylhydrazyl radical   |
| AH <sub>2</sub> | 1,2- diphenylhydrazine   |
| AM1             | The Austin Model 1   |
| AO              | Atomic orbital   |
| Au              | Atomic unit  |
| aug-cc-pVDZ     | Augmented Versions of Correlation Consistent-Polarized Valence Double Zeta |
| B3LYP           | Becke 3 term, Lee Yang, Par  |
| BSSE            | Basis Set Superposition Error  |
| cc-pV5Z         | Correlation Consistent-Polarized Valence Five Zeta                         |
| cc-pVDZ         | Correlation Consistent-Polarized Valence Double Zeta                       |
| cc-pVQZ         | Correlation Consistent-Polarized Valence Quadruple Zeta                    |
| cc-pVTZ         | Correlation Consistent-Polarized Valence Triple Zeta                       |
| CGTO            | Contracted Gaussian Type Orbitals  |
| CGTO            | Contracted Gaussian-Type Orbital   |
| CI              | Configuration Interaction  |
| C <sup>o</sup>  | Concentration (taken to be 1)  |
| CPU             | Central Processing Unit  |
| DAA             | Dehydroascorbic acid   |
| DCP             | Dream Calculator Program   |
| D-Fruc.         | D- fructose  |
| DFT             | Density Functional Theory  |

|                               |   |
|-------------------------------|---|
| DIT                           | Diiodo tyrosine                                       |
| DZ                            | Double-Zeta basis set                                 |
| E <sub>a</sub>                | Activation energy                                     |
| E <sub>e</sub>                | Electronic energy                                     |
| eV                            | Electron Volt   |
| FEP                           | Free Energy Perturbations                             |
| GGA                           | Generalized Gradient Approximation                    |
| GTOs                          | Gaussian-Type Orbitals                                |
| h                             | Planck's constant ( $6.626176 \times 10^{-34}$ Js)    |
| H <sup>+</sup>                | Hydrogen ion  |
| H <sub>2</sub> O              | Water molecule  |
| H <sub>2</sub> O <sub>2</sub> | Hydrogen peroxide                                     |
| HF                            | Hartree-Fock  |
| HOI                           | Hypoiodous acid                                       |
| HOMO                          | Highest Occupied Molecular Orbital                    |
| Hyd                           | Hydrazine   |
| Hyd <sup>+</sup>              | Hydrazinium ion                                       |
| I <sub>a</sub>                | Associative interchange mechanism                     |
| Int.                          | Intermediate  |
| K                             | Rate constant   |
| k(298.15K)                    | Reaction rate constant at Temperature(298.15K)        |
| k <sub>B</sub>                | Boltzmann constant ( $1.380662 \times 10^{-23}$ J/K); |
| kJ/mol                        | kilo Joule per mole                                   |
| LDA                           | Local Density Approximation                           |
| L-Tyr                         | L-Tyrosine  |

|                |  |
|----------------|--|
| LUMO           | Lowest Unoccupied Molecular Orbital  |
| MC             | Monte Carlo  |
| MD             | Molecular Dynamics   |
| MIT            | Monoiodo tyrosine  |
| MM             | Molecular Mechanics  |
| MNDO           | Modified Neglect of Diatomic Overlap   |
| MP2            | Møller - Plesset, Second Order Perturbation  |
| OPLS           | Optimized Parameters for Liquid Simulations  |
| PES            | Potential Energy Surface   |
| PM3            | Parameterization Method 3  |
| PM3/TM         | Parameterization Method 3 Extension For Transition Metals                              |
| PRDDO          | Partial Retention Of Diatomic Differential Overlap                                     |
| PRDDO/M        | Partial Retention Of Diatomic Differential Overlap Method                              |
| PRDDO/M/FCP    | Partial Retention Of Diatomic Differential Overlap Method using Frozen Core Potentials |
| pV             | Polarized Valence Double Zeta  |
| P <sub>x</sub> | Products x   |
| QM             | Quantum Mechanics  |
| R              | Gas Constant (8.31441 J/Mol. K)  |
| R              | Rate   |
| RAM            | Random-Access Memory   |
| R <sub>x</sub> | Reactants x  |
| SE             | Semi -Empirical  |
| STOs           | Slater-Type Orbitals   |
| SV             | Split-Valence  |

|                           |                                 |
|---------------------------|---------------------------------|
| T(298.15K)                | Temperature (298.15K)           |
| T <sub>g</sub>            | Thyroglobulin                   |
| TPO                       | Thyroid Peroxidase              |
| TS <sub>x</sub>           | Transition state x              |
| TZ                        | Triple-Zeta basis set           |
| UV                        | Ultra-Violet                    |
| VDZ                       | Valence Double Zeta             |
| VTZ                       | Valence Triple-Zeta             |
| $\Delta^\ddagger G^\circ$ | Gibbs free energy of activation |
| $\Delta^\ddagger H^\circ$ | Heat of activation              |
| $\Delta^\ddagger S^\circ$ | Entropy of activation           |
| $\Delta H_f$              | Heat of formation               |
| $\Delta_r H$              | Heat of reaction                |

## CHAPTER ONE

### 1.0 INTRODUCTION

#### 1.1 Iodine

Iodine is an essential micronutrient for mammals including humans and appears to be the heaviest required element in a diet. Iodine compounds are useful in medicine and lack of it in the diet is a cause of goiter (Pearce *et al.*, 2013; Olvera-Caltzontzin *et al.*, 2013; Doggui and El Atia, 2015). Iodine is absolutely necessary for a healthy thyroid as well as ovaries, breasts and prostate (Arroyo-Helguera *et al.*, 2006; Zimmermann, 2013; Doggui and El Atia, 2015). Iodine deficiency, though easily treated, continues to be a problem for approximately a fifth of the world population. Goitre, or enlargement of the thyroid, has been recognized for many years as symptoms of iodine deficiency. These pathological conditions are normally grouped under the common name of Iodine Deficiency Disorders (IDD) (Hetzl *et al.*, 1990; Konig *et al.*, 2011; Doggui and El Atia, 2015). Iodine deficiency is the largest preventable cause of mental retardation worldwide (Cao *et al.*, 1994; Pearce *et al.*, 2013). In severe cases, it can result in cretinism, a form of mental retardation. Mshelia *et al.* (2010) reported in their studies that volatilization from oceans and precipitation of ocean water is the origin of most iodine content of diet (Miller and Heyland, 2013) and is considered critical to compensate for metabolic losses. Goitre surveys conducted so far are limited to clinical symptoms, urinary iodine output and, to some extent, plasma thyroid hormone levels (Doggui and El Atia, 2015; Aceves *et al.*, 2013; Bizhanova and Kopp, 2009; Langer *et al.*, 2003).

The thyroid gland needs iodine to make hormones. If the thyroid doesn't have enough iodine to do its job, feedback systems in the body cause the thyroid to work harder. This can cause an enlarged thyroid gland (goiter), which becomes evident as a swollen neck. Other

consequences of not having enough iodine (iodine deficiency) are also serious. Iodine deficiency and the resulting low levels of thyroid hormone can cause women to stop ovulating, leading to infertility (Cao *et al.*, 1994). Iodine deficiency can also lead to an autoimmune disease of the thyroid and may increase the risk of getting thyroid cancer (Cao *et al.*, 1994).

Iodine is used to prevent iodine deficiency and its consequences, including goiter. It is also used for treating a skin disease caused by a fungus (*Cutaneous sporotrichosis*), treating fibrocystic breast disease; preventing breast cancer, eye disease, diabetes, and heart disease and stroke, and as an expectorant (Agarwalet *et al.*, 2008; Bonifaz *et al.*, 2007; Arora *et al.*, 2003; Cabezas *et al.*, 1996). Iodine is applied to the skin to kill germs, prevent soreness inside the mouth (mucositis) caused by chemotherapy, and treat diabetic ulcers (Mahajan *et al.*, 2010; Patrick, 2008). It is also reported that iodine has very specific protective effects against several common poisons like fluoride and bromide and, to a lesser extent, helps eliminate lead and mercury from the body (Apelqvist and Ragnarson, 1996). A number of compounds of pharmaceutical importance from a variety of chemical families, including thiocyanates, isothiocyanates, thiourea and derivatives, imidazoles, and various amines and proteins, were found to form charge transfer complexes with iodine (Yusubova and Zhdankin, 2015; Raby *et al.*, 2013; Cunningham and Nuenke, 1959; Thomas and Aune, 1977). All the studies cited showed that iodine acted as the oxidant or the electron acceptor.

These are just a few of the reasons to become interested in iodine, and truly, the study of the mechanism of oxidation of substrates by iodine has been the subject of several studies, but among which no complete agreement is found (Mshelia *et al.*, 2010; Funai and Blesa, 1984; Hasty, 1975; King *et al.*, 1978; Palmer and Lietzke, 1982; Smith and Martell, 1976;

Chernov'yantset *et al.* 2013). The mechanisms of the oxidation of substances by iodine is not only as varied as the number of authors who have published such works, but also as the number of internationally recognized peer reviewed journals in which such works were published (Klebanoff, 1967; Hasty, 1975; Smith and Martell, 1976; King *et al.*, 1978; Palmer and Lietzke, 1982; Funai and Blesa, 1984; Cao Xue *et al.*, 1994; Aghaie *et al.*, 2008, Mshelia *et al.*, 2010; Zhu *et al.*, 2013; Tang *et al.*, 2013; Chernov'yantset *et al.* 2013). A further investigation seemed desirable (Bhatnagar *et al.*, 1990; Goyal *et al.*, 1989), because all these previously cited studies showed that iodine reactions with the hydrazines and various biomolecules are of physiological importance. This study was, therefore, undertaken to provide better mechanisms of the reactions of iodine with the hydrazines and biomolecules discussed in the subsequent sub-sections (1.2 – 1.5).

## **1.2 Hydrazine and Its Derivatives**

It is well known that hydrazine and its derivatives play an important role in biological activity studies. A number of hydrazide-hydrazones are claimed to possess interesting antibacterial and antifungal (Loncle *et al.*, 2004), anticonvulsant (Sridhar *et al.*, 2002), anti-inflammatory (Gaston *et al.*, 1996) antimalarial (Gaston *et al.*, 1996) and anti-tuberculosis activities (Maccari *et al.*, 2005). It is also well known that iodine quantitatively oxidizes substances containing the -NH-NH<sub>2</sub> group. This reaction is the basis of one of the standard analytical procedures to titrate hydrazine and related substances, in particular isonicotinoyl-hydrazide which is widely used in the pharmaceutical industry because of its bacteriostatic properties against *Mycobacterium tuberculosis* (Laidler, 1978; Funai and Blesa, 1984; Sultan *et al.*, 1985; Rao and Dalvi, 1990; Cao-Xue *et al.*, 1994; Mshelia *et al.*, 2010).

1,2-Diphenylhydrazine, a derivative of hydrazine and also known as hydrazobenzene, is used as an antisludging additive to motor oil, a desuckering agent for tobacco plants, a reductant in the reclamation of rubber, a component of experimental organometallic polymers, an ingredient in photo-chromic resin compositions, and a component in polymerization reactions. It is also used in the manufacture of hydrogen peroxide (Mondal and Banerjee, 2009; Bhatnagar *et al.*, 1990; Kelly *et al.*, 1994; IPCS, 1993). Some 1,2-diphenylhydrazine derivatives are used as flame retarding agents (Ohnishi *et al.*, 2000). Several aryl hydrazine interactions in small molecule complexes were studied to see how they might react with iron and other substances (Zdilla *et al.*, 2008). The study found that a 3mM solution of benzene completely disproportionate 6 equivalents of 1,2-diphenylhydrazine into aniline and azobenzene. Their effort to shift the chemistry in a different direction was only partially successful. Several others (Globig and Freundt, 1996; Globig *et al.*, 1996; Assi *et al.*, 1996; Khalil *et al.*, 1999; Homer *et al.*, 1985) have also reported that the reactions of 1, 2-diphenylhydrazine and its derivatives are pH dependent and will yield different products depending on the pH of the reaction medium. These studies (Zdilla *et al.*, 2008; Globig and Freundt, 1996; Globig *et al.*, 1996; Assi *et al.*, 1996; Khalil *et al.*, 1999; Homer *et al.*, 1985) concluded that 1,2-diarylhydrazines and their derivatives enjoy complicated chemistries that include structural rearrangement and disproportionation and that their interactions with metal ions are complex and incompletely understood. Although 1,2-diphenylhydrazine is known to be oxidized readily by many oxidants (Ayub and Mahmood, 2013; May and Halpern, 1961; Whalley *et al.*, 1956; Blackmore *et al.*, 2008; Zarkesh *et al.*, 2008; Luu *et al.*, 2007), only in a few other cases have the reaction mechanisms been examined, especially its reaction mechanisms with iodine (Ayub and Mahmood, 2013; Shallangwa *et al.*, 2014a). It is also noteworthy to state that the various mechanisms proposed were not conclusive and needed to be revisited.

### 1.3 L-Tyrosine

The study of the oxidation of proteins and amino acids is of interest because of their biological significance and selectivity towards oxidant to yield different products (Laloo and Mahanti, 1990; Giulivi and Davies, 2001). Amino acids act not only as the building block in protein synthesis but also play a significant role in metabolism, nutrition, fortification of seeds, biochemical research and have been oxidized by a variety of oxidizing agents (Malika *et al.*, 2010; Hung and Stanbury, 2005; Faller *et al.*, 2002).

L-tyrosine (L-Tyr) is a nonessential or a semi-essential amino acid the body makes from another amino acid called phenylalanine (Xiashi and Suqin, 2010; Poustie and Wildgoose, 2010; Hoffman *et al.*, 2010). It is a building block for several important brain chemicals called neurotransmitters, including epinephrine, norepinephrine and dopamine (Webster and Wildgoose, 2013; Mahoney *et al.*, 2007). Tyrosine is used for the treatment of tuberculosis, myelitis, encephalitis, thyroid bacterial infections and as a nutritional supplement. Parkinson's disease, albinism, depression, and other mood disorders were generally found when L-tyrosine levels are abnormal (Gelenberget *et al.*, 1982; Meyers, 2000; Parry, 2001). Tyrosine also helps produce melanin, the pigment responsible for hair and skin colour. It helps in the function of organs responsible for making and regulating hormones, including the adrenal, thyroid, and pituitary glands. It is involved in the structure of almost every protein in the body (Marquez and Dunford, 1995; van Spronsen *et al.*, 2001; Tumilty *et al.*, 2011; Bergès *et al.*, 2011; Azoriet *et al.*, 2011).

It has been reported (Klebanoff, 1967; Aghaie *et al.*, 2008; Doggui and El Atia, 2015) that free iodine reacts with the protein of bacteria (presumably by iodinating tyrosine residues)

and thus kills the bacteria. At pH = 6.8, iodine reacts with tyrosine as well as with cysteine (Klebanoff, 1967; Aghaie *et al.*, 2008). Iodine deficiency is currently the most preventable cause of the world's cretinism, brain damage and thyroid disorders as well as those of ovaries, breasts and prostate (Aghaie *et al.*, 2008; Cao Xue *et al.*, 1994). These are just a few of the reasons why the study of iodine is interesting. Biologically, iodine is most essential in the synthesis of thyroid hormones, which serve in the differentiation, growth, metabolism and physiological function of virtually all tissues (Yen, 2001). In the thyroid colloid, iodide is collected and concentrated. After concentration, iodide is oxidized to  $I^+$  by the enzyme thyroid peroxidase (TPO) in the presence of  $H_2O_2$  (Aghaie *et al.*, 2008). The oxidized iodine is then bound to tyrosine residues of the protein thyroglobulin to produce monoiodothyrosine (MIT) and diiodothyrosine (DIT). Thyroglobulin (Tg) acts as the substrate for thyroid hormone (T3, T4) biosynthesis (Mallet *et al.*, 1995). Aghaie *et al.* (2008) proposed four different possible transition states for the oxidation of L-tyrosine by iodine but could not decide which of the four possible transition state would be the most favoured one. In one of the published papers from this work, Shallangwa *et al.* (2014c) revisited this reaction computationally and the authors were able to determine, energetically, the most favourable transition state.

#### **1.4 L-Ascorbic Acid**

Ascorbic acid is water soluble sugar acid with antioxidant properties or with strong reducing action and it is an important co-enzyme for internal hydroxylation reaction (Rahman *et al.*, 2007). The L-isomer of ascorbic acid is commonly known as vitamin C and is found naturally in fruits and vegetables (Kennedy *et al.*, 1989; Rahman Khan *et al.*, 2006; Dioha *et al.*, 2011; Okie *et al.*, 2008). Vitamin C (ascorbic acid) is an important component of human diet. Some of its functional roles include its use as a nutrition food additive, antioxidant, reducing agent,

stabilizer, modifier and colour stabilizer (Kapure *et al.*, 2012). Its absence in human leads to scurvy, a deficiency disease (Eitenmiller *et al.*, 2008), where the protein, collagen, cannot form fibres properly and this results in skin lesions and blood vessel fragility (Kuninori and Nishiyama, 1993; Ryley and Kajda, 1994; Cheema and Pant, 2011).

Ascorbic acid is susceptible to oxidation in acidic, basic or neutral media. The oxidation of ascorbic acid is a very important redox reaction, as it has interesting biological properties and is also a powerful reductant. Ascorbic acid is a lactone with a 2,3-endiol group (Khan and Sarwar, 2001; Matei *et al.*, 2008). It is very effective as a reducing agent and is quantitatively reversibly oxidized in aqueous solution by different oxidizing agents. The products of the oxidation depend largely on the pH of the reaction; however, its oxidation by various oxidizing agents in acid solution produces dehydroascorbic acid, a lactone whose ring can be easily hydrolyzed to give the free carboxylic group Linda (Khan and Sarwar, 2001; Matei *et al.*, 2008; Linda, 2001).

A number of articles have been written on the oxidation of ascorbic acid in acidic and basic media with various inorganic (Rajanna *et al.*, 1996; Palet *et al.*, 1994; Perolav and Pedersen, 1994; Kagayama *et al.*, 1994; Lea *et al.*, 1993; Martinez *et al.*, 1992) and organic substrates (Verma *et al.*, 1996; Rao, *et al.*, 1987; Heller *et al.*, 2001). However, the reduction of iodine with ascorbic acid though severally reported, were somewhat limited in kinetic and mechanistic details (Khan and Sarwar, 2001; Sitti and Bunbun, 2009). Given the importance of the vitamin in human health and its widespread use as an antioxidant in processed foods, study of its degradation products by iodine is worthy of investigation (Khan and Sarwar, 2001).

## 1.5 Reducing Sugars

The study of sugars or carbohydrates in general is one of the most exciting fields of biochemistry (Tao and Raffel, 2009; Bare *et al.*, 2007) and organic chemistry (Mahmood *et al.*, 2009; Finar, 1978; Olusanya and Odebunmi, 2013) and has been the subject of extensive research in recent years. Sugars serve as the major fuel for biological systems, supplying living cells with the required energy for daily functioning and, therefore, the understanding of the oxidation of sugars is of immense importance. Sugars serve as the body's primary source of energy. Abundant energy is primarily stored in the complex molecular structure of the sugars or carbohydrates (Kim *et al.*, 2002; Bond and Lovley, 2003). Carbohydrates must be burned or oxidized if energy is to be released. When complex compounds are metabolized, the atoms rearrange themselves into simpler compounds and, in the process, release the stored energy for use.

A vast amount of literature (Martin *et al.*, 2002; Hao *et al.*, 2003; Odebunmi and Owalude, 2005; Odebunmi and Owalude, 2007; Pigman and Anet, 1972; Jin *et al.*, 2014, Hietanen *et al.*, 2012; Marzorati *et al.*, 2005,) is available on the kinetics of oxidation of carbohydrates by various organic and inorganic oxidants. The oxidations of some reducing sugars by diperiodatoargentate (III), diperiodate Arsenate (III) and osmium tetroxide in alkaline medium have been reported (Rao *et al.*, 1995; Venkate and Jaya, 1995; Singh *et al.*, 1991). Oxidation of maltose and lactose by copper (II) ion and hexacyanoferrate (III) ion, have been also studied in alkaline medium (Olusanya and Odebunmi, 2011), while Okeola *et al.* (2010) investigated the kinetics of catalyzed oxidation of glucose and galactose by hexacyanoferrate (III) ion and copper sulphate in alkaline medium. Oxidation of D-glucose, D-fructose and D-mannose by 12-tungstocobaltate(III) has been investigated by several others (Banerjee *et al.*, 1988; Babasaheb *et al.*, 2012) too.

The catalyzed and non-catalyzed oxidation of sugars has been investigated in detail using organic oxidants such as N-halo compounds (Singh *et al.*, 2002; Singh *et al.*, 2004a; Singh *et al.*, 2006a; Singh *et al.*, 2006b; Lyengaret *al.*, 1990; Gowda *et al.*, 2005; Rangappa *et al.*, 1998a; Rangappa *et al.*, 1998b). Inorganic oxidants such as Cu(II), ammonical Ag(I) and Nessler's reagent have been used in the non-catalyzed oxidation of sugars in an aqueous alkaline medium (Singh *et al.*, 1975; Singh *et al.*, 1978; Singh *et al.*, 1980). The mechanism for the oxidation of some aldoses by Cr(VI), V(V) and Ce(IV) investigated in acidic media has also been reported (SenGupta *et al.*, 1998). The oxidations of sugars have been carried out in both acidic and alkaline media using such oxidants as transition metal ions, inorganic acids, organometallic complexes and enzymes.

The use of periodate in the non-catalyzed oxidation of carbohydrates and Ru(III) and the ruthenate ion-catalyzed oxidation of reducing sugars in an alkaline medium are also available (Tiziani *et al.*, 2003; Singh *et al.*, 2004b). The oxidation of sugars especially the mono and disaccharides occurs under different conditions of pH, temperature and ionic strength giving products that depend on the oxidants used. The results showed that the mechanism may depend on the nature of the substrates; in some cases, it involves the formation of intermediate complex, free radical or transition states. The mechanism of oxidation of reducing sugars, especially the mono and disaccharides, by different oxidants has been the subject of several studies, but despite the vast studies on the oxidation sugars those involving iodine are scarce. An investigation of oxidation of sugar with iodine is, therefore, desirable.

### **1.6 Statement of the Research Problem**

Iodine as an element has many uses in different areas as highlighted in the preceding sections. Iodine reduces thyroid hormone and can kill fungus, bacteria, and other microorganisms such

as amoebae. Iodine, in the form of potassium iodide, is also used to treat (but not prevent) the effects of a radioactive accident (WHO, 2002; Majidnia and Idris, 2015). It is well known that iodine quantitatively oxidizes substances such as hydrazine, hydrazine derivatives, amino acids like tyrosine, ascorbic acid, reducing sugars as highlighted in sections 1.2 - 1.5. The substrates mentioned above are, in their own rights, quite interesting molecules and deserved to be studied. But more than that, their reactions with iodine, another very interesting substance, is not well studied, and if studied the mechanisms were not well understood, or the mechanisms proposed by the various researchers were always at variance with others who studied similar or same reactions (Mshelia *et al*, 2010; Funai and Blesa, 1984).

There seemed to be a gap in knowledge related to the reaction mechanisms of iodine, a very important molecule with great physiological and biological activities and the molecules studied. May and Halpern (1961) studied the reaction of iodine with 1,2-diphenylhydrazine and gave a mechanism that was not consistent with their stoichiometry of reaction. Funai and Blesa (1984), Sultan *et al* (1985), Mshelia *et al* (2010) also investigated the reaction mechanisms of iodine with hydrazine and its derivative, and proposed dissimilar mechanisms of the same reactions. Aghaie *et al* (2008) investigated the reaction mechanism of iodine with L-tyrosine and gave a mechanism in which they proposed four different like transition states, but could not determine which of the transition states could be the most favourable one. Several groups (Morelli, 1976; Rao *et al*, 1987; Sitti and Bunbun, 2009; Canterbury, 2014) studied and gave dissimilar mechanisms for the oxidation of L-ascorbic acid by iodine. The studies of Odebunmi and Owalude (2008), Mahmood *et al* (2009), Olusanya and Odebunmi (2013) also showed that reported mechanisms of reducing sugars are varied. The dissimilar mechanisms reported are as results of the inability of the researchers to deduce the correct nature of the transition states involved in the reactions. It is documented that that

transition states of reactions have not been isolated and characterized experimentally in the laboratory.

### **1.7 Justification of the Research**

In writing a reaction mechanism, a step-by-step account of the bond (electron) reorganizations that take place in the course of a reaction is given. These mechanisms do not have any objective existence, as more often, they cannot be proven; they are merely the Chemist's attempt to represent what is going on in a reaction. Although experiments can suggest that some mechanisms are reasonable and others are not, for many reactions, there is no evidence regarding the mechanism, and the authors are free to write whatever mechanism they choose as accepted mechanistic patterns, subject only to the constraint that they have not contravened any established chemical law (Miller and Solomon, 1999; Moore and Pearson, 1980).

Reaction mechanisms offer the practicing Chemists insights into how molecules react, enable them to manipulate the course of known reactions, aid them in predicting the course of known reactions using new substrates, and help them to develop new reactions and reagents. In order to understand and write reaction mechanisms, it is essential to have a detailed knowledge of the structures of the molecules involved and to be able to notate these structures unambiguously (Miller and Solomon, 1999; Atkin and de Paula, 2006; Koch and Holthausen, 2000). But it is often difficult to predict what will actually happen in the course of a reaction, especially with regard to the intermediates and transition states, as more often the transition states cannot be isolated and characterized. This explained why there could be different mechanism for the same reaction when the mechanism is written on the basis of experiments. But modern computational methods have now been developed that could search

for the transient species, such as intermediates and transition states, and really confirm, by vibrational analysis, whether they are true transition states or not. The methods also take the further step of providing the reaction energetics for various proposed reaction pathways. This allows for the selection between mechanisms on the basis of the predicted lowest energy pathway (Jordan, 2007; Levine, 1988; Becke, 1988; Lee *et al.*, 1988; Wannan and Ruangpornvisuti, 2006).

It is these advantages that the computational methods have over the experimental that makes it possible to re-investigate the various ambiguously published reaction mechanisms of the oxidation of the following substrates: hydrazinium ion, hydrazine molecule, 1,2-diphenylhydrazine, L-tyrosine, L-ascorbic acid and D-fructose by molecular iodine. The investigation would specifically address and:

- i. resolve all the conflicts (dissimilar mechanisms for same reaction) associated with the reactions of iodine with substrates listed above and proposed new mechanisms for each of them;
- ii. establish all possible reaction pathways and the most favourable one for each reaction;
- iii. identify and characterize all the transient species which are not accessible experimentally for all the reaction pathways;
- iv. calculate thermodynamic and some physico-chemical parameters of all reactive species and products of reactions
- v. derive rate-law for each of the pathways that are consistent with the mechanisms proposed.
- vi. calculate and compare the rate constants of the reactions based on the proposed logical reaction mechanism.

## 1.8 The Research Questions

The computational chemistry modelling experiment reported in this study is exploratory. Both semi-empirical and DFT methods would be used to optimize the structures of reactants, intermediates, transition states and products of each reaction. Semi-empirical and DFT methods would be used to search for intermediates and transition state and, to calculate the thermochemical and other physicochemical properties of the optimized reactants, intermediates, transition states and products of each reaction. Logical reaction mechanisms based on the information gathered from the use of the computation tools highlighted above would be explored and derived.

To achieve the purpose of the study, the following research questions were asked and addressed. They include:

- i. What does this research want to find out or know about the optimized structures of reactants, intermediates, transition states and products of each reaction? Usually, the total energies, thermodynamic, activation and other physicochemical parameters would be sufficient.
- ii. What level of accuracy is expected from the calculations on the optimized structures of reactants, intermediates, transition states and products of each reaction to be? Semi-empirical methods use more severe approximations and/or empirical data to increase the speed of calculations, but give less accurate results, while the DFT methods are more exact but more time consuming (Springborg, 1997; Jensen, 1999; Cramer, 2002).
- iii. How much time is available for the research to be completed? The semi-empirical calculations are fast and can be completed in hours, but the DFT

calculations can take days, weeks or even months to complete depending on how large the molecules are and also depending on how big the basis set chosen. *Ab initio* methods take even longer time than the DFT methods to complete a single calculation (Parr and Yang, 1989; Ochterski, 2000).

- iv. What approximations would be made or would be acceptable? Whereas semi-empirical methods, use more severe approximations to increase the speed of calculations, the DFT methods, which are more exact in their approximations, are considered to be fairly robust (Lewars, 2003; Gao, 1996; Hehre *et al.*, 1986).

## **1.9 The Research Hypotheses**

The study was guided by the following null and alternative hypotheses:

- i. Null hypothesis:* All the published reaction mechanisms of the oxidation of substrates by iodine are correct;
- ii. Alternative hypothesis:* Some or all of the published reaction mechanisms of the oxidation of substrates by iodine needed to be modified.

## **1.10 Conceptual Framework**

The conceptual framework of the research work is as given in Figure 1.1 showing the various tasks that are expected to be carried out on the reaction of iodine with the hydrazines and biomolecules.

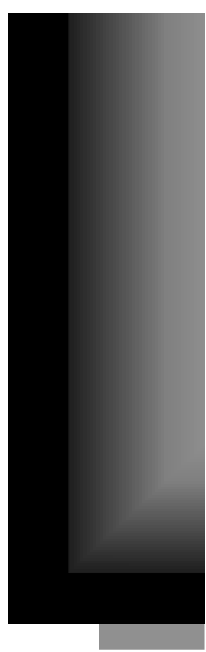


**Figure 1.1: The research conceptual framework**

## 1.11 Theoretical Framework

The past 35 years have seen rapid developments in the field of computer science and these developments have in turn brought about a rapid development of the relatively, new area of computational chemistry (Clementi, 1980; Ostlund *et al.*, 1982; Hopfinger, 1984; Leszczynski, 2000; Dykstra *et al.*, 2011; Cramer, 2013; Floudas and Pardalos, 2013). Armed by the contemporary computational power, the computational chemists are able to formulate high level theoretical models describing the real interactions between reacting species. Various methods are available for simulations of the interactions and possible behaviour. Opposed to chemical experimental procedures, computational methods are relatively fast and, combined with optimization methods, quite reliable (Jensen, 1999; Leszczynski, 2000; Cramer, 2002; Al-Hashimi and Hussein, 2010; Kortagere *et al.*, 2010; Dykstra *et al.*, 2011; Cramer, 2013; Floudas and Pardalos, 2013). As for the investigation of the reaction mechanisms of the redox reactions of some bio-substrates with molecular iodine, the best solution seems to be molecular modeling.

The primary characteristic of any mutual interaction between two molecules is the energy. Computational chemistry is capable of calculating theoretical values of such interaction at different levels of simplification (Al-Hashimi and Hussein, 2010). Like the most applications in computational chemistry, the important task is to find a proper level of simplification that allows the computations to be relatively fast, yet providing satisfactory results with regard to the real, experimentally determined behavior of the system.

For investigating interactions between a large molecule and a small molecule that binds to the larger one, there are several possibilities of addressing this problem. Probably the best-explored, and nowadays basics, are the semi-empirical and density functional theory

(DFT) methods (Mota *et al.*, 2010). This aim is realized by carrying out the tasks enumerated in the aim and objectives of this study.

### **1.12 Aim and Objectives**

The research was aimed to computationally investigate the reaction mechanisms of the oxidation of some hydrazines (hydrazinium ion, hydrazine, 1,2-diphenylhydrazine) and biomolecules (L-tyrosine, L-ascorbic acid, D-fructose) by molecular iodine. The aim would be achieved through the following objectives: To

- i. use both semi empirical and density functional theory (DFT) methods to optimize the structures of reactants, intermediates, transition states and products of each reaction.
- ii. use both semi empirical and DFT methods to search for intermediates and transition states.
- iii. calculate the thermochemical and other physico-chemical properties of the optimized reactants, intermediates, transition states and products of each reaction.
- iv. plot the potential energy surface diagrams of the various elementary steps of the reactions
- v. write a logical reaction mechanism based on the information gathered from (i) – (iv) above.
- vi. calculate the kinetic data of the reactions based on the proposed logical reaction mechanism.

## CHAPTER TWO

### 2.0 LITERATURE REVIEW

#### 2.1 Computational Approaches for Investigation of the Reaction Mechanisms

Reaction mechanism is the step by step sequence of elementary reactions by which overall chemical change occurs (Espenson, 2002; Atkins and de Paula, 2006; Tro, 2010; Masterton *et al.*, 2012). A chemical mechanism describes in detail exactly what takes place at each stage of an overall chemical reaction (Atkins and de Paula, 2006; Masterton *et al.*, 2012). It also describes each reactive intermediate, activated complex, and transition state, and which bonds are broken, and which bonds are formed. A complete mechanism must also account for all reactants used, the function of a catalyst, stereochemistry, all products formed and the amount of each (Manz and Sholl, 2010). It must also describe the relative rates of the reaction steps and the rate equation for the overall reaction (Atkins and de Paula, 2006; Tro, 2010; Masterton *et al.*, 201). Reaction intermediates are chemical species, often unstable and short-lived, which are not reactants or products of the overall chemical reaction, but are temporary products and reactants in the mechanism's reaction steps. Reaction intermediates are often free radicals or ions. Transition states can be unstable intermediate molecular states even in the elementary reactions. Transition states are commonly molecular entities involving an unstable number of bonds and/or unstable geometry. They correspond to maxima on the reaction coordinate, and to saddle points on the potential energy surface for the reaction (Lewars, 2003; Atkins and de Paula, 2006; Engel and Reid, 2006; Manz and Sholl, 2010).

There are various studies on reactions of iodine ( Bhatnagar *et al.*, 1990; Agarwal *et al.*, 2008; Zhang and Hase, 2010; Ayub and Mahmood, 2013; Raby *et al.*, 2013), hydrazines ( May and Halpern, 1961; Barca *et al.*, 1967; Funai and Blesa, 1984; Homer *et al.*, 1985;

Sultan *et al.*, 1985; Assi *et al.*, 1996; Globig *et al.*, 1996; Jia *et al.*, 2000; Blackmore *et al.*, 2008; Zdilla *et al.*, 2008; Mondal and Banerjee, 2009; Mshelia *et al.*, 2010), L-tyrosine (Azori *et al.*, 1990; Foppoli *et al.*, 1997; Giulivi and Davies, Faller *et al.*, 2002; Aghaie *et al.*, 2008; Heneberg, 2009; Barr, 2010; Malika *et al.*, 2010; Xiashi and Suqin, 2010; Karver *et al.*, 2010; Tumily *et al.*, 2011; Obiri *et al.*, 2012;), L-ascorbic acid (Khan and Sawar, 2001; Cheema and Pant, 2011; Dioha *et al.*, 2011; Kapur *et al.*, 2012; Canterbury, 2014), and D-fructose (Banerjee *et al.*, 1988; Gowda *et al.*, 2005; Mahmood *et al.*, 2009; Tao *et al.*, 2009) but for which detailed mechanisms are not available or require development. Even when information is available, identifying and assembling the relevant data from a variety of sources, reconciling discrepant values and extrapolating to different conditions can be a difficult process without expert help. Rate constants or thermochemical data are often not available in the literature, so computational chemistry techniques must be used to obtain the required parameters (Zhang and Zhang, 2007). Computational chemistry methods can also be used to calculate potential energy surfaces for reactions and determine probable mechanisms (Lewars, 2003; Schramm, 2005b; Atkins and de Paula, 2006; Zhang and Zhang, 2007; Tro, 2010; Masterton *et al.*, 2012).

A series of computational approaches can be used to overcome the limitations of experimental techniques in studying reaction mechanisms (Cummins and Gready, 2005; Atkins and de Paula, 2006; Domingo *et al.*, 2013; Shallangwa *et al.*, 2015). Identifying the most critical energetic components of the reaction is of crucial importance for understanding reaction mechanisms (Schramm, 2005b; Giraldo *et al.*, 2006; Domingo *et al.*, 2013). Several algorithms of varying accuracy and computational cost have been developed to study reaction mechanisms. From ligand binding and activation to the oxidation process itself, including formation of the transition state and final generation of products, different modelling and

simulation techniques can be applied (Bruice and Bruice, 2005; Domingo *et al.*, 2013; Barhoumi *et al.*, 2015; Hammal *et al.*, 2015). Selection of the appropriate computational tool is not straightforward; it is one of the first challenges a computational chemist must face. Therefore, no single simulation technique will be adequate to address all events occurring during oxidation – reduction processes, and it will be necessary to use a range of theoretical approaches (Araujo *et al.*, 2007; Huey *et al.*, 2008).

Nearly all of a material's physical properties can be related to free energy values. In turn, any property that is related to energies (or differences in energies) can be determined theoretically if a method exists which is both reliable and capable of accurately determining these values (Araujo *et al.*, 2007; Huey *et al.*, 2008). With the advent of high speed parallel computing, the modern theoretical methodologies required to explore atomic interactions to high degrees of accuracy are made available for routine use. *Ab initio*, Density functional theory (DFT) and semi-empirical (SE) methods are fast becoming the method of choice for exploring chemical reactivity (Jensen, 2007; Cramer, 2013). The ability of these methods to simulate bond breaking and forming events allows for valuable information to be gathered on the interactions taking place. They can also help to facilitate the elucidation of the reaction mechanisms involved (Leszczynski, 2000; Bruice and Bruice, 2005). In this chapter a brief summary of the main computational techniques used is presented, describing the underlying principles of the approaches, their applications and limitations.

The practice of chemistry, in one form or another, has been around for millennia, but only in the past two centuries has the practice of chemistry evolved from archaic alchemy to a pure and applied science. Modern chemistry is able to probe the structure, microscopic properties, and reactions of atoms and molecules through systematic laboratory methods that

include synthetic techniques, such as directly reacting a substance with another substance in a controlled environment; instrumental techniques, including the myriad of spectroscopic techniques; and, more recently, computational techniques.

With the advent of quantum mechanics in the early 20th century, the way in which chemical properties traditionally are elucidated changed dramatically. Schrödinger's wave mechanics, simultaneously introduced alongside Heisenberg's matrix mechanics, offered ways of calculating both static and dynamic properties of quantized systems. Following the construction of the first electronic computer, chemists and physicists began to submit atomic and molecular properties for calculation using Schrödinger's and Dirac's mathematics. The amount of information acquired about chemical properties during the early years of quantum mechanics was not substantial, limited primarily by the computational expense of both the underlying mathematics and the physical computational resources (i.e. storage, time, and software).

Computational chemistry has become an interdisciplinary subject that straddles physics, chemistry, biology, and geophysics. This field can also be considered as the art of the computer experiment and certainly computational chemistry or computer experiments have enlarged and deepened the scope of understanding from traditional laboratory experiments. Generally speaking, one can say that the experiment in the laboratory will tell us what happens in most cases, while in principle, computational chemistry would allow one to find out why some reactions would take place and hopefully, also predict, what will happen under certain conditions or circumstances (Tro, 2010; Masterton *et al.*, 2012). Furthermore, computer experiments can readily access reaction conditions which laboratory experiments cannot easily reach (Alfe *et al.*, 2000; Gillan *et al.*, 2006). For example, reactions can

readily be carried out at temperatures of zero or sub-zero Kelvin, and at pressures other than standard pressure, which would be out of reach in a laboratory experiment setting, yet could be computed without any particular difficulty computationally.

The key point with all simulations or computational modeling is how reliable they are and whether they accurately model reality. Traditionally, pre-parameterized empirical potentials were used to model the interaction between collections of atoms or molecules. These have achieved considerable success in many areas. Increasingly popular though, but, computationally much more expensive, are the so-called first principles approaches. In this work, a variety of first principles approaches have been applied, often with the goal of executing calculations with the highest possible accuracy.

The central task in first principles simulations is to solve the many-body Schrodinger equation and obtain the total energy and wave function of the system which are the starting point for most of the physical properties of the reacting species. There are many and varied first principles approaches. Often it is useful to categorize them as wave function based methods, e.g., quantum chemistry methods and quantum Monte Carlo, or electron-density based (density-functional theory (DFT)) methods (Zhao and Truhlar, 2008; Perdew and Schmidt, 2001). Both methods have gained great success and particularly in condensed matter electronic structure calculations, DFT predominates. One reason for this is that calculations can be done for large systems (hundreds or even thousands of atoms) at modest computational costs (Perdew *et al.*, 2005).

There is no doubt that DFT is exact in principle (Jensen, 1999). However, DFT relies on approximations to the exchange-correlation functional in practice (Cramer, 2002; Kresse *et*

*al.*, 2003; Feibelman *et al.*, 2001). Although DFT has proven to be very successful, the deficiencies of DFT are also well documented. One prominent example in surface physics is that DFT with the local density approximation (LDA) and generalized gradient approximation (GGA) predict the wrong adsorption site for CO on Pt(111) and other close-packed metal surfaces (Kresse *et al.*, 2003; Feibelman *et al.*, 2001) because of the intrinsic error in these approximations. In addition, adsorption energies of atoms and molecules on surfaces can often differ by large amounts (50%) from experiment depending on the choice of approximation for the exchange-correlation functional (Hammer *et al.*, 1999; Tran *et al.*, 2007; Fuentes-Cabrera *et al.*, 2008). Although there exists a useful scheme now for categorizing DFT exchange-correlation functionals (so-called Jacob's ladder) (Perdew and Schmidt, 2001), systematically improving DFT exchange-correlation functionals is difficult. By contrast, quantum chemistry methods which begin with Hartree-Fock as a base and gradually add in increasing accounts of electron correlation provide an alternative when high precision, beyond that available with current exchange-correlation functionals, is required. The difficulty with these wave function approaches is that they are not amenable to very large or periodic systems. Thus, applying quantum chemistry to condensed matter is not straightforward, but it is something that is becoming increasingly popular.

The ultimate goal of computational chemistry is to predict and understand the electronic structure of chemical compounds and their reactions using concepts and techniques of both the static and dynamical approaches. The first task confronting the chemist is to identify the compound reactive sites as a function of the molecular structure, and to determine their relative reactivity trends. For these, the density functional theory (DFT) provides an appealing framework of investigation in chemistry due to its relatively low cost of calculations (when compared with the more demanding calculations of *ab initio* methods),

highly accurate results and due to its offering of a perspective on the interpretation and prediction of experimental or theoretical reactivity (Perdew, 1985; Perdew and Levy, 1997).

## 2.2 Computational Chemistry

Computational chemistry can perhaps be loosely defined as chemistry modeling, based on a molecular or atomic level description. In other words, computational chemistry is a set of techniques for investigating chemical problems on a computer (Lewars, 2003). The term covers a fairly broad range of theories and methods.

Some of the common computational investigations are:

- i. *Molecular geometry*: This provides information on the shapes of molecules – bond lengths, angles, and dihedrals.
- ii. *Energies of molecules and transition states*: This tells us which conformer and/or isomer is favoured at equilibrium, and (from transition state and reactant energies) how fast a reaction can go.
- iii. *Chemical reactivity*: Knowing where the electrons are concentrated (nucleophilic sites) and where electrons are deficient (electrophilic sites) enables us to predict the reactive sites in a molecule.
- iv. *IR, UV, Raman and NMR spectra*: These can be calculated, and if the molecule is known or unknown, its properties can be studied.
- v. *The interaction of a substrate with an enzyme*: Seeing how a molecule fits into the active site of an enzyme is one approach to designing better drugs.

- vi. *The physical properties of substances*: These depend on the properties of individual molecules and on how the molecules interact in the bulk material, especially in the field of materials science.

The various methods of computational chemistry can be thought of as offering a toolbox. For different problems studied, choices must be made as to what methods are best suited. The main tools available belong to five broad classes as briefly described below.

In the present work, several different issues related to the reactions of iodine with several biomolecules and hydrazines are studied. In studying these problems an eclectic approach has been chosen, namely to attempt to find the method best suited to each problem. As a result, a fairly large number of methods have been employed and these methods again draw on different fields of theory. No attempt will be made to cover the underlying theory in any detail here. The present chapter will rather focus on presenting the various branches of computational chemistry in general terms. The introduction is intended to give general insight into the various methods, in particular their strengths, weaknesses and limitations. In addition, the terminology to be used in the following chapters and papers will be introduced.

This presentation followed the outline used by Grant and Richards (1995) in their textbook “Computational Chemistry” as well as that used by Cramer (2002) in his textbook “Essentials of Computational Chemistry”, which was also followed, to some extent, by da Silva (2005).

### **2.3 *Ab initio* (Quantum Mechanics)**

*Ab initio* calculations (*ab initio* is from the Latin: “from first principles”) are based on quantum mechanics which uses the Schrödinger equation. This is one of the fundamental

equations of modern physics and describes, among other things, how the electrons in a molecule behave. The Schrödinger equation cannot be solved exactly for any molecule with more than one electron; thus approximations are used. Regardless of the level of approximation, an *ab initio* calculation is based only on basic physical theory (quantum mechanics) and is in this sense “from first principles”.

Dirac (1929) made this statement: “*The underlying physical laws necessary for the mathematical theory of a large part of physics and the whole of chemistry are thus completely known, and the difficulty is only that exact application of these laws leads to equations much too complicated to be soluble*”. The statement attributed to Dirac regarding the laws of chemistry and physics quoted above referred mainly to the postulation of the Schrödinger equation which, in its barest and most innocent form, can be written as in equation (2.1) (Szabo and Ostlund, 1989; Levine, 2000; Young, 2001):

$$\hat{H}\Psi = E\Psi \quad (2.1)$$

$\hat{H}$  is the shorthand form of the Hamilton operator which takes into account the contributions to the energy of the system.  $E$  is the energy of the system and  $\psi$  is the wave function that describes the system. The energy has only certain allowed values, with a corresponding wave function for each allowed energy level.

The Hamiltonian operator consists of the potential and kinetic energy contributions. In the absence of external magnetic and electrical fields, and ignoring relativistic effects, it takes the form of equation (2.2) (Szabo and Ostlund, 1989; Levine, 2000; Young, 2001; Cramer, 2002; Helgaker *et al.* 2004):

$$\hat{H} = -\frac{\hbar^2}{2m_e} \sum_i \nabla_i^2 + \frac{e^2}{4\pi\epsilon_0} \left( \sum_{i>j} \frac{1}{|\vec{r}_i - \vec{r}_j|} - \sum_{iI} \frac{Z_I}{|\vec{r}_i - \vec{R}_I|} + \sum_{I>J} \frac{Z_I Z_J}{|\vec{R}_I - \vec{R}_J|} \right) \dots(2.2)$$

where  $\vec{r}_i$  are the coordinates of electron  $i$  with mass  $m_e$  and charge  $-e$ , and  $\vec{R}_I$  are the coordinates of nucleus  $I$  of atomic number  $Z_I$  and  $\hbar$  is the Planck's constant divided by  $2\pi$ . In atomic units, the prefactor  $-\hbar^2/2m_e$  in the Hamiltonian becomes  $-1/2$ , whereas  $e^2/4\pi\epsilon_0$  becomes  $1$ .  $\nabla^2$  is the Laplacian operator,  $|\vec{R}_I - \vec{R}_J|$  is the distance between particles (Helgaker *et al.* 2004). The terms represent respectively the kinetic energy of the electrons, the kinetic energy of the nuclei, the attraction between the electrons and the nucleus, the interelectronic repulsion and the internuclear repulsion. From the Hamilton operator, it could be seen that the Schrödinger equation is a set of differential equations (Cramer, 2002).

For the wave function itself, it is difficult to give a simple definition or direct physical interpretation. The product of the wave function with its complex conjugate  $|\psi^*\psi|$  does, however, have a physical interpretation; it gives the probability density for the system. For an electron,  $|\psi^*\psi|$  multiplied with a volume element would give the probability of the electron being in that volume element. The normalized integral of  $|\psi^2|$ , over all space, must be unity. The wave function can, therefore, be thought of to be a kind of road-map to how the electrons are localized (Levine, 2000; Young, 2001; Cramer, 2002; Helgaker *et al.* 2004).

There is no way to directly derive the wave function itself, but there are some conditions it must meet. It must be “well-behaved”, displaying only smooth changes and going to zero at infinity. The variational principle states that the lower the ground state energy calculated by a wave function is, the higher is the quality of the wave function (Cramer, 2002). Assuming

that each electron can be treated separately, one can operate with one electron wave functions also called atomic orbital. In a system with more than one atom, i. e. a molecule, we deal with molecular orbitals. All electrons are characterized by a spin quantum number, with two possible eigenvalues. The Pauli principle states that two electrons cannot have the same set of quantum numbers. One molecular orbital is therefore limited to two electrons with opposite spin.

The Schrödinger equation is a postulate believed to be entirely accurate (Helgaker *et al.* 2004). The complexity of it is, however, such that the largest system for which it is analytically solvable is the hydrogen atom. It was this that led Dirac to make his observation quoted above. Since Dirac made his observation, a lot of work has gone into making approximations that make it possible to make calculations on systems of practical interest. Some of the main approximations will be briefly outlined below.

### **2.3.1 The Born-Oppenheimer Approximation**

The nuclei of atoms in a system are much heavier and move much more slowly than the electrons. It is therefore assumed that the movements can be decoupled. The energy of the electrons is calculated with the nuclei of atoms in fixed positions (Young, 2001; Lewars, 2003). This approximation is in most cases entirely reasonable and universally applied.

The Born-Oppenheimer approximation tries to separate the electronic and nuclear degrees of freedom even though they are coupled by the electron-nuclear potential energy  $V_{eN}(r, R)$ . This can be done because the electrons are much lighter than the nuclei, and so with respect to the electrons, the nuclei are almost stationary. Thus, the movements can be decoupled in

the following ways (Jensen, 1999; Lewars, 2003; Helgaker *et al.* 2004; Kraka and Cremer, 2010):

- i. Fix the nuclei at some chosen configuration  $R_a$
- ii. Solve for the motion of the electrons for this nuclear configuration, giving an electronic energy  $E_e(R_a)$  and wave function  $\Psi(r; R_a)$ .
- iii. Repeat for other nuclear configurations  $R_b$  of interest, building up a potential energy surface  $E_e(R)$ .

### 2.3.2 Potential Energy Surface

A potential energy surface is a plot of the energy of a collection of nuclei and electrons against the geometric coordinates of the nuclei – essentially, plot of molecular energy versus molecular geometry (or it may be regarded as the mathematical equation that gives the energy as a function of the nuclear coordinates). The nature (minimum, saddle point or neither) of each point was discussed in terms of the response of the energy (first and second derivatives) to changes in nuclear coordinates. The potential energy surface (PES) is a central concept in computational chemistry. A PES is the relationship – mathematical or graphical – between the energy of a molecule (or a collection of molecules) and its geometry. The Born–Oppenheimer approximation says that in a molecule the nuclei are essentially stationary compared to the electrons. This is one of the cornerstones of computational chemistry because it makes the concept of molecular shape (geometry) meaningful, makes possible the concept of a PES, and simplifies the application of the Schrodinger equation to molecules by allowing us to focus on the electronic energy and add in the nuclear repulsion energy later (Combes *et al.*, 2000; Jensen, 1999; Murrel *et al.*, 1984).

The most interesting points on PES's are the stationary points, where the gradients with respect to all internal coordinates are zero; and are listed below:

- i. *Minima*: In mathematics, *minima* (or *minimums*) of a function, known collectively as *extrema* (singular: *extremum*), are the smallest value that the function takes at a point either within a given neighbourhood (*local* or *relative extremum*) or on the function domain in its entirety (*global* or *absolute extremum*) (Press *et al.* 1992). The minima correspond to stable or quasi-stable species; i.e., reactants, products, and/or intermediates (Young, 2001).
- ii. *Transition states*: By definition, the transition state is the transitory of molecular structure in which the molecule is no longer a substrate but not yet a product. All chemical reactions must go through the transition state to form a product from a substrate molecule. The transition state is the state corresponding to the highest energy along the reaction coordinate. It has more free energy in comparison to the substrate or product; thus, it is the least stable state. The specific form of the transition state depends on the mechanisms of the particular reaction (Manz and Sholl, 2010). These correspond to saddle points which are minima in all dimensions but one; a maximum in that dimension (Young, 2001).
- iii. *Higher-order saddle points*: In mathematics, a saddle point is a point in the domain of a function that is a stationary point but not a local extremum, a point at which a function of two variables has partial derivatives equal to zero but at which the function has neither a maximum nor a minimum value (Widder, 1989). These correspond to a minimum in all dimensions but  $n$ , where  $n > 1$ ; maximum in the other  $n$  dimensions (Young, 2001).

### **2.3.2.1 Hessian Index**

The Hessian index is the number of negative eigenvalues of the force constant matrix. For a stationary point, the Hessian index corresponds to the number of internal degrees of freedom along which the stationary point is a potential energy maximum. The Hessian index is 0 for minima, 1 for transition states,  $> 1$  for higher-order saddle points. The Hessian index also corresponds to the number of imaginary vibrational frequencies (Valeev and Sherrill, 2003).

A geometry optimization, when run to completion, will provide stationary point geometry. Typically, this is a potential energy minimum. However, the optimization might get stuck on a saddle point. A vibrational analysis can verify the nature of the stationary point via the Hessian index.

### **2.3.3 Geometry Optimization**

The characterization (the “location” or “locating”) of a stationary point on a potential energy surface (PES), i.e. demonstrating that the point in question exists and calculating its geometry and energy, is a geometry optimization. The stationary point of interest might be a minimum, a transition state, or, occasionally, a higher-order saddle point. Locating a minimum is often called an energy minimization or simply a minimization, and locating a transition state is often referred to specifically as a transition state optimization. Geometry optimizations are done by starting with an input structure that is believed to resemble (the closer the better) the desired stationary point and submitting this plausible structure to a computer algorithm that systematically changes the geometry until it has found a stationary point (Young, 2001; Lewars, 2003). The curvature of the PES at the stationary point, i.e. the second derivatives of energy with respect to the geometric parameters may then be determined to characterize the

structure as a minimum or as some kind of saddle point (Hehre, 1995; Foresman and Frisch, 1996).

#### **2.3.4 Hartree-Fock Self-Consistent Field Method**

Much of the difficulty of solving the Schrödinger equation stems from the need to simultaneously determine the energy of each electron in the presence of all other electrons. In the Hartree-Fock (HF) method, this is avoided by calculating the energy of each electron in the averaged static field of the others. Initially, a guess is made of the electron orbital energies. The energy of each electron orbital is then calculated in the field of the initial electron configuration. This procedure is repeated in an iterative loop until convergence (self-consistent referring to this iterative calculation) is achieved (Lewars, 2003).

The Hartree-Fock method can therefore be thought of as a kind of mean-spherical approximation at the electron level. The difference between the Hartree-Fock energy and the energy for the full Schrödinger equation is called the correlation energy. Hartree-Fock calculations are sufficiently accurate to provide insight into many problems and they are widely used. As Hartree-Fock calculations have been applied to different problems, it has however, become increasingly clear that the correlation energy is of great significance in determining the properties of a system. Efforts have, therefore, been made to improve on the Hartree-Fock energy (Jensen, 1999).

#### **2.3.5 Post Hartree-Fock Methods**

There a number of different methods that go beyond Hartree-Fock calculations, one of the widely used approaches is perturbation theory. In perturbation theory, the Hartree-Fock solution is treated as the first term in a Taylor series. The major problem in the Hartree-Fock

method is that it completely neglects correlations between electrons with same spin (beyond exchange). In quantum chemistry (Löwdin, 1959), it is common to define the energy associated with the missing electron correlation energy as:

$$E_{\text{corr}} = E_{\text{exact}} - E_{\text{HF}} \quad (2.3)$$

where  $E_{\text{exact}}$  is the exact energy of the system and  $E_{\text{corr}}$  is thus the missing energy associated with correlations in the exact many body ground state wave function.  $E_{\text{corr}}$  is negative because  $E_{\text{HF}}$  is always the upper bound of the  $E_{\text{exact}}$ . The missing correlation energy is typically a very small fraction of the total energy. However, it can be a very important contribution to many systems of physical and chemical interest. For example, the restricted Hartree-Fock method cannot describe the dissociation of  $\text{H}_2$  into two open-shell H atoms. Or, at least one quarter of the strength of hydrogen bonds between water molecules comes from correlations beyond HF (Santra *et al.*, 2007). Post-Hartree-Fock methods in quantum chemistry aim to improve on Hartree-Fock by taking account of electron correlation. These methods include configuration interaction (CI), Moller-Plesset perturbation theory, and coupled cluster (Moller and Plesset, 1934). For CI methods, a linear combination of Slater determinants rather than one single Slater determinant in Hartree-Fock is used to approximate the wave function.

The perturbation terms added involve the electron repulsion. One of the more common forms was developed by Møller and Plesset (1934). The second order perturbation form is referred to as MP2 (Szabo and Ostlund, 1982). It should be noted that the electron-electron repulsion energy is not necessarily a small perturbation. In cases where this term is large the application of perturbation theory can become more difficult (Jensen, 1999; Lewars, 2003).

There are a number of other techniques that include electron correlation which can potentially provide very accurate results. Such calculations can, however, become very time consuming and at present they tend to be used for small molecules with maybe 3-4 heavy (non-hydrogen) atoms. The molecules studied in the present work are somewhat larger and the decision has been made not to use such time consuming methods.

## 2.4 Semi-Empirical Calculations

Semi-empirical (SE) calculations, like *ab initio*, are based on the Schrödinger equation (Lewars, 2003). However, more approximations are made in solving it, and the very complicated integrals that must be calculated in the *ab initio* method are not actually evaluated in SE calculations: instead, the program draws on a kind of library of integrals that was compiled by finding the best fit of some calculated entity like geometry or energy (heat of formation) to the experimental values. This plugging of experimental values into a mathematical procedure to get the best calculated values is called parameterization (or parametrization). It is the mixing of theory and experiment that makes the method “semi-empirical”: it is based on the Schrödinger equation, but parameterized with experimental values (empirical means experimental). SE calculations have been found to give good solutions for molecules for which the program has not been parameterized (Stewart, 1990; Zerner, 1991; Hehre, 1995; Thiel, 1998; Hall, 2000; Lewars, 2003).

The advantage of semi-empirical calculations is that they are much faster than *ab initio* calculations. The disadvantage of semi-empirical calculations is that the results can be erratic and fewer properties can be predicted reliably. If the molecule being computed is similar to molecules in the database used to parameterize the method, then the results may be very good. If the molecule being computed is significantly different from anything in the

parameterization set, the answers may be very poor. However, semi-empirical methods are not as sensitive to the parameterization set as are molecular mechanics calculations. The following are some of the most commonly used semi empirical methods, especially as obtained in Spartan program package used in this work.

#### **2.4.1 Modified Neglect of Diatomic Overlap**

The modified neglect of diatomic overlap (MNDO)(Young, 2001) method has been found to give reasonable qualitative results for many organic systems. It has been incorporated into several popular semi empirical programs as well as the MNDO program. Today, it is still used, but the more accurate AM1 and PM3 methods have surpassed it in popularity.

There are some known cases where MNDO gives qualitatively or quantitatively incorrect results. Computed electronic excitation energies are underestimated. Activation barriers tend to be too high. The correct conformer is not always computed to be lowest in energy. Barriers to bond rotation are often computed to be too small. Hypervalent compounds and sterically crowded molecules are computed to be too unstable. Four-member rings are predicted to be too stable. Oxygenated functional groups on aromatic rings are predicted to be out-of-plane. The peroxide bond is too short by about 0.17Å. The ether C-O-C bond angle is too large by about 90°. Bond lengths between electronegative elements are too short. Hydrogen bonds are too weak and long (Murrell and Harget, 1972; Sadlej, 1985; Young, 2001).

#### **2.4.2 Austin Model 1**

The Austin Model 1 (AM1)(Young, 2001) method is still popular for modelling organic compounds. AM1 generally predicts the heats of formation ( $\Delta H_f$ ) more accurately than MNDO, although a few exceptions involving Br atoms have been documented (Young, 2001;

2002). Depending on the nature of the system and information desired, either AM1 or PM3 will often give the most accurate results obtainable for organic molecules with semi-empirical methods. There are some known strengths and limitations in the results obtained from these methods. Activation energies are improved over MNDO. AM1 tends to predict results for aluminium better than PM3. It tends to poorly predict nitrogen parameterization. AM1 tends to give O-Si-O bonds that are not bent enough (Murrell and Harget, 1972; Sadlej, 1985; Young, 2001).

There are some known limitations to AM1 energies, such as predicting rotational barriers to be one-third the actual barrier and predicting five-member rings to be too stable. The predicted heat of formation tends to be inaccurate for molecules with a large amount of charge localization. Geometries involving phosphorus are predicted poorly. There are systematic errors in alkyl group energies predicting them to be too stable. Nitro groups are too positive in energy. The peroxide bond is too short by about 0.17 Å. Hydrogen bonds are predicted to have the correct strength, but often the wrong orientation. On the average, AM1 predicts energies and geometries better than MNDO, but not as well as PM3. Computed bond enthalpies are consistently low.

### **2.4.3 Parameterization Method 3**

Parameterization method 3 (PM3)(Young, 2001) uses nearly the same equations as the AM1 method along with an improved set of parameters. The PM3 method is also currently extremely popular for organic systems. It is more accurate than AM1 for hydrogen bond angles, but AM1 is more accurate for hydrogen bond energies. The PM3 and AM1 methods are also more popular than other semi-empirical methods due to the availability of algorithms for including solvation effects in these calculations.

There are also some known strengths and limitations of PM3. Overall heats of formation are more accurate than with MNDO or AM1. Hypervalent molecules are also predicted more accurately. PM3 tends to predict that the barrier to rotation around the C-N bond in peptides is too low. Bonds between Si and the halide atoms are too short. PM3 also tends to predict incorrect electronic states for germanium compounds. It tends to predict  $sp^3$  nitrogen as always being pyramidal. Some spurious minima are predicted. Proton affinities are not accurate. Some polycyclic rings are not flat. The predicted charge on nitrogen is incorrect. Nonbonded distances are too short. Hydrogen bonds are too short by about  $0.1\text{\AA}$ , but the orientation is usually correct. On average, PM3 predicts energies and bond lengths more accurately than AM1 or MNDO (Murrell and Harget, 1972; Sadlej, 1985; Young, 2001).

#### **2.4.4 Partial Retention of Diatomic Differential Overlap**

The PRDDO (partial retention of diatomic differential overlap) method is an attempt to get the optimal ratio of accuracy to CPU time. It has been parameterized for the periodic elements through Br, including the 3rd row transition metals. It was parameterized to reproduce *ab initio* results. PRDDO has been used primarily for inorganic compounds, organometallics, solid-state calculations, and polymer modeling. This method has seen less use than other methods of similar accuracy mostly due to the fact that it has not been incorporated into the most widely used semi-empirical software.

There are several variations of this method. The PRDDO/M (Young, 2001) method is parameterized to reproduce electrostatic potentials. The PRDDO/M/FCP (Young, 2001) method uses frozen core potentials. PRDDO/M/NQ (Young, 2001) uses an

approximation called “not quite orthogonal orbitals” in order to give efficient calculations on very large molecules. The results of these methods are fairly good overall, although bond lengths involving alkali metals tend to be somewhat in error (Murrell and Harget, 1972; Sadlej, 1985; Young, 2001).

#### **2.4.5 Parameterization Method 3 with Extension for Transition Metals**

PM3/TM (Young, 2001) is an extension of the PM3 method to include orbitals for use with transition metals. Unlike the case with many other semi-empirical methods, PM3/TM's (Young, 2001) parameterization is based solely on reproducing geometries from X-ray diffraction results. Results with PM3/TM can be either reasonable or not depending on the coordination of the metal center. Certain transition metals tend to prefer a specific hybridization for which it works well (Murrell and Harget, 1972; Sadlej, 1985; Young, 2001).

### **2.5 Density Functional (Theory) Calculations**

Density functional calculations (often called density functional theory (DFT) calculations) are, like *ab initio* and SE calculations, based on the Schrödinger equation (Jensen, 1999). However, unlike the other two methods, DFT does not calculate a wave function, but rather derives the electron distribution (electron density function) directly. That is, density functional theory (DFT) is based on determining the electron density rather than the wave function (Jursic, 1996; Truong *et al.*, 1996; Hehre and Lou, 1997). The electron density unlike the wave function is a physically observable quantity. It has been proven (Truong *et al.*, 1996; Hehre and Lou, 1997) that, given the electron density, the Hamiltonian operator is also determined. A variational principle has also been established for DFT (Truong *et al.*, 1996; Hehre and Lou, 1997). Unlike HF theory, DFT in itself contains no approximations. There is, however, no way to derive an energy contribution in DFT known as the exchange-

correlation energy. The quality of the models is usually determined by some form of comparison with experimental data. DFT models are, in a sense, semi-empirical models and once assumptions about the exchange-correlation energy are introduced (as they must be), there is no variational principle. This means that for DFT, unlike HF and post-HF methods, there is no a priori way to establish how good a given method is and no systematic way to improve upon it (Jensen, 1999; Koch and Holthausen, 2000; Young, 2001).

It has, however, become clear that DFT methods often produce results of comparable quality to the much more expensive post-HF methods. It has also become fairly well established for what type of molecules and properties DFT methods are reliable (Jensen, 1999; Koch and Holthausen, 2000; Young, 2001). One of the most common DFT methods is the so-called B3LYP method, which is a form of hybrid between DFT and HF methods. It is considered to be fairly robust, perhaps because it balances some of the weaknesses of DFT and HF methods. B3LYP is the DFT method that was used in the present work. DFT is also relatively new (serious DFT computational chemistry goes back to the 1980's, while computational chemistry with the *ab initio* and SE approaches was been carried out since the 1960s) (Lewars, 2003; Gao, 1996; Hehre *et al.*, 1986).

### **2.5.1 Basis Sets**

HF and Perturbation Theory (Lewars, 2003) have taken us from the Schrödinger equation to a solvable set of equations (DFT offering an alternative route). In order to carry out calculations, a representation of the wave function is also needed. Each molecular orbital is constructed from linear combinations of basis functions.

For computational reasons, Gaussian type orbitals ( $e^{-\alpha r^2}$ ) are commonly used, as basis functions (Lewars, 2003). Gaussian type orbitals do not, however, have the correct shape required to reproduce the form of an electron distribution. Orbitals are therefore usually constructed as combinations of a set of Gaussians in order to reproduce the correct shape (Lewars, 2003; Cramer, 2002).

Basis-sets must be sufficiently flexible to allow the description of electron distribution in various forms of molecules and the quality of the results obtained do, in general, improve with increasing size and flexibility of the functions employed. On the other hand, calculations will also become more time consuming with increasing basis set size. One of the common approaches is to add more basis sets for the valence electrons compared to inner orbitals (Young, 2001).

In the present work, the common B3LYP and 6-311+G\*\* basis sets were utilized. 3-21G indicates a single basis set consisting of 3 Gaussian functions for inner electrons and two separate basis functions, one consisting of 2 Gaussians functions and the other 1 Gaussian function for valence electrons. In 6-31G, the number of Gaussian functions to represent the basis sets is increased and in 6-311G the number of separate basis functions for valence electrons is also increased.

It is common to add further sets of basis functions. One approach is to add higher level orbitals to electrons at a given level ((Jensen, 1999). One may, for example, add d-orbitals to electrons in a p-orbital and p-orbitals to electrons occupying s-orbitals. Such orbitals are called polarizable orbitals and the inclusions of such d-orbitals are usually indicated with a (d) and p-orbitals with (p). It is also common (Jensen, 1999; Young, 2001) to indicate the use

of polarizable orbitals with a (x, y) notation, where x is the number of polarizable orbitals on heavy (non-hydrogen) atoms and y indicates the polarizable functions on the hydrogen atoms. Another notation that is sometimes used is to indicate (d) polarization with a “\*” and (d, p) polarization with “\*\*”.

Finally, there is, in some cases, a special need to allow electrons to localize far from the atom center. Standard basis-sets are in such cases augmented with the so called diffuse basis sets. This notation is utilized in the present work, as this is the default notation type in wave function Spartan package. In the present work, such diffuse basis-sets on heavy (non-hydrogen) atoms are indicated with a “+”. If they are also included on hydrogen atoms, it is indicated with “++”. One of the circumstances in which such diffuse basis sets are required is in the accurate modeling of hydrogen bonds (Levine, 2000; Jensen, 1999; Young, 2001).

Some basis-sets are regarded as being better than others in providing quality results for a given amount of computation time. Some basis sets have therefore become standard for calculations. In the present work, all calculations were done with such widely used basis-sets. The discussions that follow try to give details as to how the notation of the Gaussian set evolved.

A commonly used highly accurate basis set of atomic orbitals involves the Slater-type orbitals (STOs) having the following form (Jensen, 1999):

$$\Phi_{l_x, l_y, l_z}^{STO}(\zeta, x, y, z) = N x^{l_x} y^{l_y} z^{l_z} e^{-\zeta r}$$

where  $N$  is normalization constant and the sum of  $l_x$ ,  $l_y$  and  $l_z$  (referred to as angular momentum,  $L = l_x + l_y + l_z$ ) determines the type of orbital ( $L = 0, 1, 2, 3, 4, 5, 6$  designated as s,

*p, d, f, g, h, i*). The orbital exponent,  $\zeta$  (zeta), controls the width of the orbital (large  $\zeta$  gives tight function, small  $\zeta$  gives diffuse function). It is based on hydrogen-like wave functions. Since computer evaluation of some integrals over STO basis set is very time consuming and not well suited to numerical manipulation, in order to speed up molecular integral evaluation, the Gaussian-type orbitals (GTOs), in turn, can be used:

$$\Phi_{l_x, l_y, l_z}^{GTO}(\zeta, x, y, z) = N x^{l_x} y^{l_y} z^{l_z} e^{-\zeta r^2}$$

where  $\zeta$  is the GTO exponent. Despite the advantages of GTOs, however, there are some serious shortcomings. Unlike the STOs, the GTOs do not have a cusp at the origin and, for  $|r| \rightarrow \infty$ , they also decay towards zero more quickly. It is found that replacing a STO by a single Gaussian function leads to unacceptable errors (Levine, 2000; Jensen, 1999; Young, 2001). However, this problem can be overcome by contracted Gaussian-type orbital (CGTO) (imitating a particular STO  $\Phi_{\mu}^{STO}(\zeta, r)$ ) represented as a linear combination of primitive GTOs.

$$\Phi_{\mu}^{CGTO}(r, n, d_{p\mu}, \zeta_{p\mu}) = \sum_{p=1}^n d_{p\mu} \Phi_{p\mu}^{GTO}(\zeta_{p\mu}, r)$$

Where  $d_{p\mu}$  is the coefficient of the primitive Gaussian function  $\Phi_{\mu}^{GTO}(\zeta_{p\mu})$  and  $n$  is the number of functions in the combination.

Although the STO basis set, relative to the GTO basis, is able to describe the motion of an electron better, especially near the nucleus, the evaluation of AO integrals and their derivatives is very intricate problem with STO basis. The recurrence relations for GTO integrals are an advantage compared to the STO for evaluating the integrals and integral

derivatives. By applying a larger number of basis functions, any deficiency of the GTO basis can finally be removed with a reasonable computational time.

According to Jensen (2007), the different types of basis sets can be extensively classified into:

*Minimal basis sets* contain the minimum number of basis functions that are needed for each inner-shell and valence-shell AO of each atom like GTO, or STO-nG  $\approx$  CGTO.

A *double-zeta (DZ) basis set* is constructed by replacing each STO of a  $\zeta$  minimal basis set by two STOs having different orbital  $\zeta$  exponents.

A *triple-zeta (TZ) basis set* can be composed similarly by splitting each function of the minimal basis into three STOs that differ in their orbital  $\zeta$  exponents.

A *split-valence (SV) basis set* is a practical simplification of previous basis sets. It uses two (or more) STOs for each valence AO but only one STO for each inner-shell (core) AO. An SV basis set is minimal for inner-shell AOs and double zeta (or triple zeta or ...) for the valence AOs. Split-valence sets are called valence double zeta (VDZ), valence triple-zeta (VTZ), etc., according to the number of STOs used for each valence AO, e.g., 3-21G or 6-21G. Here the digit before the dash (3 or 6) denotes the number of primitive GTOs in one CGTO for each core AO, the digits after dash – such numbers for inner part (2) and outer part (1) of valence AOs.

*Polarization functions:* since AOs are distorted in shape and have their centres of charge shifted upon molecule formation, the improvement of basis set for this polarization can be done by adding STOs whose  $l$  quantum numbers are greater than the maximum  $l$  of the

valence shell of the ground-state atom. In Pople-type sets, polarization functions are denoted with an asterisk,\*. A common example is a 6-31G (d) or 6-31G\* and 6-311G (d, p).

*Diffuse functions* are those basis sets with additional diffuse functions which are large by size versions of *s*- and *p*- type split valence basis sets. Diffuse orbitals spread over a larger region of space. Basis sets with diffuse functions are important for systems where electrons may be far from the nucleus. In Pople type sets, diffuse function can be denoted by a plus sign, +, while in Dunning-typesets by "aug" (from "augmented")

*Dunning's correlation consistent basis sets* are developed for post HF calculations. They include shells of polarization (correlating) functions (d, f, g, etc.) that can improve convergence of the electronic energy to the complete basis set limit. Some examples are cc-pVDZ, cc-pVTZ, cc-pVQZ, and cc-pV5Z (collectively denoted as cc-pVXZ), designed for use in calculation methods (such as configuration interaction) that include electron correlation. Here, for example, cc-pVDZ stands for correlation consistent (cc), polarized valence (pV) double zeta. Another example, aug-cc-pVDZ stands for augmented versions of cc-pVDZ in which the diffuse functions are added.

### **2.5.1.1 Basis Set Superposition Error**

When atoms interact, the basis sets allocated to each of them will overlap. This overlapping gives electrons greater freedom to localize and can result in a reduction of the energy. This reduction in energy would, however, not have occurred if the basis sets had been infinitely large. This energy reduction is therefore an artifact of working with limited basis sets. This is called the basis set superposition error (BSSE) (Valdes *et al.*, 2008; Jensen, 1999; Young, 2001).

For atoms on different molecules there are schemes to correct for the BSSE. Most common BSSE is the so-called Counterpoise correction. For interactions within the same molecule, application of such corrections is, however, more difficult (Li *et al.*, 1998; Li *et al.*, 1999; Caspar, 1995). This is of importance in the present work because some of the biomolecules display intramolecular hydrogen bonding. The BSSE is expected to become smaller with increasing basis set and in calculating intramolecular hydrogen bonds it would therefore, seem that larger basis sets are more reliable. In the present work, the general approach, therefore, adopted was to use large basis-sets in order to obtain more accurate results.

### **2.5.1.2 Temperature**

Standard quantum mechanical calculations are usually carried out on a single or small number of molecules at 0K, and without accounting for the zero-point energy (Young, 2001). The intramolecular effects of temperature are usually calculated by using the harmonic oscillator approximation. This relies on calculating the second derivative of the energy with respect to the displacement ( $r$ ). It is worthy of notice that because quantum mechanical calculations are usually carried out on very small number of molecules in vacuum, pressure effects are not accounted for (Jensen, 1999; Young, 2001).

### **2.5.1.3 Performance**

The quantum mechanics based methods are often referred to as *ab initio* methods, as none of the methods rely on parameterization to experimental data. This is an important point because it distinguishes quantum mechanical calculations from many other forms of modeling carried out in science (Jensen, 1999; Young, 2001). The development of such calculations has, however, not taken place without experimental input (this being particularly true for DFT methods). Comparison with experimental data is used to validate the calculations. Sometimes

comparisons with experiment have shown the methods to be less reliable than expected, while others have proven more reliable(Jensen, 1999; Young, 2001). This partly happens because there can occur various forms of fortuitous cancellation of errors.

It has already been noted(Jensen, 1999; Young, 2001) that quantum mechanical calculations can be time consuming. Some of the calculations in the present work took 5-7 days of CPU time. Quantum mechanical calculations can today be carried out for systems of more than 100 atoms. The calculation time can increase quite steeply when increasing the size of the basis set or using more advanced methods. In the present work, quantum mechanical calculations were used to calculate geometries and energies of the molecules.

For geometry optimization, most quantum mechanical methods are fairly reliable. High level calculations are of quality comparable to experimental data. HF calculations with smaller basis sets also tend to be reasonably accurate. Calculation of energy is in general more difficult. Results can vary quite significantly with the level of theory. Prediction of absolute energy values are difficult, but relative trends in energies can usually be calculated with reasonable accuracy (Jensen, 1999; Young, 2001).

## **2.6 Molecular Mechanics**

Quantum mechanical calculations are, as have already been mentioned, time consuming (Jensen, 1999; Young, 2001). Molecular mechanics (MM) offer a simplified form of molecular representation that makes it possible to perform significantly faster calculations. Molecular mechanics measures the energy separations between different vibrational levels, which are quantized. The typical photon energy for the excitation falls in the infra-red region of the optical spectrum (Crammer, 2002). A molecular mechanics representation can best be

summarized as soft spheres attached by springs to represent bonds. The potential energy between non-bonded atoms is usually expressed as the sum of Lennard-Jones and Coulomb potential functions as given in equation (2.4) (Jorgensen *et al.*, 1984; Jensen, 1999; Young, 2001):

$$U = \sum_{i < j} 4\epsilon_{ij} \left[ \left( \frac{\sigma_{ij}}{r_{ij}} \right)^{12} - \left( \frac{\sigma_{ij}}{r_{ij}} \right)^6 \right] + \sum_{i < j} \frac{q_i q_j}{r_{ij}} \quad \dots\dots\dots (2.4)$$

where the sums are over all pairs of interaction sites and  $\epsilon$  and  $\sigma$  are the Lennard - Jones potential parameters,  $q_i$  and  $q_j$  are the partial electric charge of interaction sites  $i$  and  $j$  respectively, and  $r_{ij}$  is the separation between interaction sites. Interaction sites are usually, but not always, atomic centers. This form of representation only accounts for two-body interactions. In a real system, many-body effects, such as three-body and four-body interactions, can also play a part. There is, therefore, an approximation involved in the form of such potential functions. To correct for this, parameters can be set to implicitly account for the many-body effects.

For bond-lengths, simple harmonic stretching functions are often used where the energy increases as the bond-length deviates from some equilibrium bond-length. For bond angles, harmonic functions of the following form are often utilized as in equation (2.5):

$$U_{\theta} = k_{\theta} (\theta - \theta_0)^2 \quad \dots\dots\dots (2.5)$$

where  $\theta$  is the bond angle and the subscript 0 denotes the equilibrium value of the bond angle.  $k_{\theta}$  is the spring constant. Dihedral angle energies around bonds are given by some form of a Fourier series. One of the common forms is the following equation (2.6):

$$U(\phi) = \sum_{i=1}^5 C_i \cos \phi^i \quad \dots\dots\dots (2.6)$$

where  $\phi$  is the dihedral angle and the  $C_i$  is a constant.

### 2.6.1 Force Field Parameterization

One of the key motivations in early force field design was the development of the energy functional that would allow facile optimization of molecular geometries (Jensen, 1999; Young, 2001). While the energy of an arbitrary structure can be interesting, real molecules vibrate thermally about their equilibrium structures, so finding the minimum energy structures is key to describing equilibrium constants. Therefore, one priority in force field development is to adopt reasonably simple functional form so as to facilitate geometry optimization (Cramer, 2002; Jensen, 1999).

The quality of the results produced by MM calculations obviously depends on the parameters chosen for the various interactions and some form of parameterization must be undertaken. A set of parameters for a single molecule or groups of molecules are called force fields.

A fairly large number of schemes have been proposed to develop force fields, partly reflecting the fact that different researchers are looking at different applications. One of the main applications is biological systems, in which case the focus is often on reproducing the structural characteristics of molecules of biological importance. A second application is the modeling of liquids. In the modeling of liquids, parameters are often chosen to reproduce the properties of liquids as determined from experimental work. There are, however, a number of different properties one can choose to reproduce. Among them are density, diffusion rates, dielectric constants and radial distribution functions. An example of such work is the

“Optimized Parameters for Liquid Simulations” (OPLS) force field developed by Jorgensen and coworkers (Jorgensen *et al.*, 1996 and Rizzo and Jorgensen 1999). In addition, there is the choice of attempting to reproduce the properties for a given temperature, or to attempt the more ambitious task of reproducing properties over a range of temperatures as done by Warshel and Levitt, (1976); Warshel, (1992); Winget *et al.*, (2000). For some solvents such as water, a fairly large body of experimental data is available (Hulsmann and Reith, 2013; Hulsmann *et al.*, 2011).

Quantum mechanical calculations are often used for setting force field parameters. They can for example be used for determining molecular geometries and atomic charges.

### **2.6.2 Atomic Charges**

One of the most important and difficult issues in the design of a force field is the selection of charges. In most common force fields, fixed charges are used and they are often, but not always, located at the atom centres (Jensen, 1999). These atomic charges are intended to reproduce the net effect of electrons and nuclei for a given atom. As electrons are not located at a single point operating with charges situated at the atomic centres does represent an approximation. Operating with fixed charges is also an approximation, as the location of electrons can be affected by the environment the molecule finds itself in.

Two main approaches to determining atomic charges can be identified in the literature. One approach is to fit the charges in simulations intended to reproduce various experimental properties. Such fitting is usually done for small organic molecules. For larger molecules, experimental data is often more sparse and the number of charges to fit is much larger. In such cases, one will often rely on atomic charges being transferable parameters. Having

determined charges for alcohol groups, amine groups and alkane groups in small molecules, one assumes these to be the same in larger molecules. The OPLS force field is based on this approach (Jorgensen *et al.*, 1996). The second approach is to determine the atomic charges from quantum mechanical calculations, an example of this is the work by Kollman and coworkers (Cornell *et al.*, 1995). This second approach is very appealing because it reduces the need for experimental data and gives the modeling a stronger predictive character (provided it works).

Even if a quantum mechanical calculation contains information about position of nucleus and electrons, the task of determining atomic charges is still a difficult one. Atomic charges are not uniquely defined and the task of assigning parts of the electron distribution to atoms in a molecule is ambiguous. The first of such schemes was the Mullikan population, which is based on determining how much each atomic basis set contributes to the wave function. While Mullikan populations have been widely used, they have come to be regarded as unreliable (Franckl and Chirlian, 2000). One of the newer schemes is to reproduce the electrostatic potential around the solute, and even for this approach, there are, however, a number of different implementations (Franckl and Chirlian, 2000). Singh and Kollmann (1984) developed a procedure based on reproducing the electrostatic potential on grid points distributed spherically around each solute atom center, outside the van der Waals volume of the solute. These types of charges are referred to by their common acronym “MK”. It has become clear that the calculated charges are sensitive to the specific procedure chosen to fit the electrostatic potential (Franckl and Chirlian, 2000). Other difficulties are that such procedures tend to work poorly for atoms buried inside a molecule and that charges can display a high degree of conformer dependency (Bayly *et al.*, 1993).

There are also schemes that attempt to use the quantum mechanical representation while at the same time reproducing some experimentally measured property. One such hybrid scheme is CM2 charges (Liet *et al.*, 1998) that reproduces experimental dipole moments.

While selection of atomic charges is a difficult issue, it should also be noted that in many contexts different force fields produce quite similar results. In such cases, one does not have to worry too much about the selection of charges. In general, different schemes to calculate atomic charges do also produce charges that are in reasonable qualitative agreement (da Silva and Svendsen, 2004).

### **2.6.3 Polarizable Force Fields**

One of the most important approximations in standard simulations with molecular mechanics representation is the use of fixed charges (Jensen, 1999). Introduction of polarizability is one way to improve the representation while avoiding the expense of quantum mechanical calculations. Such models were covered in the review by Rick and Stuart (2002). There are some main approaches to adding polarization in simulations. Among them are shell models based on polarizable point dipoles, where fixed charges are attached to each other with harmonic springs. Another form of model is based on charges being allowed to fluctuate between sites in a molecule.

The charges in a molecule do depend on the surrounding environment. It is, therefore, to be expected that a model with fixed charges will have problems representing a molecule in different states such as solids, liquids and gases. Polarizable models should have the potential to represent a molecule in different states. Another difficulty with fixed charges is that they cannot reflect changes in charge distribution that may take place as a molecule changes

conformer(Jensen, 1999). This is again something that a polarizable model has the potential to handle. On the other hand, simulations with polarizable models do take longer time than simulation with fixed charges.

Rick and Stuart (2002) concluded that polarizable models in several respects do perform better than models with fixed charges. Compared to a model with fixed charges, there are, however, a greater number of parameters to be set in a polarizable model and these present some additional challenges.

While a polarizable model is in form more realistic than a model with fixed charges, it is not given that it will (Frenkel and Smit, 2002; 2006) produce more realistic results. In using a ball and-stick representation of molecules, there is a number of assumptions involved, and in it is not given that overall performance will improve by improving on one of the approximations.

## **2.7 Simulations**

There are two forms of simulations that are used in computational chemistry: Molecular Dynamics (MD) and Monte Carlo (MC). These are used for calculations on ensembles of molecules. Simulation techniques are described in detail in the textbooks “Computer Simulations of Liquids” (Allen and Tildesley, 1987) and “Understanding Molecular Simulation” (Frenkel and Smit, 2002;2006).

Molecular dynamics calculations are based on calculating the forces between molecules and atoms in a system and allowing them to move according to Newton’s laws of motion. From the calculated forces, the acceleration and velocity of the particles in the system are

calculated. The particles are moved over a small time-step, forces and velocities are recalculated and the system is moved forward a new time-step. For each time-step, the properties of the system such as energy and temperature are monitored. A simulation is carried out for whatever number of time-steps is deemed necessary to obtain reliable averages.

Monte Carlo simulations are, on the other hand, based on random alterations of the coordinates of the system. The energy change for each alteration is calculated, the probability of the alteration being accepted depending on the associated change in energy. For changes leading to lower energy, the probability is higher. The standard approach is Metropolis sampling in which the sampling has a Boltzmann-weighted probability. As in MD, the simulation is continued for whatever number of steps deemed necessary for sampling.

Often, in simulations, the purpose is to simulate the bulk behavior of liquids. Simply placing a number of molecules in a vacuum would produce a cluster that might have properties different from bulk liquid. It is, therefore, customary both in MD and MC to do calculations with periodic boundary conditions. The cell containing the ensemble is then surrounded by replicas of itself.

Simulations are usually carried out with a molecular mechanics level representation. Simulations with such a molecular representation can be carried out on ensembles of thousands of molecules. This is significantly more than in QM calculations, but is still an extremely small number compared to the number of molecules present in even the smallest droplet of water. In the present work, most simulations are done on ensembles of less than 256 molecules. Such an ensemble is usually regarded as large enough for reliable

calculations, at the same time as such calculations can be carried out in reasonable amounts of time.

The Lennard-Jones and Coulomb interactions are usually truncated at some value. This is mainly done to save time in the calculations. The Lennard-Jones potential decays steeply as a function of distance and its truncation is unproblematic. Coulomb interactions have a slower decay, but for neutral species, the truncation can still be a reasonable simplification. For ionic species, truncation is, however, usually not an acceptable option. Although there are schemes to handle long-range forces, simulations of ionic systems are challenging. The standard way of handling long-range electrostatics is the use of Ewald sums (Harris, 1998; Yeh and Berkowitz, 1999).

Simulations are often carried out in microcanonical (NVE), canonical (NVT) and constant number of particles-constant pressure-constant temperature (NPT) ensembles. The grand-canonical ensemble with constant free energy, volume and temperature ( $\mu$ VT) is also used in some types of simulation.

When carrying out simulations, the statistical sampling is always a concern. The question of whether the system has sampled sufficiently the full set of configurations it can take on (the phase space) must be addressed. Verifying this is difficult and is not only an issue of doing a long enough simulation (Jensen, 1999).. If one can imagine the potential energy of phase space as a kind of landscape, one can think of the simulation as risking becoming trapped in a valley. As simulations are based on statistical averaging of properties, there is always some degree of statistical uncertainty in the results obtained.

While MD and MC can be used to calculate many of the same properties, they differ in some important respects(Jensen, 1999). In MC simulations, time is not a parameter and there is no easy way to obtain time-dependent properties such as diffusion-rates. MD has been developed further in handling of long-range electrostatic interactions. MC calculations can sometimes provide more efficient sampling of phase space.

### 2.7.1 Free Energy Perturbations

The free energy of solvation is the energy associated with a molecule going from the gas phase to solution and is a central concept in understanding chemistry in solution. Determination of free energies is also one of the main issues in this thesis. Kollman (1993) provided a review of the main simulation techniques for determining free energies. The main techniques are free energy perturbations (FEP), thermodynamic integration and slow growth. FEP sees the widest use and is also the technique adopted in this work. The fundamental equation that free energy perturbations are based on is the following equation (2.7) (Kollman, 1993; Dick *et al.*, 2009):

$$G_B - G_A = \Delta G = -RT \ln \left\langle e^{-\Delta H/RT} \right\rangle_A \dots\dots\dots (2.7)$$

where  $\Delta H = H_B - H_A$  are the energies of two systems, A and B, where the difference between A and B is the nonbonded terms of the solute particle, and  $\langle \rangle_A$  refers to an ensemble average over a system represented with the Hamiltonian  $H_A$ .  $R$  is the gas constant and  $T$  is the temperature of the system. If the systems differ in a significant way, the equation will, however, not lead to a meaningful result. This problem can be overcome by performing multiple simulations over intermediate steps between A and B. A coupling parameter ( $\lambda$ ) is introduced that allows the smooth conversion of system A to B. The mutation of any

geometry or potential parameter of the system can then be represented in the form of equation (2.8) (Jorgensen and Ravimohan, 1985):

$$\xi(\lambda) = \xi_0 + \lambda(\xi_1 - \xi_0) \dots\dots\dots (2.8)$$

The total free-energy change is obtained by adding together the contributions from each single perturbation. Sometimes, calculations are performed with the double-wide sampling scheme (Jorgensen and Ravimohan, 1985). In this scheme, the free energy difference for  $\lambda_i \rightarrow \lambda_{i+1}$  and  $\lambda \rightarrow \lambda_{i-1}$  are evaluated in a single ensemble.

The mutation will usually be between two different solute molecules. The essence of the FEP is to mutate one molecule into another and compute the energy associated with the transformation. FEPs are, in general, more accurate for calculating differences between molecules with similar properties. More accurate results are, for example, obtained when perturbing between molecules of the same charge, as opposed to between species with different charges. Calculating the absolute free energy of solvation is more difficult than simply calculating relative free energies.

While the general concept of FEP calculations is easily understood, the technical issues involved are far from trivial. Kofke and Cummings (1997, 1998) have concluded that perturbations that involve growth are superior to those involving shrinking or deletion of molecules. They conclude that shrinking offers loss of accuracy due to biases in the sampling. More recently, Kofke (2005) has, however, concluded that the error involved in insertion and deletion approaches may vary from system to system. The development of optimal FEP methods does, therefore, appear to be still in progress.

## **2.8 Molecular Dynamics Calculations**

Molecular dynamics calculations apply the laws of motion to molecules. Thus, one can simulate the motion of an enzyme as it changes shape on binding to a substrate, or the motion of a swarm of water molecules around a molecule of solute (Jensen, 1999; Guevara-Carrion *et al.*, 2012).

## **2.9 Computational Chemistry and Experiment**

Computational chemistry will never be a full replacement for doing experiments, which remains the final arbiter of truth about nature, but can often supplement experimental work. Furthermore, to make something, such as, new drugs, new materials, one has to go into the laboratory. Very often, neither experiment nor computational chemistry can, by itself, give us the full insight we could desire. In many cases, one must therefore piece together whatever information can be drawn from either source, to draw whatever conclusions that can be drawn. Sometimes, computational chemistry can be used to calculate properties that are not at all available from experimental work, while some issues can be difficult both in the laboratory and on the computer. Computational chemistry has grown as a field rather quickly, and many researchers are perhaps not fully aware of the potential of its methods. But, computation has become so reliable in some respects that, more and more, scientists in general are employing it before embarking on an experimental project; and the day may come when to obtain a grant for some kinds of experimental work, one will have to show to what extent one has computationally explored the feasibility of the proposal.

The approach in this work has, therefore, been somewhat pragmatic. The most effort has been put into areas where computational chemistry was thought to give the most valuable new insight.

## CHAPTER THREE

### 3.0 MATERIALS AND METHODS

#### 3.1 Materials

The following are the materials used in carrying out this computational research work:

##### A. System Softwares

- i. Microsoft windows XP professional version 2002 SP3 computer system, with Intel(R) Pentium(R) Dual CPU, E2200@2.20 GHz 219 GHz, 3.24GB of RAM.
- ii. Microsoft windows 7 ultimate version 2008 SP1 computer system, with Intel (R) Pentium(R) Dual CPU, E2200@2.20 GHz 219 GHz, 4.00 GB of RAM.
- iii. Microsoft windows 8 professional version 2012 SP1 computer system, AMD E-450 APU with Radeon(tm) HD Graphics 1.65 GHz, 4.00 GB of RAM.

##### B. Application Softwares

- i. ChemBioOffice 2008 software.
- ii. Spartan '08 V1.1.0 program package.
- iii. Spartan '14 V1.1.0 program package.
- iv. DreamCalc DCP 4.9.0 professional calculator program package .
- v. Design Science MathType 6.9 program.
- vi. GraphPad Prism 5.0

##### C. Reactants Used

- i. Iodine molecule (formula =  $I_2$ ; mol. wt.= 253.809 amu).
- ii. Hydrazine molecule (formula =  $H_4N_2$ ; mol. wt.= 32.045 amu).

- iii. Hydrazinium ion (formula =  $\text{H}_5\text{N}_2^+$ ; mol. wt.= 33.053 amu).
- iv. 1,2-diphenylhydrazine molecule (formula =  $\text{C}_{12}\text{H}_{12}\text{N}_4$ ; mol. wt.= 184.237amu).
- v. L-tyrosine molecule (formula =  $\text{C}_9\text{H}_{11}\text{NO}_3$ ; mol. wt.=176.032 amu).
- vi. L-ascorbic acid molecule (formula =  $\text{C}_6\text{H}_8\text{O}_6$ ; mol. wt.= 181.189 amu).
- vii. D-fructose molecule (formula =  $\text{C}_6\text{H}_{12}\text{O}_6$ ; mol. wt.= 180.156 amu).

### 3.2 Methodology

The Spartan '08 v1.1.0 semi-empirical (AMI, PM3 and MNDO) and DFT methods were used on Microsoft windows XP professional version 2002 SP3 computer system, with Intel(R) Pentium(R) Dual CPU,E2200@2.20 GHz 219 GHz, 3.24GB of RAM for the computational studyof the hydrazine – iodine and hydrazinium ion – iodine reaction systems.

The Spartan' 14v1.1.0 semi empirical (PM3 and MNDO) and density functional theory (DFT) methods were used on Microsoft windows7 ultimate version 2008 SP1 computer system, computer system, with Intel(R) Pentium(R) Dual CPU,E2200@2.20 GHz 219 GHz, 3.24GB of RAM for the computational study of the L-tyrosine – iodine and 1,2-diphenylhydrazine – iodine reaction systems.

The Spartan' 14v1.1.0 semi empirical (PM3 and MNDO) and density functional theory (DFT) methods were used on Microsoft windows 8 professional version 2012 SP1 computer system, AMD E-450 APU with Radeon(tm) HD Graphics 1.65 GHz, 4.00 GB of RAM for the computational study of the L-ascorbic acid – iodine and D-fructose – iodine reaction systems.

The starting geometries for all of the semi empirical and DFT calculations were first optimized using AMI, followed by PM3 and MNDO, then finally by the DFT method in the

Spartan Global calculations environment work space of the various Spartan packages as listed above. The geometries and all the electronic structure calculations included in the reaction of all substrates with iodine were fully optimized using the density functional theory (DFT) method (Hehre *et al.*, 1986; Izadyara, 2004). To check the influence of basis set, PM3, MNDO of semi empirical method and 6311+G\*\* basis set of DFT at the B3LYP level of computation were employed to optimize the geometries of the reactants, intermediates, transition states and products (Stewart, 1986; 2007; Zhang and Hase, 2010). There were marked differences between the semi empirical method and the DFT method. It thus indicated that the geometrical parameters were sensitive to the sizes of the basis sets or computational levels (Bingham, *et al.*, 1975; Dewar and Thiel, 1977; Dewar, *et al.*, 1985). The starting geometries for all the DFT calculations were at first optimized in the Spartan Global calculations environment work space at the AM1, PM3 and MNDO levels, and then followed by the DFT B3LYP calculations at 6311+G\*\* basis set level. The optimized geometries of the reactants, intermediates, transition states and products were confirmed in terms of vibrational analysis (Schlegel, 1986; Kalkanis and Shields, 1991; Kahn and Bruice, 2000). The transition state for each step was located and confirmed by animating the vibration corresponding to the reaction coordinate by selecting the imaginary frequency at the top of the list of frequencies on the IR tab. No arbitrary assumptions were imposed on finding the most likely geometries for the transition state in each case.

### **3.3 Details of the Computation Procedures**

The computational method used for calculating geometries in this work is termed a “cascade method” because of its use of molecular mechanics to remove strain energies followed by semi-empirical methods as precursors for more accurate DFT methods (Hehre, 1995). The method has been described elsewhere (Hehre, 1995; Hehre *et al.* 1998). The attractiveness of

the method lies in its ability to make calculations less computationally taxing by relegating initial geometry calculations to less computationally intensive (and possibly more inaccurate) methods. The initial calculations, which may be initialized in geometry far from that of equilibrium, are performed by those methods requiring less computational effort, allowing equilibrium geometries to be “honed in on” in later stages, leaving the refining to the more accurate and computationally intensive theories.

Details of how the computation tasks were carried out are given the subsequent sub-sections.

### **3.3.1 Geometry Optimization of Reactants, Activated Complexes, Intermediates and Products Using Semi-Empirical Methods**

To optimize a structure, first the Spartan software package was launched. On the Spartan user interface the file menu was selected. On the file menu “New build” was selected to launch the (organic, inorganic, peptide, nucleotide or substituent) tool kit for building molecules, depending on the molecule to be constructed. Atoms that constitute the molecule to be built were selected and clicked on, taking care to select the correct geometry of the atom involved, before pasting on the opened Spartan window. This step is repeated until the whole molecule is built. Next, the minimization option was clicked to remove any strain in the molecule.

After the previous steps, the “set up” menu on the open window was selected and on the drop down menu “calculation” was clicked followed by “Equilibrium Geometry” at “Ground state”. On the same interface, “Semi-empirical” at the desired level of computation was selected (usually, current or MMFF). “Total charge” of the molecule together with the calculated “multiplicity” of the molecule was also selected. “IR”, “Orbitals & Energies”, “Thermodynamic” “Vibrational Modes” and “Charges & bond Orders” tabs could

be selected. “Global Calculations” would be selected before submission. The file was then saved with the appropriate name.

The calculation was then started by clicking “Ok” on the calculation windows. After the calculation has completed, the “Display” menu was selected to see the output. On the output menu, properties, orbital energies, surfaces, spectra, Formula, spreadsheet, plots, similarities or reactions could be selected, depending on the feature wanted.

### **3.3.1.1 Geometry Optimization of Reactants, Activated Complexes, Intermediates and Products Using DFT Methods**

Since the cascade method is used (Hehre, 1995; Hehre *et al.* 1998), the optimized and saved reactants, activated complexes, intermediates and products using semi-empirical methods described in section 3.3.1 were copied and pasted on new windows. Each semi-empirical optimized molecule or specie was open anew. On the “Set Up” menu “Calculation” was clicked followed by selecting “Equilibrium Geometry” at “Ground” state with “Density Functional, BLYP, 6-311++G\*\*” level of computation in “Vacuum” selected. Next, “Current” geometry was selected. “Total charge” of the molecule together with the calculated “multiplicity” of the molecule was also selected. “IR”, “Orbitals & Energies”, “Thermodynamic” “Vibrational Modes” and “Charges & bond Orders” tabs could be selected. “Global Calculations” would be selected before submission. The file was then saved with the appropriate name.

The calculation was then started by clicking “Ok” on the calculation windows. After the calculation has completed, the “Display” menu was selected to see the output. On the output menu, properties, orbital energies, surfaces, spectra, Formula, spreadsheet, plots, similarities or reactions could be selected, depending on the feature wanted.

### **3.3.2 Calculation of HOMO and LUMO of Optimized Molecules**

The display environment for both semi-empirical and DFT calculations are the same, therefore, the calculation processes of HOMO and LUMO are the same. After the optimization process, the HOMO and LUMO could be calculated by selecting “Surfaces” on the display menu. On the surface menu, one can click on “Add” to select HOMO, LUMO, which would then display the HOMO or the LUMO of the molecule under consideration.

### **3.3.3 Determination of Chemical Reactivity of Optimized Molecules: Mapping of HOMO and LUMO Densities of Optimized Molecules**

Optimized structures of molecules that would collide to form the transition states or activated complex were copied and pasted on a new Spartan window. The two would be oriented such that the HOMO of one would be facing the LUMO of the other with the right orientations. Next, on the “search” menu “Transition State” was selected to activate the colliding molecules. To form new bond, the “Shift” key is held down, followed by a click on the atom bearing the HOMO, then the atom bearing the LUMO and back. To break a bond, the bond to be broken is clicked on followed by clicking on the centre that would accept the electrons. These operations would result in a curved arrow being drawn on the reactant structure, extending from an atom, or a centre of a bond, or the centre of a dotted line that has been drawn between atoms that were to be broken or bonded. After all reaction arrows have been properly designated, the button at the bottom right of the screen would be clicked to replace the reactants with a guess of the transition state structure.

Next, from the “set up” menu, “calculation” is then selected, followed by “Transition State Geometry” and then either “Semi-empirical” or “Density Functional” as the case may be, followed by the chosen basis set of interest. The file would be saved with a chosen name.

Before submission, all the parameters to be calculated (“IR”, “Orbitals & Energies”, “Thermodynamic” “Vibrational Modes” and “Charges & bond Orders” tabs) could be selected. “Global Calculations” would be selected as done in the optimization process discussed above (section 3.3.1 for semi-empirical and section 3.3.1.1 for DFT calculations).

When the job is completed, “Spectra” is selected from the display menu and the IR tab clicked to display the IR spectrum of the activated complex. Presence of only one imaginary frequency would be a confirmation that a transition was found. If not, the whole processes would be repeated until a transition state is found.

#### **3.3.4 Calculation of Thermodynamics, Molecular and other Physicochemical Properties of Reacting Species and Products**

After successful completion of optimization process or transition state search calculation, the “Display” menu is selected and on the Display” menu, “Molecule properties” is selected. On the “Molecule properties” menu, the following would be displayed: Formula, CAS, Energy, Energy (aq), Solvation E, E HOMO, E LUMO, Heat, T1 Heat, Weight, Dipole Moment, Pt. Group, Tautomers and Conformers.

When “thermodynamics” is selected on the Molecule properties dialogue box, the calculated thermo chemical properties, i.e.  $H^{\circ}$ ,  $S^{\circ}$ ,  $G^{\circ}$ , ZPE and  $C_v$  are displayed. The values of these data were then converted to the desired units for further use in the discussion of results.

#### **3.3.5 Construction of Potential Energy Surface Diagrams**

To construct the potential energy surface diagrams for a system,  $H^{\circ}$  for reactants, transition state and products for each proposed elementary step were tabulated and exported into Micro Soft Excel sheet or the GraphPad Prism 5 Excel sheet for plotting the diagrams. This is

achieved by copying the appropriate values for  $H^\circ$  and pasting them into columns for reactants (R), transition states (TS) and products (P). The values for reactants (R) and products (p) are usually, the sum of the reactant molecules and the sum of the product molecules, respectively, for each elementary step. The values in the three columns are then used to plot the potential energy surface diagrams.

### 3.3.6 Enthalpy of Reaction and Rate Constant Calculations (Ochterski, 2000; McQuaid and Rice, 2006; McQuaid *et al.* 2004; 2002)

The enthalpies of reaction were calculated by using the heats of formation at standard temperature of 298.15K and pressure of 1 atmosphere obtained from Spartan software package as described in section 3.3.4. The calculations were done by taking the appropriate sums and differences as given in equation (3.1).

$$\Delta_r H^\circ(298.15K) = \sum_{\text{products}} n_{\text{prod}} \Delta_f H^\circ_{\text{prod}}(298.15K) - \sum_{\text{reactants}} n_{\text{react}} \Delta_f H^\circ_{\text{react}}(298.15K) \dots\dots\dots (3.1)$$

Where  $n_{\text{prod}}$  and  $n_{\text{react}}$  are the stoichiometric coefficient of the products and reactants, respectively, and  $\Delta_r H^\circ(298.15K)$ ,  $\Delta_f H^\circ_{\text{prod}}(298.15K)$  and  $\Delta_f H^\circ_{\text{react}}(298.15K)$  are the standard heat reaction, standard heat formation of products and standard heat formation of reactants, respectively, at the specified standard temperature of 298.15K.

In instances where there were no convergences or completion of calculation during optimization, some of the thermodynamic parameters such as  $\Delta G^\circ$  and  $\Delta S^\circ$  would not be calculated by default by the Spartan software package. In such instances therefore, these parameters were calculated by using the Eyring equation (Engel and Reid, 2006; Mee, 1971) as given in equation (3.2).

$$\ln K = -\frac{\Delta G^{\circ}}{RT} = \frac{\Delta S^{\circ}}{R} - \frac{\Delta H^{\circ}}{RT} \dots\dots\dots (3.2)$$

Alternatively, the entropy of reaction and free energy of reaction can be evaluated from equations (3.3) and (3.4), respectively (McLauchlan, 2004; Sousa *et al.*, 2013).

$$\Delta_r S^{\circ}(298.15K) = \sum_{prod} n_{prod} S^{\circ}_{prod}(298.15K) - \sum_{react} n_{react} S^{\circ}_{react}(298.15K) \dots(3.3)$$

$$\Delta_r G^{\circ} = \Delta_r H^{\circ} - T \Delta_r S^{\circ} \dots\dots\dots (3.4)$$

Activation energies ( $E_a$ ) of the various elementary steps were calculated according to equation (3.5)(McQuaid and Rice, 2006; McQuaid *et al.*, 2004; 2002).

$$E_a(298.15K) = \sum_{trans} n_{trans} \Delta_f H^{\circ}_{trans}(298.15K) - \sum_{react} n_{react} \Delta_f H^{\circ}_{react}(298.15K) \dots\dots\dots (3.5)$$

Where  $n_{trans} = 1$  and  $n_{react}$  are the stoichiometric coefficient of the transition state and reactants, respectively, while  $\Delta_f H^{\circ}_{trans}(298.15K)$  and  $\Delta_f H^{\circ}_{react}(298.15K)$  are standard heat formation of transition state and standard heat formation of reactants, respectively, at the specified standard temperature of 298.15K.

For DFT calculations(McQuaid and Rice, 2006; McQuaid *et al.*, 2004; 2002),  $\Delta_f H^{\circ}_{trans}(298.15K)$  and  $\Delta_f H^{\circ}_{react}(298.15K)$  are usually written as  $E_e(trans)$  and  $E_e(react)$ , which are total electronic energies of formation of transition state and reactants, respectively.

In this case, equation (3.5) can be written as equation (3.6) below.

$$E_a(298.15K) = \sum_{trans} n_{trans} E_e(trans)(298.15K) - \sum_{react} n_{react} E_e(react)(298.15K) \dots\dots\dots (3.6)$$

The rate constant calculations were computed according to equation (3.5)(McLauchlan, 2004; Ochterski, 2000; McQuaid and Rice, 2006).

$$k(T) = \frac{k_B T}{h C^0} e^{-\Delta^\ddagger G^0 / RT} \dots\dots\dots (3.5)$$

Where  $k(T)$  = reaction rate constant at temperature(298.15K);  $k_B$ = Boltzmann constant (1.380662 x 10<sup>-23</sup> J/K);  $T$  = temperature(298.15K);  $h$  = Planck's constant (6.626176 x 10<sup>-34</sup> Js);  $C^0$  = concentration (taken to be 1);  $\Delta^\ddagger G^0$  = Gibbs free energy of activation (kJ/mol);  $R$  = gas constant (8.31441 J/mol. K).

### 3.4 Post Computation Processing

After the computation of all reactants, intermediates, transition states and products of every system, all structures were sketched using ChemBioOffice 2008 software. All equations used in this work were created with Design Science MathType 6.9 program while all calculations of the heat of formations, heat of reactions,thermodynamic parameters,activation parameters and rate constants were calculated using DreamCalc DCP 4.9.0 professional calculator program package.

## CHAPTER FOUR

### 4.0 RESULTS

#### 4.1 Structure Optimization of Reactants, Transition States, Intermediates and Products

The optimized structures of all the reaction systems studied are provided in sub-sections 4.1.1 - 4.1.5. Sub sections 4.1.1 - 4.1.6 provide the keys and explanations to Figures 4.1 – 4.10.

The mapped and calculated HOMO and LUMO of the oxidant (iodine) and the various reductant biomolecules (1,2-diphenylhydrazine, L-tyrosine, L-ascorbic acid, D-Fructose, hydrazinium ion and hydrazine) are shown in Figures 4.6 – 4.10. Each Figure showed the solid and transparent form of the mapped and calculated HOMO and LUMO of the reactants with the E HOMO and E LUMO value given.

##### 4.1.1 Optimized Geometries of 1,2-Diphenylhydrazine – Iodine Reaction System

The optimized geometries of the reactants, intermediates, transition states and products are shown in Figure 4.1, where  $I_2$  is iodine molecule;  $AH_2$  is 1,2-diphenylhydrazine;  $AH$  is 1,2-diphenyl-hydrazyl radical;  $A$  is trans-1,2-diphenyldiazene (Azobenzene);  $HI$  is hydrogen iodide;  $I$  iodide ion;  $TS_1$  is transition state 1;  $TS_2$  is transition state 2;  $TS_3$  is transition state 3 and  $TS^*$  is transition state for the one-step cyclic complex mechanism.

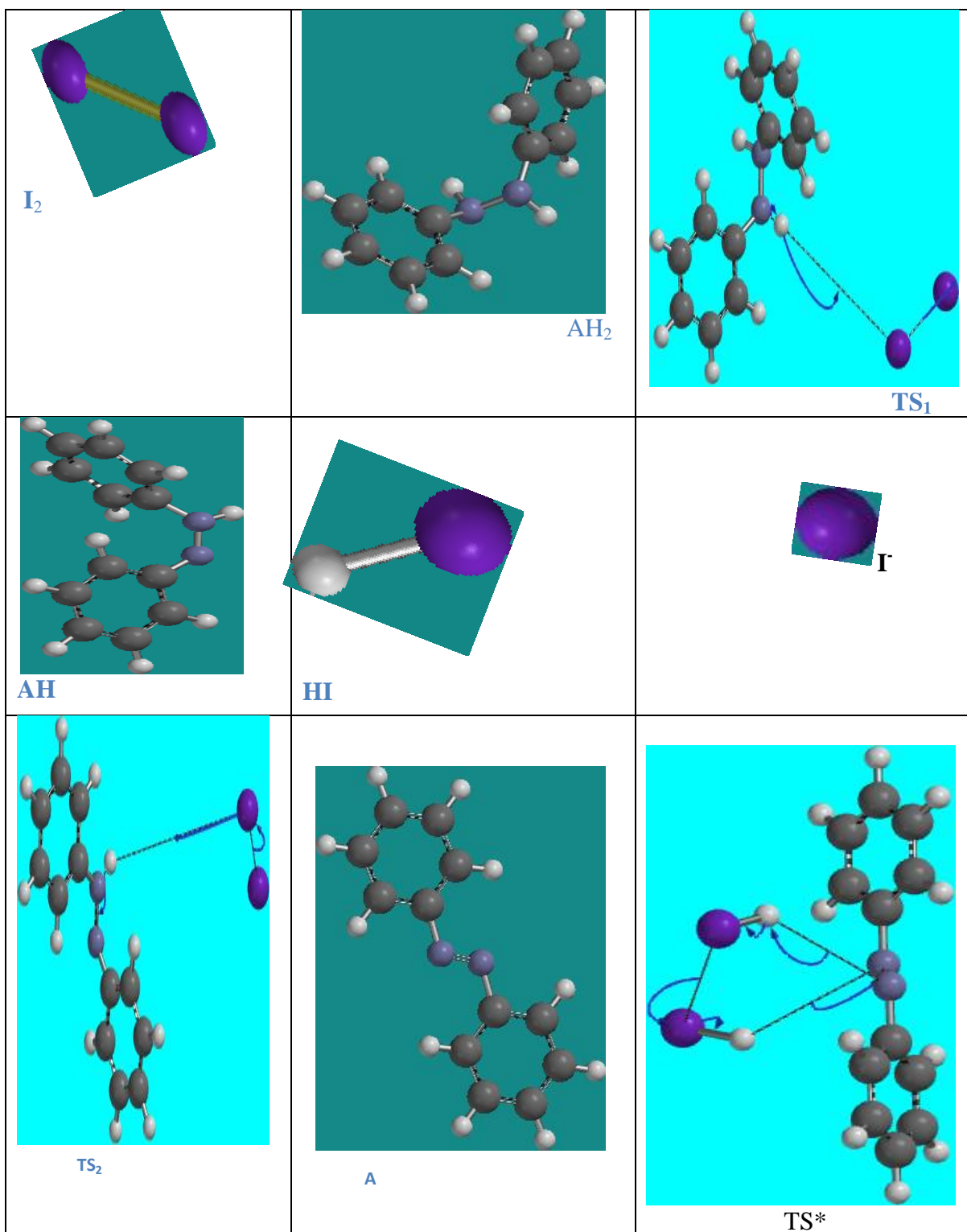
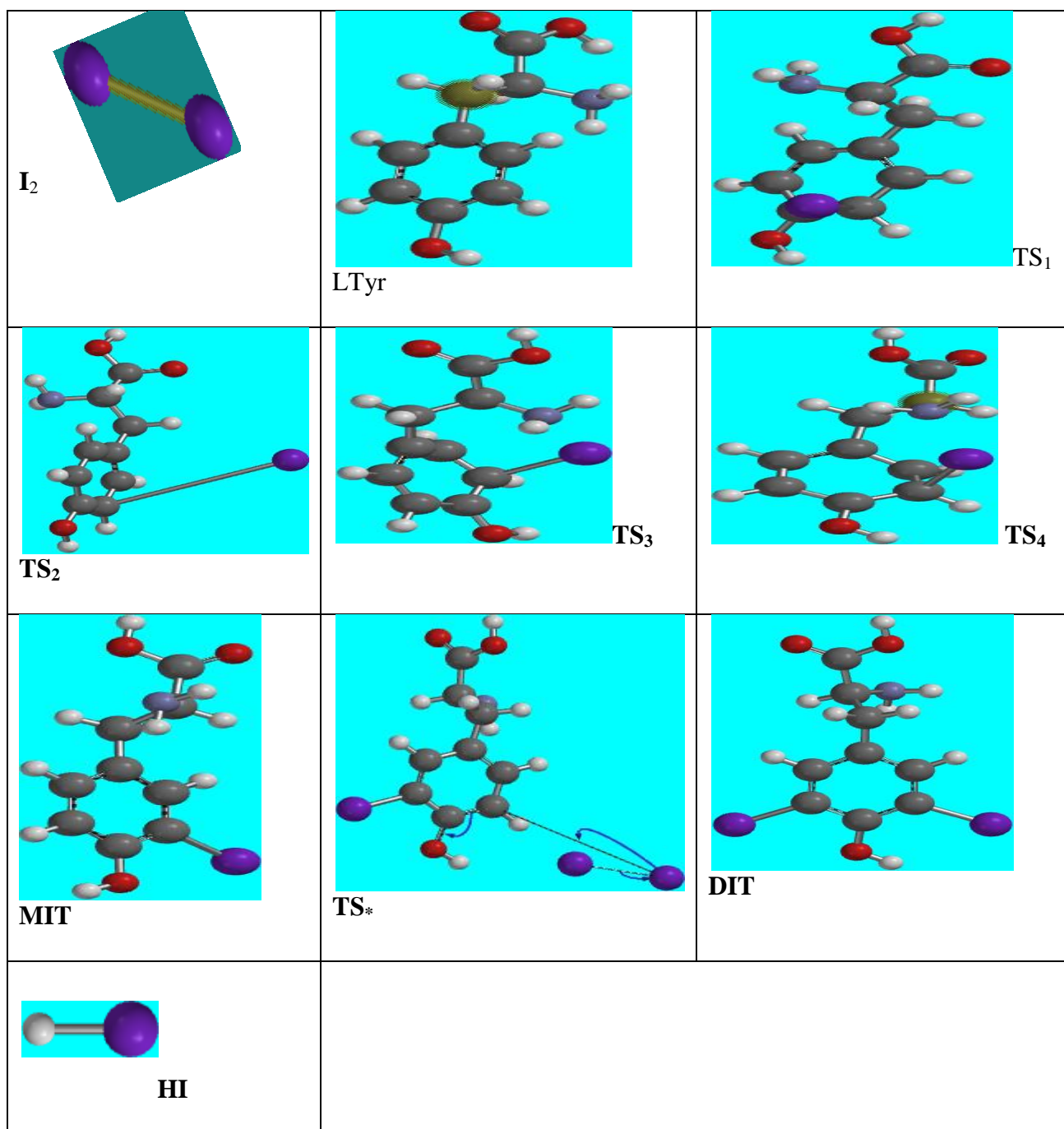


Figure 4.1: Optimized geometries of the reactants, intermediates, transition states and products for 1,2-diphenylhydrazine – iodine reaction system.

#### 4.1.2 Optimized Geometries of L-Tyrosine – Iodine Reaction System



**Figure 4.2: Optimized geometries of the reactants, intermediates, transition states and products for L-tyrosine – iodine reaction system.**

**Key:** where I<sub>2</sub> is iodine molecule; L-Tyr is L-tyrosine; MIT is monoiodo tyrosine; DIT is diiodo tyrosine; HI is hydrogen iodide; TS<sub>1</sub> is transition state 1; TS<sub>2</sub> is transition state 2; TS<sub>3</sub> is transition state 3; TS<sub>4</sub> is transition state 4 and TS\* is transition state for step 2.

### 4.1.3 Optimized Geometries of L-Ascorbic Acid – Iodine Reaction System

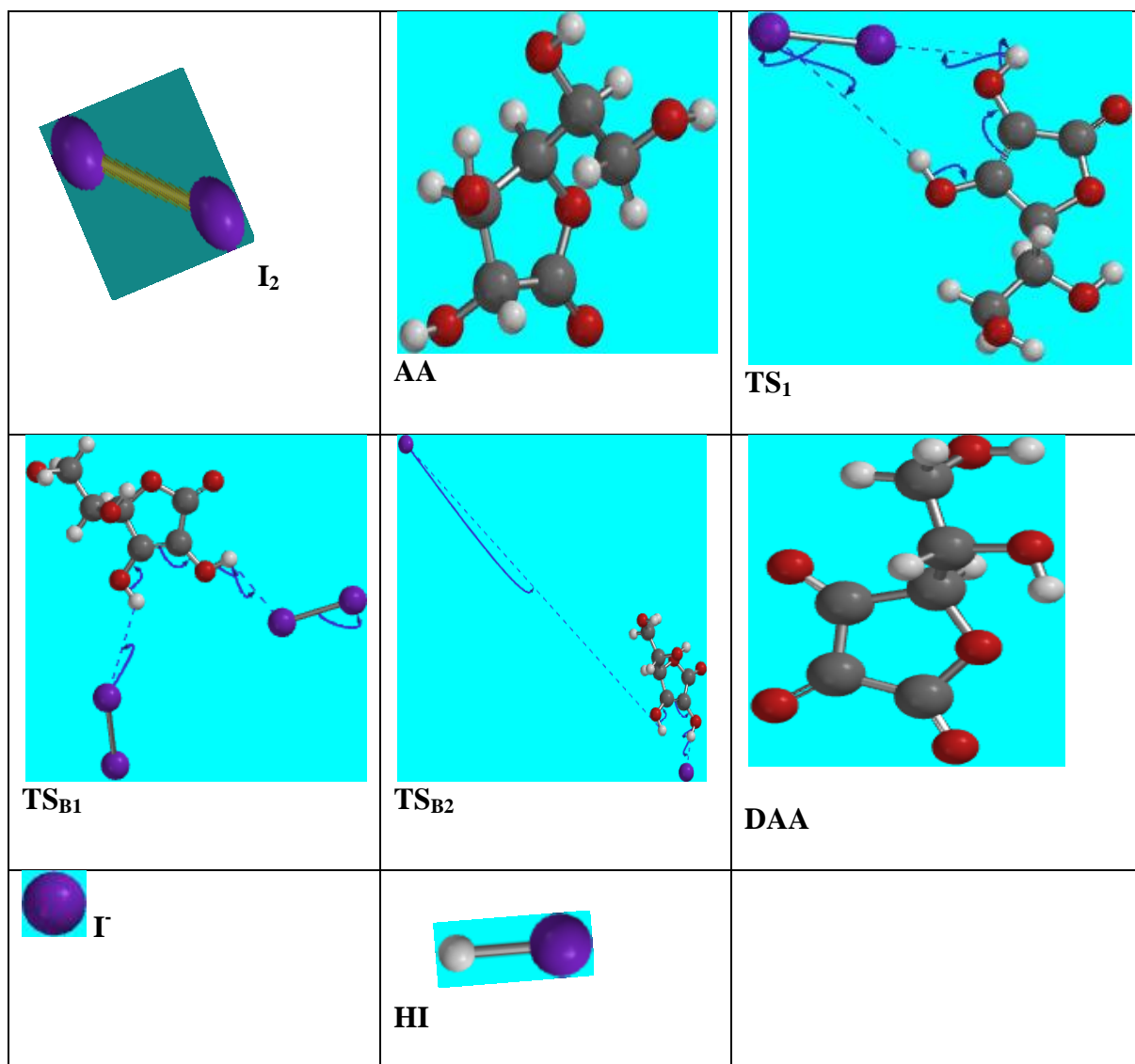


**Figure 4.3: Optimized geometries of the reactants, intermediates, transition states and products for L-ascorbic acid – iodine reaction system.**

**Key:** where I<sub>2</sub> was iodine molecule, AA was L-ascorbic acid, TS<sub>1</sub> was transition state for route 1, DAA was dehydroascorbic acid, HI was hydrogen iodide molecule. TS<sub>B1</sub> was the first transition state for route 2, I<sup>-</sup> was iodide ion, TS<sub>B2</sub> was the second transition state for route 2.

#### 4.1.4 Optimized Geometries of D-Fructose – Iodine Reaction System

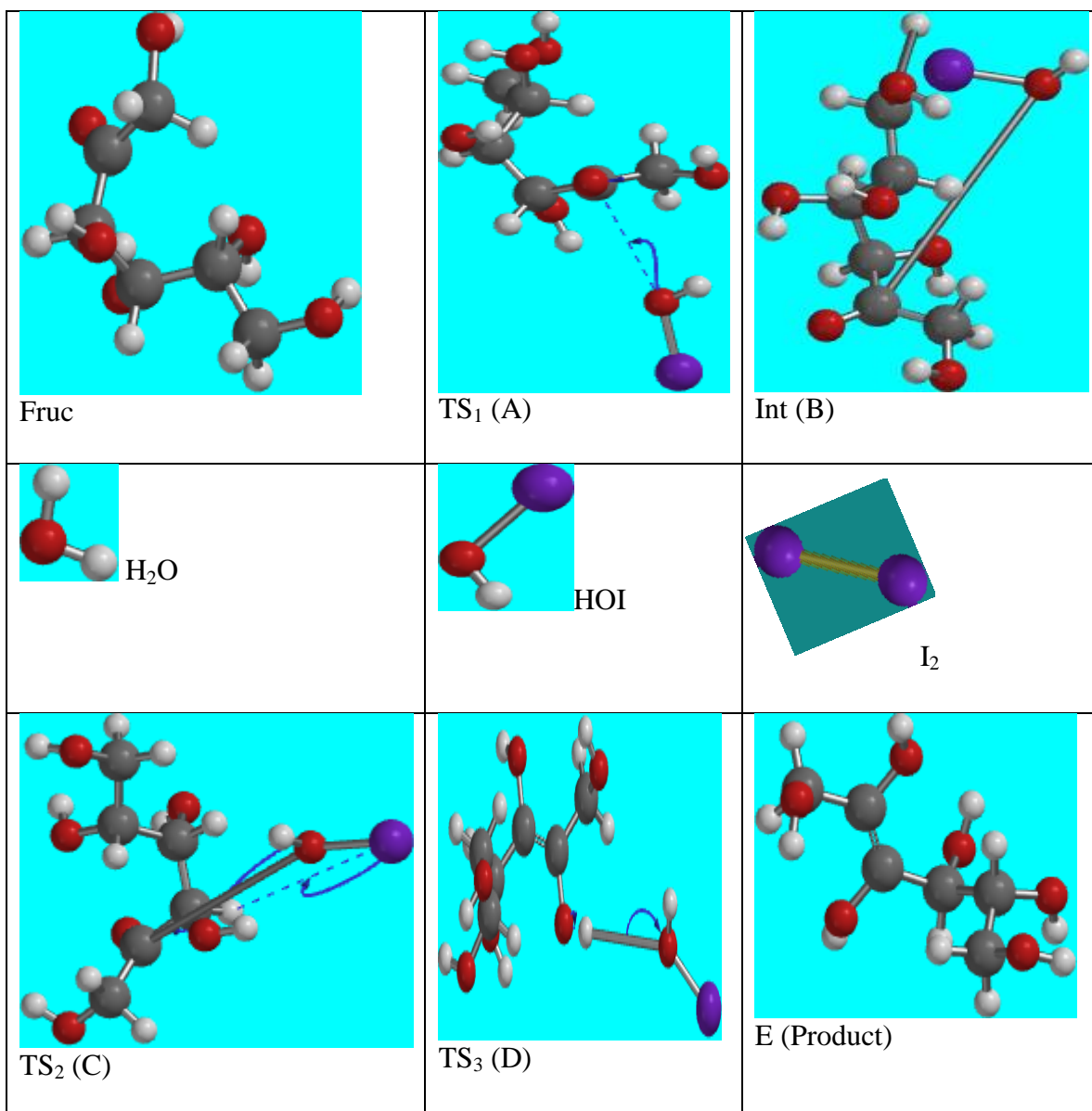


**Figure 4.4: Optimized geometries of the reactants, intermediates, transition states and products for D-fructose – iodine reaction system.**

**Key:** where I<sub>2</sub> is iodine molecule, Fruc is D-Fructose, H<sub>2</sub>O is water molecule, TS<sub>1</sub> is transition state for step1, HOI is hypiodous acid, HI is hydrogen iodide molecule, TS<sub>2</sub> and TS<sub>3</sub> are the transition states for steps 2 and 3, respectively. E is (E,4R,5R)-hex-2-ene-1,2,3,4,5,6-hexol, the product of oxidation of D-fructose.

#### 4.1.5 Optimized Geometries of Hydrazine/Hydrazinium Ion – Iodine Reaction System

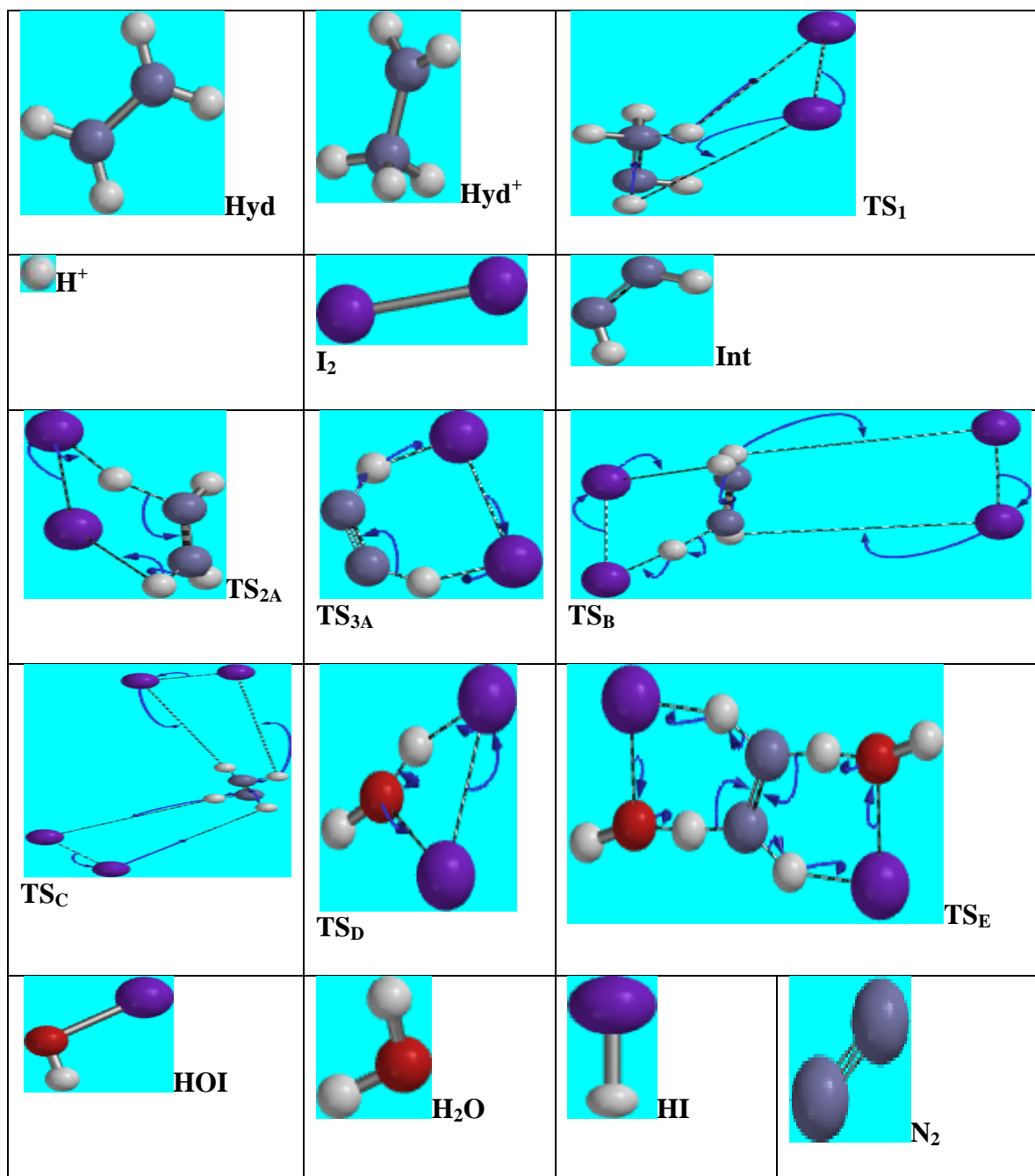


**Figure 4.5: Optimized geometries of the reactants, intermediates, transition states and products for hydrazine/hydrazinium ion – iodine reaction system.**

**Key:** where I<sub>2</sub> is iodine molecule, H<sub>2</sub>O is water molecule, Hyd<sup>+</sup> is hydrazinium ion, Hyd is hydrazine, HI is hydrogen step 1 for all the proposed four routes, N<sub>2</sub> is nitrogen molecule. TS<sub>2A</sub> and TS<sub>3A</sub> are second and third

transition states in route 1.  $TS_B$  and  $TS_C$  are the transition states for the second steps of route 2 and route 3, respectively, while  $TS_D$  and  $TS_E$  are the respective transition states for second and third steps for the proposed route 4.

#### 4.1.6 Mapping and Calculation of HOMO and LUMO of Reactants

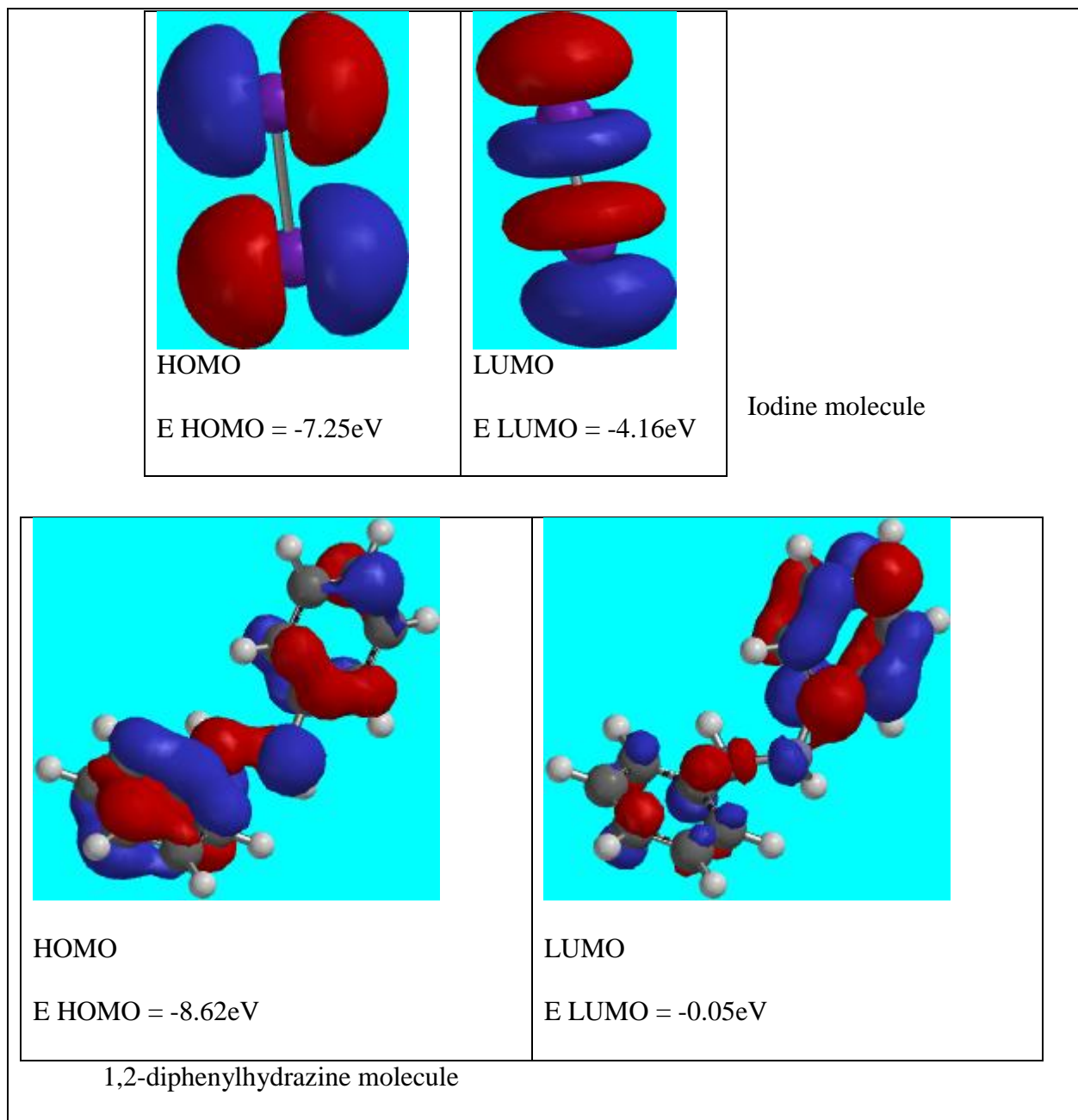


**Figure 4.6a: Solid model of HOMO and LUMO for 1,2-diphenylhydrazine – iodine reaction system**

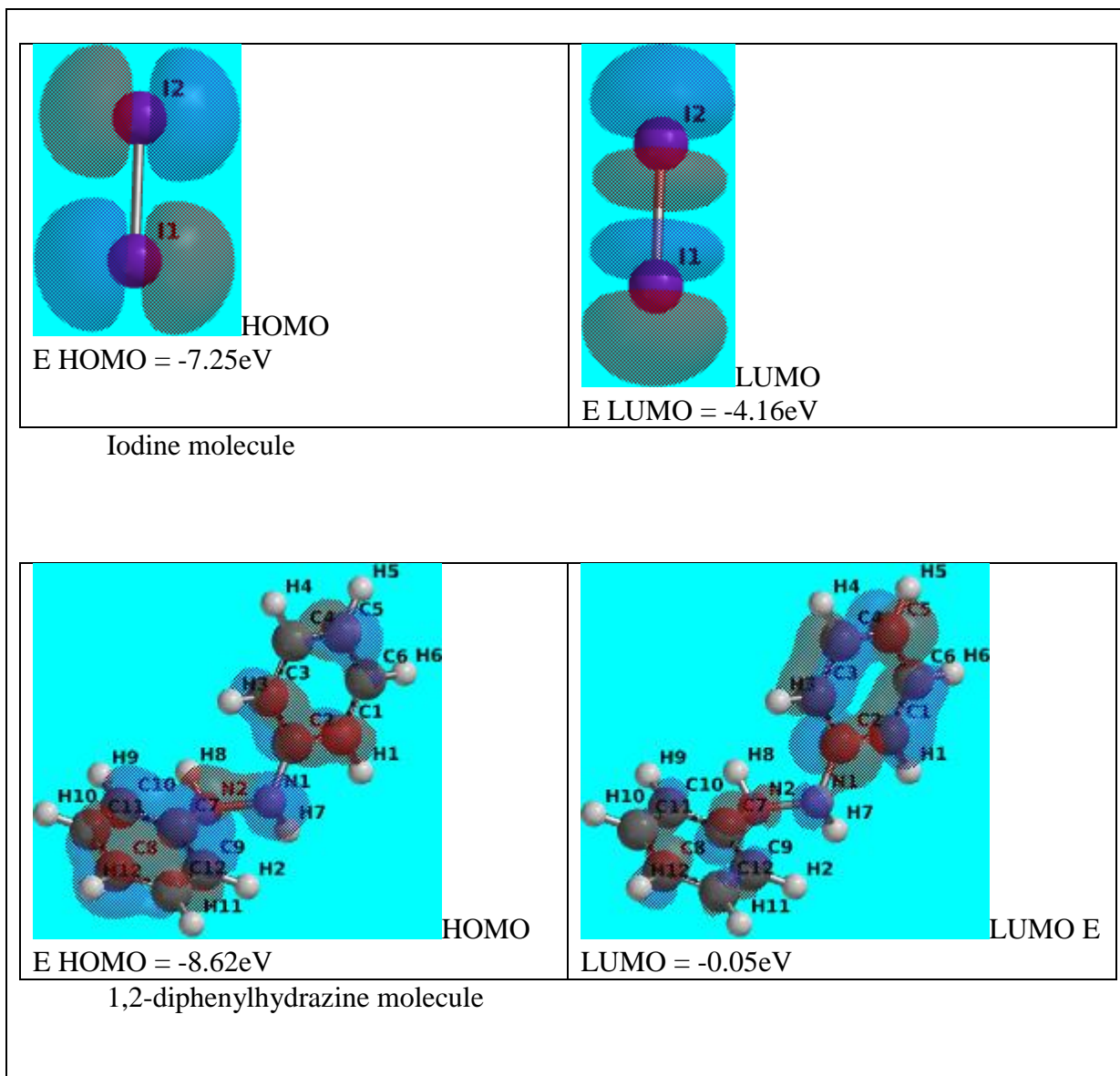


**Figure 4.6b: Transparent model of HOMO and LUMO for 1,2-diphenylhydrazine – iodine reaction system**

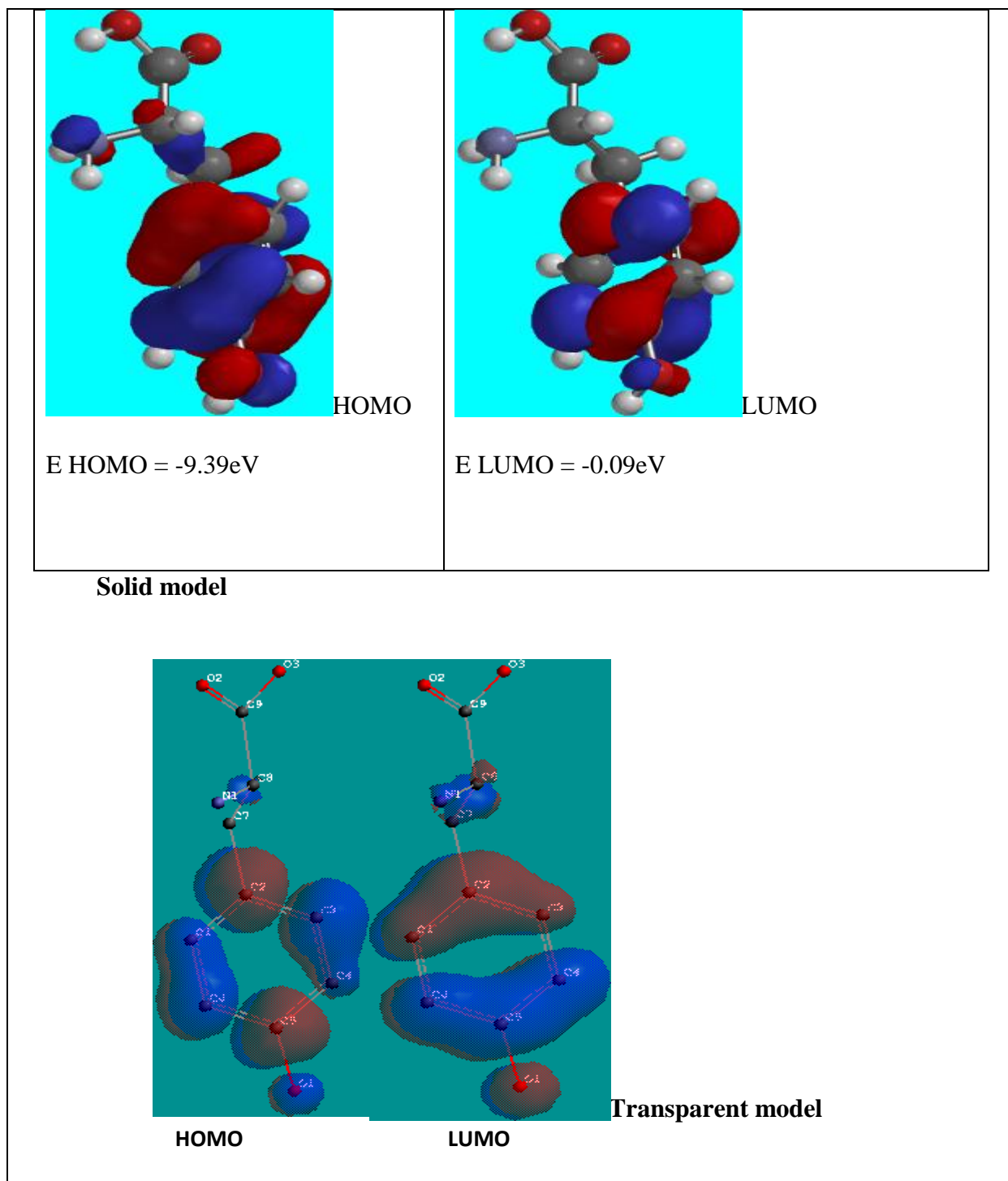


**Figure 4.7: Solid and transparent models of HOMO and LUMO for L-tyrosine**

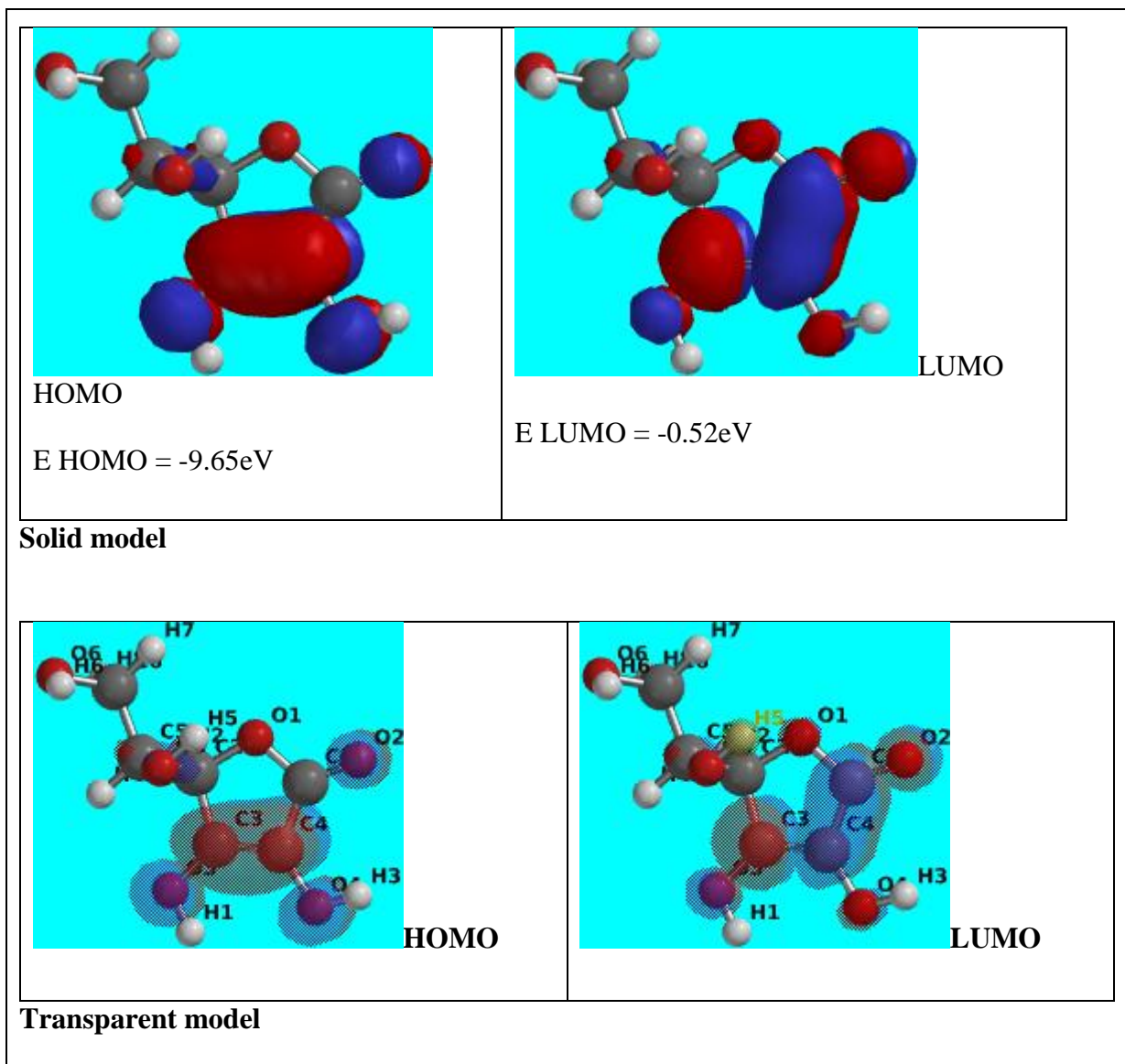
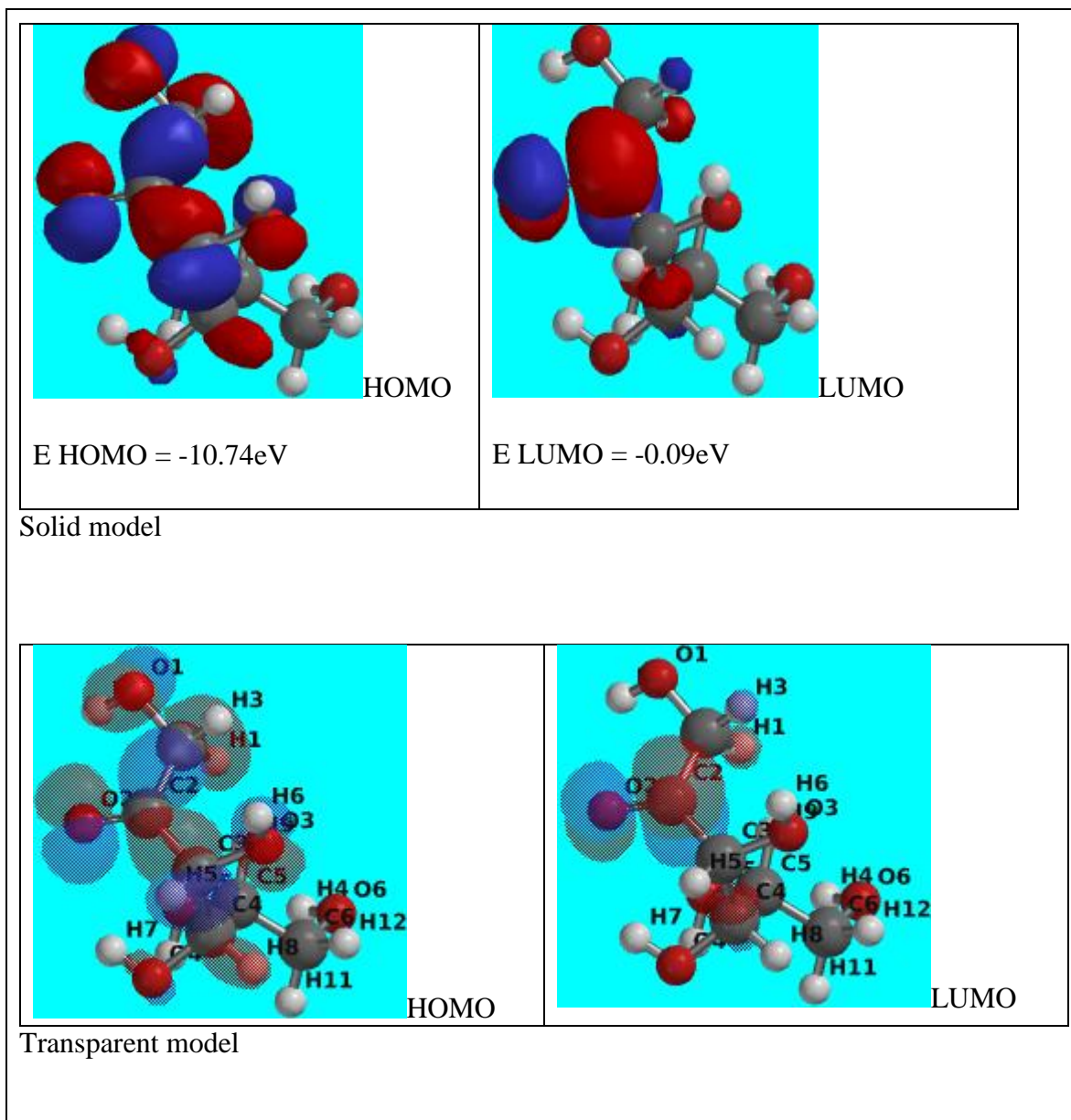
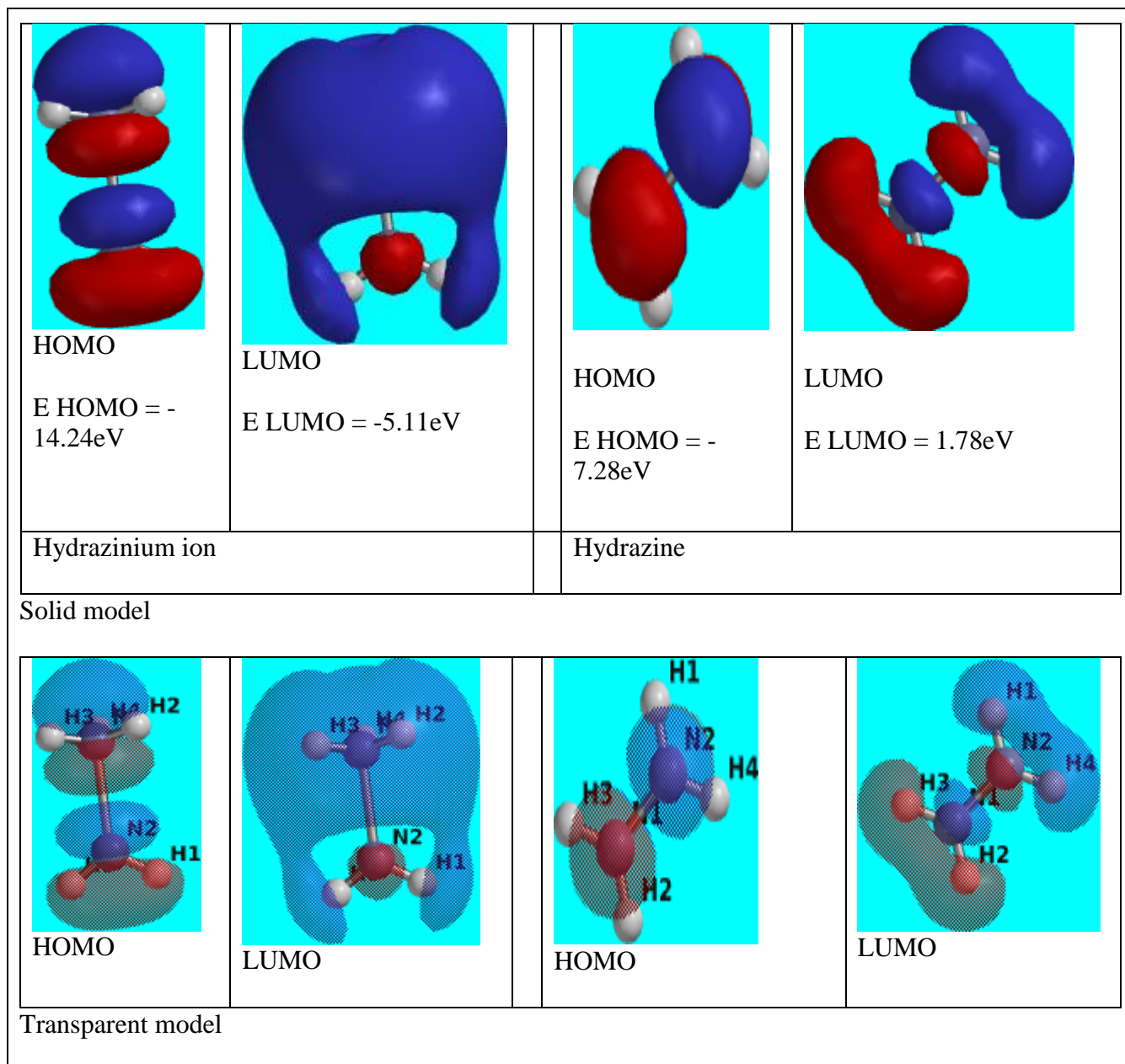


Figure 4.8: Solid and transparent models of HOMO and LUMO for L-ascorbic acid



**Figure 4.9: Solid and transparent models of HOMO and LUMO for D-fructose**



**Figure 4.10: Solid and transparent models of HOMO and LUMO for hydrazine / hydrazinium ion.**

### 4.3 Searches for Transition States and Intermediates

#### 4.3.1 Transition States and Intermediates for 1,2-Diphenylhydrazine – Iodine Reaction System

For the 1,2-diphenylhydrazine – iodine reaction system, two reaction pathways were proposed. Three transition states,  $TS_1$ ,  $TS_2$  and  $TS_3$  were found for route 1, while one transition state,  $TS^*$ , was found for the second route. The transition states are provided in Figure 4.11.

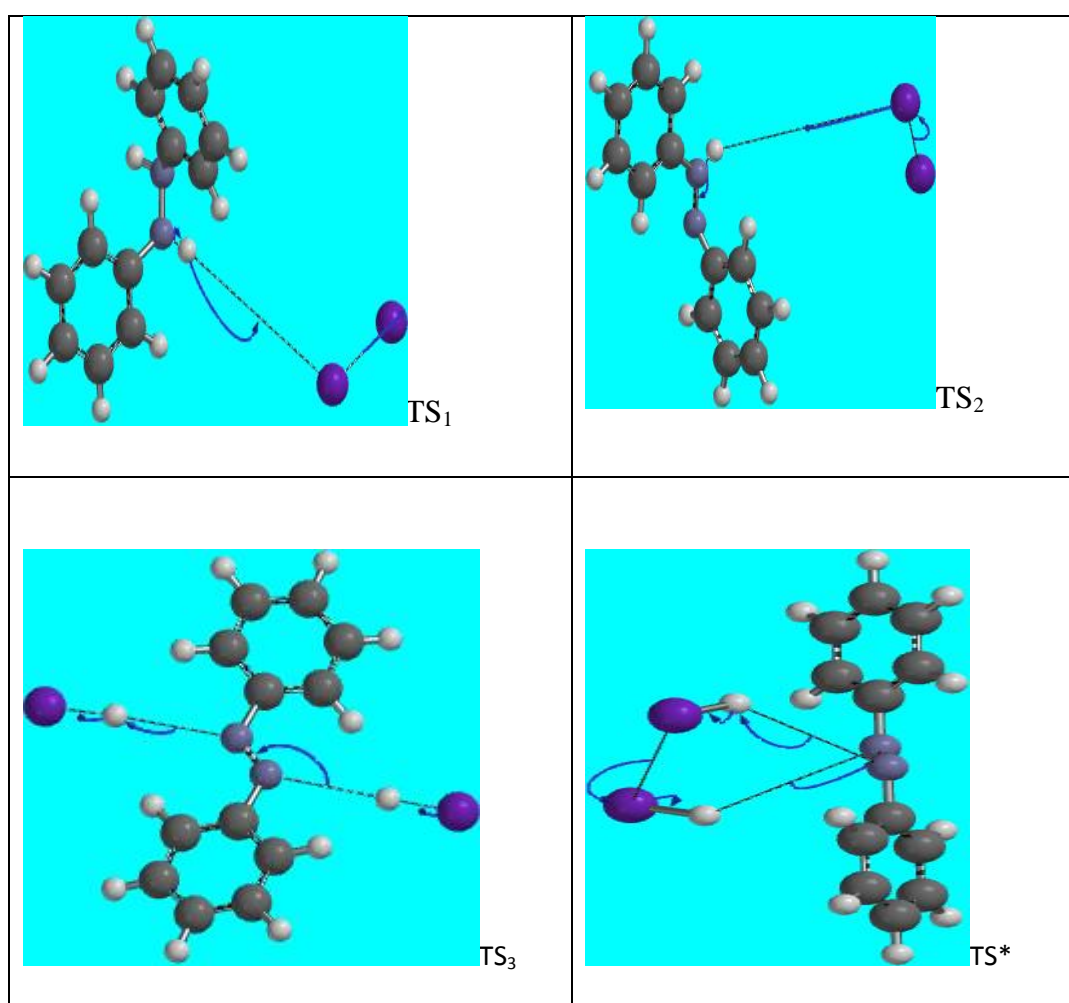


**Figure 4.11: Transition states for 1,2-diphenylhydrazine – iodine reaction system**

### 4.3.2 Transition States and Intermediates for L-Tyrosine – Iodine Reaction System

For the L-tyrosine – iodine reaction system, five transition states,  $TS_1$ ,  $TS_2$ ,  $TS_3$ ,  $TS_4$  and  $TS^*$ , were found. The transition states are provided in Figure 4.12.

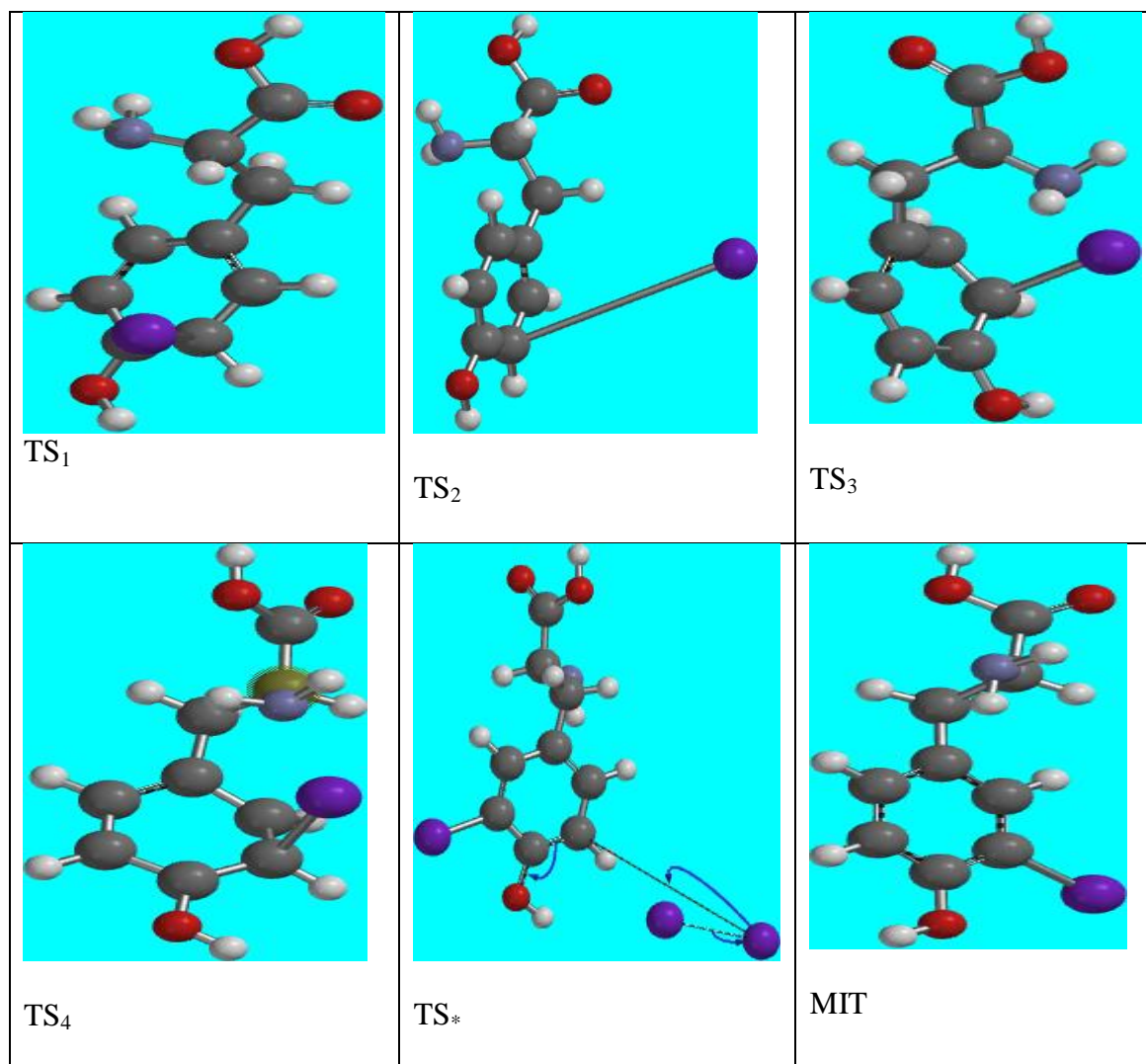
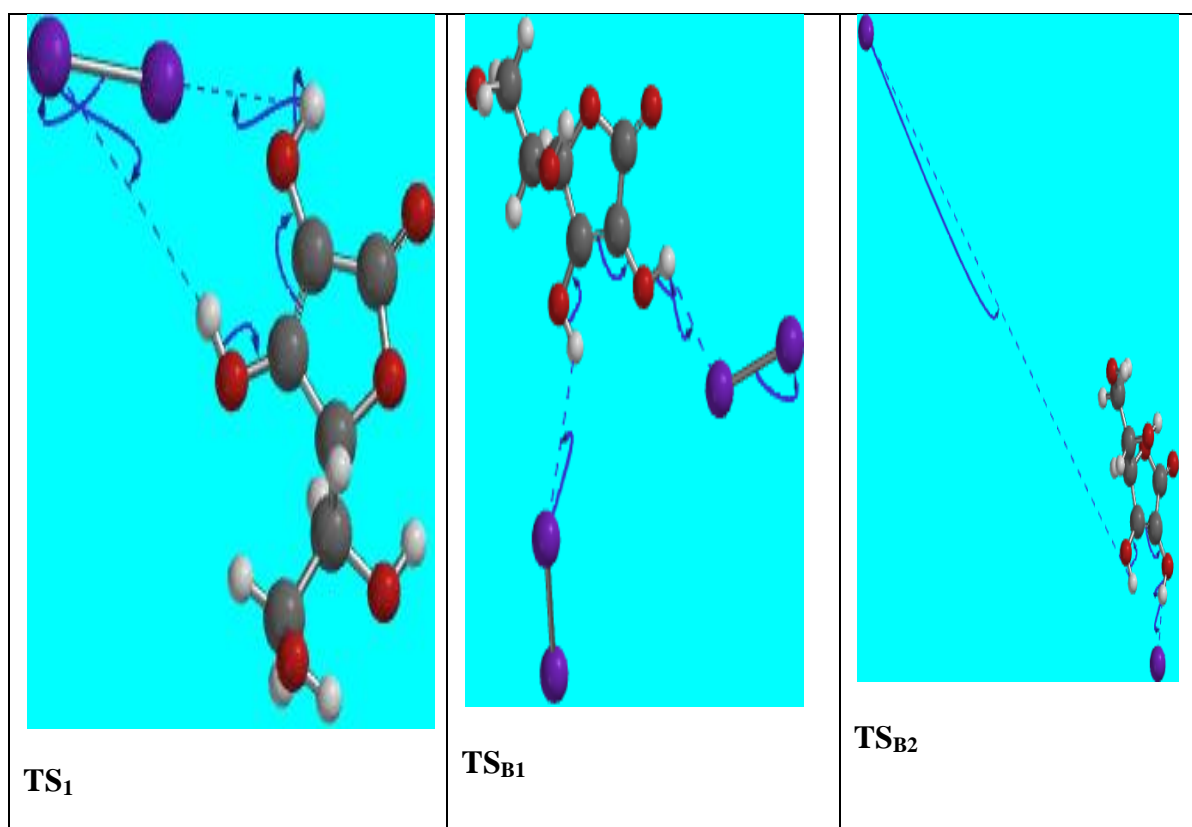


Figure 4.12: Transition states and intermediates for L-tyrosine – iodine reaction system

### 4.3.3 Transition States and Intermediates for L-Ascorbic Acid – Iodine Reaction System

For the L-ascorbic – iodine reaction system, two reaction pathways were proposed. One transition state,  $TS_1$ , was found for route 1, while two transition states,  $TS_{B1}$  and  $TS_{B2}$ , were found for the second route. The transition states are provided in Figure 4.13.



**Figure 4.13: Transition states and intermediates for L-ascorbic acid – iodine reaction system**

#### 4.3.4 Transition States and Intermediates for D-Fructose– Iodine Reaction System

For the D-fructose– iodine reaction system, three transition states,  $TS_1$ ,  $TS_2$ , and  $TS_3$ . Two intermediates, Int.(B) and Int.2 (D) were also found. The transition states and the intermediate are provided in Figure 4.14.

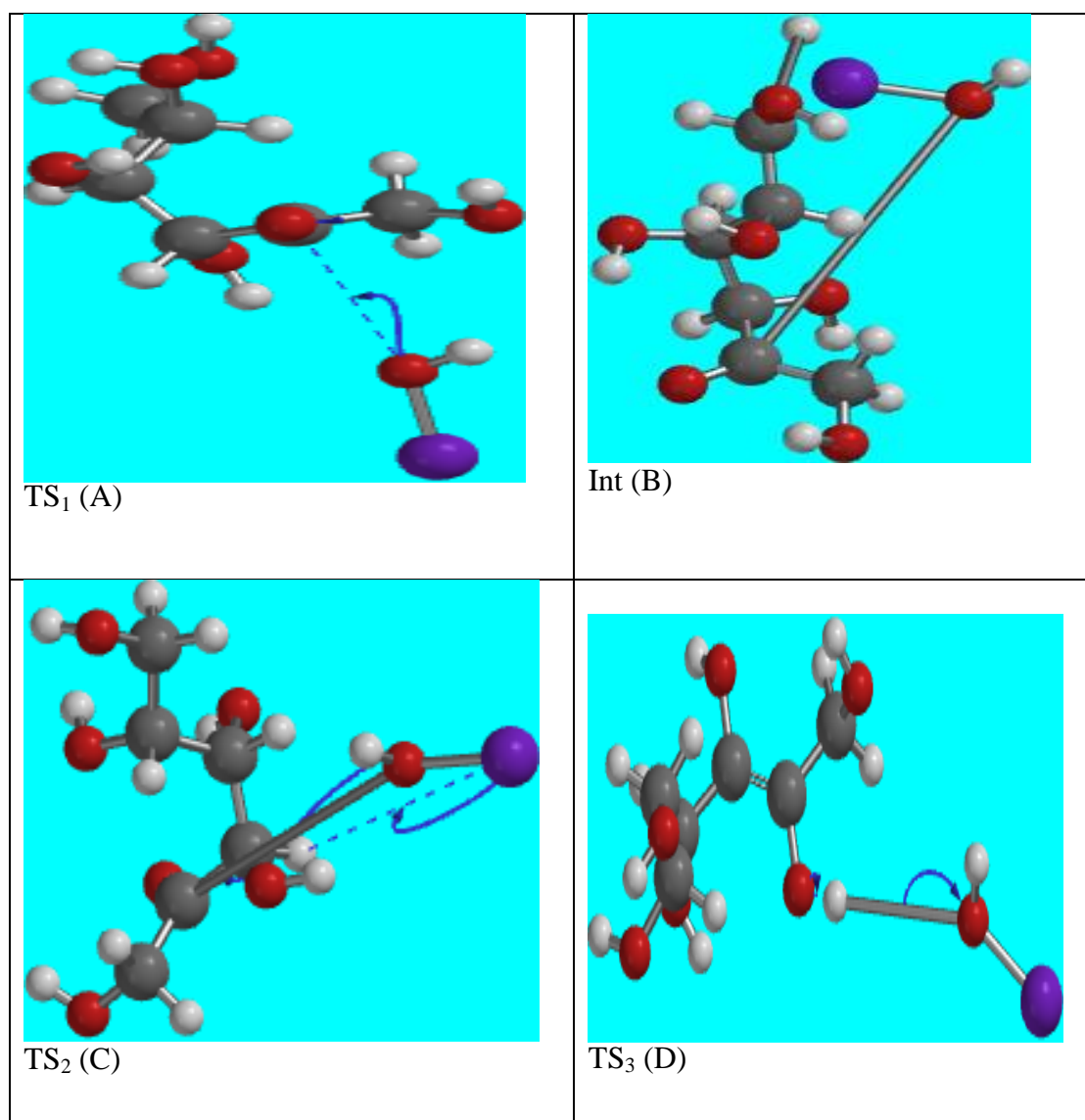


**Figure 4.14: Transition states and intermediates for D-fructose – iodine reaction system**

### 4.3.5 Transition States and Intermediates for Hydrazine/Hydrazinium Ion– Iodine Reaction System

For the hydrazine/hydrazinium ion – iodine reaction system, four reaction pathways were proposed. A total of seven transition states,  $TS_1$ ,  $TS_{2A}$ ,  $TS_{3A}$ ,  $TS_B$ ,  $TS_C$ ,  $TS_D$  and  $TS_E$ , were found for the various four routes. One intermediate, Int, was also found. The transition states and the intermediate are provided in Figure 4.15.

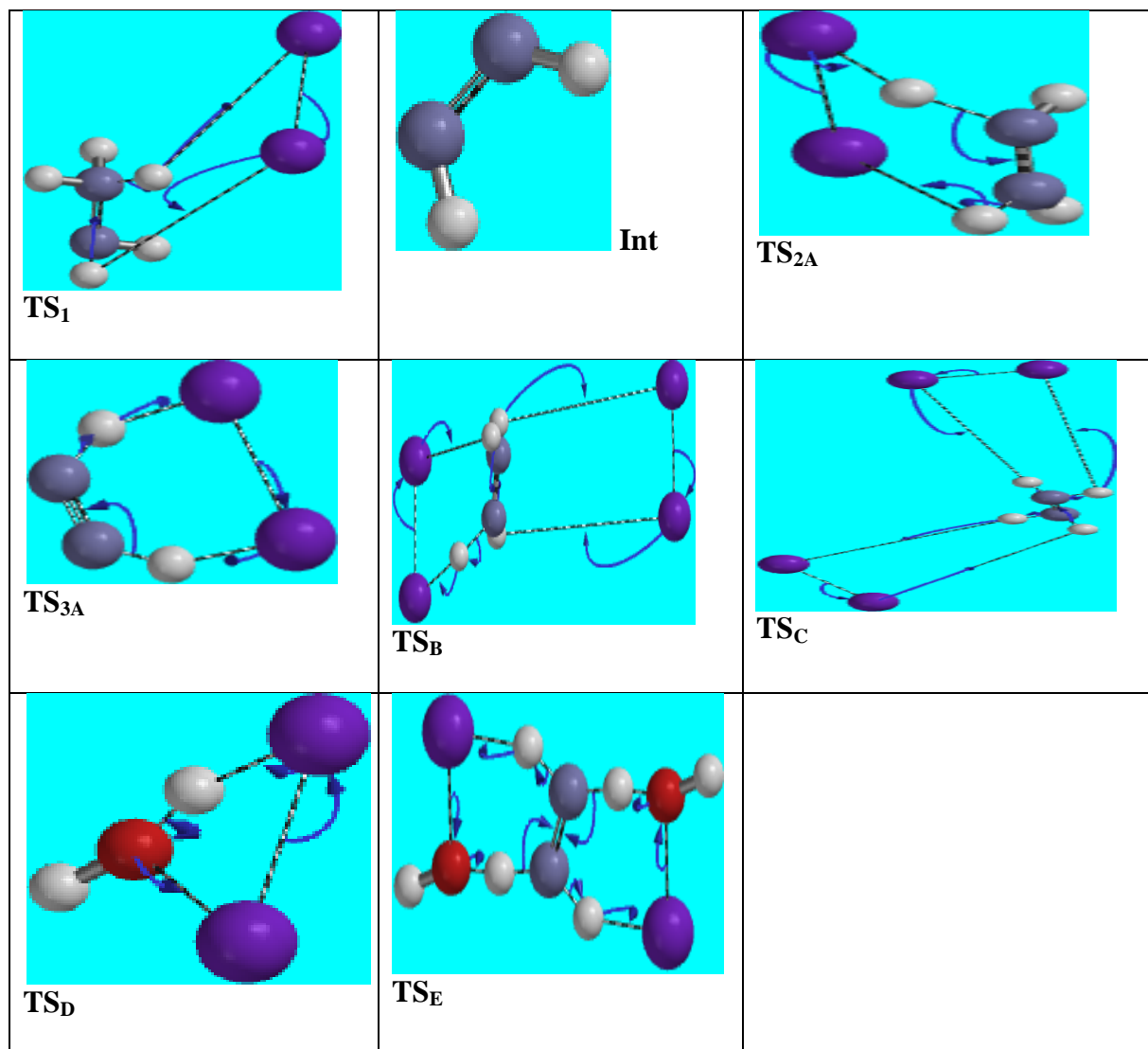


**Figure 4.15: Transition states and intermediates for hydrazine / hydrazinium ion – iodine reaction system**

#### **4.4 Calculation of Thermodynamics, Molecular and other Physicochemical Properties of Reacting Species and Products**

##### **4.4.1 Computation of Heat of Formation, Total Electronic Energy and Other Thermodynamic Parameters of Reacting Species and Products for 1,2-Diphenylhydrazine – Iodine Reaction System**

The heat of formation ( $\Delta H_f$ ), total electronic energy ( $E_e$ ) and other activation parameters of the various species for the 1,2-diphenylhydrazine – iodine system were evaluated and presented in Table 4.1, where  $I_2$  is iodine molecule;  $AH_2$  is 1,2- diphenylhydrazine ;  $AH$  is 1,2-diphenyl-hydrazyl radical;  $A$  is trans-1,2-diphenyldiazene (Azobenzene);  $HI$  is hydrogen iodide;  $I^-$  iodide ion;  $TS_1$  is transition state 1;  $TS_2$  is transition state 2;  $TS_3$  is transition state 3 and  $TS^*$  is transition state for the one step cyclic complex mechanism  $R_1 (AH_2 + I)$ ,  $R_2 (AH + I_2)$  and  $R_3 (AH_2 + 2I)$  are the reactants in steps 1, 2, 3, respectively;  $R_3 (AH_2 + 2I)$ ,  $P_2 (A + HI + I)$ , and  $P_3 (A + 2I)$  the products of the respective steps, while  $E_{a1}$ ,  $E_{a2}$  and  $E_{a3}$  are the activation energies for steps 1, 2 and 3 for the chain multi-step mechanism.  $R^* (AH_2 + I_2)$ ,  $P^* (A + 2HI)$  and  $E_{aB}$ , are the reactants, products and activation energy for the one-step cyclic complex mechanism. The activation parameters were also presented in Table 4.2.

##### **4.4.1.1 Charge Distribution and Exposed Surface Study of 1,2-Diphenylhydrazine**

The optimized 1,2-Diphenylhydrazine molecule was as shown Figure 4.16. The conformation with the lowest energy was optimized and calculated using the MNDO method. The molecular information such as hydrogen identity, bond type, bond length and exposed surface area were determined and shown in Table 4.3. The identity numbers of all hydrogen and non-hydrogen atoms of the conformer compound were labeled as in Figure 4.16.

##### **4.4.2 Computation of Heat of Formation, Total Electronic Energy and Other Activation Parameters of Reacting Species and Products for L-Tyrosine – Iodine Reaction System**

The heat of formation ( $\Delta H_f$ ), total electronic energy ( $E_e$ ) and other activation parameters of the various species for the L-tyrosine – iodine System were evaluated and presented in Table 4.4, where  $I_2$  is iodine molecule; L-Tyr, is L-tyrosine ; MIT is monoiodo tyrosine; DIT is diiodo tyrosine; HI is hydrogen iodide;  $TS_1$  is transition state 1;  $TS_2$  is transition state 2;  $TS_3$  is transition state 3;  $TS_4$  is transition state 4 and  $TS^*$  is transition state for step 2.  $R_1$  (L-Tyr +  $I_2$ ) and  $R_2$  (MIT +  $I_2$ ) are the reactants in steps 1, 2, respectively and;  $P_1$  (MIT + HI) and  $P_2$  (DIT + HI) the products of the respective steps.  $E_{a1}$  and  $E_{a2}$  are the activation energies for steps 1 and 2, respectively, and these properties and other activation parameters are also presented in Table 4.5.

#### **4.4.2.1 Charge Distribution and Exposed Surface Study of L-Tyrosine**

The optimized L- tyrosine molecule was as shown Figure 4.17. The conformation with the lowest energy was optimized and calculated using the PM3 method. The molecular information such as net charges and exposed surface areas of atoms, determined were also shown in Table 4.6. The identity numbers of all non-hydrogen atoms of the conformer compound were labeled as in Figure 4.17. The C-I and C-H bond lengths for various transition states are shown in Table 4.7.

#### **4.4.3 Computation of Heat of Formation, Total Electronic Energy and Other Activation Parameters of Reacting Species and Products for L-Ascorbic – Iodine Reaction System**

The heat of formation ( $\Delta H_f$ ), total electronic energy ( $E_e$ ), thermodynamic parameters and other activation parameters of the various species for the L-ascorbic acid – iodine system were evaluated and presented in Tables 4.8 – 4.12, where  $I_2$  is iodine molecule, AA is L-ascorbic acid,  $TS_1$  is transition state for route 1, DAA is dehydroascorbic acid, HI is hydrogen iodide molecule,  $R_1$  (AA +  $I_2$ ) are all the reactants for route 1,  $P_1$  (DAA + HI) are all the products for route 1,  $E_{a1}$  is the activation energy for route 1,  $TS_{B1}$  is the first transition state

for route 2, I is iodide ion,  $TS_{B2}$  is the second transition state for route 2,  $R_{B1}$  ( $AA + 2I_2$ ) and  $R_{B2}$  ( $AA + 2I$ ) are all the reactants in steps 1 and 2 respectively for route 2,  $P_{B1}$  ( $DAA + 2HI + 2I$ ) and  $P_{B2}$  ( $DAA + 2HI$ ) are the products of reactions for steps 1 and 2 respectively for route 2, while  $E_{aB1}$  and  $E_{aB2}$  are the activation energies for steps 1 and 2, respectively, in route 2.

#### 4.4.3.1 Charge Distribution and Exposed Surface Study of L-Ascorbic Acid

The optimized and labeled L-ascorbic acid molecule was as shown Figure 4.18. The conformation with the lowest energy was optimized and calculated using the PM3 method. The molecular information such as hydrogen identity, bond type, bond length and exposed surface area were determined and shown in 4.13. The identity numbers of all non-hydrogen atoms of the conformer compound were labeled as in Figure 4.18.

#### 4.4.4 Computation of Heat of Formation, Total Electronic Energy and Other Activation Parameters of Reacting Species and Products for D-Fructose – Iodine Reaction System

The heat of formation ( $\Delta H_f$ ), total electronic energy ( $E_e$ ), thermodynamic parameters and other activation parameters of optimized geometries of reactants, intermediates, transition states and products were presented in Tables 4.14 and 4.15 for the DFT optimization and Tables 4.16 and 4.17 for the semi-empirical PM3 optimization. Where  $I_2$  is iodine molecule, Fruc is D-Fructose,  $H_2O$  is water molecule,  $TS_1$  is transition state for step 1, HOI is hypiodous acid, HI is hydrogen iodide molecule,  $R_1(I_2 + H_2O)$  are all the reactants for step 1,  $R_2(HOI + Fruc)$  are all the reactants for step 2,  $R_3(B\ int)$  are all the products for step 3,  $TS_1$ ,  $TS_2$ ,  $TS_3$  are the transition state for steps 1, 2 and 3, respectively;  $P_1(HOI + HI)$ ,  $P_2(B\ int)$  and  $P_3(E + HOI)$  are the products of reactions for steps 1, 2 and 3, respectively, while  $E_{a1}$  is the activation energy for step 1,  $E_{a2}$  and  $E_{a3}$  are the activation energies for steps 2 and 3

respectively. D is the intermediate is step 3. The activation parameters for the DFT and PM3 studies were as presented in Tables 4.15 and 4.17, respectively.

#### 4.4.4.1 Charge Distribution and Exposed Surface Study of D-Fructose

The optimized D-fructose molecule was as shown Figure 4.19. The conformation with the lowest energy was optimized and calculated using the PM3 method. The molecular information such as net charges and exposed surface areas of atoms determined were also shown in Table 4.18. The identity numbers of all non-hydrogen atoms of the conformer compound were labeled as in Figure 4.19.

#### 4.4.5 Computation of Heat of Formation, Total Electronic Energy and Other Thermodynamic Parameters of Reacting Species and Products for Hydrazine / Hydrazinium Ion – Iodine Reaction System

The heat of formation ( $\Delta H$ ), total electronic energy ( $E_e$ ), thermodynamic parameters and other thermodynamic including activation parameters of the various species for the hydrazine / hydrazinium ion – iodine System were evaluated and presented in Tables 4.19 - 4.24 for routes 1 - 4, respectively. Where  $I_2$  is iodine molecule,  $H_2O$  is water molecule,  $Hyd^+$  is hydrazinium ion,  $Hyd$  is hydrazine,  $HI$  is hydrogen iodide molecule,  $HOI$  is hypoiodous acid,  $Int$  is intermediate (diazine),  $TS1$  is transition state for step 1,  $N_2$  is nitrogen molecule,  $R_1$  ( $H_2O + Hyd^+$ ) and  $P_1$  ( $H_3O^+ + Hyd$ ) are all the reactants and products for step 1 of all the proposed routes, respectively.  $R_{2A}$  ( $I_2 + Hyd$ ) and  $P_{2A}$  ( $Int + 2HI$ ) are the respective reactants and products of step 2, route I;  $R_B$  ( $2I_2 + Hyd$ ) and  $P_B$  ( $N_2 + 4HI$ ), respective reactants and products of step 2, route II;  $R_C$  ( $2I_2 + Hyd$ ) and  $P_C$  ( $N_2 + 4HI$ ), respective reactants and products of step 2, route III; while  $R_D$  ( $2I_2 + 2H_2O$ ) and  $P_D$  ( $2HOI + 2HI$ ), respective reactants and products of step 2, route IV.  $R_{3A}$  ( $Int + I_2$ ) and  $P_{3A}$  ( $N_2 + 2HI$ ) are the respective reactants and products of step 3, route I; while  $R_E$  ( $2HOI + Hyd$ ) and  $P_E$  ( $N_2 + 2H_2O + 2HI$ ) are the respective reactants and products of step 3, route IV.  $E_{a1}$  is the activation energy for step 1 for

all the four routes;  $E_{a2}$ ,  $E_{aB}$ ,  $E_{aC}$  and  $E_{aD}$  are the activation energy for step 2 for routes I, II, III and IV respectively.  $E_{a3}$  and  $E_{aE}$  are the respective activation energies for step 3 for routes I and IV.

#### **4.4.5.1 Charge Distribution and Exposed Surface Study of Hydrazine / Hydrazinium Ion**

The optimized hydrazine / hydrazinium ion molecules were as shown Figure 4.20. The conformation with the lowest energy was optimized and calculated using the DFT method. The molecular information such as net charges and exposed surface areas of atoms determined were also shown in Table 4.25. The identity numbers of all non-hydrogen atoms of the conformer compound were labeled as in Figure 4.20.

### **4.5 Construction of Potential Energy Surface Diagrams**

#### **4.5.1 Potential Energy Surface Diagrams of Reaction of 1,2-Diphenylhydrazine – Iodine Reaction System According to the Chain Multi Step and Cyclic Mechanism**

Reaction profiles of 1,2-diphenylhydrazine reaction with iodine were obtained by plotting the heat of formation (total electronic energy for DFT) of the reactants, transition states and products against the reaction coordinates. Figures 4.21 and 4.22 showed the energy profile diagrams for the 1,2-diphenylhydrazine reaction with iodine using DFT and MNDO methods, respectively, where  $R_1$  ( $AH_2 + I$ ),  $P_1$  ( $AH + HI + I$ ) and  $TS_1$  are reactants, products and transition states for step 1;  $R_2$  ( $AH + I_2$ ),  $P_2$  ( $A + HI + I$ ) and  $TS_2$  are reactants, products and transition states for step 2; while  $R_3$  ( $AH_2 + 2I$ ),  $P_3$  ( $A + 2I$ ) and  $TS_3$  are reactants, products and transition states for step 3, for the chain multi-step mechanism. Figures 4.23 and 4.24 are the respective energy profile diagrams using DFT and MNDO methods for the one-step cyclic complex mechanism, where  $R^*$  ( $AH_2 + I_2$ ),  $P^*$  ( $A + 2HI$ ) and  $TS^*$  are reactants, products and transition states for the one-step cyclic mechanism

**Table 4.1: Total electronic energy, heat of formation and other thermodynamic parameters of reacting species and products of 1,2-diphenylhydrazine – iodine reaction system**

| S/N | Species                               | Total electronic energy at 298.15K<br>using DFT |                        | Thermodynamic parameters at 298.15K<br>using MNDO |                 |                  |
|-----|---------------------------------------|---|------------------------|---|-----------------|------------------|
|     |                                       | E <sub>e</sub><br>(kJ/mol)                      | E <sub>e</sub><br>(au) | ΔH°<br>(kJ/mol)                                   | ΔG°<br>(kJ/mol) | ΔS°<br>(J/mol.K) |
| 1   | I <sub>2</sub>                        | -37,327,532.08                                  | -14,220.01             | 114.05  | 36.73           | 259.34           |
| 2   | AH <sub>2</sub>                       | -1,507,000.75                                   | -574.10                | 952.60  | 818.08          | 451.19           |
| 3   | TS <sub>1</sub>                       | -31,804,644.68                                  | -12,116.06             | 1,089.71  | 911.31          | 598.35           |
| 4   | AH                                    | -1,505,357.68                                   | -573.47                | 849.15  | 716.12          | 446.20           |
| 5   | HI                                    | -18,168,774.40                                  | -6,921.44              | 119.36  | 57.88           | 206.18           |
| 6   | I <sup>-</sup>                        | -18,157,470.45                                  | -6,917.13              | 0.00  | 0.00            | 0.00             |
| 7   | TS <sub>2</sub>                       | -19,669,188.83                                  | -7,493.02              | 1766.33   | 1574.84         | 642.26           |
| 8   | TS <sub>3</sub>                       | -36,834,591.95                                  | -14,032.23             | 1,193.31  | 1,001.82        | 642.39           |
| 9   | A                                     | -1,503,817.83                                   | -572.88                | 900.32  | 769.20          | 439.76           |
| 10  | TS*                                   | -37,824,591.91                                  | -14,409.37             | 1,111.05  | 934.95          | 590.65           |
| 11  | R <sub>1</sub> (AH <sub>2</sub> + I)  | -38,834,532.83                                  | -14,794.11             | 1,066.65  | 854.81          | 710.34           |
| 12  | P <sub>1</sub> (AH + HI + I)          | -37,831,602.53                                  | -14,412.04             | 968.51  | 968.51          | 652.38           |
| 13  | R <sub>2</sub> (AH + I <sub>2</sub> ) | -38,832,889.76                                  | -14,793.48             | 963.20  | 752.85          | 705.54           |
| 14  | P <sub>2</sub> (A + HI + I)           | -37,83,0062.68                                  | -14,411.45             | 1,019.68  | 827.08          | 645.94           |
| 15  | R <sub>3</sub> (AH <sub>2</sub> + 2I) | -37,821,941.65                                  | -14,408.36             | 952.60  | 818.08          | 451.19           |
| 16  | P <sub>3</sub> (A + 2I)               | -37,841,366.63                                  | -14,415.76             | 1,139.04  | 1,079.96        | 854.12           |
| 17  | E <sub>a1</sub>                       | 7,029,888.15                                    | 2,678.05               | 23.06   |                 |                  |
| 18  | E <sub>a2</sub>                       | 19,163,700.93                                   | 7,300.46               | 803.13  |                 |                  |
| 19  | E <sub>a3</sub>                       | 987,349.70                                      | 376.13                 | 240.71  |                 |                  |
| 20  | E <sub>aB</sub>                       | 1,009,940.92                                    | 384.74                 | 44.40   |                 |                  |

**Key:**where I<sub>2</sub> is iodine molecule; AH<sub>2</sub> is 1,2- diphenylhydrazine ; AH is 1,2-diphenyl-hydrazyl radical; A is trans-1,2-diphenyldiazene (Azobenzene); HI is hydrogen iodide; I<sup>-</sup> iodide ion; TS<sub>1</sub> is transition state 1; TS<sub>2</sub> is transition state 2; TS<sub>3</sub> is transition state 3 and TS\* is transition state for the one step cyclic complex mechanism R<sub>1</sub>(AH<sub>2</sub> + I), R<sub>2</sub>(AH + I<sub>2</sub>) and R<sub>3</sub>(AH<sub>2</sub> + 2I) are the reactants in steps 1, 2, 3, respectively; R<sub>3</sub>(AH<sub>2</sub> + 2I), P<sub>2</sub>(A + HI + I), and P<sub>3</sub>(A + 2I) the products of the respective steps, while E<sub>a1</sub>, E<sub>a2</sub> and E<sub>a3</sub> are the activation energies for steps 1, 2 and 3 for the chain multi-step mechanism. R\* (AH<sub>2</sub> + I<sub>2</sub>), P\* (A + 2HI) and E<sub>aB</sub>, are the reactants, products and activation energy for the one-step cyclic complex mechanism.

**Table 4.2: Heat of formation and other activation parameters of reacting species and products 1,2-diphenylhydrazine – iodine reaction system for route 1 and route according to MNDO calculations**

| Route    | Species                                | $\Delta_f H$<br>(kJ/mol) | $\Delta^\ddagger G$<br>(kJ/mol) | $\Delta^\ddagger S$<br>(J/mol) | $E_a$<br>(kJ/mol)     |
|----------|--|--------------------------|---------------------------------|--------------------------------|-----------------------|
| Route I  | R <sub>1</sub> (AH <sub>2</sub> + I)   | 1,066.65                 |                                 |                                |                       |
|          | P <sub>1</sub> (AH + HI + I)           | 968.51                   |                                 |                                |                       |
|          | TS <sub>1</sub>                        | 1,089.71                 |                                 |                                |                       |
|          | Step 1                                 |                          | 5.11x10 <sup>3</sup>            | 1.33x10 <sup>1</sup>           | 23.06                 |
|          | R <sub>2</sub> (AH + I <sub>2</sub> )  | 963.20                   |                                 |                                |                       |
|          | P <sub>2</sub> (A + HI+ I)             | 1,019.68                 |                                 |                                |                       |
|          | TS <sub>2</sub>                        | 1766.33                  |                                 |                                |                       |
|          | Step 2                                 |                          | 5.29 x10 <sup>4</sup>           | 1.74 x10 <sup>2</sup>          | 8.03 x10 <sup>2</sup> |
|          | R <sub>3</sub> (AH <sub>2</sub> + 2I)  | 952.60                   |                                 |                                |                       |
|          | P <sub>3</sub> (A +2I)                 | 1,139.04                 |                                 |                                |                       |
|          | TS <sub>3</sub>                        | 1,193.31                 |                                 |                                |                       |
|          | Step 3                                 |                          | 1.84 x10 <sup>2</sup>           | 1.91 x10 <sup>2</sup>          | 2.41 x10 <sup>2</sup> |
| Route II | R* (AH <sub>2</sub> + I <sub>2</sub> ) | 952.60                   |                                 |                                |                       |
|          | P* (A + 2HI)                           | 1,139.04                 |                                 |                                |                       |
|          | TS*                                    | 1,111.05                 |                                 |                                |                       |
|          | Step *                                 |                          | -7.11 x10 <sup>3</sup>          | 2.71 x10 <sup>1</sup>          | 44.40                 |

**Key:** where TS<sub>1</sub> is transition state 1; TS<sub>2</sub> is transition state 2; TS<sub>3</sub> is transition state 3 and TS\* is transition state for the one step cyclic complex mechanism R<sub>1</sub> (AH<sub>2</sub> + I), R<sub>2</sub> (AH + I<sub>2</sub>) and R<sub>3</sub> (AH<sub>2</sub> + 2I) are the reactants in steps 1, 2, 3, respectively; R<sub>3</sub> (AH<sub>2</sub> + 2I), P<sub>2</sub> (A + HI+ I), and P<sub>3</sub> (A +2I) the products of the respective steps, while E<sub>a1</sub>, E<sub>a2</sub> and E<sub>a3</sub> are the activation energies for steps 1, 2 and 3 for the chain multi-step mechanism. R\* (AH<sub>2</sub> + I<sub>2</sub>), P\* (A + 2HI) and E<sub>aB</sub>, are the reactants, products and activation energy for the one-step cyclic complex mechanism.

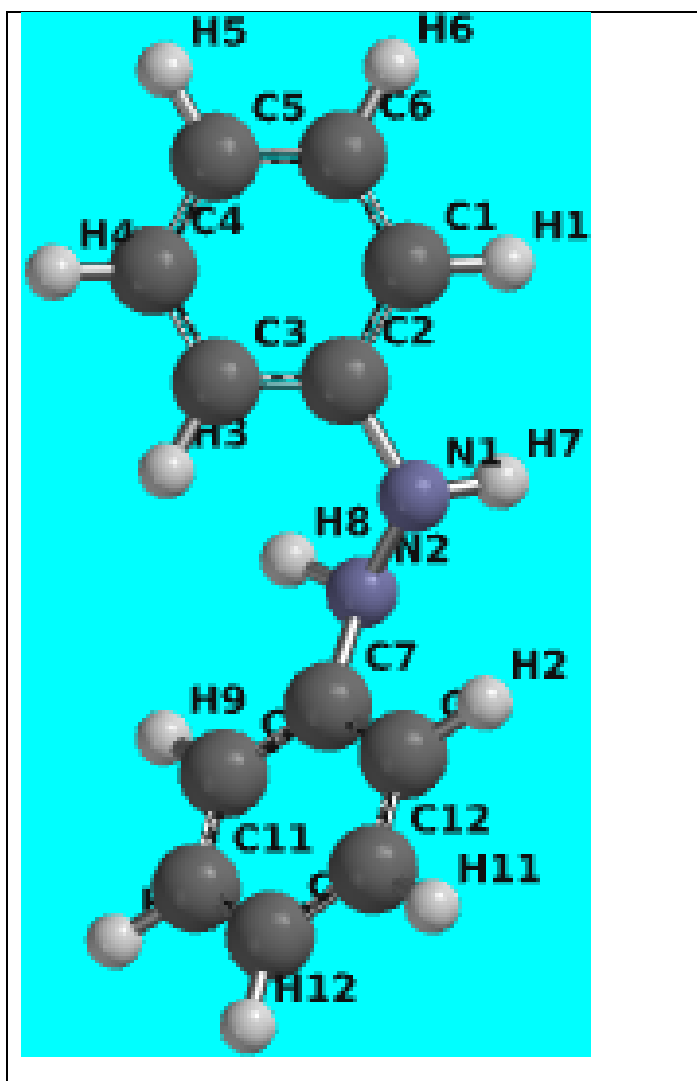


Figure 4.16: Labelled structure of 1,2-diphenylhydrazine

**Table 4.3 Bond length and exposed surface area of 1,2-diphenylhydrazine molecule**

| <b>Hydrogen Identity</b> | <b>Bond type</b> | <b>Bond Length<br/>(Å)</b> | <b>Exposed Surface<br/>Area (Å<sup>2</sup>)</b> |
|--------------------------|------------------|----------------------------|---|
| H1                       | C-H              | 1.097                      | 5.46  |
| H2                       | C-H              | 1.096                      | 5.56  |
| H3                       | C-H              | 1.097                      | 5.46  |
| H4                       | C-H              | 1.095                      | 5.44  |
| H5                       | C-H              | 1.095                      | 5.44  |
| H6                       | C-H              | 1.095                      | 5.44  |
| H7                       | N-H              | 0.998                      | 8.08  |
| H8                       | N-H              | 1.000                      | 6.58  |
| H9                       | C-H              | 1.097                      | 5.46  |
| H10                      | C-H              | 1.095                      | 5.44  |
| H11                      | C-H              | 1.095                      | 5.44  |
| H12                      | C-H              | 1.095                      | 5.44  |

**Table 4.4: Total electronic energy, heat of formation and other thermodynamic parameters of reacting species and products for L-tyrosine-iodine reaction system**

| S/N | Species                                     | Thermodynamic parameters at 298.15K using PM3 method |                              |                               | Electronic energy and thermodynamic parameters at 298.15K using DFT method* |                              |                               |
|-----|---|--|------------------------------|-------------------------------|---|------------------------------|-------------------------------|
|     |   | $\Delta H^\circ$<br>(kJ/mol)                         | $\Delta G^\circ$<br>(kJ/mol) | $\Delta S^\circ$<br>(kJ/mol.) | $E_e(\Delta H^\circ)$<br>(kJ/mol)   | $\Delta G^\circ$<br>(kJ/mol) | $\Delta S^\circ$<br>(J/mol.K) |
| 1   | I <sub>2</sub>                              | 114.05   | 36.73                        | 259.34                        | -36,334,477.09<br>-13,841.71  | -36,334,542.14<br>-13,841.73 | 260.55<br>0.10                |
| 2   | L-Tyr                                       | 100.73   | -37.67                       | 464.22                        | -1,654,299.96<br>-630.21  |                              |                               |
| 3   | TS <sub>1</sub>                             | 932.88   | 798.38                       | 451.10                        | -19,817,227.73<br>-7,549.42   | -36,998.46<br>-25.27         | -66,343.21<br>-14.09          |
| 4   | TS <sub>2</sub>                             | 1,001.15   | 844.71                       | 524.69                        | -19,817,240.74<br>-7,549.43   | -36,998.45<br>-25.27         | -66,343.26<br>-14.09          |
| 5   | TS <sub>3</sub>                             | 1,204.04   | 1,026.02                     | 597.10                        | -19,817,216.84<br>-7,549.42   | -36,998.46<br>-25.27         | -66,343.18<br>-14.09          |
| 6   | TS <sub>4</sub>                             | 1,095.16   | 946.62                       | 498.22                        | -19,816,905.20<br>-7,549.30   | -36,998.49<br>-25.27         | -66,343.17<br>-14.09          |
| 7   | MIT   | 513.01   | -11.11                       | 513.01                        | -19,816,427.88<br>-7,549.12   |                              |                               |
| 8   | HI  | 119.36   | 57.88                        | 206.18                        | -18,168,798.89<br>-6,921.45   |                              |                               |
| 9   | TS*   | 258.21   | 43.51                        | 720.09                        | -56,143,919.32<br>-21,388.16  | -40,708.64<br>-6.74          | -17,688.05<br>-15.51          |
| 10  | DIT   | 193.03   | 26.60                        | 558.22                        | -37,978,585.13<br>-14,468.03  |                              |                               |
| 11  | R <sub>1</sub><br>(L-Tyr + I <sub>2</sub> ) | 214.78   | 0.94                         | 723.56                        | -37,988,777.05<br>-14,471.92  |                              |                               |
| 12  | P <sub>1</sub><br>(MIT + HI)                | 632.37   | 46.11                        | 719.19                        | -37,985,226.77<br>-14,470.56  |                              |                               |
| 13  | R <sub>2</sub><br>(MIT + I <sub>2</sub> )   | 627.06   | 25.62                        | 772.35                        | -56,150,904.97<br>-21,390.82  |                              |                               |

\* The DFT result also presented in au units

**Key:**where I<sub>2</sub> is iodine molecule; L-Tyr is L-tyrosine ; MIT is monoiodo tyrosine; DIT is diiodo tyrosine; HI is hydrogen iodide; TS<sub>1</sub> is transition state 1; TS<sub>2</sub> is transition state 2; TS<sub>3</sub> is transition state 3; TS<sub>4</sub> is transition state 4 and TS\* is transition state for step 2. R<sub>1</sub> (L-Tyr + I<sub>2</sub>) and R<sub>2</sub> (MIT + I<sub>2</sub>) are the reactants in steps 1, 2, respectively and; P<sub>1</sub> (MIT + HI) and P<sub>2</sub> (DIT + HI) the products of the respective steps. E<sub>a1</sub> and E<sub>a2</sub> are the activation energies for steps 1 and 2, respectively.

**Table 4.5: Heat of formation, total electronic energy and other activation parameters of reacting species and products for L-tyrosine-iodine reaction system for the most favored pathway**

| S/<br>N | Species                                     | Activation parameters at 298.15K<br>using PM3 method |                                 |                                 | Electronic energy and activation parameters<br>at 298.15K using DFT method** |                                  |                                   |
|---------|---|--|---------------------------------|---------------------------------|--|----------------------------------|-----------------------------------|
|         |   | $\Delta_r H^0$<br>(kJ/mol)                           | $\Delta^\ddagger G$<br>(kJ/mol) | $\Delta^\ddagger S$<br>(J/mol.) | $E_e (\Delta_r H^0)$<br>(kJ/mol)   | $\Delta^\ddagger G$<br>(kJ/mol)  | $\Delta^\ddagger S$<br>(J/mol.)   |
| 1       | R <sub>1</sub><br>(L-Tyr + I <sub>2</sub> ) | 214.78   |                                 |                                 | -37,988,777.05<br>-14,471.92   |                                  |                                   |
| 2       | P <sub>1</sub><br>(MIT + HI)                | 632.37   |                                 |                                 | -37,985,226.77<br>-14,470.56   |                                  |                                   |
| 3       | TS <sub>2</sub>                             | 1,001.15   |                                 |                                 | -19,817,240.74<br>-75,49.43  |                                  |                                   |
| 4       | Step I                                      |  | -6.93 x10 <sup>4</sup>          | -2.32 x10 <sup>3</sup>          |  | -1.10 x10 <sup>5</sup><br>-48.76 | -1.28 x10 <sup>5</sup><br>-41.90  |
| 5       | E <sub>a1</sub>                             | 4.18x10 <sup>2</sup>                                 |                                 |                                 | 3.52 x10 <sup>3</sup><br>1.34  |                                  |                                   |
| 6       | R <sub>2</sub><br>(MIT + I <sub>2</sub> )   | 627.06   |                                 |                                 | -56,150,904.97<br>-21390.82  |                                  |                                   |
| 7       | P <sub>2</sub><br>(DIT + HI)                | 312.39   |                                 |                                 | -56,147,384.02<br>-21,389.48   |                                  |                                   |
| 8       | TS*   | 258.21   |                                 |                                 | -56,143,919.32<br>-21,388.16   |                                  |                                   |
| 9       | Step II                                     |  | -2.56 x10 <sup>4</sup>          | 7.72 x10 <sup>2</sup>           |  | -3.08 x10 <sup>5</sup><br>-72    | -1.89 x10 <sup>5</sup><br>-117.33 |
| 10      | E <sub>a2</sub>                             | 3.69x10 <sup>2</sup>                                 |                                 |                                 | 6.99 x10 <sup>3</sup><br>2.66  |                                  |                                   |

\*\* The DFT result also presented in au units

**Key:** TS<sub>1</sub> is transition state 1; TS<sub>2</sub> is transition state 2; TS<sub>3</sub> is transition state 3; TS<sub>4</sub> is transition state 4 and TS\* is transition state for step 2. R<sub>1</sub> (L-Tyr + I<sub>2</sub>) and R<sub>2</sub> (MIT + I<sub>2</sub>) are the reactants in steps 1, 2, respectively and; P<sub>1</sub> (MIT + HI) and P<sub>2</sub> (DIT + HI) the products of the respective steps. E<sub>a1</sub> and E<sub>a2</sub> are the activation energies for steps 1 and 2, respectively.

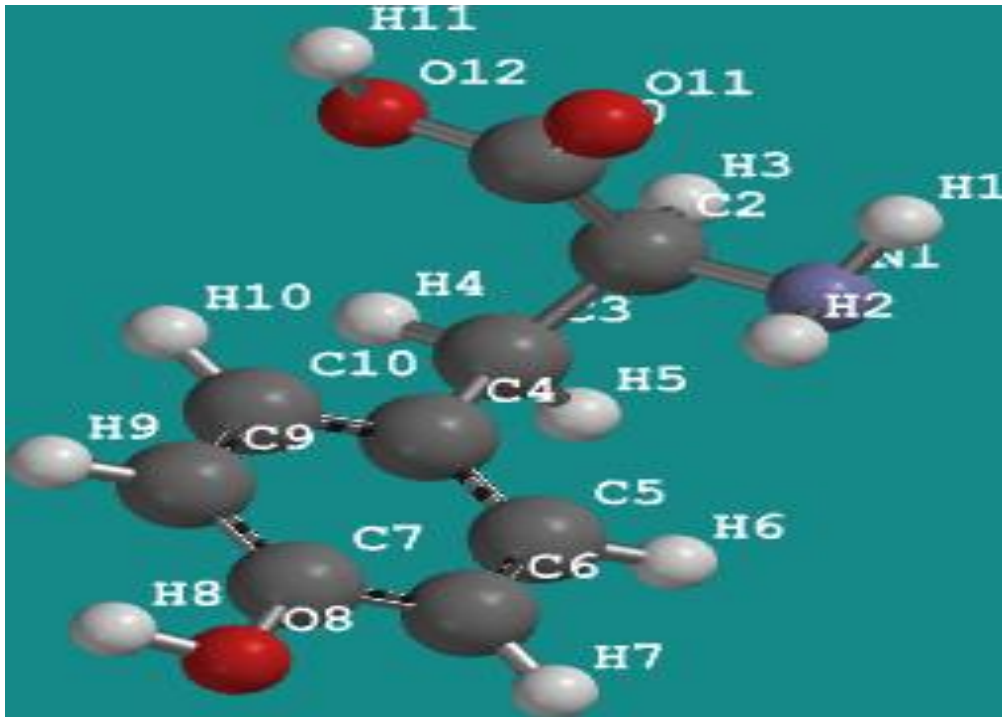


Figure 4.17: Labelled structure of L-tyrosine

**Table 4.6: Net atomic charges and exposed surface area of L-tyrosine molecule**

| No.            | Charge    | Exposed surface area (Å <sup>2</sup> ) | No.            | Charge    | Exposed surface area (Å <sup>2</sup> ) |
|----------------|-----------|--|----------------|-----------|--|
| C <sub>1</sub> | -0.003753 | 13.11                                  | C <sub>8</sub> | 0.230113  | 5.13                                   |
| C <sub>2</sub> | 0.032617  | 4.88                                   | C <sub>9</sub> | 0.765132  | 13.12                                  |
| C <sub>3</sub> | -0.015731 | 12.96                                  | O <sub>1</sub> | -0.563147 | 11.44                                  |
| C <sub>4</sub> | -0.304182 | 13.92                                  | N <sub>1</sub> | -0.845714 | 7.88                                   |
| C <sub>5</sub> | 0.535871  | 9.10                                   | O <sub>2</sub> | -0.531727 | 14.30                                  |
| C <sub>6</sub> | -0.333762 | 13.68                                  | O <sub>3</sub> | -0.553559 | 11.40                                  |
| C <sub>7</sub> | -0.166882 | 8.69                                   |                |           |  |

**Table 4.7: Bond lengths of the reactive sites of the transition states for L-tyrosine system**

| <b>Transition states</b> | <b>Bond lengths (Å)</b> |                        |                        |
|--------------------------|-------------------------|------------------------|------------------------|
|                          | <b>C<sub>6</sub>-I</b>  | <b>C<sub>6</sub>-H</b> | <b>C<sub>4</sub>-H</b> |
| <b>TS<sub>1</sub></b>    | 2.376                   | 1.092                  | 1.105                  |
| <b>TS<sub>2</sub></b>    | 2.020                   | 1.126                  | 1.105                  |
| <b>TS<sub>3</sub></b>    | 8.139                   | 1.092                  | 1.092                  |
| <b>TS<sub>4</sub></b>    | 2.376                   | 1.092                  | 1.105                  |

**Table 4.8: Total electronic energy and other thermodynamic parameter at standard condition of 1 atmosphere and 298.15K of reacting species and products of L-ascorbic acid system for DFT studies route 1**

| S/N | Species                               | $E_e$<br>(kJ/mol) | $E_e$<br>(au) | $\Delta G^\circ$<br>(kJ/mol) | $\Delta S^\circ$<br>(J/mol.K) |
|-----|---------------------------------------|-------------------|---------------|------------------------------|-------------------------------|
| 1   | I <sub>2</sub>                        | -36,327,532.08    | -13,839.06    |                              |                               |
| 2   | AA                                    | -1,801,259.01     | -686.19       |                              |                               |
| 3   | TS <sub>1</sub>                       | -38,125,652.92    | -14,524.06    | -43,700.00<br>(-48.66 au)    | -127,727.50<br>(-16.65 au)    |
| 4   | DAA                                   | -1,794,848.60     | -683.75       |                              |                               |
| 5   | HI                                    | -18,168,774.40    | -6,921.44     |                              |                               |
| 6   | R <sub>1</sub> (AA + I <sub>2</sub> ) | -38,128,791.09    | -14,525.25    |                              |                               |
| 7   | P <sub>1</sub> (DAA + HI)             | -38,132,397.40    | -14,526.63    |                              |                               |
| 8   | E <sub>a1</sub>                       | +3,138.17         | 1.20          |                              |                               |

**Key:**where I<sub>2</sub> is iodine molecule, AA is L-ascorbic acid, TS<sub>1</sub> is transition state for route 1, DAA is dehydroascorbic acid, HI is hydrogen iodide molecule, R<sub>1</sub> (AA + I<sub>2</sub>) are all the reactants for route 1, P<sub>1</sub> (DAA + HI) are all the products for route 1, E<sub>a1</sub> is the activation energy for route 1, TS<sub>B1</sub> is the first transition state for route 2, I<sup>-</sup> is iodide ion, TS<sub>B2</sub> is the second transition state for route 2, R<sub>B1</sub> (AA + 2I<sub>2</sub>) and R<sub>B2</sub> (AA + 2 I<sup>-</sup>) are all the reactants in steps 1 and 2 respectively for route 2, P<sub>B1</sub> (DAA + 2HI + 2I<sup>-</sup>) and P<sub>B2</sub> (DAA + 2HI) are the products of reactions for steps 1 and 2 respectively for route 2, while E<sub>aB1</sub> and E<sub>aB2</sub> are the activation energies for steps 1 and 2, respectively, in route 2.

**Table 4.9: Total electronic energy and other thermodynamic parameters at standard condition of 1 atmosphere and 298.15K of reacting species and products of L-ascorbic acid system for DFT studies route II**

| S/N | Species                            | $E_e$<br>(kJ/mol) | $E_e$<br>(au) | $\Delta G^\circ$<br>(kJ/mol) | $\Delta S^\circ$<br>(J/mol.K) |
|-----|------------------------------------|-------------------|---------------|------------------------------|-------------------------------|
| 1   | $I_2$                              | -36,327,532.08    | -13,839.06    |                              |                               |
| 2   | AA                                 | -1,801,259.01     | -686.19       |                              |                               |
| 3   | $TS_{B1}$                          | -74,453,171.82    | -28363.11     | -43,105.31<br>(-95.08 au)    | -249,572.59<br>(-16.42 au)    |
| 4   | DAA                                | -1,794,848.60     | -683.75       |                              |                               |
| 5   | HI                                 | -18,168,774.40    | -6921.44      |                              |                               |
| 6   | $I^-$                              | -18,167,470.45    | -6920.94      |                              |                               |
| 7   | $TS_{B2}$                          | -38,125,681.68    | -14524.07     | -43,691.96<br>(-48.66 au)    | -127,727.62<br>(-16.64 au)    |
| 8   | $R_{B1} (AA + 2I_2)$               | -74,456,323.17    | -28364.31     |                              |                               |
| 9   | $P_{B1}$<br>(DAA + 2HI + 2 $I^-$ ) | -74,467,338.30    | -28368.51     |                              |                               |
| 10  | $R_{B2} (AA + 2I^-)$               | -38,136,199.91    | -14528.08     |                              |                               |
| 11  | $P_{B2} (DAA + 2HI)$               | -38,132,397.40    | -14526.63     |                              |                               |
| 12  | $E_{aB1}$                          | +3,151.35         | 1.20          |                              |                               |
| 13  | $E_{aB2}$                          | +10,518.23        | 4.01          |                              |                               |

**Key:** where  $I_2$  is iodine molecule, AA is L-ascorbic acid,  $TS_1$  is transition state for route 1, DAA is dehydroascorbic acid, HI is hydrogen iodide molecule,  $R_1 (AA + I_2)$  are all the reactants for route 1,  $P_1 (DAA + HI)$  are all the products for route 1,  $E_{a1}$  is the activation energy for route 1,  $TS_{B1}$  is the first transition state for route 2,  $I^-$  is iodide ion,  $TS_{B2}$  is the second transition state for route 2,  $R_{B1} (AA + 2I_2)$  and  $R_{B2} (AA + 2I^-)$  are all the reactants in steps 1 and 2 respectively for route 2,  $P_{B1} (DAA + 2HI + 2I^-)$  and  $P_{B2} (DAA + 2HI)$  are the products of reactions for steps 1 and 2 respectively for route 2, while  $E_{aB1}$  and  $E_{aB2}$  are the activation energies for steps 1 and 2, respectively, in route 2.

**Table 4.10: Total electronic energy and other activation parameters at standard condition of 1 atmosphere and 298.15K of reacting species and products of L-ascorbic acid system for DFT studies route I and route II**

| Route    | Species                  | $E_e (\Delta_r H^0)$<br>(kJ/mol) | $E_e (\Delta_r H^0)$<br>(au) | $\Delta^\ddagger G$<br>(kJ/mol)   | $\Delta^\ddagger S$<br>(J/mol.K) |
|----------|--------------------------|----------------------------------|------------------------------|-----------------------------------|----------------------------------|
| Route I  | $R_1(AA + I_2)$          | -38,128,791.09                   | -14525.25                    |                                   |                                  |
|          | $P_1(DAA + HI)$          | -38,132,397.40                   | -14526.63                    |                                   |                                  |
|          | $TS_1$                   | -38,125,652.92                   | -14524.06                    |                                   |                                  |
|          | Step I                   |                                  |                              | $-2.93 \times 10^4$<br>(-48.76au) | $1.28 \times 10^5$<br>(11.16au)  |
|          | $E_{a1}$                 | $3.14 \times 10^3$               | 1.20                         |                                   |                                  |
| Route II | $R_{B1}(AA + 2I_2)$      | -74,456,323.17                   | -28364.31                    |                                   |                                  |
|          | $P_{B1}(DAA + 2HI + 2I)$ | -74,467,338.30                   | -28368.51                    |                                   |                                  |
|          | $TS_{B1}$                | -74,453,171.82                   | -28363.11                    |                                   |                                  |
|          | Step I                   |                                  |                              | $-2.99 \times 10^4$<br>(-95.24au) | $2.50 \times 10^5$<br>(11.39au)  |
|          | $E_{aB1}$                | $3.15 \times 10^3$               | 1.20                         |                                   |                                  |
|          | $R_{B2}(AA + 2I)$        | -38,136,199.91                   | -14528.08                    |                                   |                                  |
|          | $P_{B2}(DAA + 2HI)$      | -38,132,397.40                   | -14526.63                    |                                   |                                  |
|          | $TS_{B2}$                | -38,125,681.68                   | -14524.07                    |                                   |                                  |
|          | Step II                  |                                  |                              | $-2.93 \times 10^4$<br>(-48.76au) | $1.28 \times 10^5$<br>(11.16au)  |
|          | $E_{aB2}$                | $1.05 \times 10^4$               | -14525.25                    |                                   |                                  |

**Key:** where  $R_1(AA + I_2)$  are all the reactants for route 1,  $P_1(DAA + HI)$  are all the products for route 1,  $E_{a1}$  is the activation energy for route 1,  $TS_{B1}$  is the first transition state for route 2,  $I^-$  is iodide ion,  $TS_{B2}$  is the second transition state for route 2,  $R_{B1}(AA + 2I_2)$  and  $R_{B2}(AA + 2I^-)$  are all the reactants in steps 1 and 2 respectively for route 2,  $P_{B1}(DAA + 2HI + 2I^-)$  and  $P_{B2}(DAA + 2HI)$  are the products of reactions for steps 1 and 2 respectively for route 2, while  $E_{aB1}$  and  $E_{aB2}$  are the activation energies for steps 1 and 2, respectively, in route 2.

**Table 4.11: Heat of formation and other thermodynamic parameters at standard condition of 1 atmosphere and 298.15K of reacting species and products of L-ascorbic acid system for PM3 studies**

| S/N | Species                                  | Route 1                      |                              |                               | Species   | Route II                     |                              |                               |
|-----|--|------------------------------|------------------------------|-------------------------------|---|------------------------------|------------------------------|-------------------------------|
|     |  | $\Delta H^\circ$<br>(kJ/mol) | $\Delta G^\circ$<br>(kJ/mol) | $\Delta S^\circ$<br>(J/mol.K) |   | $\Delta H^\circ$<br>(kJ/mol) | $\Delta G^\circ$<br>(kJ/mol) | $\Delta S^\circ$<br>(J/mol.K) |
| 1   | I <sub>2</sub>                           | 99.61                        | 22.70                        | 257.97                        | I <sub>2</sub>                                    | 99.61                        | 22.70                        | 257.97                        |
| 2   | AA                                       | -973.83                      | -705.13                      | 451.41                        | AA  | -973.83                      | -705.13                      | 451.41                        |
| 3   | TS <sub>1</sub>                          | -462.69                      | -643.83                      | 607.55                        | TS <sub>B1</sub>                                  | -351.56                      | -590.46                      | 801.27                        |
| 4   | DAA                                      | -924.50                      | -694.55                      | 440.80                        | DAA   | -924.50                      | -694.55                      | 440.80                        |
| 5   | HI                                       | 120.53                       | 85.01                        | 207.02                        | HI  | 120.53                       | 85.01                        | 207.02                        |
| 6   | R <sub>1</sub><br>(AA + I <sub>2</sub> ) | -874.22                      |                              |                               | TS <sub>B2</sub>                                  | -632.22                      | -1286.54                     | 669.50                        |
| 7   | P <sub>1</sub><br>(DAA + HI)             | -683.44                      |                              |                               | I <sup>-</sup>                                    | 0.00                         |                              |                               |
| 8   |  |                              |                              |                               | R <sub>B1</sub><br>(AA + 2I <sub>2</sub> )        | -774.61                      |                              |                               |
| 9   |  |                              |                              |                               | P <sub>B1</sub><br>(DAA + 2HI + 2I <sup>-</sup> ) | -683.44                      |                              |                               |
| 10  |  |                              |                              |                               | R <sub>B2</sub><br>(AA + 2 I <sup>-</sup> )       | -973.83                      |                              |                               |
| 11  |  |                              |                              |                               | P <sub>B2</sub><br>(DAA + 2HI)                    | -683.44                      |                              |                               |

**Key:** where R<sub>1</sub> (AA + I<sub>2</sub>) are all the reactants for route 1, P<sub>1</sub> (DAA + HI) are all the products for route 1, E<sub>a1</sub> is the activation energy for route 1, TS<sub>B1</sub> is the first transition state for route 2, I<sup>-</sup> is iodide ion, TS<sub>B2</sub> is the second transition state for route 2, R<sub>B1</sub> (AA + 2I<sub>2</sub>) and R<sub>B2</sub> (AA + 2 I<sup>-</sup>) are all the reactants in steps 1 and 2 respectively for route 2, P<sub>B1</sub> (DAA + 2HI + 2I<sup>-</sup>) and P<sub>B2</sub> (DAA + 2HI) are the products of reactions for steps 1 and 2 respectively for route 2, while E<sub>aB1</sub> and E<sub>aB2</sub> are the activation energies for steps 1 and 2, respectively, in route 2.

**Table 4.12: Heat of formation and other activation parameter at standard condition of 1 atmosphere and 298.15K of reacting species and products of L-ascorbic acid system for PM3 studies**

| Route 1         |                                |                                 |                                 | Route II         |                                |                                 |                                 |
|-----------------|--------------------------------|---------------------------------|---------------------------------|------------------|--------------------------------|---------------------------------|---------------------------------|
| Species         | $\Delta_r H^\circ$<br>(kJ/mol) | $\Delta^\ddagger G$<br>(kJ/mol) | $\Delta^\ddagger S$<br>(J/mol.) | Species          | $\Delta_r H^\circ$<br>(kJ/mol) | $\Delta^\ddagger G$<br>(kJ/mol) | $\Delta^\ddagger S$<br>(J/mol.) |
| R <sub>1</sub>  | -874.22                        |                                 |                                 | R <sub>B1</sub>  | -774.61                        |                                 |                                 |
| P <sub>1</sub>  | -683.44                        |                                 |                                 | P <sub>B1</sub>  | -683.44                        |                                 |                                 |
| TS <sub>1</sub> | -462.69                        |                                 |                                 | TS <sub>B1</sub> | -351.56                        |                                 |                                 |
| Step I          |                                | 1.16x10 <sup>4</sup>            | 3.59 x10 <sup>1</sup>           | Step I           |                                | -1.89x10 <sup>4</sup>           | -6.61x10 <sup>1</sup>           |
| E <sub>a1</sub> | 4.12x10 <sup>2</sup>           |                                 |                                 | E <sub>aB1</sub> | 4.23x10 <sup>2</sup>           |                                 |                                 |
|                 |                                |                                 |                                 | R <sub>B2</sub>  | -973.83                        |                                 |                                 |
|                 |                                |                                 |                                 | P <sub>B2</sub>  | -683.44                        |                                 |                                 |
|                 |                                |                                 |                                 | TS <sub>B2</sub> | -632.22                        |                                 |                                 |
|                 |                                |                                 |                                 | Step II          |                                | -7.50 x10 <sup>5</sup>          | -2.51x10 <sup>3</sup>           |
|                 |                                |                                 |                                 | E <sub>aB2</sub> | 3.42x10 <sup>2</sup>           |                                 |                                 |

**Key:** where R<sub>1</sub> (AA + I<sub>2</sub>) are all the reactants for route 1, P<sub>1</sub> (DAA + HI) are all the products for route 1, E<sub>a1</sub> is the activation energy for route 1, TS<sub>B1</sub> is the first transition state for route 2, I is iodide ion, TS<sub>B2</sub> is the second transition state for route 2, R<sub>B1</sub> (AA + 2I<sub>2</sub>) and R<sub>B2</sub> (AA + 2 I) are all the reactants in steps 1 and 2 respectively for route 2, P<sub>B1</sub> (DAA + 2HI + 2I) and P<sub>B2</sub> (DAA + 2HI) are the products of reactions for steps 1 and 2 respectively for route 2, while E<sub>aB1</sub> and E<sub>aB2</sub> are the activation energies for steps 1 and 2, respectively, in route 2.



**Table 4.13: Molecular information of the optimized L-ascorbic acid molecule**

| <b>Hydrogen Identity</b> | <b>Bond Type</b> | <b>Bond Length (Å)</b> | <b>Exposed surface area (Å<sup>2</sup>)</b> |
|--------------------------|------------------|------------------------|---|
| H1                       | O-H              | 0.951                  | 8.05  |
| H2                       | C-H              | 1.115                  | 5.59  |
| H3                       | O-H              | 0.950                  | 8.06  |
| H4                       | C-H              | 1.117                  | 5.68  |
| H5                       | O-H              | 0.948                  | 7.59  |
| H6                       | O-H              | 0.949                  | 7.95  |
| H7                       | C-H              | 1.104                  | 4.93  |
| H8                       | C-H              | 1.108                  | 5.58  |

**Table 4.14: Total electronic energy and other thermodynamic parameters of reacting species and products according to the DFT method for D-fructose system**

| DFT method*** |                      |                              |                              |                              |                              |
|---------------|----------------------|------------------------------|------------------------------|------------------------------|------------------------------|
| S/<br>N       | Species              | E <sub>e</sub><br>(kJ/mol)   | ΔH <sup>o</sup><br>(kJ/mol)  | ΔG <sup>o</sup><br>(kJ/mol)  | ΔS <sup>o</sup><br>(J/mol.K) |
| 1             | I <sub>2</sub>       | -36,334,477.09<br>-13,841.71 | -36,334,465.70<br>-13,841.73 | -36,334,542.14<br>-13,841.70 | 260.55<br>0.10               |
| 2             | Fruc                 | -1,804,759.03<br>-687.53     | -1,804,217.04<br>-687.37     | -1,804,348.58<br>-687.32     | 441.18<br>0.17               |
| 3             | H <sub>2</sub> O     | -200,741.83<br>-76.47        | -200,678.03<br>-76.47        | -200,732.28<br>-76.45        | 188.64<br>0.07               |
| 4             | TS <sub>1</sub>      | -36,535,028.53<br>-13,918.12 | -36,534,957.18<br>-13,918.12 | -36,535,052.36<br>-13,918.08 | 319.24<br>0.12               |
| 5             | HOI                  | -18,366,263.09<br>-6,996.67  | -18,366,219.67<br>-6,996.68  | -18,366,295.58<br>-6,996.66  | 254.58<br>0.10               |
| 6             | HI                   | -18,168,798.89<br>-6,921.45  | -18,168,774.40<br>-6,921.46  | -18,168,835.99<br>-6,921.44  | 206.59<br>0.08               |
| 7             | A (TS <sub>2</sub> ) | -20,167,206.70<br>-7,682.75  | -20,165,007.67<br>-7,681.68  | -20,164,402.44<br>-7,681.91  | -2,029.95<br>-0.77           |
| 8             | B (int)              | -20,170,829.18<br>-7,684.13  | -20,164,777.93<br>-7,681.67  | -20,164,374.51<br>-7,681.82  | -1,353.08<br>-0.52           |
| 9             | C (TS <sub>3</sub> ) | -20,167,013.56<br>-7,682.67  | -20,160,963.46<br>-7,680.21  | -20,160,560.12<br>-7,680.37  | -1,352.81<br>-0.52           |
| 10            | D (int)              | -20,167,177.06<br>-7,682.73  | -20,166,585.18<br>-7,682.57  | -20,166,734.57<br>-7,682.51  | 501.13<br>0.19               |
| 11            | E                    | -1,804,719.71<br>-687.51     | -1,803,829.56<br>-687.22     | -1,803,960.62<br>-687.17     | 439.66<br>0.17               |

| DFT method*** |  |                              |                              |                              |                              |
|---------------|--|------------------------------|------------------------------|------------------------------|------------------------------|
| S/<br>N       | Species  | E <sub>e</sub><br>(kJ/mol)   | ΔH <sup>o</sup><br>(kJ/mol)  | ΔG <sup>o</sup><br>(kJ/mol)  | ΔS <sup>o</sup><br>(J/mol.K) |
| 12            | R <sub>1</sub> (I <sub>2</sub> + H <sub>2</sub> O) | -36,535,218.92<br>-13,918.18 | -36,535,143.73<br>-13,918.20 | -36,535,274.42<br>-13,918.15 | 449.19<br>0.17               |
| 13            | P <sub>1</sub> (HOI + HI)                          | -36,535,061.98<br>-13,918.12 | -36,534,994.07<br>-13,918.15 | -36,535,131.57<br>-13,918.09 | 461.17<br>0.17               |
| 14            | R <sub>2</sub> (HOI+ Fruc)                         | -20,171,022.12<br>-7,684.20  | -20,170,436.71<br>-7,684.05  | -20,170,644.16<br>-7,684.05  | 695.76<br>0.18               |
| 15            | P <sub>2</sub> (B int)                             | -20,170,829.18<br>-7,684.13  | -20,164,777.93<br>-7,681.67  | -20,164,374.51<br>-7,681.82  | -1,353.08<br>0.27            |
| 16            | R <sub>3</sub> (B int)                             | -20,170,829.18<br>-7,684.13  | -20,164,777.93<br>-7,681.67  | -20,164,374.51<br>-7,681.82  | -1,353.08<br>-0.52           |
| 17            | P <sub>3</sub> (E + HOI)                           | -20,170,982.80<br>-7,684.18  | -20,170,049.23<br>-7,683.91  | -20,170,256.20<br>-7,683.83  | 694.24<br>0.26               |
| 18            | E <sub>a1</sub>                                    | 190.39<br>0.07               |                              |                              |                              |
| 19            | E <sub>a2</sub>                                    | 3,815.42<br>1.45             |                              |                              |                              |
| 20            | E <sub>a3</sub>                                    | 3,815.62<br>1.45             |                              |                              |                              |

\*\*\* The DFT result also presented in au units

**Key:** Where I<sub>2</sub> is iodine molecule, Fruc is D-Fructose, H<sub>2</sub>O is water molecule, TS<sub>1</sub> is transition state for step 1, HOI is hypiodous acid, HI is hydrogen iodide molecule, R<sub>1</sub>(I<sub>2</sub> + H<sub>2</sub>O) are all the reactants for step 1, R<sub>2</sub>(HOI+ Fruc) are all the reactants for step 2, R<sub>3</sub>(B int) are all the products for step 3, TS<sub>1</sub>, TS<sub>2</sub>, TS<sub>3</sub> are the transition state for steps 1, 2 and 3, respectively; P<sub>1</sub>(HOI + HI), P<sub>2</sub>(B int) and P<sub>3</sub>(E + HOI) are the products of reactions for steps 1, 2 and 3, respectively, while E<sub>a1</sub> is the activation energy for step 1, E<sub>a2</sub> and E<sub>a3</sub> are the activation energies for steps 2 and 3 respectively. D is the intermediate is step 3.

**Table 4.15: Total electronic energy and other activation parameters of reacting species and products according to the DFT method for D-fructose system**

| Species  | $E_e$<br>(kJ/mol)                | $\Delta^\ddagger G$<br>(kJ/mol)       | $\Delta^\ddagger S$<br>(J/mol.K)     | $\Delta^\ddagger E_a$<br>(kJ/mol)  |
|--|----------------------------------|---------------------------------------|--------------------------------------|------------------------------------|
| R <sub>1</sub> (I <sub>2</sub> + H <sub>2</sub> O) | -36,535,218.92<br>(-13918.18 au) |                                       |                                      |                                    |
| P <sub>1</sub> (HOI + HI)                          | -36,535,061.98<br>(-13918.12 au) |                                       |                                      |                                    |
| TS <sub>1</sub>                                    | -36,535,028.53<br>(-13918.11 au) |                                       |                                      |                                    |
| Step I   |                                  | -4.54 x10 <sup>5</sup><br>(-46.48 au) | 1.22 x10 <sup>5</sup><br>(172.95 au) | 1.90 x10 <sup>2</sup><br>(0.07 au) |
| R <sub>2</sub> (HOI+ Fruc)                         | -20,171,022.12<br>(-7684.20 au)  |                                       |                                      |                                    |
| P <sub>2</sub> (B int)                             | -20,170,829.18<br>(-7684.13 au)  |                                       |                                      |                                    |
| A (TS <sub>2</sub> )                               | -20,167,206.70<br>(-7682.75 au)  |                                       |                                      |                                    |
| Step II  |                                  | -5.88 x10 <sup>4</sup><br>(-25.71 au) | (6.75 x10 <sup>4</sup><br>(22.40 au) | 3.82 x10 <sup>3</sup><br>(1.46 au) |
| R <sub>3</sub> (B int)                             | -20,170,829.18<br>(-7684.13 au)  |                                       |                                      |                                    |
| P <sub>3</sub> (E + HOI)                           | -20,170,982.80<br>(-7684.18 au)  |                                       |                                      |                                    |
| C (TS <sub>3</sub> )                               | -20,167,013.56<br>(-7682.67 au)  |                                       |                                      |                                    |
| Step III   |                                  | -6.78 x10 <sup>4</sup><br>(-25.68 au) | 6.74 x10 <sup>4</sup><br>(25.83 au)  | 3.82 x10 <sup>3</sup><br>(1.46 au) |

**Key:** Where R<sub>1</sub>(I<sub>2</sub> + H<sub>2</sub>O) are all the reactants for step 1, R<sub>2</sub>(HOI+ Fruc) are all the reactants for step 2, R<sub>3</sub>(B int) are all the products for step 3, TS<sub>1</sub>, TS<sub>2</sub>, TS<sub>3</sub> are the transition state for steps 1, 2 and 3, respectively; P<sub>1</sub>(HOI + HI), P<sub>2</sub>(B int) and P<sub>3</sub>(E + HOI) are the products of reactions for steps 1, 2 and 3, respectively, while E<sub>a1</sub> is the activation energy for step 1, E<sub>a2</sub> and E<sub>a3</sub> are the activation energies for steps 2 and 3 respectively. D is the intermediate in step 3.

**Table 4.16: Heat of formation and other thermodynamic parameters of reacting species and products according to the PM3 method for D-fructose system**

| S/N | Species  | $\Delta H^\circ$<br>(kJ/mol) | $\Delta G^\circ$<br>(kJ/mol) | $\Delta S^\circ$<br>(J/mol.K) |
|-----|--|------------------------------|------------------------------|-------------------------------|
| 1   | I <sub>2</sub>                                     | 99.61                        | 22.70                        | 257.97                        |
| 2   | Fruc   | -561.41                      | -790.76                      | 480.88                        |
| 3   | H <sub>2</sub> O                                   | -156.18                      | -212.30                      | 188.24                        |
| 4   | TS <sub>1</sub>                                    | 133.26                       | 34.45                        | 331.47                        |
| 5   | HOI  | -32.62                       | -107.77                      | 252.12                        |
| 6   | HI   | 120.53                       | 85.01                        | 207.02                        |
| 7   | A (TS <sub>2</sub> )                               | -602.34                      | -790.02                      | 629.62                        |
| 8   | B (int)  | -440.35                      | -611.17                      | 573.05                        |
| 9   | C (TS <sub>3</sub> )                               | -603.65                      | -782.68                      | 600.59                        |
| 10  | D (int)  | -575.45                      | -765.64                      | 638.04                        |
| 11  | E  | -543.34                      | -687.51                      | 483.64                        |
| 12  | R <sub>1</sub> (I <sub>2</sub> + H <sub>2</sub> O) | -56.57                       | -189.60                      | 446.21                        |
| 13  | P <sub>1</sub> (HOI + HI)                          | 87.91                        | -22.76                       | 459.14                        |
| 14  | R <sub>2</sub> (HOI + Fruc)                        | -604.03                      | -898.53                      | 733.00                        |
| 15  | P <sub>2</sub> (B int)                             | -440.35                      | -611.17                      | 573.05                        |
| 16  | R <sub>3</sub> (B int)                             | -440.35                      | -611.17                      | 573.05                        |
| 17  | P <sub>3</sub> (E + HOI)                           | -575.96                      | -795.28                      | 735.76                        |
| 19  | Ea <sub>1</sub>                                    | 189.83                       |                              |                               |
| 20  | Ea <sub>2</sub>                                    | 1.71                         |                              |                               |
| 21  | Ea <sub>3</sub>                                    | -163.3                       |                              |                               |

**Key:** Where I<sub>2</sub> is iodine molecule, Fruc is D-Fructose, H<sub>2</sub>O is water molecule, TS<sub>1</sub> is transition state for step 1, HOI is hypoiodous acid, HI is hydrogen iodide molecule, R<sub>1</sub>(I<sub>2</sub> + H<sub>2</sub>O) are all the reactants for step 1, R<sub>2</sub> (HOI+ Fruc) are all the reactants for step 2, R<sub>3</sub> (B int)are all the products for step 3, TS<sub>1</sub>, TS<sub>2</sub>, TS<sub>3</sub> are the transition state for steps 1, 2 and 3, respectively; P<sub>1</sub> (HOI + HI), P<sub>2</sub> (B int)and P<sub>3</sub> (E + HOI)are the products of reactions for steps 1, 2 and 3, respectively, while Ea<sub>1</sub> is the activation energy for step 1, Ea<sub>2</sub> and Ea<sub>3</sub> are the activation energies for steps 2 and 3 respectively. D is the intermediate is step 3.

**Table 4.17: Heat of formation and other activation parameters of reacting species and products according to the PM3 method at 298.15K for D-fructose system**

| Species  | $\Delta_f H^\circ$<br>(kJ/mol) | $\Delta^\ddagger G$<br>(kJ/mol) | $\Delta^\ddagger S$<br>(J/mol.K) | $\Delta^\ddagger E_a$<br>(kJ/mol) |
|--|--------------------------------|---------------------------------|----------------------------------|-----------------------------------|
| R <sub>1</sub> (I <sub>2</sub> + H <sub>2</sub> O) | -56.57                         |                                 |                                  |                                   |
| P <sub>1</sub> (HOI + HI)                          | 87.91                          |                                 |                                  |                                   |
| TS <sub>1</sub>                                    | 133.26                         |                                 |                                  |                                   |
| Step I   |                                | -1.51 x10 <sup>5</sup>          | 5.06 x10 <sup>2</sup>            | 1.90 x10 <sup>2</sup>             |
| R <sub>2</sub> (HOI+ Fruc)                         | -604.03                        |                                 |                                  |                                   |
| P <sub>2</sub> (B int)                             | -440.35                        |                                 |                                  |                                   |
| A (TS <sub>2</sub> )                               | -602.34                        |                                 |                                  |                                   |
| Step II  |                                | 8.57 x10 <sup>4</sup>           | -2.90 x10 <sup>2</sup>           | 1.71                              |
| R <sub>3</sub> (B int)                             | -440.35                        |                                 |                                  |                                   |
| P <sub>3</sub> (E + HOI)                           | -575.96                        |                                 |                                  |                                   |
| C (TS <sub>3</sub> )                               | -603.65                        |                                 |                                  |                                   |
| Step III   |                                | 2.45 x10 <sup>5</sup>           | -8.47 x10 <sup>2</sup>           | 1.63 x10 <sup>2</sup>             |

**Key:** Where R<sub>1</sub>(I<sub>2</sub> + H<sub>2</sub>O) are all the reactants for step 1, R<sub>2</sub>(HOI+ Fruc) are all the reactants for step 2, R<sub>3</sub>(B int) are all the products for step 3, TS<sub>1</sub>, TS<sub>2</sub>, TS<sub>3</sub> are the transition state for steps 1, 2 and 3, respectively; P<sub>1</sub>(HOI + HI), P<sub>2</sub>(B int) and P<sub>3</sub>(E + HOI) are the products of reactions for steps 1, 2 and 3, respectively, while E<sub>a1</sub> is the activation energy for step 1, E<sub>a2</sub> and E<sub>a3</sub> are the activation energies for steps 2 and 3 respectively. D is the intermediate is step 3.



Figure 4.19: Labeled structure of D-fructose

**Table 4.18: Net atomic charges and exposed surface area of D-fructose molecule**

| Atom           | Charge | Exposed surface area (Å <sup>2</sup> ) | Atom           | Charge | Exposed surface area (Å <sup>2</sup> ) | Atom            | Charge | Exposed surface area (Å <sup>2</sup> ) |
|----------------|--------|--|----------------|--------|--|-----------------|--------|--|
| C <sub>1</sub> | 0.001  | 13.80                                  | O <sub>1</sub> | -0.606 | 12.11                                  | H <sub>1</sub>  | 0.401  | 6.67                                   |
|                |        |  |                |        |  | H <sub>2</sub>  | 0.124  | 5.46                                   |
|                |        |  |                |        |  | H <sub>3</sub>  | 0.146  | 5.48                                   |
| C <sub>2</sub> | 0.551  | 6.91                                   | O <sub>2</sub> | -0.516 | 11.89                                  |                 |        |  |
| C <sub>3</sub> | -0.081 | 6.06                                   | O <sub>3</sub> | -0.671 | 10.24                                  | H <sub>6</sub>  | 0.443  | 5.39                                   |
|                |        |  |                |        |  | H <sub>5</sub>  | 0.135  | 5.47                                   |
| C <sub>4</sub> | 0.015  | 5.48                                   | O <sub>4</sub> | -0.653 | 11.43                                  | H <sub>7</sub>  | 0.420  | 5.37                                   |
|                |        |  |                |        |  | H <sub>8</sub>  | 0.075  | 5.47                                   |
| C <sub>5</sub> | 0.226  | 5.29                                   | O <sub>5</sub> | -0.627 | 10.50                                  | H <sub>10</sub> | 0.409  | 7.70                                   |
|                |        |  |                |        |  | H <sub>9</sub>  | 0.102  | 5.24                                   |
| C <sub>6</sub> | -0.062 | 13.06                                  | O <sub>6</sub> | -0.595 | 12.10                                  | H <sub>4</sub>  | 0.403  | 5.42                                   |
|                |        |  |                |        |  | H <sub>11</sub> | 0.106  | 5.42                                   |
|                |        |  |                |        |  | H <sub>12</sub> | 0.116  | 5.48                                   |

**Table 4.19: Total electronic energy and other thermodynamic parameters at standard condition of 1 atmosphere and 298.15K of reacting species and products for route I for hydrazine / hydrazinium ion – iodine reaction system**

| S/N | Species                       | $E_e (\Delta H^\circ)$<br>(kJ/mol) | $\Delta G^\circ$<br>(kJ/mol)     | $\Delta S^\circ$<br>(J/mol.K)     |
|-----|-------------------------------|------------------------------------|----------------------------------|-----------------------------------|
| 1   | I <sub>2</sub>                | -36,334,465.70<br>(-13,841.70 au)  | -36,334,542.14<br>(-13841.73au)  | 260.55<br>(0.10au)                |
| 2   | H <sub>2</sub> O              | -200,678.03<br>(-76.45au)          | -200,732.28<br>(-76.47au)        | 188.64<br>(0.07au)                |
| 3   | H <sub>3</sub> O <sup>+</sup> | -201,317.55<br>(-76.69au)          | -201,375.65<br>(-76.71au)        | 194.90<br>(0.07au)                |
| 4   | Hyd <sup>+</sup>              | -294,265.02<br>(-112.10au)         | -294,343.59<br>(-112.13au)       | 263.55<br>(0.10au)                |
| 5   | Hyd                           | -293,512.76<br>(-111.81au)         | -293,585.77<br>(-111.84au)       | 244.93<br>(0.09au)                |
| 6   | HI                            | -18,168,774.40<br>(-6,921.44au)    | -18,168,835.99<br>(-6,921.46au)  | 206.59<br>(0.08au)                |
| 7   | Int.                          | -290,042.75<br>(-110.49au)         | -290,100.30<br>(-110.51au)       | 364.75<br>(0.14au)                |
| 8   | N <sub>2</sub>                | -287,570.90<br>(-109.55au)         | -287,627.96<br>(-109.57au)       | 191.57<br>(0.07au)                |
| 9   | TS <sub>1</sub>               | -494,142.06<br>(-188.24au)         | -494,634.72<br>(-188.43au)       | 6.2 x10 <sup>4</sup><br>(1.65 au) |
| 10  | TS <sub>3A</sub>              | -36,527,976.45<br>(-1,3915.42au)   | -36,528,075.41<br>(-13,915.46au) | 331.95<br>(0.13au)                |
| 11  | TS <sub>2A</sub>              | -36,618,245.67<br>(-13,949.81au)   | -36,625,511.49<br>(-13,952.58au) | 24.37<br>(0.01au)                 |

| S/N | Species                                  | $E_e (\Delta H^\circ)$<br>(kJ/mol) | $E_e (\Delta H^\circ)$<br>(kJ/mol) | $E_e (\Delta H^\circ)$<br>(kJ/mol) |
|-----|--|------------------------------------|------------------------------------|------------------------------------|
| 12  | $R_1(\text{H}_2\text{O} + \text{Hyd}^+)$ | -494,943.05<br>(-188.55au)         | -494,318.05<br>(-188.31au)         | 452.39<br>(0.17au)                 |
| 13  | $P_1(\text{H}_3\text{O}^+ + \text{Hyd})$ | -494,830.31<br>(-188.51au)         | -494,961.42<br>(-188.56au)         | 439.83<br>(0.17au)                 |
| 14  | $R_2(\text{I}_2 + \text{Hyd})$           | -36,627,978.46<br>(-13,953.52au)   | -36,628,127.91<br>(-13,953.57au)   | 505.48<br>(0.19au)                 |
| 15  | $P_2(\text{Int} + 2\text{HI})$           | -36,627,591.55<br>(-13,953.37au)   | -36,627,772.28<br>(-13,953.44au)   | 777.93<br>(0.30au)                 |
| 16  | $R_{3A}(\text{Int} + \text{I}_2)$        | -36,624,508.45<br>(-13,952.19au)   | -36,624,642.44<br>(-13,952.24au)   | 625.3<br>(0.24au)                  |
| 17  | $P_{3A}(\text{N}_2 + 2\text{HI})$        | -72,962,668.50<br>(-27,795.30au)   | -36,625,299.94<br>(-13,952.50au)   | 604.75<br>(0.23au)                 |
| 18  | $E_{a1}$                                 | 800.99<br>(0.31au)                 |                                    |                                    |
| 19  | $E_{a2}$                                 | 100,002.01<br>(38.10au)            |                                    |                                    |
| 20  | $E_{a3}$                                 | 6,262.78<br>(2.39au)               |                                    |                                    |

**Key:** Where  $\text{I}_2$  is iodine molecule,  $\text{H}_2\text{O}$  is water molecule,  $\text{Hyd}^+$  is hydrazinium ion, Hyd is hydrazine, HI is hydrogen iodide molecule, HOI is hypoiodous acid, Int is intermediate (diazine), TS1 is transition state for step 1,  $\text{N}_2$  is nitrogen molecule,  $R_1(\text{H}_2\text{O} + \text{Hyd}^+)$  and  $P_1(\text{H}_3\text{O}^+ + \text{Hyd})$  are all the reactants and products for step 1 of all the proposed routes, respectively.  $R_{2A}(\text{I}_2 + \text{Hyd})$  and  $P_{2A}(\text{Int} + 2\text{HI})$  are the respective reactants and products of step 2, route I;  $R_B(2\text{I}_2 + \text{Hyd})$  and  $P_B(\text{N}_2 + 4\text{HI})$ , respective reactants and products of step 2, route II;  $R_C(2\text{I}_2 + \text{Hyd})$  and  $P_C(\text{N}_2 + 4\text{HI})$ , respective reactants and products of step 2, route III; while  $R_D(2\text{I}_2 + 2\text{H}_2\text{O})$  and  $P_D(2\text{HOI} + 2\text{HI})$ , respective reactants and products of step 2, route IV.  $R_{3A}(\text{Int} + \text{I}_2)$  and  $P_{3A}(\text{N}_2 + 2\text{HI})$  are the respective reactants and products of step 3, route I; while  $R_E(2\text{HOI} + \text{Hyd})$  and  $P_E(\text{N}_2 + 2\text{H}_2\text{O} + 2\text{HI})$  are the respective reactants and products of step 3, route IV.  $E_{a1}$  is the activation energy for step 1 for all the four routes;  $E_{a2}, E_{aB}, E_{aC}$  and  $E_{aD}$  are the activation energy for step 2 for routes I, II, III and IV respectively.  $E_{a3}$  and  $E_{aE}$  are the respective activation energies for step 3 for routes I and IV.

**Table 4.20: Total electronic energy and other thermodynamic parameters at standard condition of 1 atmosphere and 298.15K of reacting species and products for route II for hydrazine / hydrazinium ion – iodine reaction system**

| S/N | Species   | E <sub>e</sub> (kJ/mol)           | ΔG <sup>o</sup> (kJ/mol)          | ΔS <sup>o</sup> (J/mol.K)         |
|-----|---|-----------------------------------|-----------------------------------|-----------------------------------|
| 1   | I <sub>2</sub>  | -36,334,465.70<br>(-13,841.70 au) | -36,334,542.14<br>(-13,841.73au)  | 260.55<br>(0.10 au)               |
| 2   | H <sub>2</sub> O                                      | -200,678.03<br>(-76.45au)         | -200,732.28<br>(-76.47au)         | 188.64<br>(0.07au)                |
| 3   | H <sub>3</sub> O <sup>+</sup>                         | -201,317.55<br>(-76.69au)         | -201,375.65<br>(-76.71au)         | 194.90<br>(0.07au)                |
| 4   | Hyd <sup>+</sup>                                      | -294,265.02<br>(-112.10au)        | -294,343.59<br>(-112.13au)        | 263.55<br>(0.10au)                |
| 5   | Hyd   | -293,512.76<br>(-111.81au)        | -293,585.77<br>(-111.84au)        | 244.93<br>(0.09au)                |
| 6   | HI  | -18,168,774.40<br>(-6,921.44au)   | -18,168,835.99<br>(-6,921.46au)   | 206.59<br>(0.08au)                |
| 7   | N <sub>2</sub>  | -287,570.90<br>(-109.55au)        | -287,627.96<br>(-109.57au)        | 191.57<br>(0.07au)                |
| 8   | TS <sub>1</sub>                                       | -494,142.06<br>(-188.24au)        | -494,634.72<br>(-188.43au)        | 6.2 x10 <sup>4</sup><br>(1.65 au) |
| 9   | TS <sub>B</sub>                                       | -72,948,708.06<br>(-27,789.98au)  | -72,963,181.09<br>(-27,795.50 au) | 48.54<br>(0.02au)                 |
| 10  | R <sub>1</sub> (H <sub>2</sub> O + Hyd <sup>+</sup> ) | -494,943.05<br>(-188.55au)        | -494,318.05<br>(-188.31au)        | 452.39<br>(0.17au)                |
| 11  | P <sub>1</sub> (H <sub>3</sub> O <sup>+</sup> + Hyd)  | -494,830.31<br>(-188.51au)        | -494,961.42<br>(-188.56au)        | 439.83<br>(0.17au)                |
| 12  | R <sub>B</sub> (2I <sub>2</sub> + Hyd)                | -72,962,444.16<br>(-27,795.21au)  | -72,962,670.05<br>(-27795.30au)   | 766.03<br>(0.29au)                |
| 13  | P <sub>B</sub> (N <sub>2</sub> + 4HI)                 | -72,962,668.50<br>(-27,795.30au)  | -72,962,971.92<br>(-27,795.42au)  | 1,017.93<br>(0.39au)              |
| 14  | E <sub>a1</sub>                                       | 800.99<br>(0.31au)                |                                   |                                   |
| 15  | E <sub>aB</sub>                                       | 13,736.10<br>(5.23au)             |                                   |                                   |

**Key:** Where I<sub>2</sub> is iodine molecule, H<sub>2</sub>O is water molecule, Hyd<sup>+</sup> is hydrazinium ion, Hyd is hydrazine, HI is hydrogen iodide molecule, HOI is hypoiodous acid, Int is intermediate (diazine), TS<sub>1</sub> is transition state for step 1, N<sub>2</sub> is nitrogen molecule, R<sub>1</sub> (H<sub>2</sub>O + Hyd<sup>+</sup>) and P<sub>1</sub> (H<sub>3</sub>O<sup>+</sup> + Hyd) are all the reactants and products for step 1 of all the proposed routes, respectively. R<sub>2A</sub> (I<sub>2</sub> + Hyd) and P<sub>2A</sub> (Int + 2HI) are the respective reactants and products of step 2, route I; R<sub>B</sub> (2I<sub>2</sub> + Hyd) and P<sub>B</sub> (N<sub>2</sub> + 4HI), respective reactants and products of step 2, route II; R<sub>C</sub> (2I<sub>2</sub> + Hyd) and P<sub>C</sub> (N<sub>2</sub> + 4HI), respective reactants and products of step 2, route III; while R<sub>D</sub> (2I<sub>2</sub> + 2H<sub>2</sub>O) and P<sub>D</sub> (2HOI + 2HI), respective reactants and products of step 2, route IV. R<sub>3A</sub> (Int + I<sub>2</sub>) and P<sub>3A</sub> (N<sub>2</sub> + 2HI) are the respective reactants and products of step 3, route I; while R<sub>E</sub> (2HOI + Hyd) and P<sub>E</sub> (N<sub>2</sub> + 2H<sub>2</sub>O + 2HI) are the respective reactants and products of step 3, route IV. E<sub>a1</sub> is the activation energy for step 1 for all the four routes; E<sub>a2</sub>, E<sub>aB</sub>, E<sub>aC</sub> and E<sub>aD</sub> are the activation energy for step 2 for routes I, II, III and IV respectively. E<sub>a3</sub> and E<sub>aE</sub> are the respective activation energies for step 3 for routes I and IV.

**Table 4.21: Total electronic energy and other thermodynamic parameters at standard condition of 1 atmosphere and 298.15K of reacting species and products for route III for hydrazine / hydrazinium ion – iodine reaction system**

| S/N | Species   | $E_e$ ( $\Delta H^\circ$ )<br>(kJ/mol) | $\Delta G^\circ$<br>(kJ/mol)      | $\Delta S^\circ$<br>(J/mol.K)     |
|-----|---|--|-----------------------------------|-----------------------------------|
| 1   | I <sub>2</sub>  | -36,334,465.70<br>(-13,841.70 au)      | -36,334,542.14<br>(-13,841.73au)  | 260.55<br>(0.10 au)               |
| 2   | H <sub>2</sub> O                                      | -200,678.03<br>(-76.45au)              | -200,732.28<br>(-76.47au)         | 188.64<br>(0.07au)                |
| 3   | H <sub>3</sub> O <sup>+</sup>                         | -201,317.55<br>(-76.69au)              | -201,375.65<br>(-76.71au)         | 194.90<br>(0.07au)                |
| 4   | Hyd <sup>+</sup>                                      | -294,265.02<br>(-112.10au)             | -294,343.59<br>(-112.13au)        | 263.55<br>(0.10au)                |
| 5   | Hyd   | -293,512.76<br>(-111.81au)             | -293,585.77<br>(-111.84au)        | 244.93<br>(0.09au)                |
| 6   | HI  | -18,168,774.40<br>(-6,921.44au)        | -18,168,835.99<br>(-6,921.46au)   | 206.59<br>(0.08au)                |
| 7   | N <sub>2</sub>  | -287,570.90<br>(-109.55au)             | -287,627.96<br>(-109.57au)        | 191.57<br>(0.07au)                |
| 8   | TS <sub>1</sub>                                       | -494,142.06<br>(-188.24au)             | -494,634.72<br>(-188.43au)        | 6.2 x10 <sup>4</sup><br>(1.65 au) |
| 9   | TS <sub>C</sub>                                       | -72,948,830.75<br>(-27,790.03 au)      | -72,963,303.79<br>(-27,795.54 au) | 451.51<br>(0.17au)                |
| 10  | R <sub>1</sub> (H <sub>2</sub> O + Hyd <sup>+</sup> ) | -494,943.05<br>(-188.55au)             | -494,318.05<br>(-188.31au)        | 452.39<br>(0.17au)                |
| 11  | P <sub>1</sub> (H <sub>3</sub> O <sup>+</sup> + Hyd)  | -494,830.31<br>(-188.51au)             | -494,961.42<br>(-188.56au)        | 439.83<br>(0.17au)                |
| 12  | R <sub>C</sub> (2I <sub>2</sub> + Hyd)                | -72,962,444.16<br>(-27,795.21au)       | -72,962,670.05<br>(-27795.30au)   | 766.03<br>(0.29au)                |
| 13  | P <sub>C</sub> (N <sub>2</sub> + 4HI)                 | -72,962,668.50<br>(-27,795.30au)       | -72,962,971.92<br>(-27,795.42au)  | 1,017.93<br>(0.39au)              |
| 14  | E <sub>a1</sub>                                       | 800.99<br>(0.31au)                     |                                   |                                   |
| 15  | E <sub>aC</sub>                                       | 13,736.10<br>(5.23au)                  |                                   |                                   |

**Key:** TS<sub>1</sub> is transition state for step 1, N<sub>2</sub> is nitrogen molecule, R<sub>1</sub> (H<sub>2</sub>O + Hyd<sup>+</sup>) and P<sub>1</sub> (H<sub>3</sub>O<sup>+</sup> + Hyd) are all the reactants and products for step 1 of all the proposed routes, respectively. R<sub>2A</sub> (I<sub>2</sub> + Hyd) and P<sub>2A</sub> (Int + 2HI) are the respective reactants and products of step 2, route I; R<sub>B</sub> (2I<sub>2</sub> + Hyd) and P<sub>B</sub> (N<sub>2</sub> + 4HI), respective reactants and products of step 2, route II; R<sub>C</sub> (2I<sub>2</sub> + Hyd) and P<sub>C</sub> (N<sub>2</sub> + 4HI), respective reactants and products of step 2, route III; while R<sub>D</sub> (2I<sub>2</sub> + 2H<sub>2</sub>O) and P<sub>D</sub> (2HOI + 2HI), respective reactants and products of step 2, route IV. R<sub>3A</sub> (Int + I<sub>2</sub>) and P<sub>3A</sub> (N<sub>2</sub> + 2HI) are the respective reactants and products of step 3, route I; while R<sub>E</sub> (2HOI + Hyd) and P<sub>E</sub> (N<sub>2</sub> + 2H<sub>2</sub>O + 2HI) are the respective reactants and products of step 3, route IV. E<sub>a1</sub> is the activation energy for step 1 for all the four routes; E<sub>a2</sub>, E<sub>aB</sub>, E<sub>aC</sub> and E<sub>aD</sub> are the activation energy for step 2 for routes I, II, III and IV respectively. E<sub>a3</sub> and E<sub>aE</sub> are the respective activation energies for step 3 for routes I and IV.

**Table 4.22: Total electronic energy and other thermodynamic parameters at standard condition of 1 atmosphere and 298.15K of reacting species and products for route IV for hydrazine / hydrazinium ion – iodine system**

| <b>S/<br/>N</b> | <b>Species</b>                | <b>E<sub>e</sub><br/>(kJ/mol)</b> | <b>ΔG°<br/>(kJ/mol)</b>          | <b>ΔS°<br/>(J/mol.K)</b>          |
|-----------------|-------------------------------|-----------------------------------|----------------------------------|-----------------------------------|
| 1               | I <sub>2</sub>                | -36,334,465.70<br>(-13,841.70 au) | -36,334,542.14<br>(-13,841.73au) | 260.55<br>(0.10au)                |
| 2               | H <sub>2</sub> O              | -200,678.03<br>(-76.45au)         | -200,732.28<br>(-76.47au)        | 188.64<br>(0.07au)                |
| 3               | H <sub>3</sub> O <sup>+</sup> | -201,317.55<br>(-76.69au)         | -201,375.65<br>(-76.71au)        | 194.90<br>(0.07au)                |
| 4               | HOI                           | -18,366,219.67<br>(-6,996.65 au)  | -18,366,295.58<br>(-6,996.68 au) | 254.58<br>(0.20 au)               |
| 5               | Hyd <sup>+</sup>              | -294,265.02<br>(-112.10au)        | -294,343.59<br>(-112.13au)       | 263.55<br>(0.10au)                |
| 6               | Hyd                           | -293,512.76<br>(-111.81au)        | -293,585.77<br>(-111.84au)       | 244.93<br>(0.09au)                |
| 7               | HI                            | -18,168,774.40<br>(-6,921.44au)   | -18,168,835.99<br>(-6,921.46au)  | 206.59<br>(0.08au)                |
| 8               | N <sub>2</sub>                | -287,570.90<br>(-109.55au)        | -287,627.96<br>(-109.57au)       | 191.57<br>(0.07au)                |
| 9               | TS <sub>1</sub>               | -494,142.06<br>(-188.24au)        | -494,634.72<br>(-188.43au)       | 6.2 x10 <sup>4</sup><br>(1.65 au) |
| 10              | TS <sub>D</sub>               | -36,534,957.18<br>(-13,918.08au)  | -36,535,052.36<br>(-13,918.12au) | 319.24<br>(0.12au)                |
| 11              | TS <sub>E</sub>               | -37,019,091.68<br>(-14,102.51au)  | -37,056,036.73<br>(-14,116.58au) | 123.91<br>(0.05au)                |

| S/<br>N | Species   | E <sub>e</sub><br>(kJ/mol)       | ΔG°<br>(kJ/mol)                   | ΔS°<br>(J/mol.K)   |
|---------|---|----------------------------------|-----------------------------------|--------------------|
| 12      | R <sub>1</sub> (H <sub>2</sub> O + Hyd <sup>+</sup> )     | -494,943.05<br>(-188.55au)       | -494,318.05<br>(-188.31au)        | 452.39<br>(0.17au) |
| 13      | P <sub>1</sub> (H <sub>3</sub> O <sup>+</sup> + Hyd)      | -494,830.31<br>(-188.51au)       | -494,961.42<br>(-188.56au)        | 439.83<br>(0.17au) |
| 14      | R <sub>D</sub> (2I <sub>2</sub> + 2H <sub>2</sub> O)      | -36,535,143.73<br>(-13,918.15au) | -73,070,548.84<br>(-27,836.40au)  | 898.38<br>(0.34au) |
| 15      | P <sub>D</sub> (2HOI + 2HI)                               | -36,534,994.07<br>(-13,918.09au) | -73,070,263.14<br>(-27,836.29 au) | 922.34<br>(0.35au) |
| 16      | R <sub>E</sub> (2HOI + Hyd)                               | -37,025,952.10<br>(-14,105.12au) | -37,026,176.93<br>(-14,105.21au)  | 754.09<br>(0.29au) |
| 17      | P <sub>E</sub> (N <sub>2</sub> + 2H <sub>2</sub> O + 2HI) | -37,026,475.76<br>(-14,10532au)  | -37,026,764.50<br>(-14,105.43au)  | 982.03<br>(0.37au) |
| 18      | E <sub>a1</sub>   | 800.99<br>(0.31au)               |                                   |                    |
| 19      | E <sub>aD</sub>   | 186.55<br>(0.07au)               |                                   |                    |
| 20      | E <sub>aE</sub>   | 6,860.42<br>(2.61au)             |                                   |                    |

**Key:** Where I<sub>2</sub> is iodine molecule, H<sub>2</sub>O is water molecule, Hyd<sup>+</sup> is hydrazinium ion, Hyd is hydrazine, HI is hydrogen iodide molecule, HOI is hypiodous acid, Int is intermediate (diazine), TS<sub>1</sub> is transition state for step 1, N<sub>2</sub> is nitrogen molecule, R<sub>1</sub>(H<sub>2</sub>O + Hyd<sup>+</sup>) and P<sub>1</sub>(H<sub>3</sub>O<sup>+</sup> + Hyd) are all the reactants and products for step 1 of all the proposed routes, respectively. R<sub>2A</sub>(I<sub>2</sub> + Hyd) and P<sub>2A</sub>(Int + 2HI) are the respective reactants and products of step 2, route I; R<sub>B</sub>(2I<sub>2</sub> + Hyd) and P<sub>B</sub>(N<sub>2</sub> + 4HI), respective reactants and products of step 2, route II; R<sub>C</sub>(2I<sub>2</sub> + Hyd) and P<sub>C</sub>(N<sub>2</sub> + 4HI), respective reactants and products of step 2, route III; while R<sub>D</sub>(2I<sub>2</sub> + 2H<sub>2</sub>O) and P<sub>D</sub>(2HOI + 2HI), respective reactants and products of step 2, route IV. R<sub>3A</sub>(Int + I<sub>2</sub>) and P<sub>3A</sub>(N<sub>2</sub> + 2HI) are the respective reactants and products of step 3, route I; while R<sub>E</sub>(2HOI + Hyd) and P<sub>E</sub>(N<sub>2</sub> + 2H<sub>2</sub>O + 2HI) are the respective reactants and products of step 3, route IV. E<sub>a1</sub> is the activation energy for step 1 for all the four routes; E<sub>a2</sub>, E<sub>aB</sub>, E<sub>aC</sub> and E<sub>aD</sub> are the activation energy for step 2 for routes I, II, III and IV respectively. E<sub>a3</sub> and E<sub>aE</sub> are the respective activation energies for step 3 for routes I and IV.

**Table 4.23: Total electronic energy and other activation parameters at standard condition of 1 atmosphere and 298.15K of reacting species for routes I and II for hydrazine / hydrazinium ion – iodine reaction system**

| Route   | Species             | $E_e$<br>(kJ/mol)                 | $\Delta^\ddagger G$<br>(kJ/mol)    | $\Delta^\ddagger S$<br>(J/mol.K)     | $\Delta^\ddagger E_a$<br>(J/mol)      |                                 |
|---------|---------------------|-----------------------------------|------------------------------------|--------------------------------------|---------------------------------------|---------------------------------|
| Route I | $R_1(H_2O + Hyd^+)$ | -494,943.05<br>(-188.55au)        |                                    |                                      |                                       |                                 |
|         | $P_1(H_3O^+ + Hyd)$ | -494,830.31<br>(-188.51au)        |                                    |                                      |                                       |                                 |
|         | $TS_1$              | -494,142.06<br>(-188.24au)        |                                    |                                      |                                       |                                 |
|         | Step I              |                                   | $-2.76 \times 10^4$<br>(-10.51au)  | $-1.75 \times 10^3$<br>(0.67au)      | $8.01 \times 10^2$<br>(0.31au)        |                                 |
|         | $R_2(I_2 + Hyd)$    | -36,627,978.46<br>(-13,953.52 au) |                                    |                                      |                                       |                                 |
|         | $P_2(Int + 2HI)$    | -36,627,591.55<br>(-13,953.37au)  |                                    |                                      |                                       |                                 |
|         | $TS_{2A}$           | -36,618,245.67<br>(-13,949.81au)  |                                    |                                      |                                       |                                 |
|         | Step II             |                                   | $-2.70 \times 10^4$<br>(-10.29 au) | $-1.73 \times 10^5$<br>(-65.90 au)   | $1.00 \times 10^5$<br>(38.10 au)      |                                 |
|         | $R_{3A}(Int + I_2)$ | -36,624,508.45<br>(-13,952.19 au) |                                    |                                      |                                       |                                 |
|         | $P_{3A}(N_2 + 2HI)$ | -72,962,668.50<br>(-27,795.30 au) |                                    |                                      |                                       |                                 |
|         | $TS_{3A}$           | -36,527,976.45<br>(-1,3915.42 au) |                                    |                                      |                                       |                                 |
|         | Step III            |                                   |                                    | $-1.52 \times 10^7$<br>(-5,790.48au) | $-3.66 \times 10^7$<br>(-13,942.71au) | $6.26 \times 10^3$<br>(2.38 au) |

| Route    | Species             | $E_e$<br>(kJ/mol)                 | $\Delta^\ddagger G$<br>(kJ/mol)   | $\Delta^\ddagger S$<br>(J/mol.K)  | $\Delta^\ddagger E_a$<br>(J/mol) |
|----------|---------------------|-----------------------------------|-----------------------------------|-----------------------------------|----------------------------------|
| Route II | $R_1(H_2O + Hyd^+)$ | -494,943.05<br>(-188.55au)        |                                   |                                   |                                  |
|          | $P_1(H_3O^+ + Hyd)$ | -494,830.31<br>(-188.51au)        |                                   |                                   |                                  |
|          | (TS <sub>1</sub> )  | -494,142.06<br>(-188.24au)        |                                   |                                   |                                  |
|          | Step I              |                                   | $-2.76 \times 10^4$<br>(-10.51au) | $-1.75 \times 10^3$<br>(0.67au)   | $8.01 \times 10^2$<br>(0.31au)   |
|          | $R_B(2I_2 + Hyd)$   | -72,962,444.16<br>(-27,795.21 au) |                                   |                                   |                                  |
|          | $P_B(N_2 + 4HI)$    | -72,962,668.50<br>(-27,795.30 au) |                                   |                                   |                                  |
|          | TS <sub>B</sub>     | -72,948,708.06<br>(-27,789.98 au) |                                   |                                   |                                  |
| Step II  |                     |                                   | $-5.91 \times 10^4$<br>(-22.51au) | $-2.45 \times 10^5$<br>(-93.33au) | $1.37 \times 10^4$<br>(5.22au)   |

**Key:** TS<sub>1</sub> is transition state for step 1, N<sub>2</sub> is nitrogen molecule, R<sub>1</sub> (H<sub>2</sub>O + Hyd<sup>+</sup>) and P<sub>1</sub> (H<sub>3</sub>O<sup>+</sup> + Hyd) are all the reactants and products for step 1 of all the proposed routes, respectively. R<sub>2A</sub> (I<sub>2</sub> + Hyd) and P<sub>2A</sub> (Int + 2HI) are the respective reactants and products of step 2, route I; R<sub>B</sub> (2I<sub>2</sub> + Hyd) and P<sub>B</sub> (N<sub>2</sub> + 4HI), respective reactants and products of step 2, route II; R<sub>C</sub> (2I<sub>2</sub> + Hyd) and P<sub>C</sub> (N<sub>2</sub> + 4HI), respective reactants and products of step 2, route III; while R<sub>D</sub> (2I<sub>2</sub> + 2H<sub>2</sub>O) and P<sub>D</sub> (2HOI + 2HI), respective reactants and products of step 2, route IV. R<sub>3A</sub> (Int + I<sub>2</sub>) and P<sub>3A</sub> (N<sub>2</sub> + 2HI) are the respective reactants and products of step 3, route I; while R<sub>E</sub> (2HOI + Hyd) and P<sub>E</sub> (N<sub>2</sub> + 2H<sub>2</sub>O + 2HI) are the respective reactants and products of step 3, route IV. E<sub>a1</sub> is the activation energy for step 1 for all the four routes; E<sub>a2</sub>, E<sub>aB</sub>, E<sub>aC</sub> and E<sub>aD</sub> are the activation energy for step 2 for routes I, II, III and IV respectively. E<sub>a3</sub> and E<sub>aE</sub> are the respective activation energies for step 3 for routes I and IV.

**Table 4.24: Total electronic energy and other activation parameters at standard condition of 1 atmosphere and 298.15K of reacting species and products for routes III and IV for hydrazine / hydrazinium ion – iodine reaction system**

| Route     | Species   | $\Delta_r H^\circ$<br>(kJ/mol)       | $\Delta^\ddagger G$<br>(kJ/mol)      | $\Delta^\ddagger S$<br>(kJ/mol.K)  | $\Delta^\ddagger E_a$<br>(kJ/mol) |
|-----------|---|--------------------------------------|--------------------------------------|------------------------------------|-----------------------------------|
| Route III | R <sub>1</sub> (H <sub>2</sub> O + Hyd <sup>+</sup> ) | -494,943.05<br>(-188.55au)           |                                      |                                    |                                   |
|           | P <sub>1</sub> (H <sub>3</sub> O <sup>+</sup> + Hyd)  | -494,830.31<br>(-188.51au)           |                                      |                                    |                                   |
|           | (TS <sub>1</sub> )                                    | -494,142.06<br>(-188.24au)           |                                      |                                    |                                   |
|           | Step I  |                                      | -2.76 x10 <sup>4</sup><br>(-10.51au) | -1.75 x10 <sup>3</sup><br>(0.67au) | 8.01 x10 <sup>2</sup><br>(0.31au) |
|           | R <sub>C</sub> (2I <sub>2</sub> + Hyd)                | -72,962,444.16<br>(-27,795.21au)     |                                      |                                    |                                   |
|           | P <sub>C</sub> (N <sub>2</sub> + 4HI)                 | -72,962,668.50<br>(-27,795.30au)     |                                      |                                    |                                   |
|           | TS <sub>C</sub>                                       | -72,948,830.75<br>(-27,790.03 au)    |                                      |                                    |                                   |
| Step II   |   | -7.37 x10 <sup>4</sup><br>(-28.08au) | 1.23 x10 <sup>5</sup><br>(46.86au)   | 1.37 x10 <sup>4</sup><br>(5.22 au) |                                   |
| Route IV  | R <sub>1</sub> (H <sub>2</sub> O + Hyd <sup>+</sup> ) | -494,943.05<br>(-188.55au)           |                                      |                                    |                                   |
|           | P <sub>1</sub> (H <sub>3</sub> O <sup>+</sup> + Hyd)  | -494,830.31<br>(-188.51au)           |                                      |                                    |                                   |
|           | (TS <sub>1</sub> )                                    | -494,142.06<br>(-188.24au)           |                                      |                                    |                                   |

| Route | Species   | $\Delta_r H^\circ$<br>(kJ/mol)   | $\Delta^\ddagger G$<br>(kJ/mol)         | $\Delta^\ddagger S$<br>(kJ/mol.K)  | $\Delta^\ddagger E_a$<br>(kJ/mol) |
|-------|---|----------------------------------|---|------------------------------------|-----------------------------------|
|       | Step I  |                                  | $-2.76 \times 10^4$<br>(-10.51au)       | $1.75 \times 10^3$<br>(0.67au)     | $8.01 \times 10^2$<br>(0.31au)    |
|       | R <sub>D</sub> (2I <sub>2</sub> + 2H <sub>2</sub> O)      | -36,535,143.73<br>(-13,918.15au) |   |                                    |                                   |
|       | P <sub>D</sub> (2HOI + 2HI)                               | -36,534,994.07<br>(-13,918.09au) |   |                                    |                                   |
|       | TS <sub>D</sub>   | -36,534,957.18<br>(-13,918.08au) |   |                                    |                                   |
|       | Step II   |                                  | $-1.57 \times 10^9$<br>(-598,095.24 au) | $5.40 \times 10^6$<br>(2,057.14au) | $1.87 \times 10^2$<br>(0.07au)    |
|       | R <sub>E</sub> (2HOI + Hyd)                               | -37,025,952.10<br>(-14,105.12au) |   |                                    |                                   |
|       | P <sub>E</sub> (N <sub>2</sub> + 2H <sub>2</sub> O + 2HI) | -37,026,475.76<br>(-14,10532au)  |   |                                    |                                   |
|       | TS <sub>E</sub>   | -37,019,091.68<br>(-14,102.51au) |   |                                    |                                   |
|       | Step III  |                                  | $-8.01 \times 10^4$<br>(30.51au)        | $1.24 \times 10^6$<br>(472.38au)   | $6.86 \times 10^3$<br>(2.61au)    |

**Key:** TS<sub>1</sub> is transition state for step 1, N<sub>2</sub> is nitrogen molecule, R<sub>1</sub> (H<sub>2</sub>O + Hyd<sup>+</sup>) and P<sub>1</sub> (H<sub>3</sub>O<sup>+</sup> + Hyd) are all the reactants and products for step 1 of all the proposed routes, respectively. R<sub>2A</sub> (I<sub>2</sub> + Hyd) and P<sub>2A</sub> (Int + 2HI) are the respective reactants and products of step 2, route I; R<sub>B</sub> (2I<sub>2</sub> + Hyd) and P<sub>B</sub> (N<sub>2</sub> + 4HI), respective reactants and products of step 2, route II; R<sub>C</sub> (2I<sub>2</sub> + Hyd) and P<sub>C</sub> (N<sub>2</sub> + 4HI), respective reactants and products of step 2, route III; while R<sub>D</sub> (2I<sub>2</sub> + 2H<sub>2</sub>O) and P<sub>D</sub> (2HOI + 2HI), respective reactants and products of step 2, route IV. R<sub>3A</sub> (Int + I<sub>2</sub>) and P<sub>3A</sub> (N<sub>2</sub> + 2HI) are the respective reactants and products of step 3, route I; while R<sub>E</sub> (2HOI + Hyd) and P<sub>E</sub> (N<sub>2</sub> + 2H<sub>2</sub>O + 2HI) are the respective reactants and products of step 3, route IV. E<sub>a1</sub> is the activation energy for step 1 for all the four routes; E<sub>a2</sub>, E<sub>aB</sub>, E<sub>aC</sub> and E<sub>aD</sub> are the activation energy for step 2 for routes I, II, III and IV respectively. E<sub>a3</sub> and E<sub>aE</sub> are the respective activation energies for step 3 for routes I and IV.

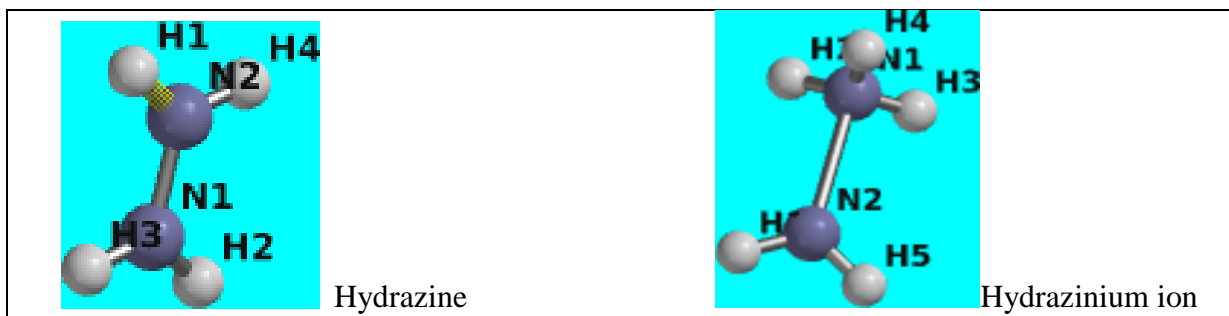


**Figure 4.20: Labeled structures of hydrazine molecule and hydrazinium ion**

**Table 4.25: Bond lengths and exposed surface areas of hydrazine molecule and hydrazinium ion**

| Hydrogen Identity | Bond type | Hydrazine       |  | Hydrazinium ion |  |
|-------------------|-----------|-----------------|--|-----------------|--|
|                   |           | Bond Length (Å) | Exposed Surface Area (Å <sup>2</sup> ) | Bond Length (Å) | Exposed Surface Area (Å <sup>2</sup> ) |
| H1                | N-H       | 0.098           | 9.09                                   | 1.026           | 9.38                                   |
| H2                | N-H       | 0.098           | 9.09                                   | 1.016           | 9.30                                   |
| H3                | N-H       | 0.098           | 9.09                                   | 1.016           | 9.30                                   |
| H4                | N-H       | 0.098           | 9.09                                   | 1.026           | 9.30                                   |
| H5                | N-H       |                 |  | 1.026           | 9.38                                   |

#### **4.5.2 Potential Energy Surface Diagrams of Reactions of L-Tyrosine – Iodine Reaction System according to the PM3 and DFT Methods respectively**

Reaction profiles of L-tyrosine reaction with iodine were obtained by plotting the heat of formation (total electronic energy for DFT) of the reactants, transition states and products against the reaction coordinates. Figures 4.25 and 4.26 showed the energy profile diagrams for L-tyrosine reaction with iodine using PM3 and DFT methods, respectively, where  $R_1$  (L-Tyr +  $I_2$ ),  $R_2$  (MIT +  $I_2$ ), were reactants for steps 1 and 2;  $P_1$  (MIT + HI),  $P_2$  (DIT + HI) were products for steps 1 and 2;  $TS_{1-4}$ ,  $TS^*$  were transition states for steps 1 and 2. Figure 4.27 show the reaction profile of the reaction mechanism involving the favored transition state ( $TS_2$ ).

#### **4.5.3 Potential Energy Surface Diagrams of Reaction of L-Ascorbic Acid – Iodine Reaction System According to the DFT and PM3 Studies**

The scaled energy diagram of the reaction of L-ascorbic acid with iodine according to the DFT were as shown in Figures 4.28 and 4.29 while those for PM3 studies were as shown in Figures 4.30 and 4.31, where  $R_1$  ( $AA + I_2$ ) are the reactants in route 1, with  $TS_1$  as the searched transition states and  $P_1$  (DAA + HI), the products of the same reaction. While  $R_{B1}$  ( $AA + 2I_2$ ) and  $R_{B2}$  ( $AA + 2I$ ) are all the reactants in steps 1 and 2, respectively, for route 2,  $P_{B1}$  (DAA + 2HI + 2I) and  $P_{B2}$  (DAA + 2HI) are the products of reactions for steps 1 and 2, respectively, for route 2,  $TS_{B1}$  is the first transition state for route 2, and  $TS_{B2}$  is the second transition state for route 2.

#### **4.5.4 Potential Energy Surface Diagrams of Reaction of D-Fructose – Iodine Reaction System for the Respective DFT and PM3 studies**

Plots of the potential energy profile diagrams are shown in Figure 4.32 for the DFT studies and Figure 4.33 for the PM3 studies, respectively, clearly showing the reacting species and the saddle points on the diagrams, where  $R_1$  ( $I_2 + H_2O$ ),  $TS_1$  and  $P_1$  (HOI + HI) are reactants,

transition states respectively for the first step; while  $R_2$  (HOI+ Fruc) and  $R_3$  (B int) are reactants,  $TS_2$  (A) and  $TS_3$  (C) are transition states, int. (B) and int.2 (D) were intermediates in second and third steps, respectively.  $P_3$  (E + HOI) are the final products of the reaction.

#### **4.5.5 Potential Energy Surface Diagrams of Reactions of Hydrazine / Hydrazinium Ion – Iodine Reaction System According to the DFT Methods for Routes 1 - 4, respectively**

Plots of the potential energy profile diagrams are shown in Figures 4.34 – 4.37 for the DFT studies for routes 1-4, respectively, clearly showing the reacting species and the saddle points on the diagrams.

$R_1$  ( $H_2O + Hyd^+$ ) and  $P_1$  ( $H_3O^+ + Hyd$ ) are all the reactants and products for step 1 of all the proposed four routes, respectively.  $R_{2A}$  ( $I_2 + Hyd$ ) and  $P_{2A}$  (Int + 2HI) are the respective reactants and products of step 2, route I;  $R_B$  ( $2I_2 + Hyd$ ) and  $P_B$  ( $N_2 + 4HI$ ), respective reactants and products of step 2, route II;  $R_C$  ( $2I_2 + Hyd$ ) and  $P_C$  ( $N_2 + 4HI$ ), respective reactants and products of step 2, route III; while  $R_D$  ( $2I_2 + 2H_2O$ ) and  $P_D$  ( $2HOI + 2HI$ ), respective reactants and products of step 2, route IV.  $R_{3A}$  (Int +  $I_2$ ) and  $P_{3A}$  ( $N_2 + 2HI$ ) are the respective reactants and products of step 3, route I; while  $R_E$  ( $2HOI + Hyd$ ) and  $P_E$  ( $N_2 + 2H_2O + 2HI$ ) were the respective reactants and products of step 3, route IV.

$TS_1$ ,  $TS_2$  and  $TS_{3A}$  are the three transition states for route I.  $TS_1$  and  $TS_B$  are the two transition states for route II.  $TS_1$  and  $TS_C$  are the two transition states for route III.  $TS_1$ ,  $TS_D$  and  $TS_E$  are the three transition states for route IV.

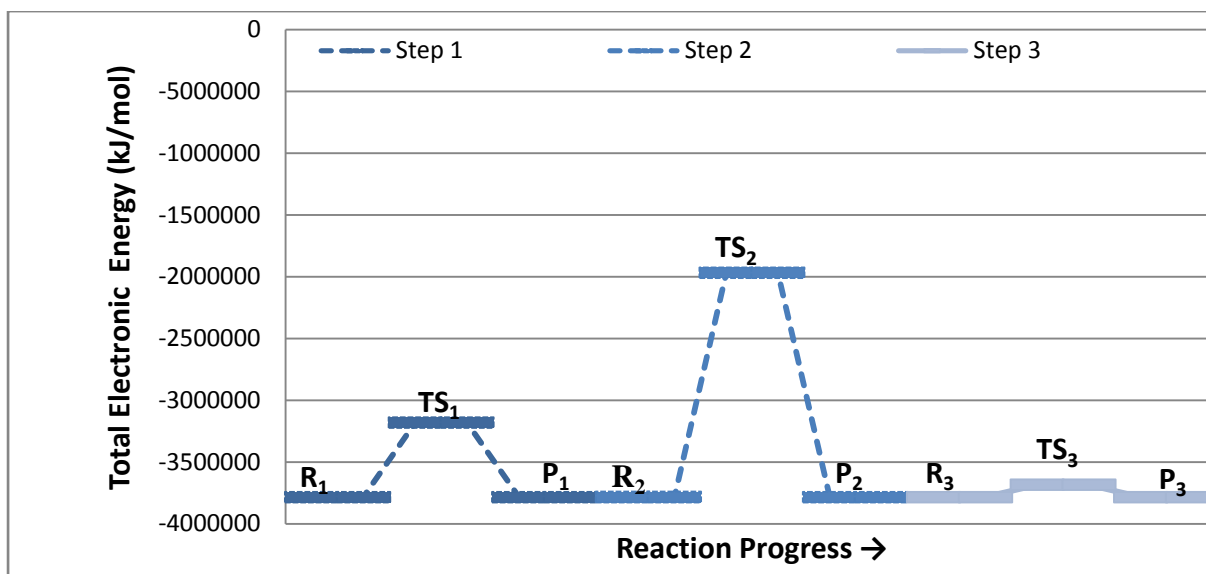


**Figure 4.21: Energy profile of the oxidation of 1,2-diphenylhydrazine by iodine as per the DFT calculations**

**Key:** where  $R_1$  ( $AH_2 + I$ ),  $P_1$  ( $AH + HI + I$ ) and  $TS_1$  are reactants, products and transition states for step 1;  $R_2$  ( $AH + I_2$ ),  $P_2$  ( $A + HI + I$ ) and  $TS_2$  are reactants, products and transition states for step 2; while  $R_3$  ( $AH_2 + 2I$ ),  $P_3$  ( $A + 2I$ ) and  $TS_3$  are reactants, products and transition states for step 3, for the chain multi-step mechanism.

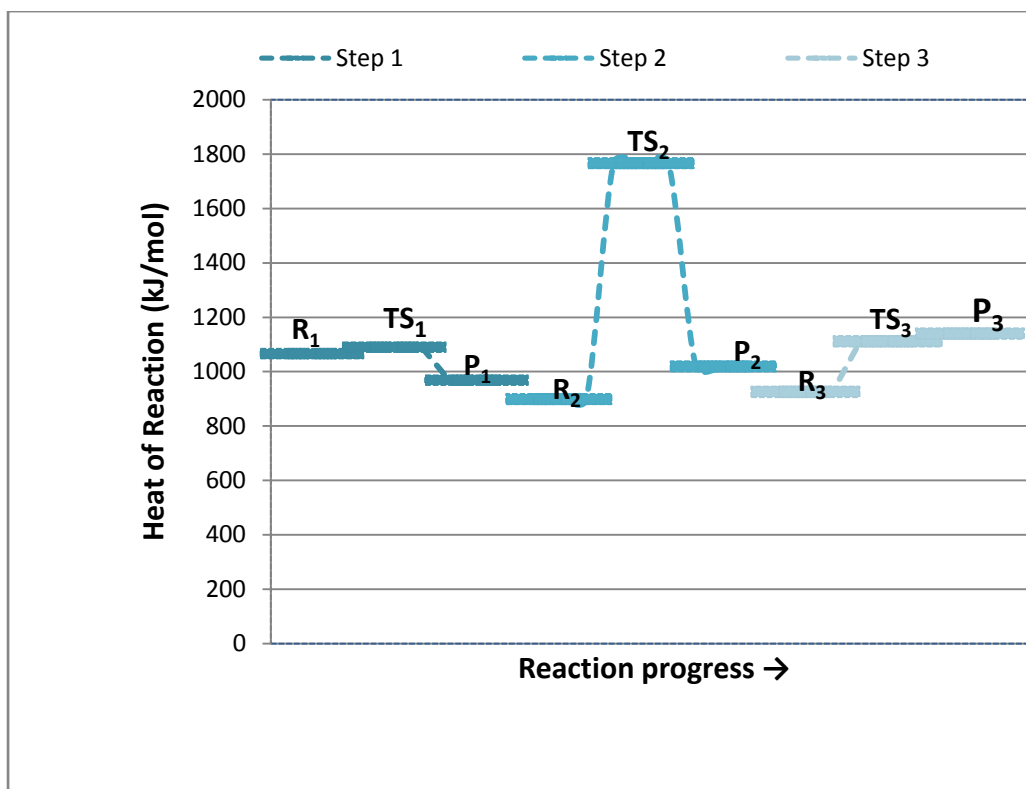


**Figure 4.22: Energy profile of the oxidation of 1,2-diphenylhydrazine by iodine as per the MNDO calculations**

**Key:** where  $R_1$  ( $AH_2 + I$ ),  $P_1$  ( $AH + HI + I$ ) and  $TS_1$  are reactants, products and transition states for step 1;  $R_2$  ( $AH + I_2$ ),  $P_2$  ( $A + HI + I$ ) and  $TS_2$  are reactants, products and transition states for step 2; while  $R_3$  ( $AH_2 + 2I$ ),  $P_3$  ( $A + 2I$ ) and  $TS_3$  are reactants, products and transition states for step 3, for the chain multi-step mechanism.

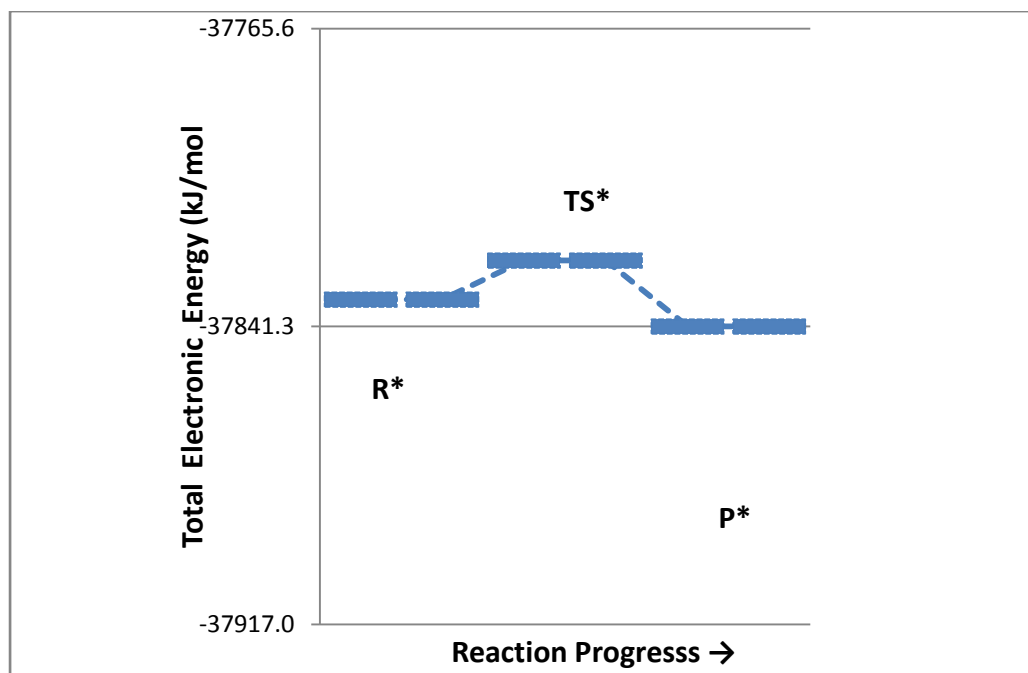


**Figure 4.23: Energy profile of the oxidation of 1,2-diphenylhydrazine by iodine via the cyclic activated complex for the DFT calculations**

**Key:** where R\* ( $AH_2 + I_2$ ), P\* ( $A + 2HI$ ) and TS\* are reactants, products and transition states for the one-step cyclic mechanism.

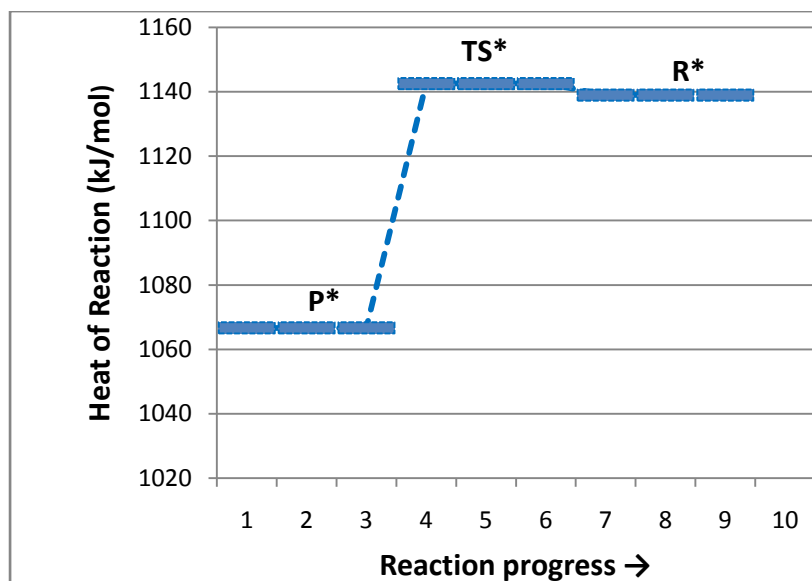


**Figure 4.24: Energy profile of the oxidation of 1,2-diphenylhydrazine by iodine via the cyclic activated complex for the MNDO calculations**

**Key:** where R\* ( $AH_2 + I_2$ ), P\* ( $A + 2HI$ ) and TS\* are reactants, products and transition states for the one-step cyclic mechanism.

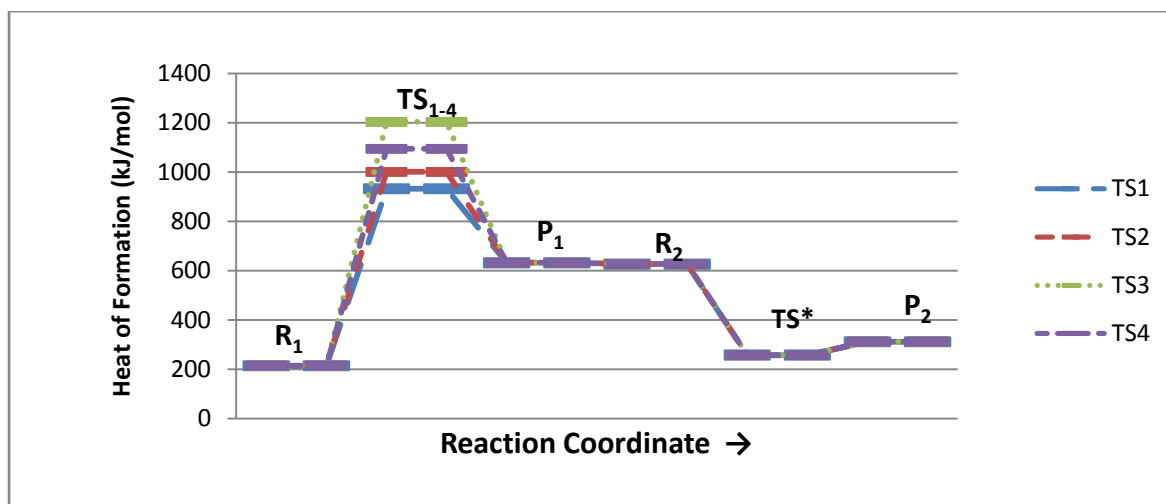


**Figure 4.25: Energy profile of the oxidation of L-tyrosine by iodine according to the PM3 calculations**

**Key:** where  $R_1$  (L-Tyr + I<sub>2</sub>),  $R_2$  (MIT + I<sub>2</sub>), re reactants for steps 1 and 2;  $P_1$  (MIT + HI),  $P_2$  (DIT + HI) are products for steps 1 and 2; TS<sub>1-4</sub>, TS\* were transition states for steps 1 and 2.

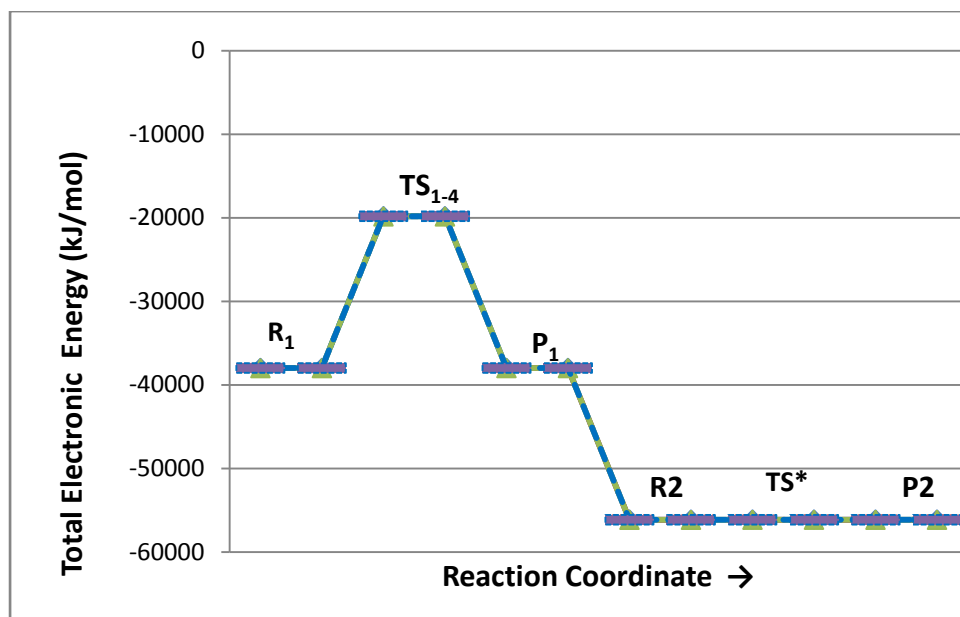


**Figure 4.26: Energy profile of the oxidation of L-tyrosine by iodine according to the DFT calculations**

**Key:** where R<sub>1</sub> (L-Tyr + I<sub>2</sub>), R<sub>2</sub> (MIT + I<sub>2</sub>), re reactants for steps 1 and 2; P<sub>1</sub> (MIT + HI), P<sub>2</sub> (DIT + HI) are products for steps 1 and 2; TS<sub>1-4</sub>, TS\* were transition states for steps 1 and 2.

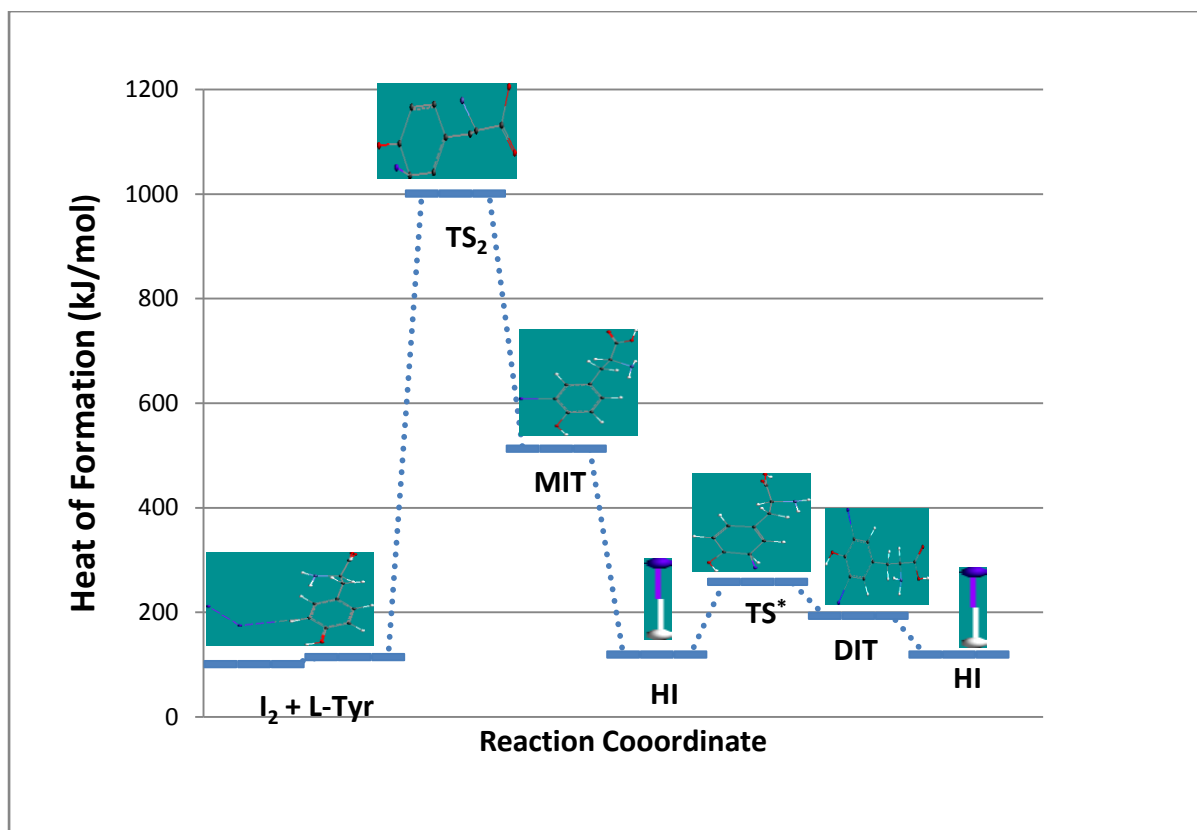


**Figure 4.27: Energy profile of the oxidation of L-tyrosine by iodine according to the most favored route showing the position of the optimized reacting species**

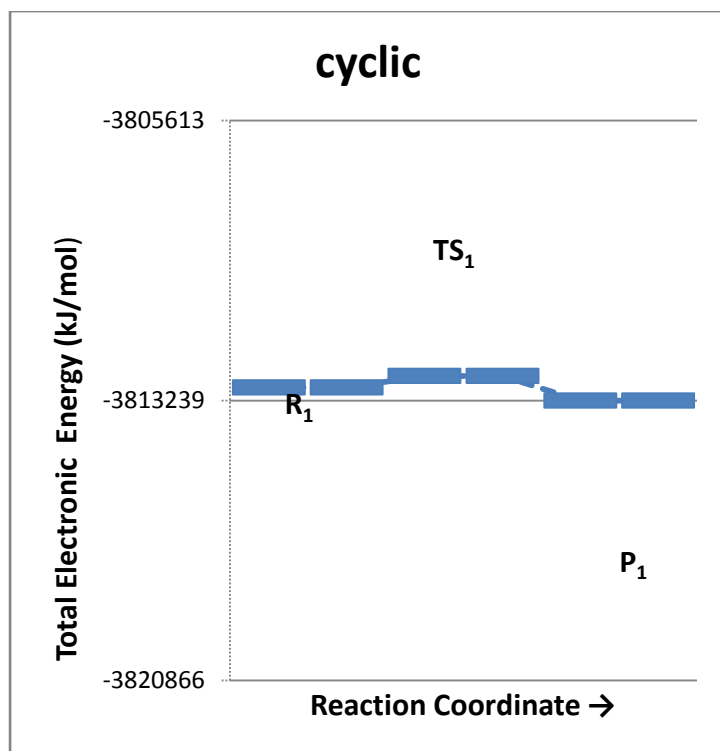


**Figure 4.28: Energy profile of the oxidation of L-ascorbic acid by iodine according to the DFT studies route 1 proposed mechanism**

**Key:** where  $R_1$  ( $AA + I_2$ ) are the reactants in route 1, with  $TS_1$  as the searched transition states and  $P_1$  ( $DAA + HI$ ), the products of the same reaction.

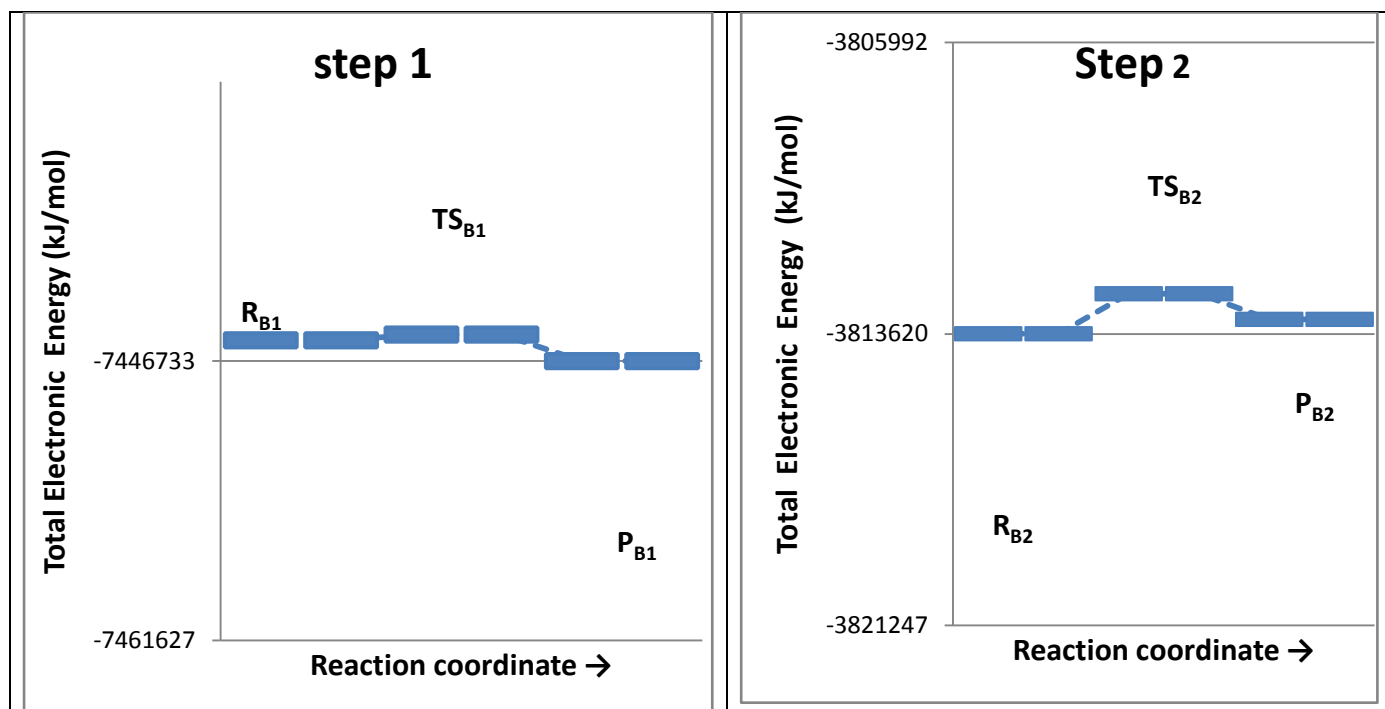


**Figure 4.29:** Energy profile of the oxidation of L-ascorbic acid by iodine according to the DFT studies route 2 proposed mechanisms

**Key:** While  $R_{B1}$  ( $AA + 2I_2$ ) and  $R_{B2}$  ( $AA + 2 I$ ) are all the reactants in steps 1 and 2, respectively, for route 2,  $P_{B1}$  ( $DAA + 2HI + 2I$ ) and  $P_{B2}$  ( $DAA + 2HI$ ) are the products of reactions for steps 1 and 2, respectively, for route 2,  $TS_{B1}$  is the first transition state for route 2, and  $TS_{B2}$  is the second transition state for route 2.

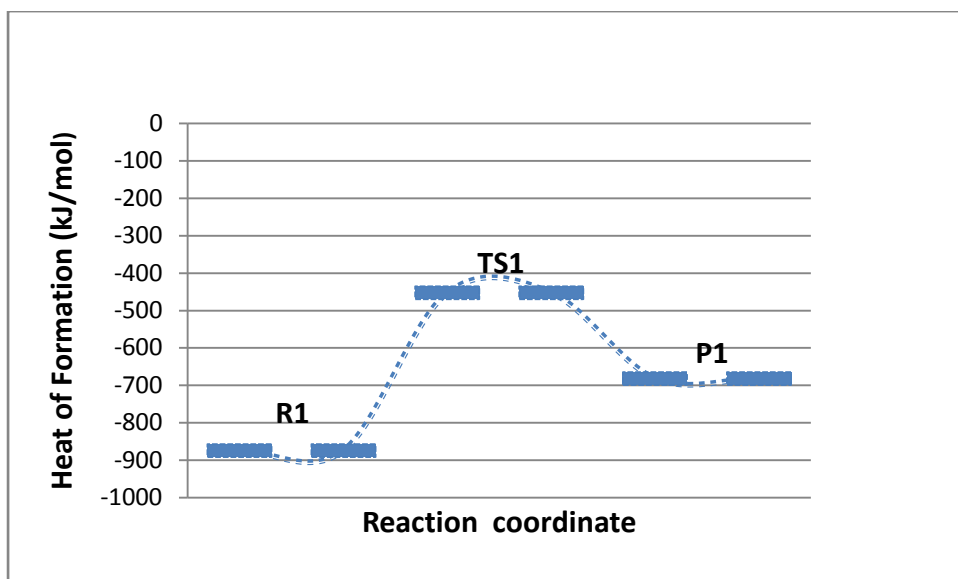


**Figure 4.30: Energy profile of the oxidation of L-ascorbic acid by iodine according to the PM3 studies route1 proposed mechanism**

**Key:** where  $R_1$  ( $AA + I_2$ ) are the reactants in route 1, with  $TS_1$  as the searched transition states and  $P_1$  ( $DAA + HI$ ), the products of the same reaction.

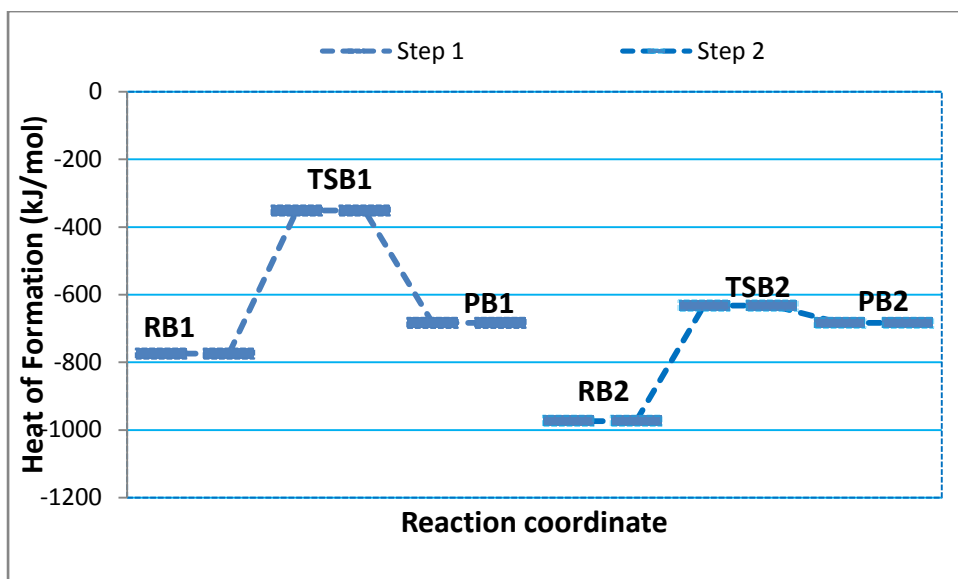


**Figure 4.31: Energy profile of the oxidation of L-ascorbic acid by iodine according to the PM3 studies route 2 proposed mechanism**

**Key:** While  $R_{B1}$  ( $AA + 2I_2$ ) and  $R_{B2}$  ( $AA + 2I$ ) are all the reactants in steps 1 and 2, respectively, for route 2,  $P_{B1}$  ( $DAA + 2HI + 2I$ ) and  $P_{B2}$  ( $DAA + 2HI$ ) are the products of reactions for steps 1 and 2, respectively, for route 2,  $TS_{B1}$  is the first transition state for route 2, and  $TS_{B2}$  is the second transition state for route 2.

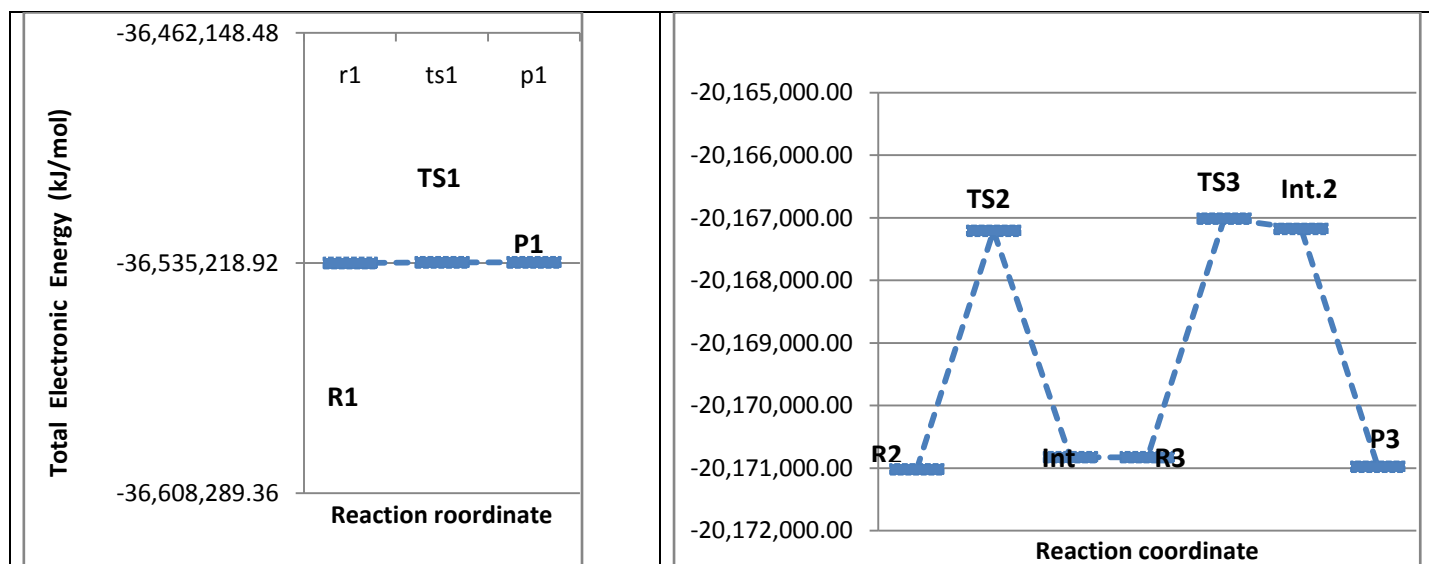


**Figure 4.32: Energy profile of the oxidation of D-fructose by iodine according to the DFT studies proposed mechanism**

**Key:** where  $R_1$  ( $I_2 + H_2O$ ),  $TS_1$  and  $P_1$  ( $HOI + HI$ ) are reactants, transition states respectively for the first step; while  $R_2$  ( $HOI + Fruc$ ) and  $R_3$  ( $B \text{ int}$ ) are reactants,  $TS_2$  ( $A$ ) and  $TS_3$  ( $C$ ) are transition states,  $int.$  ( $B$ ) and  $int.2$  ( $D$ ) were intermediates in second and third steps, respectively.  $P_3$  ( $E + HOI$ ) are the final products of the reaction.

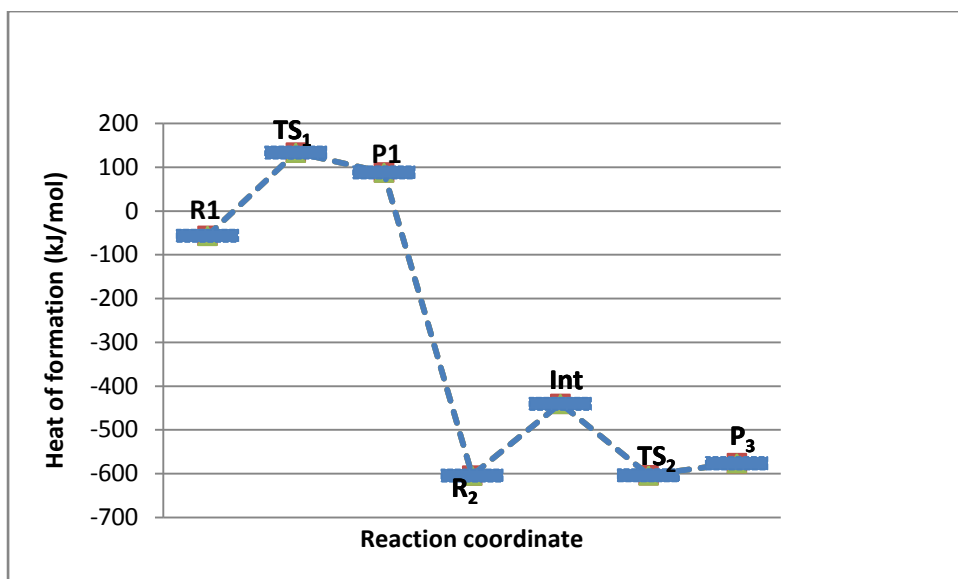


**Figure 4.33: Energy profile of the oxidation of D-fructose by iodine according to the PM3 studies proposed mechanism**

**Key:** where R<sub>1</sub> (I<sub>2</sub> + H<sub>2</sub>O), TS<sub>1</sub> and P<sub>1</sub> (HOI + HI) are reactants, transition states respectively for the first step; while R<sub>2</sub> (HOI + Fruc) and R<sub>3</sub> (B int) are reactants, TS<sub>2</sub> (A) and TS<sub>3</sub> (C) are transition states, int. (B) and int.2 (D) were intermediates in second and third steps, respectively. P<sub>3</sub> (E + HOI) are the final products of the reaction.

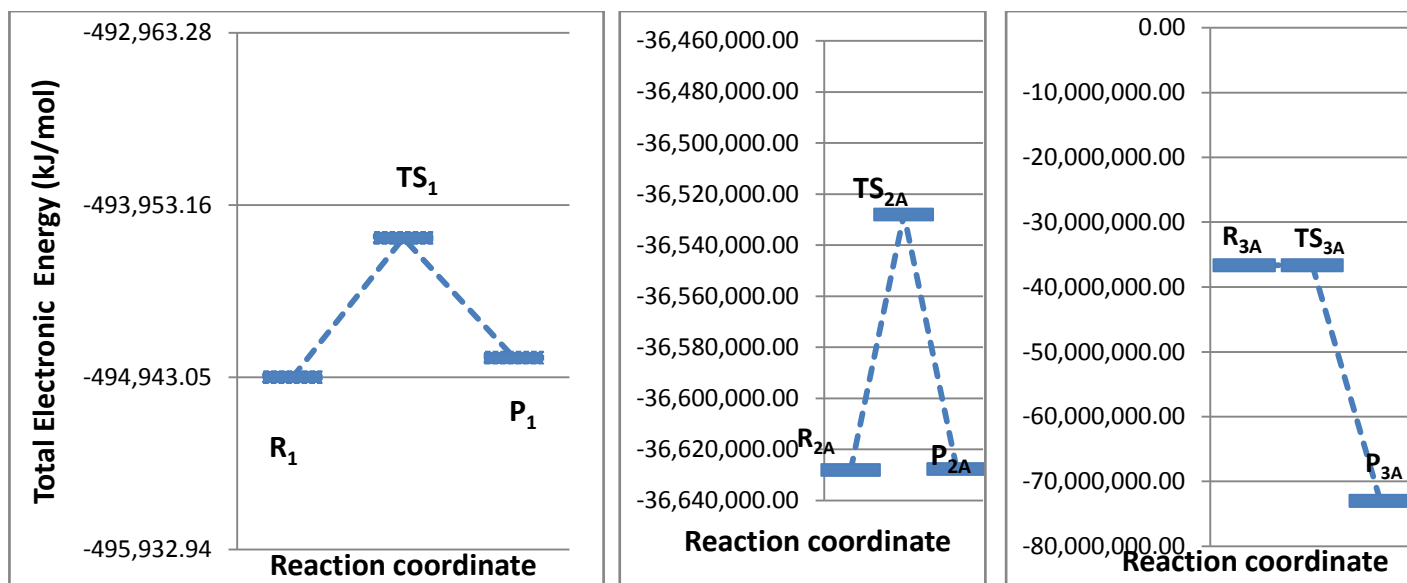


**Figure 4.34: Energy profile of the oxidation of hydrazine / hydrazinium ion by iodine according to the route 1 proposed mechanism**

**Key:** where  $R_1$  ( $H_2O + Hyd^+$ ) and  $P_1$  ( $H_3O^+ + Hyd$ ) are all the reactants and products for step 1.  $TS_1$ ,  $TS_2$  and  $TS_{3A}$  are the three transition states for route I.  $R_{2A}$  ( $I_2 + Hyd$ ) and  $P_{2A}$  ( $Int + 2HI$ ) are the respective reactants and products of step 2.  $R_{3A}$  ( $Int + I_2$ ) and  $P_{3A}$  ( $N_2 + 2HI$ ) are the respective reactants and products of step 3.

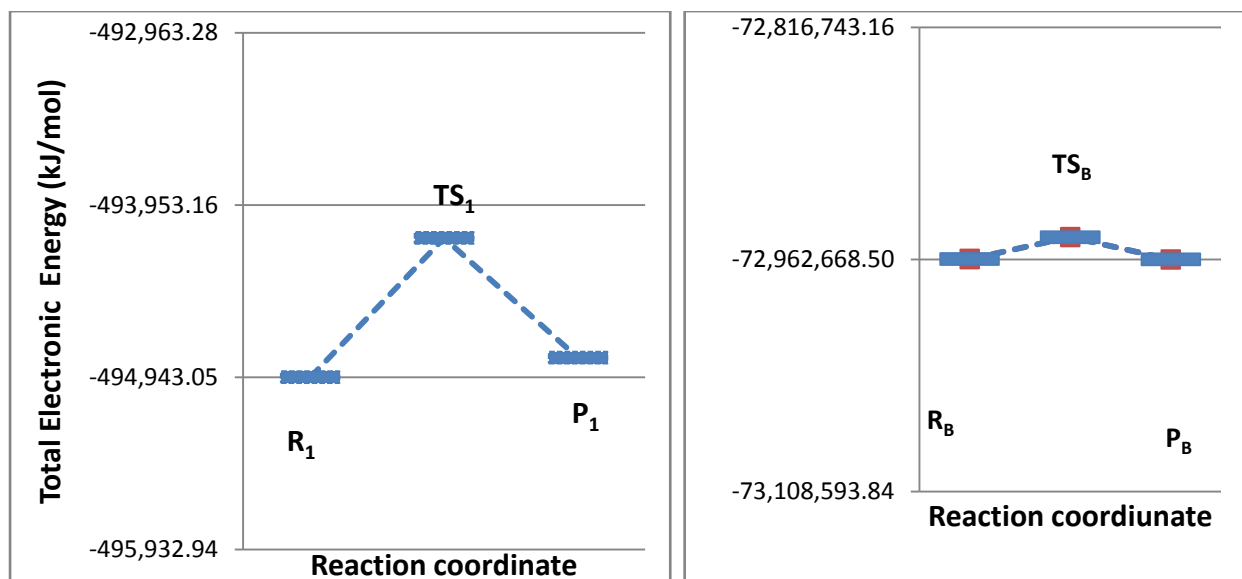


**Figure 4.35: Energy profile of the oxidation of hydrazine / hydrazinium ion by iodine according to the route II proposed mechanisms**

**Key:** where  $R_1$  ( $H_2O + Hyd^+$ ) and  $P_1$  ( $H_3O^+ + Hyd$ ) are all the reactants and products for step 1.  $TS_1$  and  $TS_B$  are the two transition states for route II.  $R_B$  ( $2I_2 + Hyd$ ) and  $P_B$  ( $N_2 + 4HI$ ) are the respective reactants and products of step 2.

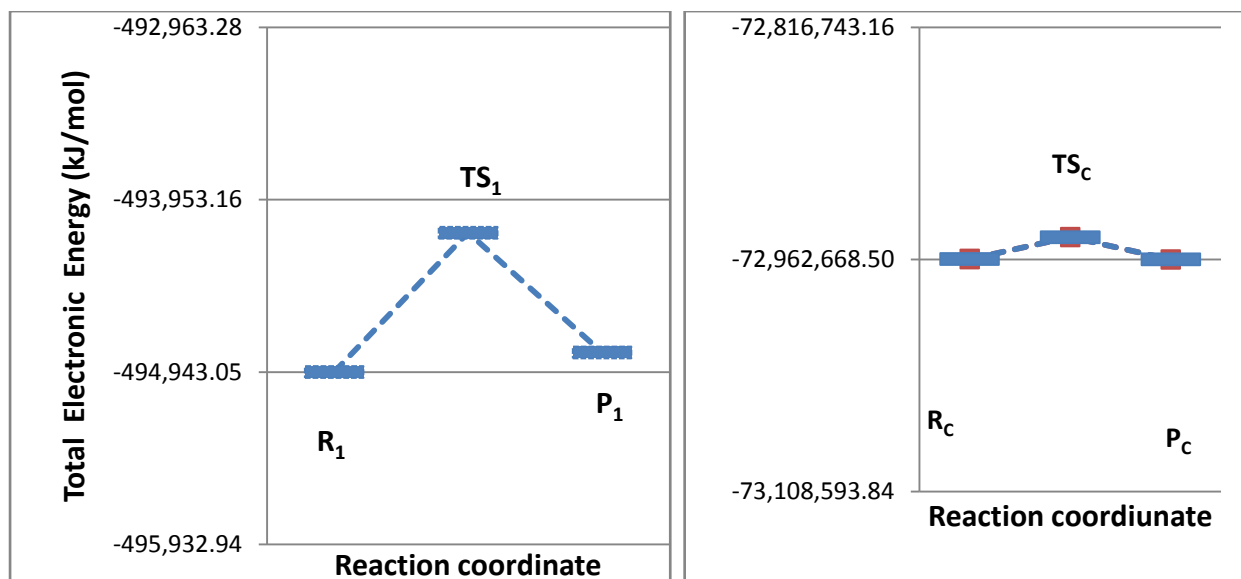


**Figure 4.36: Energy profile of the oxidation of hydrazine / hydrazinium ion by iodine according to the route III proposed mechanisms**

**Key:** where R<sub>1</sub> (H<sub>2</sub>O + Hyd<sup>+</sup>) and P<sub>1</sub> (H<sub>3</sub>O<sup>+</sup> + Hyd) are all the reactants and products for step 1. TS<sub>1</sub> and TS<sub>C</sub> are the two transition states for route III. R<sub>B</sub> (2I<sub>2</sub> + Hyd) and P<sub>B</sub> (N<sub>2</sub> + 4HI) are the respective reactants and products of step 2.

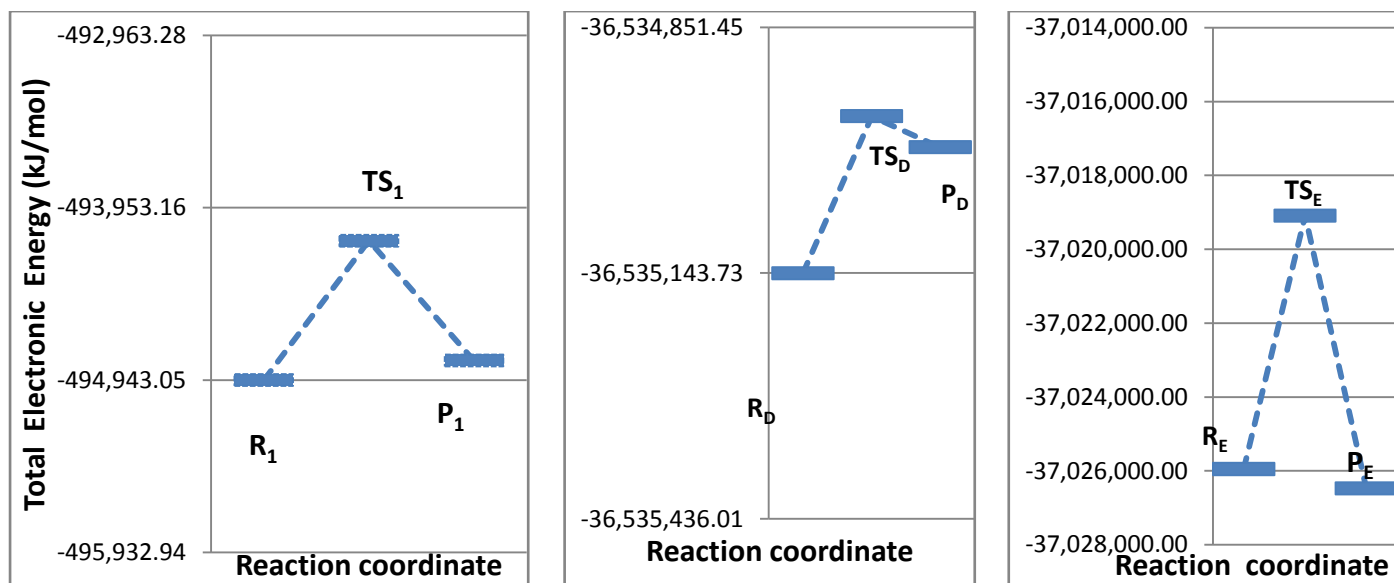


**Figure 4.37: Energy profile of the oxidation of hydrazine / hydrazinium ion by iodine according to the route IV proposed mechanisms**

**Key:** where  $R_1$  ( $H_2O + Hyd^+$ ) and  $P_1$  ( $H_3O^+ + Hyd$ ) are all the reactants and products for step 1.  $TS_1$ ,  $TS_D$  and  $TS_E$  are the three transition states for route IV; while  $R_D$  ( $2I_2 + 2H_2O$ ) and  $P_D$  ( $2HOI + 2HI$ ), respective reactants and products of step 2.  $R_E$  ( $2HOI + Hyd$ ) and  $P_E$  ( $N_2 + 2H_2O + 2HI$ ) were the respective reactants and products of step 3.

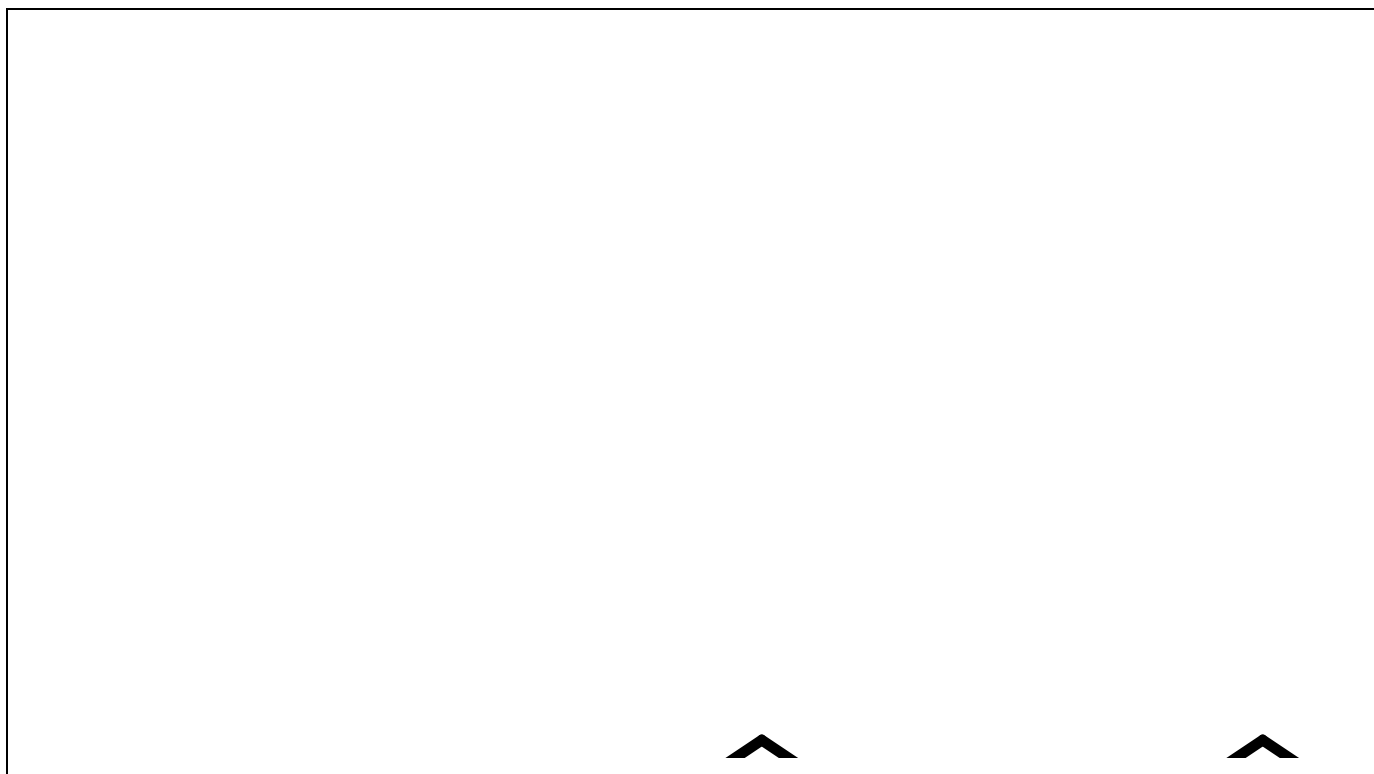
#### **4.6 Proposal of More Plausible Mechanisms for the Biomolecules - Iodine Reaction Systems**

##### **4.6.1 More Plausible Mechanisms for Reaction of 1,2-Diphenylhydrazine – Iodine Reaction System According to the Chain Multi Step and Cyclic Mechanism**

**Scheme 4.1: Proposed multi-step mechanism for the 1,2-diphenylhydrazine reaction with iodine**

**Scheme 4.2: The one-step mechanism with cyclic activated complex for the 1,2-diphenylhydrazine reaction with iodine**

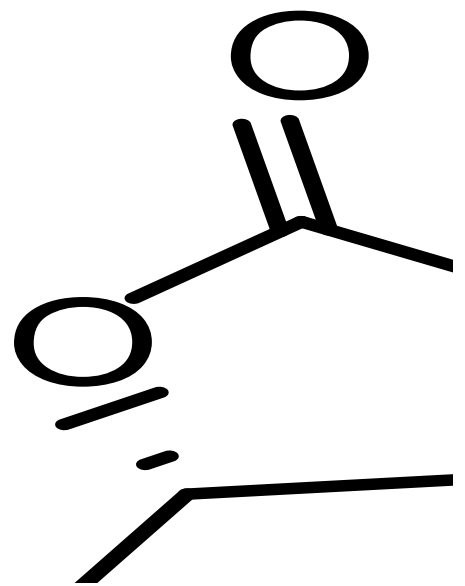
#### 4.6.2 More Plausible Mechanisms for Reactions of L-Tyrosine – Iodine Reaction System



**Scheme 4.3:** The reaction mechanism of L-tyrosine as modified by this study

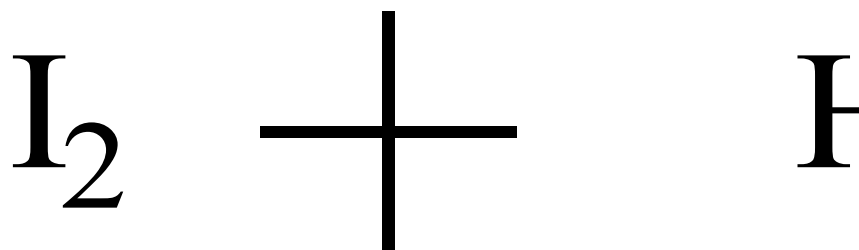
### **4.6.3 More Plausible Mechanisms for Reaction of L-Ascorbic Acid – Iodine Reaction System**

**Scheme 4.4: The one-step reaction mechanism via the cyclic activated complex for the L-ascorbic acid reaction with iodine**



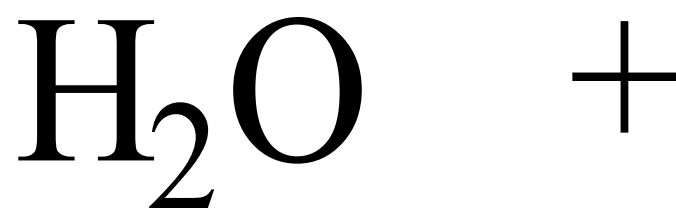
**Scheme 4.5: The two-steps reaction mechanism for the L-ascorbic acid reaction with iodine**

#### 4.6.4 More Plausible Mechanisms for Reaction of D-Fructose – Iodine Reaction System



**Scheme 4.6:** Proposed reaction mechanism for the oxidation of D-fructose with iodine.

**4.6.5 More Plausible Mechanisms for Reactions of Hydrazine / Hydrazinium Ion – Iodine Reaction System According to the DFT Methods for Routes 1 - 4, respectively**



**Scheme 4.7: The first proposed mechanism for the hydrazine / hydrazinium ion reaction with iodine (Route I)**

**Scheme 4.8: The second proposed mechanism for the hydrazine / hydrazinium ion reaction with iodine (Route II)**

**Scheme 4.9: The third proposed mechanism for the hydrazine / hydrazinium ion reaction with iodine (Route III)**

**Scheme 4.10: The fourth proposed mechanism for the hydrazine / hydrazinium ion reaction with iodine (Route IV)**

## CHAPTER FIVE

### 5.0 DISCUSSION

#### 5.1 Geometry Optimization of Reactants, Activated Complexes, Intermediates and Products

Geometry optimization of the reactants, intermediates, transition states and products in the 1,2-diphenylhydrazine, L-tyrosine, D-ascorbic acid, D-fructose and hydrazine / hydrazinium ion reaction systems with iodine were executed. The geometry optimizations of these species were successfully completed. The geometries of the reactants, transition states, intermediate and products were optimized using molecular mechanics to remove strain energies. This was followed by semi empirical optimizations at AM1, MNDO and PM3 theory levels. Finally, DFT Becke's three parameter nonlocal exchange functional with the nonlocal correlation functional of Lee, Yang, Parr (B3LYP) with 6-311+G\*\* basis set calculations was employed (Stewart, 1986; 2007; Zhang and Hase, 2010).

The optimized geometries of the reactants, intermediates, transition states and products are shown in Figure 4.1 for the 1,2-diphenylhydrazine – iodine reaction system. Figure 4.2 is for the L-tyrosine – iodine reaction system, Figure 4.3 for the D-ascorbic acid– iodine reaction system, Figure 4.4 for the D-fructose– iodine reaction system and Figure 4.5 for the hydrazine/ hydrazinium ion – iodine reaction system.

#### 5.2 Mapped and Calculated HOMO and LUMO of Reactants

Chemists have developed a variety of methods for describing electrons in molecules. Lewis structures are the most familiar. These drawings assign pairs of electrons either to single atoms (lone pairs) or pairs of atoms (bonds). The quantum mechanical equivalents are atomic and molecular orbitals which arise from solution of (approximate) Schrödinger equations for atoms and molecules, respectively, (Spartan, 2014). Molecular orbitals are spread throughout

the entire molecule, that is, they are delocalized. Because of this, they are typically more difficult to interpret than Lewis structures (Spartan, 2014).

Molecular orbitals provide important clues about chemical reactivity. The Spartan-generated images (Figures 4.6 – 4.10) depict the same orbital as a surface of constant value. The surface is accurate in that it is derived from an authentic (but approximate) calculated solution to the quantum mechanical equations of electron motion. Equally important, the images are three-dimensional, and can be manipulated and looked at from a variety of different perspectives. Note that an orbital surface actually consists of two distinct surfaces represented by different colours (Spartan, 2014). They identify regions where the orbital takes on a significant value, either positive (blue) or negative (red). The orbital node is not shown, but we can guess that it lies midway between the two surfaces (this follows from the fact that the orbital's value can only change from positive to negative by passing through zero).

Atomic orbitals (descriptions of atoms) are the fundamental building blocks from which molecular orbitals (descriptions of molecules) are assembled. The familiar atomic orbitals for the hydrogen atom are, in fact, exact solutions of the Schrödinger equation for this one-electron system (Lynam *et al.*, 1998). They form an infinite collection (a complete set), the lowest-energy member representing the best location for the electron, and higher-energy members representing alternative locations. Orbitals for real many-electron atoms are normally assumed to be similar in form to those of hydrogen atom, the only difference being that, unlike hydrogen, more than the lowest-energy atomic orbital is utilized. In practical quantum chemical calculations, atomic orbitals for many-electron atoms are made up of sums and differences of finite collection of hydrogen-like orbitals (Lynam *et al.*, 1998).

The plots of the HOMO and LUMO of iodine are shown in Figure 4.6a and 4.6b. It could be seen that the frontier electron densities of both HOMO and LUMO orbitals are on the two atoms that formed the iodine molecule. Specifically, HOMO and LUMO levels determine how a chemical molecule shares its valence electron in the occupied molecular orbitals and donates (or accepts) electrons to ligand, and thus the HOMO-LUMO energy gap has been suggested as an indicator of the stability of molecules (Lynam *et al.*, 1998). The HOMO-LUMO energy gap, ( $\Delta E = -3.09$  eV) is smaller than all the HOMO-LUMO gaps in the other bio substrate reactants. This value showed that, compared to the other reactants, the iodine molecule would be a better electron donor than the others, according to Fukui's frontier orbital theory (Fukui, 1964; 1974; 1982; Ya-Yin Fang, 2002).

The plots of the HOMO and LUMO of 1,2-diphenylhydrazine are also shown in Figure 4.6a and 4.6b. The HOMO-LUMO energy gap, ( $\Delta E = -8.57$  eV), of the 1,2-diphenylhydrazine is larger than that of the iodine molecule. This would make the 1,2-diphenylhydrazine as the electron acceptor, or, the reductant.

The plots of the HOMO and LUMO of L-tyrosine are shown in Figure 4.7. It could be seen that the frontier electron densities of atoms C<sub>4</sub> and C<sub>6</sub> in both HOMO and LUMO orbitals are larger than those of the other atoms. These, according to Fukui's frontier orbital theory (Fukui, 1964; 1974; 1982; Ya-Yin Fang, 2002), coupled with the fact that these same atoms carried the most negative charges were pointers to their being the most capable reactive site in the molecule. In addition, the bonding contribution of LUMO (-0.09 eV) for bond cleavage was smaller than that of HOMO (-9.39 eV) for bond formation; thus it showed that there would be bond formation between L-tyrosine and the other molecules. The HOMO-LUMO energy gap,  $\Delta E$ , of L-tyrosine is -8.57 eV. This may also indicate that the

substitution reaction occurred by the associative interchange ( $I_a$ ) mechanism, as there were both bond breakage and bond formation, with the bond formation dominating (Housecroft and Sharpe, 2008).

The HOMO and LUMO plot for D-ascorbic acid is as shown in Figure 4.8. The most reactive sites are C3, C4, O3, and O4. The HOMO-LUMO energy gap,  $\Delta E$ , of D-ascorbic acid is -9.13 eV.

The plots of the HOMO and LUMO of D-fructose are shown in Figure 4.9. It could be seen that the HOMO and LUMO are centered on atoms C<sub>2</sub>, C<sub>3</sub>, O<sub>2</sub>, H<sub>5</sub> and H<sub>8</sub> of the optimized D-fructose molecule. These, according to Fukui's frontier orbital theory (Fukui, 1964, 1982; Fang, 2002), were pointers to their being the most capable reactive site in the molecule. In addition, the bonding contribution of LUMO (-10.74 eV) for bond cleavage is smaller than that of HOMO (-0.09 eV) for bond formation, while the HOMO-LUMO energy gap,  $\Delta E$ , is -10.69 eV.

The plots of the HOMO and LUMO of hydrazine / hydrazinium ion are shown in Figure 4.10. The HOMO-LUMO energy gaps for hydrazine and hydrazinium ion are -9.06 eV and -9.13 eV, respectively. Both values are larger than the energy gap for iodine, the electron donor.

The trends in the E HOMO, E LUMO and  $\Delta E$  for the iodine molecule and the bio molecules were as expected, with that of iodine (the oxidant) being the least and those the bio substrates (the reductants) being larger.

### 5.3 Searched Transition States and Intermediates

The energy of a molecule depends on its geometry. Even small changes in structure can lead to quite large changes in total energy. Proper choice of molecular geometry is therefore quite important in carrying out modeling studies. Experimental geometries, where available, would certainly be suitable. While experimental equilibrium geometries are available for many stable molecules, the problem is that, many more have not been determined (Spartan, 2014). Also, experimental data for reactive or otherwise short-lived molecules are scarce, and data for transition states are completely lacking. In the final analysis, there is no alternative to obtaining geometries from calculation. Fortunately, this is not difficult, although it may be demanding in terms of computer time.

Determination of geometry (geometry optimization) is an iterative process. The energy and energy gradient (first derivative of the energy with respect to all geometrical coordinates) are calculated for the initial geometry, and this information is then used to project a new geometry (Spartan, 2014). This process continues until three criteria are satisfied. First, the gradient must closely approach zero. This ensures that the optimization is terminating in a flat region of the potential surface (either the bottom of energy well in the case of equilibrium geometry or the top of an energy hill in the case of transition-state geometry). Second, successive iterations must not change any geometrical parameter by more than a specified (small) value. Third, successive iterations must not change the total energy by more than a specified (small) value.

Chemists recognize a transition state as the structure that lies at the top of a potential energy surface connecting reactant and product (Figures 4.21 - 4.37 in section 4.5 on potential energy surfaces). More precisely, a transition state is a point on the potential energy surface

for which the gradient is zero, but for which the diagonal representation of the Hessian has one and only one negative element, corresponding to the reaction coordinate (Spartan, 2014). All the other elements are positive. In other words, a transition state is a structure that is an energy minimum in all dimensions except one, for which it is an energy maximum. Mathematically, such a structure is referred to as a first-order saddle point (Spartan, 2014; Lynam *et al.*, 1998).

### **5.3.1 Transition States and Intermediates for 1,2-Diphenylhydrazine – Iodine Reaction System**

Geometry optimization of the reactants, intermediates, transition states and products in the 1, 2-diphenylhydrazine reaction with iodine was executed. For the 1,2-diphenyl hydrazine – iodine reaction system, two reaction pathways were proposed. Two transition states, TS<sub>1</sub> and TS<sub>2</sub> were found for route 1, while one transition state, TS\*, was found for the second route. The transition states are provided in Figure 4.11. All the transition states were found to occupy saddle points on the potential surface diagrams (Figures 4.21- 4.24). They were also confirmed by animating the vibration corresponding to the reaction coordinate by selecting the imaginary frequency at the top of the list of frequencies on the IR tab. The computed heat of formation (total electronic energy for DFT) of the intermediates and transition states together with those of other optimized structures were evaluated and presented in Tables 4.1 and 4.2.

### **5.3.2 Transition States and Intermediates for L-Tyrosine – Iodine Reaction System**

For the L-tyrosine – iodine reaction system, five transition states, TS<sub>1</sub>, TS<sub>2</sub>, TS<sub>3</sub>, TS<sub>4</sub> and TS\*, were found. The transition states are provided in Figure 4.12. All the transition states were found to occupy saddle points on the potential surface diagrams (Figures 4.25- 4.27). Only the transition state production and the values of the active energies can really reveal

whether the reactions occur or not and also how they occur if they do. In order to better understand the mechanism, dynamic calculations of the transition state was also investigated. The bond lengths of C<sub>6</sub>-I, C<sub>6</sub>-H and C<sub>4</sub>-H (the reactive sites) of the various optimized transition states (Aghaie*et al.*, 2008) were examined to see if there were any differences.

The bond lengths for C<sub>6</sub>-H and C<sub>4</sub>-H in the optimized L-tyrosine are 1.091 and 1.090, respectively, while all the other C-H bond lengths are 1.092 (Table 4.7). In the activated complex, TS<sub>2</sub>, the bond lengths for C<sub>6</sub>-H and C<sub>4</sub>-H, increased from 1.091 and 1.090 to 1.126 and 1.105, respectively, thus indicating that the respective H-atoms were pushed further away from the respective C-atoms, ready to be replaced by incoming substituent. On the other hand, the same C-H bond lengths under consideration in TS<sub>2</sub>, TS<sub>3</sub> and TS<sub>4</sub> remained unaffected. Also, considering the C<sub>6</sub>-I bond lengths in TS<sub>1</sub>, TS<sub>2</sub>, TS<sub>3</sub>, and TS<sub>4</sub>, respectively, TS<sub>2</sub> had the shortest bond length, and that also showed that the C-I bond in TS<sub>2</sub> was more stabilized than in the others.

### **5.3.3 Transition States and Intermediates for L-Ascorbic Acid – Iodine Reaction System**

Geometry optimization of intermediates and transition states as well as reactants and products in the L-ascorbic acid reaction with iodine was executed. For the L-ascorbic – iodine reaction system, two reaction pathways were proposed. One transition state, TS<sub>1</sub>, was found for route 1, while two transition states, TS<sub>B1</sub> and TS<sub>B2</sub>, were found for the second route. The transition states are provided in Figure 4.13. All the transition states were found to occupy saddle points on the potential surface diagrams (Figures 4.28- 4.31). They were also confirmed by animating the vibration corresponding to the reaction coordinate by selecting the imaginary frequency at the top of the list of frequencies on the IR tab. The heat of

formation (total electronic energy for DFT) at standard condition of 1 atmosphere and 298.15K were evaluated and presented together with other thermodynamic parameters in Table 4.8 for DFT studies route 1; Table 4.9 for DFT studies route 2; and Table 4.11 for the PM3 studies for both routes 1 and 2. The activation parameters are given in Tables 4.10 and 4.12, respectively.

### **5.3.4 Transition States and Intermediates for D-Fructose– Iodine Reaction System**

For the D-fructose– iodine reaction system, three transition states, TS<sub>1</sub>, TS<sub>2</sub>, and TS<sub>3</sub>. One intermediate, Int, was also found. The transition states and the intermediate are provided in Figure 4.14. All the transition states were found to occupy saddle points on the potential surface diagrams (Figures 4.32 and 4.33). They were also confirmed by animating the vibration corresponding to the reaction coordinate by selecting the imaginary frequency at the top of the list of frequencies on the IR tab. The computed heat of formation (total electronic energy for DFT) of the intermediates and transition states together with those of other optimized structures were evaluated and presented in Tables 4.14 – 4.17.

### **5.3.5 Transition States and Intermediates for Hydrazine/Hydrazinium Ion– Iodine Reaction System**

For the hydrazine/hydrazinium ion – iodine reaction system, four reaction pathways were proposed. A total of seven transition states, TS<sub>1</sub>, TS<sub>2A</sub>, TS<sub>3A</sub>, TS<sub>B</sub>, TS<sub>C</sub>, TS<sub>D</sub> and TS<sub>E</sub>, were found for the various four routes. One intermediate, Int, was also found. The transition states and the intermediate are provided in Figure.15. All the transition states were found to occupy saddle points on the potential surface diagrams (Figures 4.34- 4.37). They were also confirmed by animating the vibration corresponding to the reaction coordinate by selecting the imaginary frequency at the top of the list of frequencies on the IR tab. The computed heat of formation (total electronic energy for DFT) of the intermediates and transition states

together with those of other optimized structures for the various routes proposed were evaluated and presented in Tables 4.18 – 4.22.

#### **5.4 Calculation of Thermodynamics, Molecular and other Physico-chemical Properties of Reacting Species and Products**

In addition to molecular geometry, the energy is one of the most important quantities to come out of molecular modeling. Energy can be used to reveal which of several isomers is most stable, to determine whether a particular chemical reaction will have a thermodynamic driving force (an exothermic reaction) or be thermodynamically uphill (an endothermic reaction), and to ascertain how fast a reaction is likely to proceed (Spartan, 2014).

There is more than one way to express the energy of a molecule. Most common to chemists is the heat of formation,  $\Delta H_f$ . This is the heat of a hypothetical chemical reaction that creates a molecule from the well defined (but arbitrary) standard states of each of its constituent elements (Spartan, 2014; Smith and Sutcliffe, 1997).

An alternative, total energy is the heat of a hypothetical reaction that creates a molecule from a collection of separated nuclei and electrons. Like the heat of formation, total energy cannot be measured directly, and is used solely to provide a standard method for expressing and comparing energies. Total energies are always negative numbers and, in comparison with the energies of chemical bonds, are very large. By convention, they are expressed in so-called atomic units\* or au (1 au = 2625 kJ/mol), but may be converted to other units as desired (Spartan, 2014).

##### **5.4.1 1,2-Diphenylhydrazine – Iodine System**

Geometry optimization of the reactants, intermediates, transition states and products in the 1, 2-diphenylhydrazine reaction with iodine was executed. The geometry optimizations

of all the species were successfully completed. The optimized geometries of the reactants, intermediates, transition states and products are shown in Figure 4.1 and the computed heat of formation (total electronic energy for DFT) were evaluated and presented in Table 4.1. The activation parameters are as shown in Table 4.2.

#### **5.4.1.1 Charge Distribution, Bond Length and Exposed Surface Area of 1,2-diphenylhydrazine**

The starting 1,2-diphenylhydrazine molecule was optimized. The conformation with the lowest energy was optimized and calculated using the PM3 and DFT methods. The oxidation of 1,2-diphenylhydrazine by the various groups previously reported (Whalley *et al.*, 1956; May and Halpern, 1961; Sengupta and Sen, 1979; Kelly *et al.*, 1994; Jia *et al.*, 2000) showed that hydrogen ( $H^+$ ) ions were abstracted from the ascorbic acid molecule. The identity numbers of all the atoms of the 1,2-diphenylhydrazine molecule are labelled as in Figure 4.16.

Molecular information such as how all the 12 hydrogen atoms were bonded (either as C-H or N-H), their bond lengths, the exposed surface areas of various hydrogen atoms available for reactions were obtained and presented in Table 4.3.

Among the 12 hydrogen atoms of the 1,2-diphenylhydrazine molecule, H1, H2, H3, H4, H5, H6, H9, H10, H11 and H12 were bonded to carbon atoms while H7 and H8 were bonded to nitrogen atoms. The bond lengths of all the C-H bonds (ranging from 1.094 – 1.098 Å) were longer than the N-H bonds (ranging from 0.998 – 1.000 Å). However, these hydrogen atoms bonded to nitrogen atoms had the largest exposed surfaces of 8.08 Å<sup>2</sup> and 6.56 Å<sup>2</sup>. The hydrogen atoms bonded to carbon atoms all have smaller exposed surface areas ranging from 5.44 – 5.46 Å<sup>2</sup>. The large exposed surfaces of the 2 hydrogen atoms attached to nitrogen

centres showed that these atoms were active hydrogen atoms and can react easily (Ya-Yin, 2002). In addition, the bonding contribution of LUMO (-0.05eV) for bond cleavage was smaller than that of HOMO (-8.62eV) for bond formation; thus it showed that there was bond formation between 1,2-diphenylhydrazine molecule and the electrophiles.

#### 5.4.2 L-Tyrosine – Iodine System

Geometry optimization of the reactants, intermediates, transition states and products in the L-tyrosine reaction with iodine was executed. The geometry optimizations of all these species were successfully completed and the heat of formation at 298.15K (total electronic energy for DFT) were evaluated and presented together with other activation parameters in Tables 4.4 and 4.5.

If the heat of formation of the various optimized transition states as proposed by Aghaieet *al.* (2008) were considered, TS<sub>1</sub> has the least enthalpy of formation(932.15 kJ/mol), followed by TS<sub>2</sub> with 1001.15 kJ/mol, TS<sub>4</sub> with 1095.16 kJ/mol and TS<sub>3</sub> with 1204.04 kJ/mol according to the PM3 calculations (Table 4.4). The trend with the DFT calculations was not quite different only that TS<sub>2</sub> was most favoured and was therefore, the most stabilized of the four possible transition states (TS<sub>1</sub>-TS<sub>4</sub>). The potential energy surface diagrams (Figures 4.25 - 4.27) showed the energy profiles of the optimized reacting species, where R<sub>1</sub> were the reactants in step 1, with TS<sub>1-4</sub> as the possible transition states and P<sub>1</sub>, the products of the same step; whereas R<sub>2</sub>, TS\* and P<sub>2</sub> were the reactants, transition state and products of the second step respectively.

Figure 4.25 showed TS<sub>1-4</sub> as saddle points as expected but unfortunately failed to do for TS\*. This showed the deficiency of the semi empirical calculations. Figure 4.26 was able to show

TS<sub>1-4</sub> and TS\* as saddle points as expected because of the accuracy of the DFT calculations. For the DFT calculations, total electronic energies for the various species ( $R_2 = -56150904.97$  kJ/mol, TS\* =  $-56143919.32$  kJ/mol and  $P_2 = -56147384.02$  kJ/mol) were close but that of TS\* was still slightly higher.

#### 5.4.2.1 Charge Distribution, Bond Length and Exposed Surface Area of L-Tyrosine

The starting L- tyrosine molecule was optimized. The conformation with the lowest energy was optimized and calculated using the PM3 method. Then molecular information such as net charges, electron density, molecular orbital energies were obtained. The identity numbers of all non-hydrogen atoms of the conformer compound were labelled as in Figure 4.17.

The more negative charges that an atom possesses, the more the ability of the atom to react with electrophiles. On the other hand, the more positive charges that an atom possesses, the more the capacity of the atom to react with nucleophiles or nucleophilic reagents. In this work, the net charges as well as the exposed areas of non-hydrogen atoms of the reactant, L- tyrosine, were shown in Table 4.6. Atoms C<sub>1</sub>, C<sub>3</sub>, C<sub>4</sub>, C<sub>6</sub>, C<sub>7</sub>, O<sub>1</sub>, N<sub>1</sub>, O<sub>2</sub> and O<sub>3</sub>, possessed more negative charges, while C<sub>2</sub>, C<sub>5</sub>, C<sub>8</sub> and C<sub>9</sub> possessed more positive charges. Among these, atoms C<sub>4</sub>, C<sub>6</sub>, N<sub>1</sub>, O<sub>1</sub>, O<sub>2</sub> and O<sub>3</sub> possessed the most net charges and were capable reactive sites. Because atoms N<sub>1</sub> of the amino group, O<sub>1</sub> of the hydroxyl group, and O<sub>2</sub>, O<sub>3</sub> of the carboxyl group can be stabilized or be made inactive when they form zwitterions, they have not been considered (Laloo and Mahanti, 1990; Giulivi and Davies, 2001; Faller *et al.*, 2002; Malika *et al.*, 2010; Trouillaset *et al.*, 2010). Amino acids with aromatic side chain were oxidized more rapidly than the alkyl side chain amino acids. Thus, atoms C<sub>4</sub> and C<sub>6</sub> were the reactive sites. The calculated exposed areas of the atoms as captured in Table 4.6 also showed atoms C<sub>4</sub> and C<sub>6</sub> presented more surfaces for reactivity (Spartan, 2003).

### 5.4.3 L-Ascorbic Acid – Iodine System

Geometry optimization of the reactants, intermediates, transition states and products in the ascorbic acid reaction with iodine was executed. The geometry optimizations of all these species were successfully completed and the heat of formation (total electronic energy for DFT) at standard condition of 1 atmosphere and 298.15K were evaluated and presented together with other thermodynamic parameters in Table 4.8 for DFT studies route 1; Table 4.9 for DFT studies route 2; and Table 4.11 for the PM3 studies for both routes 1 and 2. Tables 4.10 and 4.12 showed the results of the activation parameters according to the DFT and PM3 methods, respectively.

#### 5.4.3.1 Charge Distribution, Bond Length and Exposed Surface Area of L-Ascorbic Acid

The starting ascorbic acid molecule was optimized. The conformation with the lowest energy was optimized and calculated using the PM3 method. The oxidation of ascorbic acid by the various groups previously reported (Morelli, 1976; Rahmawati and Bundjali, 2009; Canterbury, 2014) showed that hydrogen ( $H^+$ ) ions were abstracted from the ascorbic acid molecule. The identity numbers of all the atoms of the Ascorbic acid molecule labelled as in Figure 4.18.

Molecular information such as how all the eight hydrogen atoms were bonded (either as C-H or O-H), their bond lengths, the exposed surface of various hydrogen atoms available for reactions were obtained and presented in Table 4.13.

Among the eight hydrogen atoms of the ascorbic acid molecule, H1, H3, H5 and H6 were bonded to oxygen atoms while the rest were bonded to carbon atoms. The bond lengths of all the C-H bonds were longer than the O-H bonds. But of all the O-H bonds, H1 and H3 had the longest bond lengths of  $0.951\text{\AA}$  and  $0.950\text{\AA}$  respectively. These same hydrogen atoms had the

largest exposed surfaces of 8.05 Å and 8.06 Å. The large exposed surfaces of these 2 hydrogen atoms showed that these atoms were active hydrogen atoms and can react easily (Ya-Yin, 2002). In addition, the bonding contribution of LUMO (-0.52eV) for bond cleavage was smaller than that of HOMO (-9.65eV) for bond formation; thus it showed that there was bond formation between ascorbic acid molecule and the electrophiles.

#### **5.4.4 D-Fructose – Iodine System**

Geometry optimization of the reactants, intermediates, transition states and products in the D-fructose reaction with iodine was executed. The geometry optimizations of all these species were successfully completed and the heat of formation at 298.15K (total electronic energy for DFT) were evaluated and presented together with other thermodynamic and activation parameters in Tables 4.14 and 4.15 for the DFT optimization and Tables 4.16 and 4.17 for the semi-empirical PM3 optimization.

Looking at the respective values of TS<sub>1</sub>, TS<sub>2</sub> and TS<sub>3</sub> for the DFT studies in Table 4.14, it was clear they were true transition states, and these were confirmed by vibrational analysis studies. However, for the less accurate semi-empirical PM3 method, it was only TS<sub>1</sub> that was observed to be a true transition state. Plots of the potential energy surface profiles as shown in Figures 4.32 and 4.33, respectively, clearly showed the TS<sub>1</sub>, TS<sub>2</sub> and TS<sub>3</sub> for the DFT studies were true saddle points. But as expected, and as pointed out above, only TS<sub>1</sub> for the PM3 studies was a saddle point.

##### **5.4.4.1 Charge Distribution, Bond Length and Exposed Surface Area of D-Fructose**

The starting D-fructose molecule was optimized. The conformation with the lowest energy was optimized and calculated using semi-empirical PM3 and the DFT methods. Molecular

information such as net charges, electron density, molecular orbital energies were obtained. The identity numbers of all non-hydrogen atoms of the conformer compound were labeled as in Figure 4.19.

The more negative charges that an atom possesses, the more the ability of the atom to react with electrophiles. On the other hand, the more positive charges that an atom possesses, the more the capacity of the atom to react with nucleophiles or nucleophilic reagents. In this study, the net charges as well as the exposed areas of non-hydrogen atoms of the reactant, D-fructose, were shown in Table 4.18. Among the carbon atoms C<sub>1</sub> and C<sub>6</sub> have the largest exposed surface areas followed by C<sub>2</sub>, C<sub>3</sub>, C<sub>4</sub> and C<sub>4</sub> in that respective order. But C<sub>2</sub> has the largest net atomic charges of 0.551, with C<sub>1</sub> and C<sub>2</sub>, having the least values. The possession of large exposed surface area coupled with large net atomic charges would make C<sub>2</sub> a reactive site for nucleophilic attack. All the six oxygen atoms have negative net atomic charges, with O<sub>2</sub> attached to C<sub>2</sub> having the least negative charge of -0.516 and a relatively large exposed surface area of 11.89 Å<sup>2</sup>. This also makes O<sub>2</sub> a capable reactive site. Analyses of the hydrogen atoms' exposed surface areas and net atomic charges showed that H<sub>5</sub> attached to C<sub>3</sub> and H<sub>8</sub> attached to C<sub>4</sub> were the most active hydrogen atoms. Thus, the calculated exposed areas and the net atomic charges of the atoms showed atoms C<sub>2</sub>, O<sub>2</sub>, H<sub>5</sub> and H<sub>8</sub> were the most reactive sites of the optimized D-fructose molecule. This information was then used in proposing a mechanism for the reaction.

#### 5.4.5 Hydrazine / Hydrazinium Ion – Iodine System

Geometry optimization of the reactants, intermediates, transition states and products in the hydrazinium ion reaction with iodine was executed. The geometry optimizations of all these species were successfully completed and the heat of formation (total electronic energy for

DFT) at standard condition of 1 atmosphere and 298.15K were evaluated and presented together with other thermodynamic parameters in Tables 4.19 for route 1, Table 4.20 for route 2, Table 4.21 for route 3 and Table 4.22 for route 4. Tables 4.23 and 4.24 contained the activation parameters for the various routes.

In all the four routes proposed, the first step always started by the hydrolysis of the hydrazinium ion or abstraction of hydrogen ion by water to yield hydrazine. In fact, the abstraction of hydrogen ion or the hydrolysis of hydrazinium ion by water to yield hydrazine has been reported by several authors (Sisler *et al.*, 1957; Barca *et al.*, 1967; Jia *et al.*, 2000).

#### **5.4.5.1 Charge Distribution, Bond Length and Exposed Surface Area of Hydrazine/Hydrazinium Ion**

The starting hydrazine molecule and hydrazinium ion were optimized. The conformations with the lowest energies were optimized and calculated using the DFT method. Molecular information such as net charges, electron density, molecular orbital energies were obtained. The identity numbers of all atoms of the conformers were labelled as in Figure 4.20

The more negative charges that an atom possesses, the more the ability of the atom to react with electrophiles. On the other hand, the more positive charges that an atom possesses, the more the capacity of the atom to react with nucleophiles or nucleophilic reagents. In this study, the net charges as well as the exposed areas of hydrogen atoms of the reactants, hydrazine molecule and hydrazinium ion, were shown in Table 4.25.

The hydrazine molecule has four hydrogen atoms attached to two different nitrogen atoms (Figure 4.20). The bond lengths of each of the four N-H bonds were calculated as 0.998 Å. The four hydrogen atoms have exposed surface areas of 9.09 Å<sup>2</sup> each. The hydrazinium ion, on the other hand, has five hydrogen atoms attached to two nitrogen atoms (Figure 4.20). The

N-H bond length for H1 and H5 were calculated as 1.026 Å each, while those for H2, H3 and H4 were obtained as 1.016 Å each. The exposed surface areas of the five hydrogen atoms also followed the same pattern of their bond lengths, with H1 and H5 having the largest exposed areas of 9.38 Å<sup>2</sup> while the rest have 9.30 Å<sup>2</sup> each.

Sengupta and Sen (1979) and others (Jia *et al.*, 2000; Mshelia *et al.*, 2010) have reported that hydrazine and hydrazinium ion are known to be powerful reducing agents and are known to be oxidized to N<sub>2</sub> gas. This information, together with the others, gathered from the molecular properties were used to propose mechanisms for the hydrazine / hydrazinium ion – iodine reaction systems.

## 5.5 Construction of Potential Energy Surface Diagrams

Potential energy surfaces are special cases of a general type of plot in which the variation in energy is given as a function of reaction coordinate. Such diagrams provide the essential connections between important chemical observables - structure, stability, reactivity and selectivity - and energy (Spartan, 2014, Jensen, 2007).

The positions of the energy minima along the reaction coordinate give the equilibrium structures of the reactant and product. Similarly, the position of the energy maximum gives the structure of the transition state. Both energy minima (which correspond to stable molecules) and the energy maximum (which may correspond to a transition state) are well defined. However, the path connecting them (reaction coordinate) is not well defined, in the sense that there are many possible paths. Liken this to climbing a mountain. The starting and ending points are well defined as is the summit, but there can be many possible routes (Spartan, 2014; Norrby, 2000).

Equilibrium structure (geometry) may be determined from experiment, given that the molecule can be prepared and is sufficiently long-lived to be subject to measurement. On the other hand, the geometry of a transition state may not be experimentally established. This is simply because a transition state is not an energy well which can trap molecules (Jensen, 2007; Olsen and Jensen, 2003). Therefore, it is impossible to establish a population of molecules on which measurements may be performed.

Both equilibrium and transition-state structures may be determined from quantum chemical calculations. The fact that a molecule may not be stable enough to be detected and characterized (or even exist) is not important. Equilibrium and transition-state structures can be distinguished from one another simply by inspecting the shape of the potential energy surface in the vicinity of the structure (Spartan, 2014). A better (more general) indicator is the set of frequencies associated with the vibrational motions around the structure, the same quantities measured by infrared spectroscopy. Structures for which all frequencies are real numbers correspond to stable molecules (energy minima), while structures which have one (and only one) vibrational frequency which is an imaginary number may be transition states (Jensen, 2007; Jensen, 1994; Menger and Sherrod, 1990). The coordinate (vibrational motion) associated with this imaginary frequency is the reaction coordinate.

All the transition states in the schemes proposed in this work were found to be true transition states or activated complexes. They all have higher energies compared to other species in their respective elementary steps as can be seen in Tables 4.1 – 4.24. They all occupied saddle points on scaled potential energy surface diagrams as drawn in Figures 4.21 – 4.37. The trueness of the transition states were also confirmed by animating the

vibration corresponding to the reaction coordinate by selecting the imaginary frequency at the top of the list of frequencies on the IR tab.

## 5.6 Proposal of More Plausible Mechanisms for the Biomolecules - Iodine Reaction Systems

### 5.6.1 1,2-Diphenylhydrazine – Iodine Reaction system

The outline of the published mechanism of the reaction of 1,2-diphenylhydrazine with iodine as given by May and Halpern (1961) is shown in scheme 5.1 for the chain multi-step mechanism.



**Scheme 5.1: Published multi-step mechanism for the 1,2- diphenylhydrazine reaction with iodine**

According to the mechanisms outlined above where  $AH_2$  is 1,2- diphenylhydrazine;  $AH.$  a 1,2-diphenyl-hydrazyl radical;  $A$ , the trans-1,2-diphenyldiazene (azobenzene);  $I_2$ , iodine molecule;  $HI$ , hydrogen iodide and  $I.$  iodide ion, the overall equation of reaction should be as in (5.5) below, if equations 5.1-5.5 are summed up.



Whalley *et al* (1956), in their work, published a similar mechanism for the reaction of 1,2-diphenylhydrazine with persulphate. However, these two separate studies by May and Halpern (1961) on the one hand, and Whalley *et al* (1956) on the other, gave stoichiometry equations of the type as in (5.6), which is not consistent with their given mechanisms. In fact,

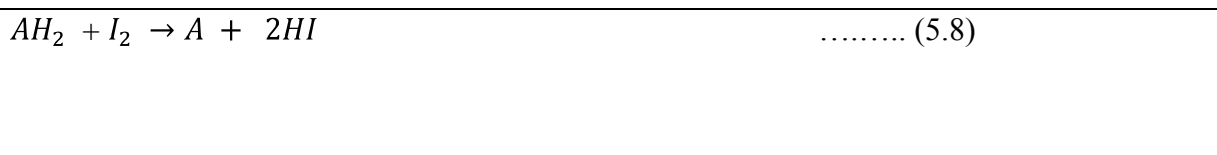
it is this inconsistency observed that partly necessitate the re-investigation of this reaction system.



Another study (Cao Xue, 1994) in which 1,2- diphenylhydrazine was oxidized by molecular oxygen was reported to show a stoichiometry similar to (5.6). The equation is given in (5.7) below.



May and Halpern (1961) did provide an alternative one-step mechanism in which "cyclic" activated complex was formed which disproportionate to give products that are consistent with equation (5.6). The authors (May and Halpern, 1961) were of the opinion that both the chain multi-step mechanism proposed in scheme 1 and the one step mechanism, as shown in equation (5.8) in scheme 5.2, were plausible mechanisms. It is this seeming inconsistency that informed the desire of this study to investigate whether the popular multi-step mechanism (Whalley *et al.*, 1956; May and Halpern, 1961) or, the latter proposed one-step mechanism is the most plausible one; and/or if both routes are possible, which one would be the most favored?



**Scheme 5.2: The published one-step mechanism with cyclic activated complex for the 1,2- diphenylhydrazine reaction with iodine**

According to the discussion that will follow on the basis of the semi-empirical calculations as well as the DFT calculations, the mechanism shown in Scheme 4.1 for the chain multi-step

mechanism is more plausible than the version published by May and Halpern (1961). Scheme 4.1 can be presented in a simplified form as equations 5.9 through 5.11



So that the overall equation of the reaction is as given in equation (5.12)



Or, as in (5.13) which is in agreement with (5.6) above. Equation (5.13) is also consistent with the mechanism proposed in this work.



*Step 1, (eq 5.9):* The optimized 1,2-diphenylhydrazine (AH<sub>2</sub>) reacted with the iodine molecule (I<sub>2</sub>) to yield a 1,2-diphenylhydrazyl radical (AH·), hydrogen iodide (HI) and iodine radical (I·) via the transition state TS<sub>1</sub>. This step is in agreement with equation (1) proposed by May and Halpern (1961).

*Step 2, (eq 5.10):* The optimized 1,2-diphenylhydrazyl radical (AH·) reacted with another iodine molecule (I<sub>2</sub>) to give trans-1,2-diphenyldiazene (A), the reported product of 1,2-diphenylhydrazine oxidation via the transition state TS<sub>2</sub>. This step was the rate determining step, as shown by the high value of ΔH<sub>f</sub>(total electronic energy for DFT) in table 4.1. Equation (5.10) differed with equation (5.2) but rather agreed with equation (5.3).

*Step 3, (eq 5.11):* Another optimized 1,2-diphenylhydrazine (AH<sub>2</sub>) reacted with iodine radicals produced in steps 1 and 2. This reaction was fast to yield another oxidation product,

trans-1,2-diphenyldiazene (A) plus two molecules of hydrogen iodide. The energy for the combination of two molecules 1,2-diphenylhydrazyl radicals (AH.), as reported by May and Halpern (1961) in equation (5.4), was very high in comparison to that required for equation(5.11) reported for this study. That means that the chain multi-step mechanism proposed in this work would be more favorable than the one proposed by May and Halpern (1961).

The summation of equations (5.9), (5.10) and (5.11) gave (5.12), which was reduced to (5.13). Equation (5.13) is the exact stoichiometric equation for the oxidation of 1,2-diphenylhydrazine as reported by previous works (Whalley *et al.*, 1956; May and Halpern, 1961; Kelly *et al.*, 1994) but which was not consistent with the mechanisms they published.

Figures 4.21 and 4.22 depicted the chain multi-step mechanism or, in other words, the three steps mechanism of the oxidation of 1,2-diphenylhydrazine by iodine diagrammatically, as per the DFT and semi-empirical calculations respectively, with the positions of the various species (R, reactants; TS<sub>1-3</sub>, transition states and, P, products) indicated. From the scaled potential energy surface diagrams it was evident that step 2 was the rate determining step as shown by the high position of the transition state, TS<sub>2</sub> in both diagrams. Based on the optimized geometries of the reacting species, an attempt was made to search the transition states in each of the steps 1, 2 and 3. Only one transition state was found for each step (transition state in Step 1:TS<sub>1</sub> and in Step 2: TS<sub>2</sub>) as shown in Figures 4.21 and 4.22, and summarized in Table 4.1. Vibrational analysis confirmed that TS<sub>1</sub> and TS<sub>2</sub> were actually the transition state in each step, while TS<sub>3</sub> was not a true transition state. The total electronic energies of TS<sub>1</sub>and TS<sub>2</sub> were calculated to be -31,804,644.68 kJ/mol (-5,258.91 au) and -19,669,188.83 kJ/mol (-7,493.02 au), respectively, for the DFT calculations while for the

semi-empirical calculations the heat of formation values were 1089.71 and 1766.33 kJ/mol, respectively. Based on the above results, the apparent activation energies for the steps 1 to 3 were estimated by subtracting the  $\Delta H_f$ (total electronic energy for DFT) of the starting geometry from that of the transition state in each step in order to determine the rate-determining step. As shown in Figures 4.21 and 4.22, it was found that the transition state TS<sub>2</sub> had the largest  $\Delta H_f$ (total electronic energy for DFT). Thus, the apparent activation energy for step 2 was estimated to be 18,163,700.93kJ/mol (6,919.52 au) for the DFT estimations and 803.13kJ/mol for the MNDO estimations, whereas for step 1, it was found to be just 6,029,888.15kJ/mol (2,297.10 au) or 23.06 kJ/mol, respectively. This clearly indicated that Step 1 proceeded very smoothly. On the other hand, in step 2, the activation energy was significantly large, 18,163,700.93kJ/mol (6,919.52 au) for DFT or 803.13 kJ/mol for semi-empirical, in comparison with those in other steps. For step 3, true transition state was not found.

For the one step mechanism (Scheme 4.2) in which "cyclic" activated complex was formed, the energy diagrams, according to the DFT and MNDO estimations for the reaction were as given in Figures 4.23 and 4.24. Based on the optimized geometries of the reacting species, an attempt was also made to search for the transition states, which was found and confirmed by vibrational analysis. The transition state, TS\*, as optimized and shown in Figure 4.11, has the total electronic energy, estimated to be -37,824,591.91kJ/mol (-14,409.37 au) for the DFT calculations or heat of formation of 1,111.05 kJ/mol for the semi-empirical calculations, respectively. The apparent activation energy was estimated to be 9,940.92 kJ/mol (3.79 au) for DFT or 44.40 kJ/mol for semi-empirical, thus indicating that the reaction could proceed smoothly too. In fact, the activation barrier of 9,940.92 kJ/mol (3.79 au) for DFT or 44.40 kJ/mol for semi-empirical, for the limiting step of the "cyclic" activated

complex mechanism was a pointer that this mechanism would be more favoured than the multi-step chain mechanism which had an activation barrier of 18,163,700.93kJ/mol (6,919.52 au) for DFT or 803.13 kJ/mol for semi-empirical, for the rate limiting step.

### 5.6.2 L-Tyrosine – Iodine Reaction system

The outline of the published mechanism of the oxidation of L- tyrosine with iodine as given by Aghaie *et al* (2008) is shown in scheme 5.3 below. Scheme 5.3 can be presented in a more simplified form as a two- steps reaction mechanisms as in equations 5.16 and 5.17.

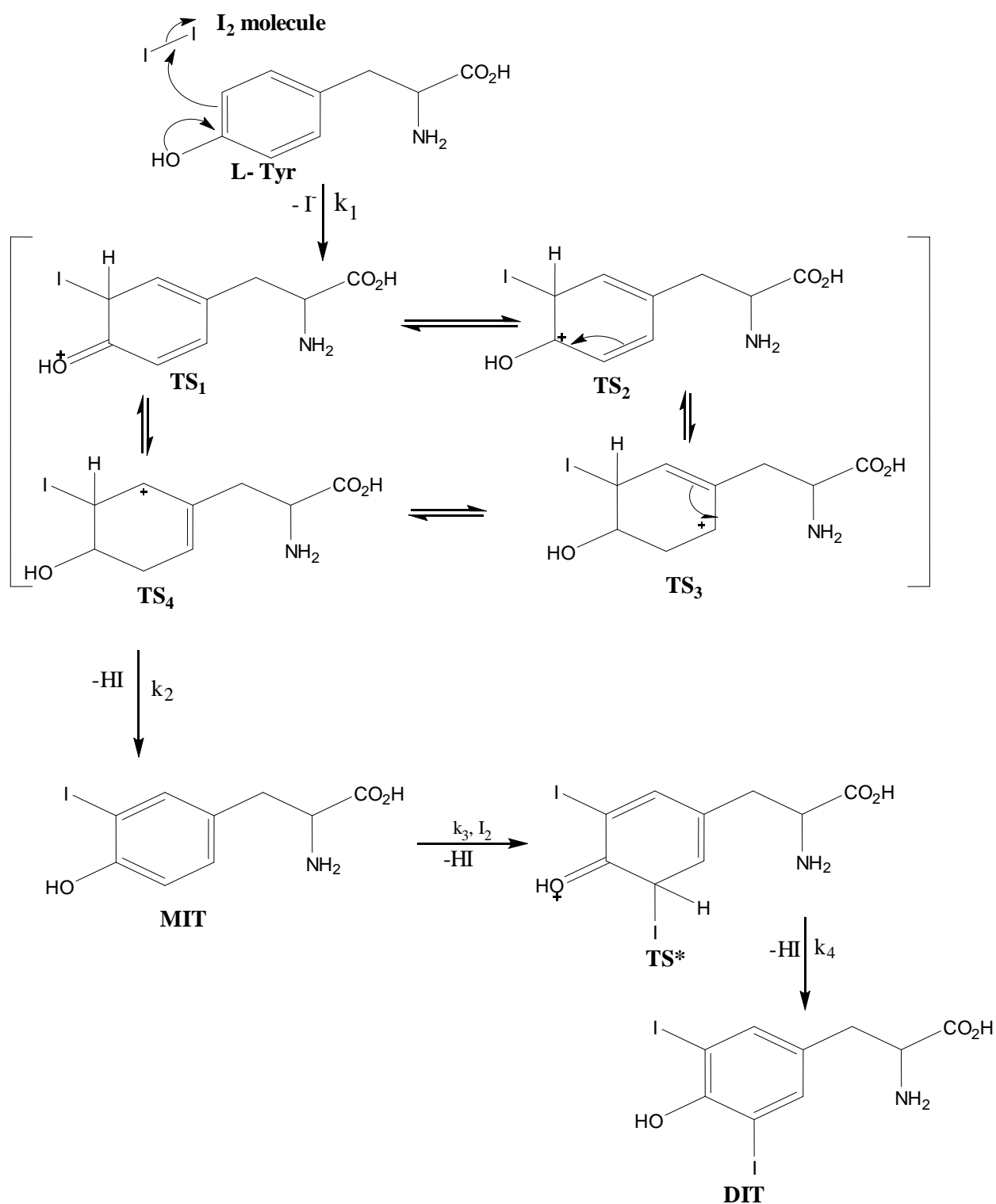


The stoichiometric equation of the reaction would, therefore, be as in equation (5.18).



Aghaie *et al.* (2008) were of the opinion that the transition state, [TS], in equation (5.16) can exist as different equilibrium conformers represented as [TS<sub>1</sub> –TS<sub>4</sub>] in scheme 5.3. It was the desire of this work to find out if all the conformers could exist, and if they do, which one would be the most favorable one energetically and thus, propose a mechanism based on this finding.

Based on the discussion of the optimized L-tyrosine's activated C<sub>4</sub> and C<sub>6</sub>, the net charges, electron density, molecular orbital energies, the heat of formation of the various proposed transition states (Tables 4.4 and 4.5) and their C<sub>4</sub>-H, C<sub>6</sub>-H, C<sub>6</sub>-I bond lengths (Table 4.7), it became obvious that TS<sub>2</sub> was the most stabilized and favored transition state, and therefore, the reaction mechanism would be as given in the Scheme 4.3.



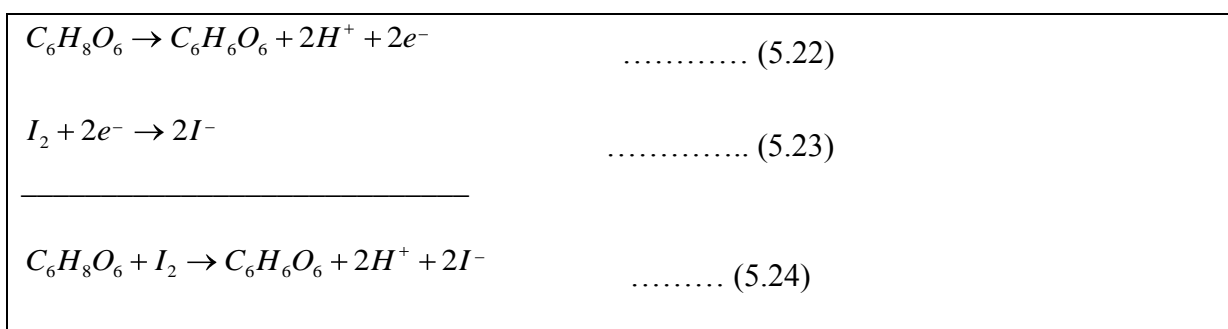
**Scheme 5.3: The reaction mechanism as proposed by Aghaie *et al.* (2008)**

The mechanism proposed in this study is not quite different from that proposed by Aghaie *et al.* (2008). In fact, the only difference between the mechanism proposed here (Scheme 4.3)

and that proposed by Aghaie *et al* (2008) (Scheme 5.3) is that, this study was able to demonstrate that the reaction would likely to go through TS<sub>2</sub> instead of the other three proposed by Aghaie *et al* (2008).

### 5.6.3 L-Ascorbic Acid – Iodine Reaction system

The outline of the published mechanism of the oxidation of ascorbic acid with iodine as given by several groups (Morelli, 1976; Rahmawati and Bundjali, 2009; Canterbury, 2014) is shown in Scheme 5.4 below.



**Scheme 5.4: The reaction mechanism of L-ascorbic acid as proposed by several groups (Morelli, 1976; Rahmawati and Bundjali, 2009; Canterbury, 2014)**

The various groups have shown that reaction between ascorbic acid and iodine would yield dehydroascorbic acid with H<sup>+</sup> and I<sup>-</sup> as byproducts. But both H<sup>+</sup> and I<sup>-</sup> are very reactive species and would not remain as ions in the reaction medium. It is the desire of this work to find out if the fate of these ions could be account for or, if the mechanism presented in Scheme 5.4 could even be modified. Two proposed schemes were presented for this study in Scheme 4.4 and Scheme 4.5 as route 1 and route 2 for the DFT studies, respectively. The same reactions were also studied using semi-empirical PM3 method.

Considering the structure of the optimized ascorbic acid molecule, the frontier molecular orbital studies, the bond length studies and the exposed surface areas studied there are two

possible schemes of writing the reaction mechanism. These were presented as route 1 (Scheme 4.4) and route 2 (Scheme 4.5), respectively.

### 5.6.3.1 Route I

In route 1 the optimized ascorbic acid molecule reacted with an iodine molecule to form a cyclic activated complex,  $TS_1$ , which on disproportionation, two hydrogen atoms were abstracted to give the products, a molecule of dehydroascorbic acid plus two molecules of hydrogen iodide. Even though the calculations have shown the reaction mechanism of route 1 is possible, it is doubted if the mechanism would be the most favoured pathway. This is because H1 and H3 of the optimized ascorbic acid molecule were *trans*- to each other and therefore, the possibility of the same molecule of iodine attacking the hydrogen atoms at the same time is very limited. The route I mechanism is as given in Scheme 4.4.

### 5.6.3.2 Route II

Route II described a two-step scheme in which the optimized ascorbic acid molecule reacted with two different iodine molecules to yield dehydroascorbic acid plus two molecules of hydrogen iodide and two iodine ions in the first step. In the second step, another ascorbic acid molecule reacted with the two iodine ions generated in the first step to yield another dehydroascorbic acid molecule plus two molecules of hydrogen iodide. The route II mechanisms seemed more feasible, especially as the two activated complexes  $TS_{B1}$  and  $TS_{B2}$  were true transition states. They both occupied saddle points along the energy profile of the reactions. The transition states were also confirmed by animating the vibration corresponding to the reaction coordinate by selecting the imaginary frequency at the top of the list of frequencies on the IR tab. The route II mechanism was also given in scheme 4.5.

### 5.6.3.3 DFT Studies

If the heat of formation of the various optimized reaction species for route 1 were considered, the transition states,  $TS_1$ , with total electronic energy of  $-38,125,652.92\text{kJ/mol}$  ( $-14,524.06$  au) was observed to be a true transition state because its position was a saddle point on the scaled potential energy diagram of the reaction (Figure 4.28). It was also confirmed by animating the vibration corresponding to the reaction coordinate by selecting the imaginary frequency at the top of the list of frequencies on the IR tab. The potential energy diagram (Figures 4.28) showed this vividly, where  $R_1$  were the reactants in route 1, with  $TS_1$  as the possible transition states and  $P_1$ , the products of the same reaction. The reaction appeared to be exothermic with activation energy,  $E_{a1}$ , of  $3,138.17\text{kJ/mol}$  ( $1.20$  au).

On the other hand,  $TS_{B1}$  and  $TS_{B2}$  were also transition states with heats of formation (total electronic energy) of  $-74,453,171.82\text{kJ/mol}$  ( $-28,363.11$  au) and  $-38,125,681.68\text{kJ/mol}$  ( $-14,524.0$  au), respectively, in the two-steps mechanism as proposed in route II.  $TS_{B1}$  and  $TS_{B2}$  were real saddle points in the reaction. They were also confirmed by animating the vibration corresponding to the reaction coordinate by selecting the imaginary frequency at the top of the list of frequencies on the IR tab. The potential energy diagram (Figure 4.29) showed this vividly also. The second step for the 2-steps reaction was the rate determining step with an activation barrier or energy,  $E_{aB2}$ , of  $10,518.23\text{kJ/mol}$  ( $4.01$  au). The first step had activation barrier or energy,  $E_{aB1}$ , of only  $3,151.35\text{kJ/mol}$  ( $1.20$  au).

### 5.6.3.4 Semi-Empirical PM3 Studies

For the semi-empirical PM3 studies, if the heat of formation of the various optimized reaction species for route 1 were considered, the transition states  $TS_1$  with heat of formation of  $-462.29\text{kJ/mol}$  was observed to be a transition state because its position was a saddle point on

the scaled potential energy diagram of the reaction. It was also confirmed by animating the vibration corresponding to the reaction coordinate by selecting the imaginary frequency at the top of the list of frequencies on the IR tab. The potential energy diagram (Figures 4.30) showed this vividly, where  $R_1$  were the reactants in route 1, with  $TS_1$  as the possible transition states and  $P_1$ , the products of the same reaction.

On the other hand,  $TS_{B1}$  and  $TS_{B2}$  were also transition states with heats of formation of -351.56 kJ/mol and -632.22kJ/mol, respectively, in the two-step mechanism as proposed in route 2.  $TS_{B1}$  and  $TS_{B2}$  were real saddle points in the reaction. They were also confirmed by animating the vibration corresponding to the reaction coordinate by selecting the imaginary frequency at the top of the list of frequencies on the IR tab. The energy diagram (Figures 4.31) showed this vividly also.

#### **5.6.4 D-Fructose – Iodine Reaction system**

The published mechanisms of the oxidation of sugar with different oxidants were varied. Odebunmi and Owalude (2008) gave the reaction products of their study of the oxidation of some simple reducing sugars by permanganate ion in alkaline medium as formic acid and lower sugars; Sengupta *et al* (2009) gave the reaction products as aldonic acids; Olusanya and Odebunmi (2013) reported the formation of enediol intermediate in the course of their reactions; while Mahmood *et al*(2009) also gave aldonic acid as the reaction product of the reaction of reducing sugars with iodine.

Looking at the respective values of  $TS_1$ ,  $TS_2$  and  $TS_3$  for the DFT studies in Table 4.14, it was clear they were true transition states, and these were confirmed by vibrational analysis studies. However, for the less accurate semi-empirical PM3 method, it was only  $TS_1$  that was observed to be a true transition state. Plots of the potential energy surface profiles as shown

in Figures 4.32 and 4.33, respectively, clearly showed the  $TS_1$ ,  $TS_2$  and  $TS_3$  for the DFT studies were true saddle points. But as expected, and as pointed out above, only  $TS_1$ , for the PM3 studies was a saddle point.

Based on the discussion of the optimized D-fructose's activated atoms ( $C_2$ ,  $C_3$ ,  $O_2$ ,  $H_5$  and  $H_8$ ), their net charges, exposed surface, electron density, molecular orbital energies, and their heat of formation, as well as the determination of the various transition states and potential energy surface diagrams discussed in the previous sections, a plausible mechanism for the reaction was proposed as shown in Scheme 4.6.

#### **5.6.4.1 Step 1**

In step1, the optimized water molecule ( $H_2O$ ) reacted with iodine ( $I_2$ ) molecule to form a cyclic activated complex,  $TS_1$ , which on disproportionation, gave hydrogen iodide ( $HI$ ) and hypoiodous acid ( $HOI$ ) as the products. Both DFT and PM3 studies showed that  $TS_1$  is a true transition state, which occupied a saddle point on the reaction coordinate.

#### **5.6.4.2 Step 2**

The hypoiodous generated in step 1 attacked the D-fructose molecule to form an activated complex  $TS_2$  (also represented as A), to yield an intermediate (Int), (also represented B).  $TS_2$  (A), in the DFT studies, was confirmed as a true transition state but not in the PM3 studies.

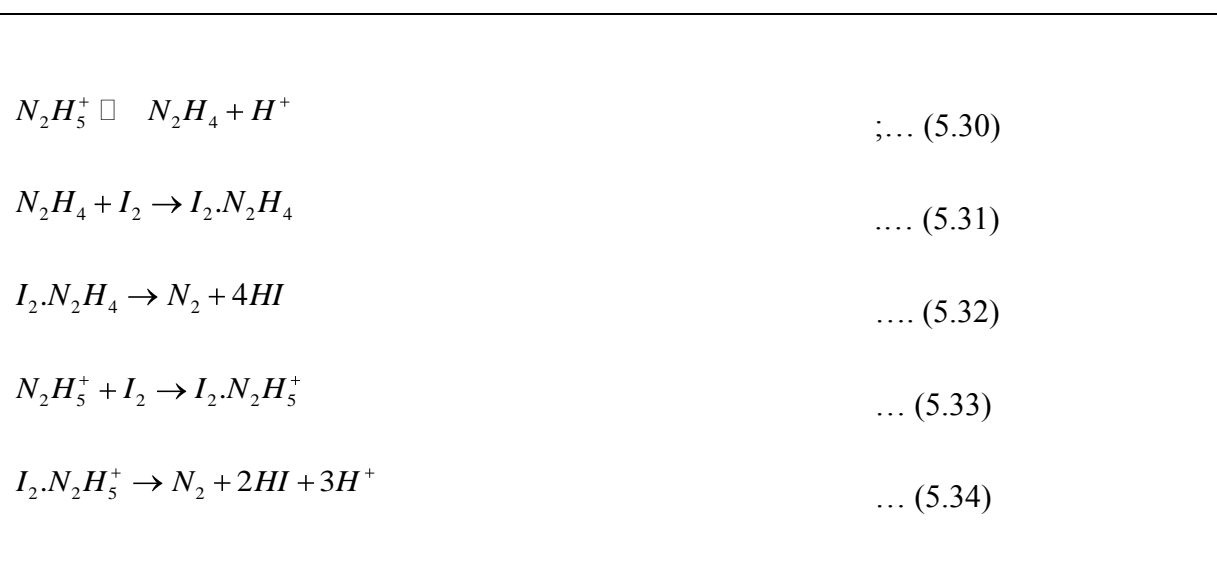
#### **5.6.4.3. Step 3**

Actually, steps 2 and 3 can be combined as a complex reaction step because, the intermediate (B), in step 2 was converted to a activated complex,  $TS_3$ , ( otherwise represented as C) which, in turn, was transformed into another intermediate, D (Int.2), an enediol intermediate as reported in the work of Olusanya and Odebunmi (2013) which finally yielded the

products(E,4R,5R)-hex-2-ene-1,2,3,4,5,6-hexol represented (represented as E) (Olusanya and Odebunmi, 2013) plus a HOI molecule. The more accurate DFT method showed that all transition states occupied saddle points on the PES diagram (Figure 4.13) and the intermediates positions were troughs or valleys on the PES diagram. Unfortunately, the less accurate PM3 method was less exact in showing the true saddle points and valleys on the PES diagram (Figure 4.33).

### 5.6.5 Hydrazine / Hydrazinium Ion – Iodine Reaction System

The outline of the published mechanism of the oxidation of hydrazinium ion with iodine as given by several groups (Mshelia *et al.*, 2010) is shown in scheme 5.5 below.



**Scheme 5.5: The reaction mechanism as proposed by Mshelia *et al* (2010)**

Mshelia *et al* (2010) gave the stoichiometry of their reaction as equation (5.35) below.



The mechanism as proposed in Scheme 5.5 by Mshelia *et al* (2010) was not consistent with their stated equation of stoichiometry. Whereas the number of all atoms on the reactants side

and those on the products side were balanced, the number of positive charges on the products was twice that on the reactants side. However, it was noted that their stoichiometry was consistent with their other data but not in agreement with their written mechanism. It therefore, showed that the problem was with the mechanism they proposed. It is the desire of this work to find out if mechanisms that are consistent with the stoichiometry or, better still, mechanisms that are more favorable energetically than the one proposed by Mshelia *et al* (2010) could be formulated in current study. Four mechanisms were proposed and presented in schemes 4.7-4.10 as routes 1, 2, 3 and 4, respectively.

Based on the discussion of the DFT calculations of the various optimized reacting species, the four reaction routes or mechanisms shown in Scheme 4.7 - 4.10 are more plausible than the mechanism version (Scheme 5.5) published by Mshelia *et al* (2010).

#### **5.6.5.1 Route I**

In this scheme (4.7), water reacted with the hydrazinium ion to yield hydrazine and hydroxonium ion via the transition state  $TS_1$ . The hydrazine molecule formed in the first step then reacted with an iodine molecule via transition state  $TS_2$  to give a diazine molecule and two molecules of HI. Finally, the diazine molecule reacted with another iodine molecule via transition state  $TS_3$  to give a nitrogen molecule plus two molecules of HI.

#### **5.6.5.2 Route II**

In this scheme(4.8), water reacted with the hydrazinium ion to yield hydrazine and hydroxonium ion via the transition state  $TS_1$ . The hydrazine formed is then attacked concurrently by two molecules of iodine via the transition state  $TS_B$  to yield the products of nitrogen molecule plus four molecules of HI.

### 5.6.5.3 Route III

This was another two-step pathway just like the previous one. The only difference was that each of the two molecules of iodine attacked and abstracted two hydrogen atoms attached to the same nitrogen atoms of the hydrazine molecule. In the previous route, each iodine molecule attacked and abstracted two hydrogen atoms attached to different nitrogen atoms of the hydrazine molecule.

### 5.6.5.4 Route IV

This scheme (4.10) started as usual with water reacting with the hydrazinium ion to yield hydrazine and hydroxonium ion via the transition state  $TS_1$  in the first step. In the second step, two molecules of iodine reacted with two molecules water via the transition state  $TS_D$  to yield two molecules of hypoiodous acid plus two molecules of HI. In the final step, two molecules of hypoiodous acid intermediate attacked and abstracted two hydrogen atoms attached to different nitrogen atoms of the hydrazine molecule via transition state  $TS_D$  to give back the two water molecules, used as catalyst in step two, plus the products of nitrogen molecule and two molecules of HI.

The stoichiometry of four the proposed mechanisms are the same, and are consistent with each of the proposed scheme. In the scheme published by Mshelia *et al* (2010) their stoichiometry was not consistent with their proposed mechanism, in relation to the net charges carried by reacting species. The stoichiometric equation of all the proposed mechanisms is as given below.



Route 1 of the four mechanisms proposed had three saddle points, TSF, TS<sub>1</sub> and TS<sub>2</sub> as can be seen in Table 4.19 and Figure 4.34. Evidently, step 2 was the rate determining step with an activation barrier, E<sub>a2</sub>, of 100,002.01kJ/mol. Routes II and III were both two-step mechanisms. Step 2 for both schemes were the rate determining steps with respective activation energies, E<sub>aB</sub> and E<sub>aC</sub>, of 13,736.10 kJ/mol and 13,613.41 kJ/mol, respectively. The fourth route proposed, a water catalyzed mechanism scheme, had three elementary steps with the third step being the rate determining step. The rate determining step had an activation barrier, E<sub>aE</sub>, of 6,860.42 kJ/mol. In comparing the rate determining steps of the four proposed schemes, the fourth route had the least activation barrier of 6,860.42 kJ/mol, followed by the third with activation energy of 13,613.41 kJ/mol, then the second route with activation energy of 13,736.10 kJ/mol, and lastly the first route with highest activation barrier of 100,002.01kJ/mol. Evidently, the fourth scheme proposed would be the most favorable mechanism energetically, and the reaction, in every likelihood, would follow the path of least energy (Engel and Reid, 2006).

### **5.7 Enthalpy of Reaction and Rate Constant Calculations for the Biomolecules - Iodine Reaction Systems (Ochterski, 2000; Engel and Reid, 2006; Spartan, 2014)**

In addition to molecular geometry, the energy is one of the most important quantities to come out of molecular modeling. Energy can be used to reveal which of several isomers is most stable, to determine whether a particular chemical reaction will have a thermodynamic driving force (an exothermic reaction) or be thermodynamically uphill (an endothermic reaction), and to ascertain how fast a reaction is likely to proceed (Ochterski, 2000; Spartan, 2014).

There is more than one way to express the energy of a molecule. Most common to chemists is the heat of formation,  $\Delta H_f$ . This is the heat of a hypothetical chemical reaction that creates a

molecule from the well defined (but arbitrary) standard states of each of its constituent elements (Spartan, 2014; Jensen, 2007; Ochterski, 2000). An alternative, total energy, is the heat of a hypothetical reaction that creates a molecule from a collection of separated nuclei and electrons. Like the heat of formation, total energy cannot be measured directly, and is used solely to provide a standard method for expressing and comparing energies. Total energies are always negative numbers and, in comparison with the energies of chemical bonds, are very large. By convention, they are expressed in so-called atomic units or au (1 au = 2625 kJ/mol), but may be converted to other units as desired (Spartan, 2014).

It makes no difference which reference reaction (heat of formation or total energy) is used to calculate the thermochemistry of a balanced chemical reaction (reactant 1 + reactant 2 + . . . → product 1 + product 2 + . . .) (Spartan, 2014):

$$\Delta E_{(\text{reaction})} = E_{\text{product 1}} + E_{\text{product 2}} + \dots - E_{\text{reactant 1}} - E_{\text{reactant 2}} - \dots$$

Total energies will be used in the discussion that follows. A negative  $\Delta E$  indicates an exothermic (thermodynamically favourable) reaction, while a positive  $\Delta E$  an endothermic (thermodynamically unfavorable) reaction (Ochterski, 2000; Morris, 1972).

Total energies may also be used to calculate activation energies,  $\Delta E^\ddagger$ :

$$\Delta E^\ddagger = E_{\text{transition state}} - E_{\text{reactant 1}} - E_{\text{reactant 2}} - \dots$$

Here,  $E_{\text{transition state}}$  is the total energy of the transition state. Activation energies will always be positive numbers (Ochterski, 2000; Spartan, 2014), meaning that the transition state is always less stable than reactants (and products as well). Reaction and activation energies are sufficient to know whether a reaction is exothermic or endothermic or whether it proceeds with small or large activation barrier (Ochterski, 2000; Spartan, 2014).

There are, however, other situations where energies need to be replaced by Gibbs energies in order to take proper account of the role of entropy. For example, a proper account of the equilibrium concentrations of reactants and products requires calculation of the equilibrium constant,  $K_{eq}$ , which, according to the Boltzmann equation, is related to the Gibbs energy of reaction,  $\Delta G_{rxn}$ :

$$K_{eq} = \exp(-\Delta G_{rxn}/RT)$$

where R is the gas constant and T is the temperature (K).

Although  $\Delta G_{rxn}$  depends on both enthalpy and entropy, there are many reactions for which the entropy contribution is small and can be neglected (Ochterski, 2000; Spartan, 2014). Further assuming that  $\Delta H_{rxn} \approx \Delta E_{rxn}$ , equilibrium constants can then be estimated according to the Boltzmann equation (Ochterski, 2000; Spartan, 2014):

$$K_{eq} \approx \exp(-E_{rxn}/RT) \approx \exp(-1060 E_{rxn}) .$$

Reaction rate constants,  $k_{rxn}$ , are also related to Gibbs energies. As before, if entropy contributions can be neglected, the rate constant can be obtained directly from the activation energy,  $\Delta E^\ddagger$ , according to the Arrhenius equation (Ochterski, 2000; Spartan, 2014):

$$k_{rxn} \approx (k_B T/h) [\exp(-E^\ddagger/RT)]$$

Where,  $k_B$  and h are the Boltzmann and Planck constants, respectively.

### 5.7.1 1,2-Diphenylhydrazine – Iodine Reaction System

The enthalpies of reaction were calculated by using the Spartan software to calculate heats of formation at standard temperature of 298.15K, and the appropriate sums and differences taken as given in equation (3.1) reproduced here as equation (5.37).

$$\Delta_r H^\circ_{298.15K} = \sum_{products} n_{prod} \Delta_f H^\circ_{prod, 298.15K} - \sum_{reactants} n_{react} \Delta_f H^\circ_{react, 298.15K} \dots (5.37)$$

The computed enthalpies of reaction at standard conditions was 72.39 kJ/mol for both the mechanisms considered in this work compared to the computed enthalpies of reaction of the mechanism proposed by May and Halpern (1961), which was 128.87 kJ/mol at 298.15K.

The rate constant calculations were computed according to equation (3.5) also reproduced here as equation (5.38).

$$k_{298.15K} = \frac{k_B T}{h c^o} e^{-\Delta^\ddagger G^o / RT} \dots\dots\dots (5.38)$$

where  $k_{(298.15K)}$  = reaction rate at temperature (298.15K);  $k_B$  = Boltzmann constant ( $1.380662 \times 10^{-23}$  J/K);  $T$  = temperature (298.15K);  $h$  = Planck's constant ( $6.626176 \times 10^{-34}$  Js);  $C^o$  = concentration (taken to be 1);  $\Delta^\ddagger G^o$  = Gibbs free energy of activation (kJ/mol);  $R$  = gas constant (8.31441 J/mol. K).

The rate constants,  $k_1$  and  $k_2$ , for this study, as proposed in the mechanisms in Scheme 4.1, are  $7.85 \text{ dm}^3\text{mol}^{-1} \text{ sec}^{-1}$  and  $1.88 \times 10^9 \text{ dm}^3\text{mol}^{-1} \text{ sec}^{-1}$ , respectively, as opposed to the mechanisms in Scheme 5.1 published previously (May and Halpern, 1961), where  $k_1 = 5.76 \times 10^8 \text{ dm}^3\text{mol}^{-1} \text{ sec}^{-1}$  and  $k_2 = 3.35 \times 10^8 \text{ dm}^3\text{mol}^{-1} \text{ sec}^{-1}$ , respectively. The fore-going showed that the mechanisms proposed in Scheme 4.1 are more favourable than those proposed in scheme 5.1 published by May and Halpern (1961), as it was reported that the larger the value of the rate constant, the faster the reaction (Szajewski and Whiteside, 1980). The rate constant for the one-step cyclic activated complex mechanism was computed to be  $5.67 \times 10^{-2} \text{ dm}^3\text{mol}^{-1} \text{ sec}^{-1}$ . The multi-step mechanisms were less favoured than the one-step mechanism; especially if we take into account that activation barrier of 18,163,700.93kJ/mol (6,919.51 au) in the limiting step for the multi-step mechanisms for the DFT calculations which was far more than the 9,940.92kJ/mol (3.79 au) for the limiting step of the one step cyclic activated complex mechanism.

### 5.7.2 L-Tyrosine – Iodine Reaction System

The enthalpies of reaction were calculated by using the Spartan software package to calculate heats of formation at standard temperature of 298.15K, and the appropriate sums and differences taken as given in equation (5.37).

The mechanism proposed here (Scheme 4.3) is still consistent with that published by Aghaie *et al* (2008) only that the transition state, TS<sub>2</sub>, for step1 which was also the rate determining step (equation 5.16), was found to be more favorable for all the reasons highlighted above. TS<sub>2</sub> was therefore adopted as shown in Figure 4.7, while TS<sub>1</sub>, TS<sub>3</sub> and TS<sub>4</sub> were rejected for the same reasons discussed above. Computed enthalpies of the oxidation reaction at standard conditions for the PM3 and DFT calculation were 216.97kJ/mol and -36,327,404.72kJ/mol (13,839.01 au), respectively. Other activation parameters of the reaction at standard conditions, ΔG° and ΔS°, for the PM3 studies were calculated by the Spartan software package by default and were as provided in table 1. ΔG° and ΔS° for the DFT studies were computed using the Eyring equation (5.39) (Mee, 1971; Morris, 1972).

$$\ln K = -\frac{\Delta G^\circ}{RT} = \frac{\Delta S^\circ}{R} - \frac{\Delta H^\circ}{RT} \dots\dots\dots (5.39)$$

The rate constant calculations were computed according to equation (5.38).

The rate constants, k<sub>1</sub>, for this study was calculated to be 4.41 x 10<sup>12</sup>dm<sup>3</sup>mol<sup>-1</sup> sec<sup>-1</sup> and 1.89 x 10<sup>19</sup>dm<sup>3</sup>mol<sup>-1</sup> sec<sup>-1</sup> for the PM3 and DFT studies, respectively.

### 5.7.3 L-Ascorbic Acid – Iodine Reaction System

The enthalpies of reaction were calculated using the Spartan software package to calculate heats of formation at standard temperature of 298.15K and pressure of 1 atmosphere. The calculations were done by taking the appropriate sums and differences as given in equation (5.37).

The computed enthalpies of reaction at standard conditions for the DFT studies were -3,606.31kJ/mol (-1.38 au) and -7,212.78kJ/mol (-2.75 au) for Scheme 4.4 and Scheme 4.5, respectively; while the computed enthalpies of reaction at standard conditions the semi-empirical PM3 studies were 190.78kJ/mol and 381.56kJ/mol for Scheme 4.4 and Scheme 4.5, respectively. The enthalpy of reaction for route 2 was exactly twice that for route 1 since route 2 used twice the amount of reactants used in route 1. These showed that the same amount of energy is released in the course of the reactions of the two schemes proposed in this work. Both routes showed that reactions were exothermic. For the DFT studies, the activation barrier for the one-step reaction (Scheme 4.4) was calculated as 3,138.17kJ/mol. (1.20 au); while those of the two-steps mechanism (Scheme 4.5) was calculated as 3,151.35kJ/mol (1.20 au) and 10,518.23kJ/mol (4.01 au) for each of the respective steps. For the semi-empirical PM3 studies, the activation barrier for the one step reaction (Scheme 4.4) was calculated as 411.53kJ/mol.; while that of the two steps mechanism (Scheme 4.5) was calculated as 423.05kJ/mol and 341.61kJ/mol for each of the respective steps. Evidently, step 2 was the rate determining step for Scheme 5.6. In comparing activation barriers for the rate determining steps of Scheme 4.4 (3,138.17kJ/mol) and Scheme 4.5 (10,518.23kJ/mol) for the DFT studies, the difference was appreciably large (7,380.06 kJ/mol). This showed that even though the two routes proposed in this work were possible, route 1 would be faster, despite the fact that the optimized structure of the ascorbic acid would suggest that the two-step scheme should have been more favoured. For the semi-empirical PM3 studies, the less accurate method, the activation barrier for the rate determining steps of Scheme 4.4 (411.53kJ/mol) and Scheme 4.5 (423.05kJ/mol), the difference is only 11.52kJ/mol.

The proposed mechanisms also accounted for ions generated in the course of the reactions rather than leaving  $H^+$  and  $I^-$  in the reaction medium after the reactions were completed as

seemed to have been suggested by the earlier workers in Scheme 5.4 (Morelli, 1976; Rahmawati and Bundjali, 2009; Canterbury, 2014).  $\Delta G^\circ$  and  $\Delta S^\circ$  for the DFT studies were computed by using the Eyring (Mee, 1971; Morris, 1972) equation (5.38).

For the semi-empirical PM3 studies,  $\Delta G^\circ$  and  $\Delta S^\circ$  were calculated by the Spartan software package by default and were as provided in Table 4.11. The rate constant calculations were computed according to equation (5.37). For the DFT studies, the rate constant,  $k_1$  for route 1 was calculated to be  $1.37 \times 10^5 \text{ dm}^3 \text{ mol}^{-1} \text{ sec}^{-1}$ . For route 2,  $k_1$  and  $k_2$  were calculated as  $1.74 \times 10^5 \text{ dm}^3 \text{ mol}^{-1} \text{ sec}^{-1}$  and  $1.38 \times 10^5 \text{ dm}^3 \text{ mol}^{-1} \text{ sec}^{-1}$ , respectively. Whereas for the semi-empirical PM3 studies, the rate constant,  $k_1$  for route 1 was calculated to be  $1.07 \times 10^6 \text{ dm}^3 \text{ mol}^{-1} \text{ sec}^{-1}$ . For route 2,  $k_1$  and  $k_2$  were calculated as  $4.80 \times 10^{-4} \text{ dm}^3 \text{ mol}^{-1} \text{ sec}^{-1}$  and  $2.51 \times 10^{13} \text{ dm}^3 \text{ mol}^{-1} \text{ sec}^{-1}$ , respectively.

#### 5.7.4 D-Fructose – Iodine Reaction System

The enthalpies of reaction were calculated using the Spartan software package to calculate heats of formation at standard temperature of 298.15K and pressure of 1 atmosphere. The calculations were done by taking the appropriate sums and differences as given in equation (5.37).

The computed enthalpies of reaction at standard conditions were 196.32 kJ/mol (0.07 au) and 172.55.78kJ/mol for the DFT and PM3 studies respectively. The DFT studies showed that that step 3 was the rate determining step for the reaction. The activation barrier for the rate determining step for the DFT studies was calculated as 3,815.62kJ/mol (1.45 au); while the poor semi-empirical showed the activation barrier for the same to be -163.3kJ/mol.

The rate constant calculations were computed according to equation (5.38). For the DFT studies, the rate constant,  $k_1$  for step 1, was calculated to be  $1.04 \times 10^{-27} \text{ dm}^3 \text{ mol}^{-1} \text{ sec}^{-1}$ .  $k_2$  and

$k_3$  for steps 2 and 3 were  $5.00 \times 10^{-11} \text{ dm}^3\text{mol}^{-1} \text{ sec}^{-1}$  and  $1.33 \times 10^{-12} \text{ dm}^3\text{mol}^{-1} \text{ sec}^{-1}$  respectively. According to the semi-empirical calculations,  $k_1$ ,  $k_2$  and  $k_3$  were calculated as  $3.48 \times 10^{-27} \text{ dm}^3\text{mol}^{-1} \text{ sec}^{-1}$ ,  $3.07 \times 10^{-16} \text{ dm}^3\text{mol}^{-1} \text{ sec}^{-1}$  and  $6.96 \times 10^{-42} \text{ dm}^3\text{mol}^{-1} \text{ sec}^{-1}$ , respectively.

### 5.7.5 Hydrazine/Hydrazinium Ion – Iodine Reaction System

The enthalpies of reaction were calculated by using the Spartan software package to calculate heats of formation at standard temperature of 298.15K and pressure of 1 atmosphere. The calculations were done by taking the appropriate sums and differences as given in equation (5.37).

The computed enthalpy of reaction at standard conditions was 357.96kJ/mol for each of the four proposed pathways. This is because they all have the same stoichiometry. The computed enthalpy of reaction also showed the reactions were endothermic. The potential energy surface diagrams (Figures 4.34 – 4.37) also confirmed this.  $\Delta G^\circ$  and  $\Delta S^\circ$  were also computed by using the Spartan software package, but for some species where there was no convergence, these parameters were calculated by using the Eyring equation (5.39) (Mee, 1971; Morris, 1972).

The rate constant calculations were computed according to equation (5.38). The first step for all the four proposed schemes is the same. The rate constants,  $k_1$ , for this step was calculated to be  $68.02 \times 10^3 \text{ dm}^3\text{mol}^{-1} \text{ sec}^{-1}$ . However,  $k_2$  was calculated as  $1.84 \times 10^{-5} \text{ dm}^3\text{mol}^{-1} \text{ sec}^{-1}$  for route 1.  $k_2$  for routes 2, 3, and 4 were calculated as  $22.29 \times 10^9 \text{ dm}^3\text{mol}^{-1} \text{ sec}^{-1}$ ,  $8.02 \times 10^{12} \text{ dm}^3\text{mol}^{-1} \text{ sec}^{-1}$  and  $5.68 \times 10^{12} \text{ dm}^3\text{mol}^{-1} \text{ sec}^{-1}$  respectively. The fourth scheme proposed which, incidentally, is the most preferred mechanism, energetically had the third step as the

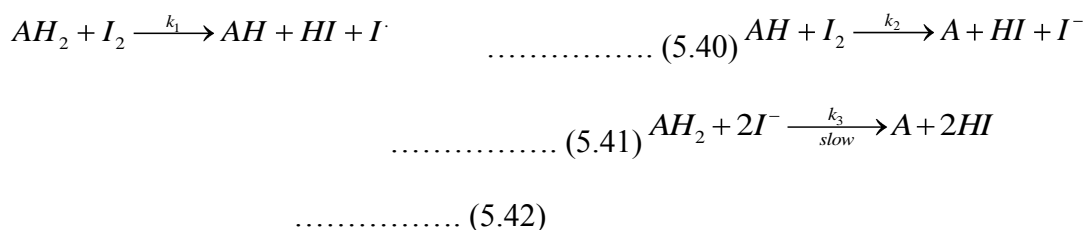
rate determining step. The rate constant,  $k_3$ , for this scheme was calculated to be  $108.48 \times 10^{12} \text{ dm}^3 \text{ mol}^{-1} \text{ sec}^{-1}$ . Again, in comparing the rate constants for the rate determining steps for the four proposed pathways, it showed that even kinetically, the fourth scheme was the most favoured yet, as it was reported that the larger the value of the rate constant, the faster the reaction (Szajewski and Whiteside, 1980).

## 5.8 Rate Laws for the Proposed Mechanisms of Reactions

### 5.8.1 Rate laws for 1,2-Diphenylhydrazine – Iodine Reaction System

Two mechanisms were proposed for the 1,2-diphenylhydrazine – iodine reaction system, the chain multi-step mechanism (Scheme 4.1) and the one-step cyclic activated complex mechanism (Scheme 4.2). The rate laws for the two mechanisms are as given in sub-sections 5.8.1.1 and 5.8.1.2, respectively.

#### 5.8.1.1 The chain multi-step mechanism



The slowest step of the reaction is the rate determining step and therefore, the rate of consumption of  $AH_2$  can be given as:

$$r = k_3 AH_2 [I^-]^2 \quad \dots\dots\dots (5.43)$$

$$\text{Rate of formation of } [I]: k_1 AH_2 I_2 + k_2 AH I_2 \quad \dots\dots\dots (5.44)$$

$$\text{Rate of decomposition of } [I]: k_3 AH_2 [I^-]^2 \quad \dots\dots\dots (5.45)$$

At the steady state, equilibrium is set, therefore:

$$[I^-]^2 = \frac{k_1 AH_2 I_2 + k_2 AH I_2}{k_3 AH_2} \dots\dots\dots (5.46)$$

$$\text{Hence, } r = k_3 AH_2 \left( \frac{k_1 AH_2 I_2 + k_2 AH I_2}{k_3 AH_2} \right) \dots\dots\dots (5.47)$$

$$= k_1 AH_2 I_2 + k_2 AH I_2 \dots\dots\dots (5.48)$$

$$\text{Rate of formation of [AH]: } k_1 AH_2 I_2 \dots\dots\dots (5.49)$$

$$\text{Rate of decomposition of [AH]: } k_2 AH I_2 \dots\dots\dots (5.51)$$

$$\text{At equilibrium: } AH = \frac{k_1 AH_2 I_2}{k_2 I_2} = \frac{k_1 AH_2}{k_2} \dots\dots\dots (5.52)$$

$$\text{Therefore, } r = k_1 AH_2 I_2 + k_1 AH_2 I_2 \dots\dots\dots (5.53)$$

$$= k AH_2 I_2 \dots\dots\dots (5.54)$$

$$\text{Where, } k = (1 + 1)k_1 \dots\dots\dots (5.55)$$

= 1.57 x 10<sup>1</sup> dm<sup>3</sup> mol<sup>-1</sup> sec<sup>-1</sup> for the DFT studies.

### 5.8.1.2 The One-Step Cyclic Activated Complex Mechanism

This mechanism is a one- step mechanism where I<sub>2</sub> reacted with the the1,2-diphenylhydrazine via a cyclic activated complex to yield the products of reaction.



$$\text{Therefore, the rate, } \frac{-d[AH_2]}{dt} = k_1[AH_2][I_2] \dots\dots\dots (5.56)$$

Therefore, k<sub>1</sub> = k = 5.67 x 10<sup>-2</sup> dm<sup>3</sup> mol<sup>-1</sup> sec<sup>-1</sup> for the DFT studies.

### 5.8.2 L-Tyrosine – Iodine Reaction system

The rate law for the proposed mechanism of the oxidation of L- tyrosine with iodine as given

by Aghaie *et al* (2008) and modified by this study as shown in Scheme 4.3 is presented here.

The reaction is a two- steps reaction mechanism.



The first step is the rate determining step and therefore,

$$\frac{-d L-Tyr}{dt} = k_1 I_2 L-Tyr \quad \dots\dots\dots (5.59)$$

Therefore,  $k_1 = k = 4.41 \times 10^{12} \text{ dm}^3 \text{ mol}^{-1} \text{ sec}^{-1}$  for the DFT studies.

### 5.8.3 L-Ascorbic Acid – Iodine Reaction System

Two mechanisms were proposed for the ascorbic acid – iodine reaction system, a one-step cyclic activated complex mechanism which disproportionate to give the reaction products (Scheme 4.4) and a two-step mechanism Scheme 4.5). The rate laws for the two mechanisms are as given in sub-sections 5.8.3.1 and 5.8.3.2, respectively.

#### 5.8.3.1 The One-Step Cyclic Activated Complex Mechanism

This mechanism is a one- step mechanism where  $I_2$  reacted with the ascorbic acid via a cyclic activated complex (M) to yield the products of reaction.



Therefore, the rate (r) of the consumption of the ascorbic acid or the iodine molecule is as given below.

$$r = k_1 AA I_2 \quad \dots\dots\dots (5.61)$$

Therefore,  $k_1 = k = 1.37 \times 10^5 \text{ dm}^3 \text{ mol}^{-1} \text{ sec}^{-1}$  for the DFT studies.

### 5.8.3.2 The Two-Steps Mechanism



The second step is the slowest step and thus is the rate limiting step.

$$\text{Therefore, } r = k_2 AA [I^-]^2 \quad \dots\dots\dots (5.64)$$

From the first step, at equilibrium,

$$k_1 AA I_2^2 = k_{-1} DA HI^2 [I^-]^2 \quad \dots\dots\dots (5.65)$$

$$\text{Hence, } [I^-]^2 = \frac{k_1 AA I_2^2}{k_{-1} DA HI^2} \quad \dots\dots\dots (5.66)$$

Substituting for  $[I^-]^2$ , the rate (r) becomes,

$$r = k_2 AA \left( \frac{k_1 AA I_2^2}{k_{-1} DA HI^2} \right) \quad \dots\dots\dots (5.67)$$

$$r = \frac{k_1 k_2}{k_{-1}} \left( \frac{AA^2 I_2^2}{DA HI^2} \right) \quad \dots\dots\dots (5.68)$$

$$r = k_1 \frac{AA^2 I_2^2}{DA HI^2} \quad \dots\dots\dots (5.69)$$

$$\text{Where, } k = \frac{k_1 k_2}{k_{-1}} \quad \dots\dots\dots (5.70)$$

Therefore,  $k = 1.17 \times 10^4 \text{ dm}^3 \text{ mol}^{-1} \text{ sec}^{-1}$  for the DFT studies.

### 5.8.4 D-Fructose – Iodine Reaction System

The rate law for the mechanism of the oxidation of D-fructose with iodine as proposed in this study is shown in Scheme 4.6 is presented here. The reaction is a four-step reaction mechanism.



The third step is the slowest step and thus is the rate limiting step.

Therefore, the rate,  $r = k_3 [B]$  ..... (5.75)

Rate of formation of [B]:  $k_2[Fruc][HOI]$

Rate of consumption of [B]:  $k_3[B]$

At the steady state condition:  $[B] = \frac{k_2[Fruc][HOI]}{k_3}$  ..... (5.76)

Therefore,  $r = k_3 \frac{k_2[Fruc][HOI]}{k_3}$  ..... (5.77)

$r = k_2[Fruc][HOI]$  ..... (5.78)

Rate of formation of [HOI]:  $k_1[I_2][H_2O]$

Rate of consumption of [HOI]:  $k_{-1}[HOI][HI] + k_2[HOI][Fruc]$

At the steady state condition:  $[HOI] = \frac{k_1[I_2][H_2O]}{k_{-1}[HI] + k_2[Fruc]}$  ..... (5.79)

Hence,  $r = k_2[Fruc] \frac{k_1[I_2][H_2O]}{k_{-1}[HI] + k_2[Fruc]}$  ..... (5.80)

$k_1 k_2 [Fruc] [I_2] [H_2O] \square \frac{1}{k_{-1}[HI] + k_2[Fruc]}$  ..... (5.81)

Therefore,  $r = \frac{k[Fruc][I_2][H_2O]}{k_{-1}[HI]}$  ..... (5.82)

$$\text{Where, } k = \frac{k_1 k_2}{k_{-1} [HI]} \dots\dots\dots (5.83)$$

$k_{-1}$  is approx. zero

Therefore,  $k = 5.20 \times 10^{-38} \text{ dm}^3 \text{ mol}^{-1} \text{ sec}^{-1}$  for the DFT studies.

### 5.8.5 Hydrazine/Hydrazinium Ion – Iodine Reaction System

Four different mechanisms were proposed for the hydrazine/hydrazinium ion – iodine reaction system, tagged route I to route IV (Schemes 4.7 – 4. 10). The rate laws for the two mechanisms are as given in sub-sections 5.8.5.1 to 5.8.5.4, respectively.

#### 5.8.5.1 Route I

Route 1 is a three-step reaction mechanism as given in Scheme 4.7.



The second step is the slowest and this is the rate determining step. Therefore,

$$\text{Rate, } r = k_2 I_2 N_2H_4 \dots\dots\dots (5.87)$$

At the steady state, rate of formation of  $[N_2H_2]$  = rate of consumption of  $[N_2H_2]$

$$k_1 H_2O [N_2H_5^+] = k_{-1} N_2H_4 [H_3O^+] \dots\dots\dots (5.88)$$

$$\text{Hence, } N_2H_4 = \frac{k_1 H_2O [N_2H_5^+]}{k_{-1} [H_3O^+]} \dots\dots\dots (5.89)$$

Therefore,

$$r = k_2 I_2 \left( \frac{k_1 H_2O [N_2H_5^+]}{k_{-1} [H_3O^+]} \right) \dots\dots\dots (5.90)$$

$$r = \frac{k_1 k_2}{k_{-1}} \frac{I_2 H_2O [N_2H_5^+]}{[H_3O^+]} \dots\dots\dots (5.91)$$

$$r = k \left( \frac{I_2 H_2O [N_2H_5^+]}{[H_3O^+]} \right) \dots\dots\dots (5.92)$$

Where,  $k = \frac{k_1 k_2}{k_{-1}} \dots\dots\dots (5.93)$

Therefore,  $k = 1.00 \times 10^{-4} \text{ dm}^3 \text{ mol}^{-1} \text{ sec}^{-1}$  for the DFT studies

### 5.8.5.2 Route II

Route II is a two-step reaction mechanism as given in Scheme 4.8.



The second step is the slowest and this is the rate determining step. Therefore,

Rate,  $r = k_2 I_2^2 N_2H_4 \dots\dots\dots (5.96)$

At the steady state, equilibrium is set up and, therefore,

$$N_2H_4 = \frac{k_1 H_2O [N_2H_5^+]}{k_{-1} [H_3O^+]} \dots\dots\dots (5.97)$$

Hence,  $r = k_2 I_2^2 \left( \frac{k_1 H_2O [N_2H_5^+]}{k_{-1} [H_3O^+]} \right) \dots\dots\dots (5.98)$

$$r = \frac{k_1 k_2}{k_{-1}} \frac{I_2^2 H_2O [N_2H_5^+]}{[H_3O^+]} \dots\dots\dots (5.99)$$

$$r = k \left( \frac{I_2^2 H_2O [N_2H_5^+]}{[H_3O^+]} \right) \dots\dots\dots (5.100)$$

$$\text{Where, } k = \frac{k_1 k_2}{k_{-1}} \dots\dots\dots (5.101)$$

Therefore,  $k = 1.21 \times 10^{13} \text{ dm}^3 \text{ mol}^{-1} \text{ sec}^{-1}$  for the DFT studies

### 5.8.5.2 Route III

Route III is another two - steps reaction mechanism as given in Scheme 5.12. The rate law is exactly the same as that of route II (Scheme 4.9). That is,



The second step is the slowest and this is the rate determining step. Therefore,

$$\text{Rate, } r = k_2 I_2^2 N_2H_4 \dots\dots\dots (5.104)$$

At the steady state, equilibrium is set up and, therefore,

$$N_2H_4 = \frac{k_1 H_2O [N_2H_5^+]}{k_{-1} [H_3O^+]} \dots\dots\dots (5.105)$$

$$\text{Hence, } r = k_2 I_2^2 \left( \frac{k_1 H_2O [N_2H_5^+]}{k_{-1} [H_3O^+]} \right) \dots\dots\dots (5.106)$$

$$r = \frac{k_1 k_2}{k_{-1}} \frac{I_2^2 H_2O [N_2H_5^+]}{[H_3O^+]} \dots\dots\dots (5.107)$$

$$r = k \left( \frac{I_2^2 H_2O [N_2H_5^+]}{[H_3O^+]} \right) \dots\dots\dots (5.108)$$

$$\text{Where, } k = \frac{k_1 k_2}{k_{-1}} \dots\dots\dots (5.109)$$

Therefore,  $k = 4.36 \times 10^{13} \text{ dm}^3 \text{ mol}^{-1} \text{ sec}^{-1}$  for the DFT studies

### 5.8.5.4 Route IV

Route IV is a three - steps reaction mechanism as given in Scheme 5.10



The third step is the slowest and this is the rate determining step. Therefore,

$$r = k_3 [HOI]^2 [N_2H_4] \quad \dots\dots\dots (5.113)$$

At the steady state, equilibrium is set up and, therefore,

$$[HOI]^2 = \frac{k_2 [I_2]^2 [H_2O]^2}{k_{-2} [HI]^2}, \text{and} \quad \dots\dots\dots (5.114)$$

$$[N_2H_4] = \frac{k_1 [H_2O] [N_2H_5^+]}{k_{-1} [H_3O^+]} \quad \dots\dots\dots (5.115)$$

$$\text{Hence, } r = k_3 \left( \frac{k_2 [I_2]^2 [H_2O]^2}{k_{-2} [HI]^2} \right) \left( \frac{k_1 [H_2O] [N_2H_5^+]}{k_{-1} [H_3O^+]} \right) \quad \dots\dots\dots (5.116)$$

$$r = \frac{k_1 k_2 k_3}{k_{-1} k_{-2}} \left( \frac{[I_2]^2 [H_2O]^3 [N_2H_5^+]}{[HI]^2 [H_3O^+]} \right) \quad \dots\dots\dots (5.117)$$

$$r = k \left( \frac{[I_2]^2 [H_2O]^3 [N_2H_5^+]}{[HI]^2 [H_3O^+]} \right) \quad \dots\dots\dots (5.118)$$

$$\text{Where, } k = \frac{k_1 k_2 k_3}{k_{-1} k_{-2}} \quad \dots\dots\dots (5.119)$$

$k_{-2}$  is approx. zero

Therefore,  $k = 4.19 \times 10^{31} \text{ dm}^3 \text{ mol}^{-1} \text{ sec}^{-1}$  for the DFT studies.

### 5.9 Comparison of Rate Constants

For the 1,2-diphenylhydrazine system, this research established two possible pathways. The most favourable pathway have an overall rate constant of  $k = 5.56 \times 10^2 \text{ dm}^3 \text{ mol}^{-1} \text{ sec}^{-1}$  while the other pathway have, rate constant,  $k = 1.57 \times 10^1 \text{ dm}^3 \text{ mol}^{-1} \text{ sec}^{-1}$ . May and Halpern (1961)

who studied the same reaction did not give the overall rate constant for the reaction; they only gave some expressions for calculating the rate constants for the elementary steps, e.g. for first step they gave  $k_1 = 4.4 \times 10^{11} e^{[-10,000/RT]}$ . For the hydrazine/ hydrazinium system, four different reaction pathways were established, with  $k = 1.0 \times 10^{-4} \text{ dm}^3\text{mol}^{-1} \text{ sec}^{-1}$ ;  $k = 1.21 \times 10^{13} \text{ dm}^3\text{mol}^{-1} \text{ sec}^{-1}$ ;  $k = 4.36 \times 10^{13} \text{ dm}^3\text{mol}^{-1} \text{ sec}^{-1}$  and  $k = 4.19 \times 10^{31} \text{ dm}^3\text{mol}^{-1} \text{ sec}^{-1}$ , respectively. Mshelia *et al* (2010) who investigated the same system obtained,  $k = 1.96 \times 10^5 \text{ dm}^3\text{mol}^{-1} \text{ sec}^{-1}$  while Funai and Blesa (1984) obtained,  $k = 3.1 \times 10^{-1} \text{ dm}^3\text{mol}^{-1} \text{ sec}^{-1}$  for the same system and,  $k = 5.69 \times 10^8 \text{ dm}^3\text{mol}^{-1} \text{ sec}^{-1}$  for a derivative of isonicotinoylhydrazide. Both Mshelia *et al* (2010), and Funai and Blesa (1984) rate constants fell within the extremes obtained for this work.

For the L-tyrosine system the rate constant obtained was  $k = 4.41 \times 10^{12} \text{ dm}^3\text{mol}^{-1} \text{ sec}^{-1}$ . Aghaie *et al* (2008) reported  $k = 7.2 \times 10^{-1} \text{ dm}^3\text{mol}^{-1} \text{ sec}^{-1}$ . There seems to be a large difference between their study and ours.

For the L-ascorbic system, two possible pathways were established for this research. The rate constants for the respective pathways were  $k = 1.17 \times 10^4 \text{ dm}^3\text{mol}^{-1} \text{ sec}^{-1}$  and  $k = 1.37 \times 10^4 \text{ dm}^3\text{mol}^{-1} \text{ sec}^{-1}$ . Morelli (1976), Sitti and Bunbun (2009) and Canterbury (2014) all reported the oxidation of L-ascorbic acid by iodine without giving the kinetic data. However, their reaction products obtained were the same with the ones obtained in this research.

For the D-fructose system, only one possible pathway, with  $k = 5.20 \times 10^{-38} \text{ dm}^3\text{mol}^{-1} \text{ sec}^{-1}$ , was established for this research. Mahmood *et al* (2009) studied the same reaction and gave rate constants for the elementary steps but only reported the expression for obtaining the

overall rate constant. Mahmood *et al* (2009) gave,  $k = \frac{k_1 k_2}{k_{-1} + k_2}$  and, whereas  $k_1$  and  $k_2$  were provided, their investigation did not provide for  $k_{-1}$ .

It is noteworthy to state that for the works previously done (May and Halpern, 1961; Morelli, 1976; Funai and Blesa, 1984; Aghaie *et al.*, 2008; Sitti and Bunbun, 2009; Mahmood *et al.*, 2009; Mshelia *et al.*, 2010; Canterbury, 2014) all studies were carried in very dilute solutions, a condition very necessary for any good kinetic work (Mee, 1971; Espenson, 2002; Atkin and de Paula, 2006). All the works cited were also concentration dependent. So, if there appeared to be differences in rate constants in some of the cited works and those obtained in this research, it is because the experimental kineticist must of necessity work in very dilute solution (Mee, 1971; Espenson, 2002; Atkin and de Paula, 2006) whereas the computational researcher (Ochterski, 2000; McQuaid *et al.* 2002; 2004; McQuaid and Rice, 2006; Spartan, 2014) is required to use concentration of 1 (which ever unit chosen).

On a final note, this work has shown that the oxidation by iodine of the molecules investigated are in the following order: hydrazine/ hydrazinium ion > L-tyrosine > L-ascorbic acid > 1,2-diphenylhydrazine >> D-fructose.

## CHAPTER SIX

### 6.0 SUMMARY, CONCLUSION AND RECOMMENDATIONS

#### 6.1 Summary

The research work designed to investigate the reactions between iodine molecule and the following substrates: hydrazinium ion, hydrazine molecule, 1,2-diphenylhydrazine, L-tyrosine, L-ascorbic acid and D-fructose. In the course of the investigation the following were specifically addressed and:

- i. resolved all the conflicts (dissimilar mechanisms for same reaction) associated with the reactions of iodine with substrates listed above and proposed new mechanisms for each of them;
- ii. established all possible reaction pathways and the most favourable one for each reaction;
- iii. identified and characterized all the transient species which are not accessible experimentally for all the reaction pathways;
- iv. calculated thermodynamic and some physico-chemical parameters of all reactive species and products of reactions
- v. derived rate-law for each of the pathways that are consistent with the mechanisms proposed.
- vi. calculated and compare the rate constants of the reactions based on the proposed logical reaction mechanism.

This work also showed that the oxidation by iodine of the molecules investigated were in the following order: hydrazine/ hydrazinium ion > L-tyrosine > L-ascorbic acid > 1,2-diphenylhydrazine >> D-fructose.

## 6.2 Conclusion

The mechanism of the reaction of 1,2-diphenylhydrazine, L-tyrosine, D-ascorbic acid, D-fructose and hydrazine / hydrazinium ion with iodine were respectively studied using computational semi empirical and density functional theory methods. The semi-empirical methods used were either at the MNDO or PM3 levels while all the DFT calculations were executed using 6311+G\*\* basis set of DFT at the B3LYP level of computation. In all cases, comparison of the two methods used showed that the DFT calculations were more exact. The results of the various studies were compared with previously published works on the reaction of iodine with the respective substrates investigated.

In this work, all the reacting species, including transition states and products, were optimized at the various basis sets used for the study. The best conformer, energetically for the reacting species, were always searched and when found were chosen as the starting molecules or species for each study. The study was able to demonstrate clearly that for each system, there were more than one plausible reaction mechanisms. But the most energetically favoured pathways were always chosen as the most possible mechanism of reaction. Previous published works on the reactions of iodine with the various biomolecules used in this work were ambiguous or incomplete because the researchers were not able to propose clear transition states for their reactions. Through computational means, transition states of the various reactions which could not be determined experimentally in the laboratory, were searched out and determined for the various systems studied in this work (Manz and Sholl, 2010, Spartan, 2014). Apart from the transition states determined, other activation parameters for the reacting species and products were also determined and calculated in this work. These, together with the transition states found, lend credence to the various reaction mechanisms proposed in this study.

The study was, therefore, able to address the ambiguities and short comings in the previously published works on the reactions of 1,2-diphenylhydrazine, L-tyrosine, D-ascorbic acid, D-fructose and hydrazine / hydrazinium ion with iodine, respectively by obtaining the various transition states of the reactions.

### **6.3 Recommendation**

There are several ways in which the present work can be expanded and improved upon. Study of reaction mechanisms in aqueous and other media can be undertaken using computational means to gain greater insight into mechanisms of reactions of iodine with the various biomolecules studied. Computational chemistry methods can also be utilized together with experimental spectroscopy works to obtain a more detailed understanding of the various species present in the reactions of iodine with biomolecules of interest.

It is also worthy of note to state that computers and the methods of computational chemistry are in continuous development, and it is almost certain that the calculations of reaction energies presented in this work can be improved upon. The present work has shown that computational chemistry tools can be successfully applied to further the understanding of reaction mechanisms of reacting systems. It is also likely that the same methods as applied in the present work can be applied to study other reactions of interest.

In light of the above therefore, it is recommended that Chemistry Department of Ahmadu Bello University, Zaria:

I should purchase modern high-performance computers that can be used for computational studies.

- II should purchase subscriptions or, licenses for computational soft wares, such as, Spartan, HyperChem, Firefly, GAMESS, etc., for use in computational studies.
- III should set up computational chemistry laboratory after obtaining items in I and II above.

## REFERENCES

- Agarwal, S., Gopal, K. and Kumar, B. (2008). Sporotrichosis in Uttarakhand (India): a report of nine cases. *International Journal of Dermatology*, **47**(4):367-371.
- Aghaie, M., Mirzaie, M., Zare, K., Monajjemi, M. and Aghaie, H. (2008). Kinetic and Mechanism Studies of the Reaction between L-Tyrosine and Iodine on the Basis of UV -Vis Spectrophotometric Method. *Asian Journal of Biochemistry*, **3**(5): 290-296.
- Alfie, D., Gillan, M.J. and Price, G.D. (2000). Constraints on the composition of the Earth's core from *ab initio* calculations. *Nature*, **405**: 172 - 175.
- Al-Hashimi, N.A and Hussein, Y. H.A. (2010). Ab initio study on the formation of triiodide CT complex from the reaction of iodine with 2,3-diaminopyridine. *Spectrochimica Acta Part A: Molecular and Biomolecular Spectroscopy*, **75**:198–202.  
[doi:10.1016/j.saa.2009.10.012](https://doi.org/10.1016/j.saa.2009.10.012)
- Allen, M. P. and Tildesley, D. J. (1987). *Computer Simulations of Liquids*, Clarendon Press, Oxford, UK, pp.18,155-159,182.
- Apelqvist, J. and Ragnarson, T.L.G., (1996). Cavity foot ulcers in diabetic patients: a comparative study of cadexomer iodine ointment and standard treatment. *Acta DermVenereologica*, **76**:231-235.
- Araujo, J, C., de Mesquita Carneiro, J, W., de Araujo, M, T., Leited, F, H, A., Tarantod, A, and G. (2008). *Bioorganic and Medicinal Chemistry*, **16**: 5021-5029.
- Araujo, J, C., de Mesquita Carneiro, J, W., de Araujo, M, T., Leited, F, H, A., Tarantod, A, G. (2008). Interaction between artemisinin and heme. A Density Functional Theory study of structures and interaction energies, *Bioorganic and Medicinal Chemistry*, **16**: 5021-5029.
- Arora, U., Aggarwa, I A. and Arora, R.K. (2003). Sporotrichosis in Amritsar - a case report. *Indian Journal of Pathology and Microbiology*, **46**:442-443.
- Assi, A., Globig, S. and Koelbel, C. (1996). PH-dependent reaction types of hydrazobenzene in gastric juice and hydrous solution. 37th Spring Meeting of the German Society for Experimental and Clinical Pharmacology and Toxicology, Mainz, Germany, March 12-14, 1996, *Naunyn Schmiedeberg's Archives of Pharmacology*, **353**(4 SUPPL.): R112, 1996.
- Atkins, P. and de Paula, J, (2006). *Physical Chemistry*, 8th ed., W.H. Freeman, pp.816-818, 884-886, 892-893.
- Ayub, K. and Mahmood, T. (2013). DFT studies of halogen bonding abilities of nitrobenzene with halogens and chlorofluorocarbons. *Journal of The Chemical Society of Pakistan*, **35**, 617- 821.

- Azori, J.M., Bovie, Ph., Widme, J., Jeanningros, R., Tissot, R. (1990). L-Tyrosine and L-Tryptophan Membrane Transport in Erythrocytes and antidepressant drug choice. *Biological Psychiatry*, **27(7)**:723-734.
- Babasaheb, D. B. and Gavisiddappa S. G. (2012). Kinetics and mechanism of ruthenium(III) catalyzed oxidation of d-glucose by  $\text{K}_2\text{S}_2\text{O}_8$ -tungstocobaltate(III) in aqueous hydrochloric acid medium. *Advances in Applied Science Research*, **3(2)**:785-792.
- Banerjee, P., Saha, S. K. and Gupta, M. (1988). Kinetics and mechanism of the reduction of dodecatungstocobaltate (III) by D-fructose, D-glucose, and D-mannose: comparison between keto- and aldohexoses. *Journal of the Chemical Society, Perkin Transaction* **2, 1988**, 1781- 1785. DOI: 10.1039/P29880001781, Paper
- Barca, R., Ellis, J., Tsao, M.S. and Willmarth, W. K. (1967). The pentacyano complexes of cobalt(III). IV. Kinetics and mechanism of the substitution of water in  $\text{Co}(\text{CN})_5\text{OH}_2$  - by pyridine, ammonia, hydrazine, and hydrazinium ion. *Inorganic Chemistry*, **6(2)**, 243–248.
- Bare, W. D., Pham, C.V., Cuber, M. and Demas, J. N. (2007). An improved method for studying the enzyme-catalyzed oxidation of glucose using luminescent probes. *Journal of Chemistry Education*, **84**:1511–1514.
- Barhoumi, A., Zeroual, A., Bakkas, S. and El Hajbi, A. (2015). Theoretical study of the regioselectivity of the reaction between tetrachloromethane and triethyl phosphite using DFT B3LYP/6-31G (d). *Journal of Computational Methods in Molecular Design*, **5(2)**: 8-15.
- Barr, A. J. (2010) Protein tyrosine phosphatases as drug targets: Strategies and challenges of inhibitor development, *Future Medicinal Chemistry*, **2**: 1563-1576. 62.
- Bayly, C. I., Cieplak, P., Cornell, W. D. and Kollman, P. A. (1993). A Well Behaved Electrostatic Potential Based Method Using Charge Restraints for Deriving Atomic Charges: The RESP Model. *The Journal of Physical*, **97(40)**, 10269-10280. DOI: 10.1021/j100142a004
- Becke, A. D. (1988). Density-functional exchange-energy approximation with correct asymptotic behavior. *Physical Review A*, **38(6)**: 3098–3100.
- Bergès, J., Trouillas, P. and Houée-Levin, C. (2011). *Journal of Physics: Conference Series* 261(2011) 012003. DOI:10.1088/1742-6596/261/1/0120
- Bhatnagar, P., Mittal, R.K. and Gupta, Y.K. (1990). Stoichiometry, Kinetics, and Mechanism of the Oxidation of Hyponitrous Acid by Iodine in Acetate Buffers. *Journal of the Chemical Society, Dalton Transactions*, 3669-3673.
- Bingham, R.C., Dewar, M. J. S. and Lo, D. H. (1975). An improved version of the MINDO Semi empirical SCF-MO Method. *Journal of the American Chemical Society*, **97(18)**: 1285-1294.

- Blackmore, K. J., Lal, N., Ziller, J. W. and Heyduk, A. F. (2008). Catalytic reactivity of a zirconium(IV) redox-active ligand complex with 1,2-diphenylhydrazine. *Journal of the American Chemical Society*, **130**(9): 2728–2729.
- Bond, D.R. and Lovley, D.R.(2003). Electricity production by *Geobacter sulfur reducens* attached to electrodes. *Applied and Environmental Microbiology*, **69**: 1548-1555.
- Bonifaz, A., Saúl, A., Paredes-Solis, V., Fierro, L.Rosales, A., Palacios, C. and Araiza, J. (2007). Sporotrichosis in childhood: clinical and therapeutic experience in 25 patients. *Pediatric Dermatology*, **24**:369-372.
- Bruice, T. C. and Bruice, P. Y. (2005). Covalent intermediates and enzyme proficiency. *Journal of American Chemical Society*, **127**: 12478-12479.
- Cabezas, C., Bustamante, B., Holgado, W. and Begue, R. E. (1996). Treatment of cutaneous sporotrichosis with one daily dose of potassium iodide. *The Pediatric Infectious Disease Journal*, **15**(4): 352-354.
- Canterbury, (2014). University of Canterbury, Determination of Vitamin C Concentration by Titration, [www.outreach.canterbury.ac.nz](http://www.outreach.canterbury.ac.nz) – accessed 03/02/2014
- Cao Xue, Y. I., Jiang, X.M., Kareem A., Dou, Z.H., Rakeman, M.A., Zhan, M.L. and Dulong G.R. (1994). Iodination of irrigation waters as a method of supplying iodine to a severely Iodine deficient population in Xinjing, China. *The Lancet*, **344**: 107-109.
- Caspar, D.L. (1995). MINIREVIEW: Problems in simulating macromolecular movements. Insufficient sampling of conformational sub-states by current molecular dynamics simulations accounts for deficiencies in representations of the fluctuating interatomic separations in macromolecules. *Structure*, **15**(3):327-329.
- Cheema, S.K. and Pant M. R. (2011). Estimation Of Vitamin C In Seven Cultivated Varieties Of Capsicum Annuum L. *International Journal of Pharmaceutical Sciences*, **3**(2):1397-1401.
- Chernov'yants, M. S. and Burykin, I. V., Starikova, Z. A., Tereznikov, A. Y. and Kolesnikova, T. S. (2013). Spectroscopic and structural study of novel interaction product of pyrrolidine-2-thione with molecular iodine. Presumable mechanisms of oxidation. *Journal of Molecular Structure*, **1047**: 204–208.  
<http://dx.doi.org/10.1016/j.molstruc.2013.04.062>
- Clementi, E. (1980). Evolution of Computational Chemistry and Trends in the Computer Industry, *Abstracts of Papers of the American Chemical Society*, **180**: 17.
- Combes, P., Lombard, F., Quinson, M. and Suter, F.(2000). A Scalable Approach to Network Enabled Servers. In *Advances in Computing Science - ASIAN 2002*, volume **2550** of Lecture Notes in computer Science
- Cornell, W. L. Cieplak, P., Bayly, C. I., Gould, I. R., Merz, K. M., Ferguson, D. M., Spellmeyer, D. C., Fox, T., Caldwell, J. W. and Kollman, P. A. (1995). A Second Generation Force Field for the Simulation of Proteins, Nucleic Acids, and Organic Molecules. *Journal of the American Chemical Society*, **117**: 5179-5197.
- Cramer, C. J. (2002). *Essentials of Computational Chemistry*. John Wiley & Sons, UK. Cumming Co., California, pp. 1-14, 17, 40-46, 95-100, 121-149, 153-188, 233-371, 385.

- Cummins, P. L. and Gready, J. E. (2005). Computational methods for the study of enzymic reaction mechanisms III: A perturbation plus QM/MM approach for calculating relative free energies of protonation. *Journal Computational Chemistry*, **26**: 561-568.
- Cunningham, L. W. and Nuenke, B. J. (1959). Physical and Chemical Studies of a Limited Reaction of Iodine with Proteins. *Journal of Biological Chemistry*, **234**:1447-1451. <http://www.jbc.org/content/234/6/1447>.
- da Silva, E. F. and Svendsen, H. F. (2004). *Ab initio* study of the reaction of carbamate formation from CO<sub>2</sub> and alkanolamine. *Industrial and Engineering Chemistry Research*, **43(13)**: 3413 -3418.
- da Silva, E.F.(2005). Computational Chemistry Study of Solvents for Carbon Dioxide Absorption (Doctoral Thesis). *Norwegian University of Science and Technology*.
- Dewar, M. J. S., Zebisch, E.G., Healy, E. F. and Stewart, J. J. P. (1985). AM1: A New General Purpose Quantum Mechanical Molecular Model, *Journal of the American Chemical Society*, **107**: 3902-3909.
- Dewar, M. J. S. and Thiel, W. (1977). Ground States of Molecules. 38. The MNDO Method. Approximations and Parameters. *Journal of the American Chemical Society*, **99(15)**: 4899-4907.
- Dick, T. J., Wierzbicki, A. and Madura, J. D. (2009). CO<sub>2</sub>(aq) Parameterization Through Free Energy Perturbation/Monte Carlo Simulations for Use in CO<sub>2</sub> Sequestration. In: Leszczynski, J. and Shukla, M. K. (Eds). *Practical Aspects of Computational Chemistry - Methods, Concepts and Applications*, Springer, Dordrecht, pp.337-358.
- Dioha, I. J., Olugbemi O., Onuegbu T. U. and Shahru, Z. (2011). Determination of ascorbic acid content of some tropical fruits by iodometric titration. *International Journal of Biological and Chemical Sciences*, **5(5)**: 2180-2184.
- Dirac, P.A.M.(1929). Quantum Mechanics of Many-Electron Systems. *Proceedings of the Royal Society, London, A1929*, **123**: 714-733.
- Doggui, R. and El Atia, J. (2015). Iodine deficiency: Physiological, clinical and epidemiological features, and pre-analytical considerations. *Annales d'Endocrinologie (Annals of Endocrinology)*, **76**: 59-66. <http://dx.doi.org/10.1016/j.ando.2014.12.002>
- Domingo, L. R., Pérez, P. and Sáez, J. A. (2013). Understanding the local reactivity in polar organic reactions through electrophilic and nucleophilic Parr function, *RSC Advances*, **3**: 1486–1494.
- Eitenmiller, R. R., Ye L., Landen W. O. (2008). *Vitamin analysis for the health and food sciences*. CRC Press, Taylor & Francis Group, UK.
- Engel, T. and Reid, P. (2006). *Physical Chemistry*, Pearson Prentice Hall, Upper saddle River, NJ, p.924.
- Espenson, J. H. (2002) *Chemical Kinetics and Reaction Mechanisms*, 2nd ed., McGraw-Hill, London, UK, pp.112, 156-160.

- Faller, P., Rutherford, A.W. and Debus, R.J. (2002). Tyrosine D oxidation at cryogenic temperature in photosystem II. *Biochemistry*, **41**: 12914–12920.
- Feibelman, P. J., Hammer, B. Norskov, J. K., Wagner, F., Scheffler, M., Stumpf, R., Watwe, R. and Dumesic, J. (2001). The CO/Pt(111) Puzzle. *The Journal of Physical Chemistry*, **B105**: 4018-4025.
- Finar, I.L. (1978). *Organic Chemistry*, Longman Limited: London, UK. Pp.503 – 524.
- Foppoli, C., De Marco, C., Blarzino, C., Coccia, R., Mosca, L., Roesi, M.A. (1997). Dimers formation by cytochrome c-catalyzed oxidation of tyrosine and enkephalins, *Amino Acids*, **13**: 273–280.
- Foresman, J. B. and Frisch, Æ. (1996). *Exploring chemistry with electronic structure methods*, 2<sup>nd</sup> edn. Gaussian Inc., Pittsburgh, PA, pp 173–211, 272.
- Franckl, M. M. and Chirlian, L. (2000). in: Lipkowitz, K. B., Boyd, D. B., (Eds.), *Reviews in Computational Chemistry*, Volume **14**, Wiley-VCH, pp. 1-31.
- Frenkel, D. and Smit, B. (2002). *Understanding molecular simulation: From Algorithms to Applications*, 2<sup>nd</sup> edn, Academic Press, San Diego, USA, p.638.
- Frenkel, D. and Smit, B. (2006). *Understanding Molecular Simulation: From Algorithms to Applications*; Academic Press: Waltham, MA, USA, pp.375 – 387.
- Fuentes-Cabrera, M., Baskes, M.I., Melechko, A.V. and Simpson, M.L. (2008). Bridge structure for the graphene/Ni(111) system: A first principles study. *Physical Review*, **B 77**: 035405. DOI: <http://dx.doi.org/10.1103/PhysRevB.77.035405>
- Fukui, K. (1964). in: P.O. Lowdin, B. Pullman (Eds.), *Molecular Orbitals in Chemistry, Physics and Biology*, Academic Press, New York, p. 513
- Fukui, K. (1974) In: Daudel, R. and Pullman, B. (Eds.), *The World of Quantum Chemistry*, Reidel, Dordrecht, p. 113.
- Fukui, K., (1982). Chemical Reactivity Theory - Its Pragmatism and Beyond, *Pure & Applied Chemistry*, **54(10)**: 1825-1836,
- Funai, I.A. and Blesa, M.A.(1984). Kinetics and mechanism of the reaction of Iodine with isonicotinoylhydrazide. *Canadian Journal of Chemistry*, **62**: 2923 - 2928.
- Gao J. (1996). In: Lipkowitz, K. B., Boyd, D. B., (Eds.), *Reviews in Computational Chemistry*, Volume 7, Wiley-VCH, pp. 119-185.
- Gaston, M. A., Dias, L. R., Freitas, A. C., Miranda A. L and Barreiro, P. (1996). Synthesis and Analgesic Properties of New 4-Arylhydrazone 1-H Pyrazole [3,4-b] Pyridine Derivatives. *Pharmaceutica Acta Helvetiae*, **71(2)**: 213-219. Doi: 10.1016/0031-6865(96)00012-X.
- Gelenberg, A. J., Gibson, C. J. and Wojcik, J. D. (1982). Neurotransmitter precursors for the treatment of Depression. *Psychopharmacology Bulletin*, **18(1)**: 7–18.

- Gillan, M.J., Alfe, D., Brodholt, J., Vocadlo, L. and Price, G.D. (2006). First-principles modeling of Earth and planetary materials at high pressures and temperatures. *Reports on Progress in Physics*, **69**, 2365 - 2442
- Giraldo, J., Roche, D., Rovira, X and Serra, J. (2006). The catalytic power of enzymes: conformational selection or transition state stabilization? *FEBS Letters*, **580**: 2170-2177.
- Giulivi, C. and Davies, K. J. A. (2001). Mechanism of the formation and proteolytic release of H<sub>2</sub>O<sub>2</sub>-induced dityrosine and tyrosine oxidation products in hemoglobin and red blood cells. *The Journal of Biological Chemistry*, **276(26)**: 24129–24136.
- Globig, S. and Freundt, K.J. (1996). Metabolism of hydrazobenzene in rat liver homogenate. Autumn Meeting of the Deutsche Gesellschaft Fuer Experimentelle Und Klinische Pharmakologie Und Toxikologie (German Society for Experimental and Clinical Pharmacology and Toxicology), Dresden, Germany, September 10-12, 1996, *Naunyn-Schmiedeberg's Archives of Pharmacology*, **354 (4 SUPPL. 1)**:R28.
- Globig, S., Killguss, M. and Freundt, K.J. (1996). Metabolism of hydrazobenzene and azobenzene in rat hepatocytes in primary culture. Autumn Meeting of the Deutsche Gesellschaft Fuer Experimentelle Und Klinische Pharmakologie Und Toxikologie (German Society for Experimental and Clinical Pharmacology and Toxicology), Dresden, Germany, September 10-12, 1996, *Naunyn-Schmiedeberg's Archives of Pharmacology* **354(4 SUPPL. 1)**:R419.
- Gowda, B.T., Damodara, N. and Jyothi, K. (2005). Kinetics and mechanism of D-fructose and D-glucose by sodium salts of N-chloro-mono/di substituted benzenesulfonamide in aqueous alkaline medium. *International Journal of Chemical Kinetics*, **37**: 572-582.
- Goyal, M. R., Bhatnagar, P., Mittal, R. K. and Gupta, Y. K. (1989). Redox chemistry of hyponitrous acid. 4. Stoichiometry, kinetics and mechanism of oxidation by cerium (iv) in acid sulfate-solutions, and determination of hyponitrous acid in acid perchlorate solutions. *Indian Journal of Chemistry Section A-Inorganic Bio-Inorganic Physical Theoretical & Analytical Chemistry*, **28(5)**: 382-387.
- Grant, G. H. and Richards, W. G. (1995). *Computational Chemistry*. Oxford University Press, UK. p.113
- Griffiths D. J., (1995). *Introduction to Quantum Mechanics*, Prentice-Hall, Engelwood Cliffs, NJ. Pp. 1-17.
- Guevara-Carrion, G., Hasse, H. and Vrabec, J. (2012). *Multiscale Molecular Methods in Applied Chemistry*, In: Kirschner, B., Vrabec, J., (Eds.); Series: *Topics in Current Chemistry*, Volume 307; Springer: Berlin/Heidelberg, Germany, 2012; pp.201 - 249.
- Gupta, A., Gupta, R. K. and Gupta, G. S. (2009). Targeting cells for drug and gene delivery: Emerging applications of mannans and mannan binding lectins. *Journal of Scientific and Industrial Research*, **68**: 465-483.

- Hall, M. B. (2000). Perspective on “The Spectra and Electronic Structure of the Tetrahedral Ions  $\text{MnO}_4^-$ ,  $\text{CrO}_4^-$ , and  $\text{ClO}_4^-$ ”. *Theoretical Chemistry Account*, **103**(3-4): 221-224.
- Hammal, R., Benharref, A. and El Hajbi, A. (2015). Exploration of the mechanism and selectivity of [1+2] cycloaddition reaction between  $\alpha$ -cis-himachalene and dibromocarbene using DFT-based reactivity indices. *Journal of Computational Methods in Molecular Design*, **5**(2): 16-24.
- Hammer, B., Hansen, L. B. and Norskov, J. K. (1999). Improved adsorption energetics within density-functional theory using revised Perdew-Burke-Ernzerhof functionals. *Physical Review. B* 59: 7413. DOI: <http://dx.doi.org/10.1103/PhysRevB.59.7413>
- Hao, X.H., Quo, L.J., Mao, X., Zhang, X. M. and Chen, X. J. (2003). Hydrogen production from glucose used as model compound of biomass gasified in supercritical water. *International Journal of Hydrogen Energy*, **28**: 55-64.
- Harris, F. E.(1998). Ewald Summations in Systems with Two-Dimensional Periodicity, *International Journal of Quantum Chemistry*, **68**:385-404.
- Hasty, R. A. (1975).The kinetics of the reduction of iodine by hydrazine.*Zeitschrift für Physikalische Chemie*, **94**(1-3): 53-61.
- Hehre, W. J. 1995. *Practical Strategies for Electronic Structure Calculations*, Wavefunction Inc., Irvine, CA., p 9-14.
- Hehre, W. J. and Lou, L. (1997). *A Guide to Density Functional Calculations in Spartan*, Wavefunction Inc., Irvine CA. pp.7-10, 21-30.
- Hehre, W. J., Radom, L., Schleyer, P. V. R. and Pople, J. A. (1986). *Ab Initio Molecular Orbital Theory*; John Wiley & Sons, Inc.: New York. Sections 6.2 – 6.3.
- Hehre, W. J., Shusterman, A. J. and Nelson, J. E. (1998). *The Molecular Modeling Workbook for Organic Chemistry*, Wavefunction Inc., Irvine, CA., pp.1-19, 59-67.
- Helgaker, T., Jorgensen, P., Olsen, J. and Klopper, W. (2004). *Wave Function–Based Quantum Chemistry*. In: Patri ck Bultinck, P., Winter, H. D., Langenaeker, W. and Tollenaere, J. P. (Eds.), *Computational Medicinal Chemistry for Drug Discovery*, Marcel Dekker, Inc., New York, pp.57-88.
- Heller, R., Unbehaun, A., Schellenberg, B., Mayer, B., Werner-Felmayer, G. and Werner, E. R. (2001). L-Ascorbic Acid Potentiates Endothelial Nitric Oxide Synthesis via a Chemical Stabilization of Tetrahydrobiopterin. *The Journal of Biological Chemistry*, **276**(1): pp. 40–47.
- Heneberg, P. (2009) Use of protein tyrosine phosphatase inhibitors as promising targeted therapeutic drugs, *Current Medicinal Chemistry*, **16**: 706-733. 63.
- Hetzl, B.S., Potter, B. J. and Dulberg, E. M. (1990).The iodine deficiency disorders, nature, Pathogenesis and epidemiology. *World review of nutrition and dietetics*, **62**: 59-79.
- Hietanen, A. and Kanerva, L. T. (2012). One-Pot Oxidation-Hydrocyanation Sequence Coupled to Lipase-Catalyzed Diastereoresolution in the Chemoenzymatic Synthesis of Sugar Cyanohydrin Esters. **2012**: 2729. DOI: 10.1002/ejoc.201200086.

- Hoffman, J.R., Ratamess, N. A., Gonzalez, A., Beller, N. A., Hoffman, M.W., Olson, M., Purpura, M. and Jäger, R. (2010). The effects of acute and prolonged CRAM supplementation on reaction time and subjective measures of focus and alertness in healthy college students. *Journal of the International Society Sports Nutrition*, **7**:39. Dec 15, 2010. <http://www.jissn.com/content/7/1/39>
- Homer, R. B., Cannon, R. D. and Kim, S. S.B. (1985). The oxidation of hydrazobenzene by oxygen catalysed by CO(2MeOsalen) in methanol. *Bulletin of Korean Chemical Society*, **16** (2): 115-118.
- Hopfinger, A. J. (1984). Computational Chemistry, Molecular Graphics and Drug Design, *Pharmacy International*, **5**: 224-228.
- Housecroft, C.E. and Sharpe, A.G., (2006). *Inorganic Chemistry*, 3<sup>rd</sup> edn., Pearson Prentice Hall, Milan, pp.882-883.
- Huey, R., Morris, G. M., Olson, A. J., Goodsell, D. S. (2007). A semi-empirical free energy force field with charge-based desolvation. *Journal of Computational Chemistry*, **28**, 1145-1152.
- Hulsmann, M. and Reith, D. (2013). SpaGrOW—A Derivative-Free Optimization Scheme for Intermolecular Force Field Parameters Based on Sparse Grid Methods, *Entropy*, **15**: 3640-3687; Doi:10.3390/e15093640.
- Hulsmann, M., Muller, T. J., Koddermann, T., and Reith, D. (2011). Automated force field optimisation of small molecules using a gradient-based workflow package. *Molecular Simulation*, **36**:1182–1196.
- Hung, M. and Stanbury, D.M. (2005). Catalytic and direct oxidation of Cysteine by Octacyanomolybdate(V), *Inorganic Chemistry*, **44**(10):3541-3550.
- IPCS (1993). *International Chemical Safety Card for 1,2-Diphenylhydrazine*. In: International Programme for Chemical Safety WHO, editor. Geneva, 1993.
- Isgro, T. A. (2003). Structural Characterization of N-Acetyl-2-Aminofluorene and its Guanine and Deoxyguanosine Adducts via a Molecular Mechanics, Semi-empirical, and Density Functional Theory Cascade Method (M.Sc. Thesis), *The Cooper Union for the Advancement of Science and Art Albert Nerken School of Engineering*.
- Izadyara, M., Gholami, M. R., Haghgu, M., (2004). DFT calculations on the retro-ene reactions, part II: allyln-propylsulfide pyrolysis in the gas phase. *Journal of Molecular Structure: (THEOCHEM)*, **686**, 37–42.
- Jensen, F. (1994), Transition structure modelling by intersecting potential energy surfaces, *Journal of Computational Chemistry*, **15**(11): 1199-1216. DOI: 10.1002/jcc.540151103
- Jensen, F. (1999). *Introduction to Computational Chemistry*; John Wiley & Sons Ltd. Chichester, West Sussex. pp.74-85, 171.
- Jensen, F. (2007). *Introduction to Computational Chemistry*; 2<sup>nd</sup> edn., John Wiley & Sons Ltd. Chichester, West Sussex. pp.192-204.

- Jia, Z., Salaita, M. G. and Margerum, D. W. (2000), Kinetics and Mechanisms of the Oxidation of Hydrazinium Ion ( $N_2H_5^+$ ) by Aqueous  $Br_2$ ,  $Cl_2$ , and  $BrCl$ . Electrophilicity Scale for Halogens and Interhalogens. *Inorganic Chemistry*, **39(9)**: 1974–197.
- Jin, Y., Edler, K. J., Marken, F. and Scott, J. L. (2014). Voltammetric optimisation of TEMPO-mediated oxidations at cellulose fabric. *Green Chemistry*, **16**: 3322. DOI: 10.1039/c4gc00306c
- Jordan, R.B. (2007). *Reaction Mechanisms of Inorganic and Organometallic Systems*, 3<sup>rd</sup> Edition, Oxford University press, New York, pp.23-27, 167-194, 403.
- Jorgensen, W. L. and Ravimohan, C. (1985). Monte Carlo simulation of differences in free energies of hydration. *Journal of Chemical Physics*, **83**: 3050-3054.
- Jorgensen, W.L., Madura, J. D. and Swenson, C. J. (1984). Optimized Intermolecular Potential Functions for Liquid Hydrocarbons. *Journal of American Chemical Society*, **106**: 6638-6646.
- Jorgensen, W. L., Maxwell, D. S. and Tirado-Rives, J. (1996). Development and Testing of the OPLS All-Atom Force Field on Conformational Energetics and Properties of Organic Liquids *Journal of American Chemical Society*, **118**: 11225-11236.
- Jursic, B. S. (1996). The density functional theory investigation of the equilibrium structures of OOF, FOOF, OOF<sub>2</sub>, and FOOF. *Journal of molecular structures*, **336**: 97-103.
- Kagayama, N., Sekiguchi, M., Inada, Y., Takagi, H. D. and Fanahashi, S. (1994). Mechanistic Study of the Reaction of L-Ascorbic Acid with Hexacyanometalate(III) Ions of Iron(III), Ruthenium(III), and Osmium(III) in Aqueous Acidic Solution at Elevated Pressures. *Inorganic Chemistry*, **33(9)**: 1881–1885.
- Kahn, K. (1999). Theoretical study of intermediates in the urate oxidase reaction. *Bioorganic Chemistry*, **27(5)**: 351 – 362.
- Kahn, K. and Bruice, T. C. (2000). Transition state and ground state structures and their interaction with the active site residues in catechol O-methyltransferase. *Journal of American Chemical Society*, **12(1)**: 46 – 51.
- Kalkanis, G. H. and Shields, G.C. (1991). AMI and PM3 Calculations of the Potential Energy Surfaces for  $CH_2OH$  Reactions with  $NO$  and  $NO_2$ . *The Journal of Physical Chemistry*, **95(13)**, 5085-5089.
- Kapur, A., Hasković, A., Čopra-Janićijević, A., Klepo, L., Topčagić, A., Tahirović, I. and Sofić, E. (2012). Spectrophotometric analysis of total ascorbic acid content in various fruits and vegetables. *Bulletin of the Chemists and Technologists of Bosnia and Herzegovina*, **38**: 39-42,
- Karver, M. R., Krishnamurthy, D., Bottini, N., and Barrios, A. M. (2010) Gold(I) phosphine mediated selective inhibition of lymphoid tyrosine phosphatase, *Journal of Inorganic Biochemistry*, **104**: 268-273.

- Kelly, T. J., Mukund, R., Spicer, C.W. (1994). Concentrations and transformations of hazardous air pollutants. *Environmental Science & Technology*, **28(8)**: 378A–387A.
- Kennedy, J. F., White, C. A., Warner, F. P., Lloyd, L. L and Rivera, Z. S. (1989). The identification and analysis of the oxidation products of L-ascorbic acid by HPLC. *Journal of Micronutrient Analysis*, **5**: 91-109.
- Khalil, M.S., Kelada, N., Sawyer, B., Zenz, D.R., Tata, P. and Lue-Hing, C. (1999). Comparison of onestep acidic extraction versus two-step basic and acidic extraction procedures for semi volatile analysis of wastewater. *Water Environment Research*, **71(3)**: 348–352.
- Khan, M. N. and Sarwar, A. (2001). The Influence of Transition Metal Ions on the Kinetics of Ascorbic Acid Oxidation by Methylene Blue in Strongly Acidic Media. *Turkish Journal of Chemistry*, **25**: 433 – 440.
- Kim, K.H., Tucker, M.P. and Nguyen, Q. A., (2002). Effect of pressing lignocellulosic biomass on sugar yield in two-stage dilute-acid hydrolysis process. *Biotechnology Progress*, **18**: 489-494.
- King, S. E., Cooper, J. N. and Crawford, R. D. (1978). Oxidation of hydrazine by iodine in aqueous perchloric acid. *Inorganic Chemistry*, **17(11)**: 3306–3307. DOI: 10.1021/ic50189a073
- Klebanoff, S.J. (1967). Iodination of bacteria: A bactericidal mechanism. *The Journal of Experimental Medicine*, **126(6)**: 1063 -1078.
- Koch, W. and Holthausen, M. C. (eds.) (2000). *A Chemist's Guide to Density Functional Theory*. Wiley-VCH, Weinheim, Germany. In: Thomas, S.H. (2013). From macromolecules to electrons – grand challenges in theoretical and computational chemistry, *Frontiers in Chemistry*, **1, Article 6**: 1-4.
- Kofke, D. A. (2005). Free energy methods in molecular simulation, *Fluid Phase Equilibria*, **228-229**: 41-48.
- Kofke, D. A. and Cummings, P. T. (1997). Quantitative comparison and optimization of methods for evaluating the chemical potential by molecular simulation. *Molecular Physics*, **92**: 973–996.
- Kofke, D. A. and Cummings, P. T. (1998). Precision and accuracy of staged free energy perturbation methods for computing the chemical potential by molecular simulation. *Fluid Phase Equilibria*, **150-151**: 41-49.
- Kollman, P. (1993). Free Energy Calculations: Applications to Chemical and Biochemical Phenomena. *Chemical Reviews*, **93**: 2395-2417. DOI: 10.1021/cr00023a004.
- Konig, F., Andersson, M., Hotz, K., Aeberli, I. and Zimmermann, M. B. (2011). Ten repeat collections for urinary iodine from spot samples or 24-hour samples are needed to reliably estimate individual iodine status in women. *Journal of Nutrition*, **141**: 2049–2054.
- Kortagere, S., Krasowski, M. D., Reschly, E. J., Venkatesh, M., Mani, S. and Ekins, S. (2010). Evaluation of Computational Docking to Identify Pregnane X Receptor Agonists in

- the ToxCast Database. *Environmental Health Perspectives*, **118(10)**:1412–1417.  
[doi:10.1289/ehp.1001930](https://doi.org/10.1289/ehp.1001930)
- Kraka, E. and Cremer, D. (2010). Review of computational approaches to the potential energy surface and some new twists, the unified reaction valley approach URVA. *Accounts of Chemical Research*, **43**:591–601.
- Kresse, G., Gil, A., and Sautet, P. (2003). Significance of single-electron energies for the description of CO on Pt(111). *Physical Review*, **B 68**: 07340.  
[DOI: http://dx.doi.org/10.1103/PhysRevB.68.073401](https://doi.org/10.1103/PhysRevB.68.073401)
- Kuninori, T. and Nishiyama, J. (1993). Advances in cereal chemistry and technology in Japan. Recent advances in dough improvement with ascorbic acid and its derivatives. *Cereal Foods World*, **38**: 554 – 559.
- Laidler, K.J. (1978). *Physical Chemistry with Biological Applications*, Benjamin Cummings, Menlo Park, NC, pp. 365-426.
- Laloo, D. and Mahanti, M.K. (1990). Kinetics of oxidation of amino acids by alkaline hexacyanoferrate(III), *Journal of the Chemical Society, Dalton Transactions*, 311–313.
- Leal, J. M., Domingo, P. L., Garcia, B. and Ibeas, S. (1993). Alkali-metal ion catalysis of the oxidation of L-ascorbic acid by hexacyanoferrate (III) in strongly acidic media, *Journal of the Chemical Society, Faraday Transactions*, **89**: 3571-3577.
- Lee, C., Yang, W. and Parr, R. G. (1988). Development of the Colle-Salvetti correlation-energy formula into a functional of the electron density. *Physical Review B*, **37**, 785–789.
- Leszczynski, J. (2000). Computational chemistry. *Parallel Computing*, **26**: 817-818.  
[doi:10.1016/S0167-8191\(00\)00013-2](https://doi.org/10.1016/S0167-8191(00)00013-2)
- Levine, I.N. (2000). *Quantum chemistry*, 5th edn. Prentice Hall, Upper Saddle River, NJ, pp. 305-315, 494-498, 629-631, 652-664.
- Levine, I.N. (1988). *Physical Chemistry*, 3rd edn.; McGraw-Hill, New York. pp. 2, 27, 34, 58 – 61, 305-315, 494-498.
- Lewars, E (2003). *Introduction to the Theory and Applications of Molecular and Quantum Mechanics*, Kluwer Academic Publishers, Dordrecht. pp. 1-4, 9-39, 81-95, 159-231, 339-437.
- Li, J., Zhu, T., Cramer, C. J. and Truhlar, D. G. (1998). New Class IV Charge Model for Extracting Accurate Partial Charges from Wave Functions. *Journal of Physical Chemistry*, **102A**:1820-1831.
- Li, J., Zhu, T., Hawkins, G. D., Winget, P., Daniel A. Liotard, D. A., Cramer, C. J. and Truhlar, D. G. (1999). Extension of the platform of applicability of the SM5.42R universal solvation model. *Theoretical Chemistry Accounts*, **103**: 9-63.
- Linda Lloyd Agilent Technologies Inc. (2011). [www.agilent.com/chem](http://www.agilent.com/chem) © Agilent Technologies, Inc. 2011 Published in UK, May 20, 2011 5990-8217EN.

- Loncle, C., Brunel, J. M. Vidal, N., Dherbomez, M. and Letourneux, Y. (2004). Synthesis and Antifungal Activity of Cholesterol-Hydrazone Derivatives. *European Journal of Medicinal Chemistry*, **39(12)**: 1067- 1071. Doi:10.1016/j.ejmech.2004.07.005.
- Löwdin, P. O. (1959). *Advances in Chemical Physics*, **2**: 207–322. In: P.O. Löwdin (Ed.), *Molecules and the Solid State*. Academic Press, New York (1966), pp.105- 121.
- Luu, T. X. U., Christensen, P., Duus, F. and Le, T. N. (2007). Inorganic salt supported potassium permanganate promoted oxidation of aniline into azobenzene. *Journal of Chemistry*, **45**: 105–1110.
- Lyengar, T.A., Puttaswamy, M. R. and Mahadewappa, D. S. (1990). Oxidation of some aldopentoses by chloramines B in alkaline medium. *Carbohydrate Research*, **204**: 197-206.
- Lynam, M., Kutty, M., Damborsky, J., Koca, J., and Adriaens, P. (1998). Molecular orbital calculations to describe microbial reductive dechlorination of polychlorinated dioxins. *Environmental Toxicology and Chemistry*, **17**: 988–997. doi:10.1002/etc.5620170603
- Maccari, R. Ottana, R. and Vigorita, M.G. (2005). In Vitro Advanced Antimycobacterial Screening of Isoniazid-Related Hydrazones, Hydrazides and Cyanoboranes: Part 14, *Bioorganic and Medicinal Chemistry Letters*, **15(10)**: 2509-2513. Doi:10.1016/j.bmcl.2005.03.065.
- Mahajan, V. K., Sharma, N. L., Shanker, V., Poonam, G. and Kavita, M. (2010). Cutaneous sporotrichosis: unusual clinical presentations. *Indian Journal of Dermatology, Venereology and Leprology*, **76**:276-8
- Mahmood, T., Haque, Q., Mahmood, I., Asghar Ali, S. and Maqsood, Z.T. (2009) Study of the Non-Catalyzed Molecular Reaction of Reducing Sugars. *Scientia Iranica Transactions C: Chemistry and Chemical Engineering*, **16(1)**: 22-28.
- Mahoney, C.R., Castellani, J., Kramer, F. M., Young, A. and Lieberman. H.R. (2007). Tyrosine supplementation mitigates working memory decrements during cold exposure. *Physiology and Behavior*, **92(4)**: 575 – 582.
- Majidnia, Z. and Idris, A. (2015). Photocatalytic reduction of iodine in radioactive waste water using maghemite and titania nanoparticles in PVA-alginate beads. *Journal of the Taiwan Institute of Chemical Engineers*, **54**:137-144. <http://dx.doi.org/10.1016/j.jtice.2015.03.005>
- Malika, M.A., Basahel, S. N., Obaid, A. Y. and Khan, Z. (2010). Oxidation of tyrosine by permanganate in presence of cetyltrimethyl ammonium bromide. *Colloids and Surfaces B: Biointerfaces*, **76**: 346–353.
- Mallet, B., Lejeune, P., Baudry, N., Niccoli, P., Carayon, P. and Franc, J. (1995). N-glycans modulate in vivo and vitro thyroid hormone synthesis: Study at the N-Terminal Domain of thyroglobin. *The journal of biological chemistry*, **270(50)**: 29881-29888.

- Manz, T. A. and Sholl, D. S. (2010). A dimensionless reaction coordinate for quantifying the lateness of transition states. *Journal of Computational Chemistry*, 31(7): 1528–1541. DOI: 10.1002/jcc.21440
- Maron, S.H. and Lando, J.B. (1974). *Fundamentals of Physical Chemistry*, Macmillan Publishing Co. Inc., UK., pp.94-145.
- Marquez, L. A., and Dunford, H. B. (1995). Kinetics of Oxidation of Tyrosine and Dityrosine by Myeloperoxidase Compounds I and II. *The journal of biological chemistry*, **270(51)**: 30434–30440.
- Martin, C., Galbe, M., Wahlbom, C.F., Hahn-Hagerdal, B. and Jonsson, L. J. (2002). Ethanol production from enzymatic hydrolysis of sugarcane bagasse using recombinant xylose-utilising *Saccharomyces cerevisiae*. *Enzyme and Microbial Technology*, **31**: 274-282.
- Martinez P., Zuluaga, J., Noheda, P. and Van Eldik, R. (1992). Kinetics of the oxidation of L-ascorbic acid by diaquatetraamminecobalt(III) in acidic aqueous solution. Application of the Fuoss model and the Marcus-Sutin cross-relationship for electron-transfer processes. *Inorganica Chimica Acta*, **195(2)**: 249–253.
- Marzorati, M., Danieli, B., Haltrich, D. and Riva, S. (2005). Selective laccase-mediated oxidation of sugars derivatives. *Green Chemistry*, **7(5)**: 310-315.
- Masterton, W. L., Hurley, C. N. and Neith, E. J. (2012). *Chemistry: Principles and Reactions*, 7<sup>th</sup> edn., Brooks/Cole – Cengage Learning, Belmont, USA. Pp.202-208, 646-650.
- Matei, N., Birghila, S., Popescu, V., Dobrinas, S., Soceanu, A., Oprea, C. and Magearu, V. (2008). Kinetic Study of Vitamin C Degradation From Pharmaceutical Products, *Romanian Journal of Physics*, **53(1– 2)**: 343–351,
- May, J.W. and Halpern, J. (1961). Kinetics of the Oxidation of Hydrazobenzene by Iodine and Triiodide. *Canadian Journal of Chemistry*, **39(6)**: 1377-1385.
- McLauchlan, K. A. (2004). *Molecular Physical Chemistry: A Concise Introduction*. The Royal Society of Chemistry, Thomas Graham House, Science Park, Milton Road, Cambridge CB4 0WF, UK, pp. 89-99.
- McQuaid, M. J. and Rice, B. M. (2006). *Computational Chemistry-Based Enthalpy-of-Formation, Enthalpy-of-Vaporization, and Enthalpy-of-Sublimation Predictions for Azide-Functionalized Compounds*. ARL-TR-2806, U.S. Army Research Laboratory, Aberdeen Proving Ground, MD, pp. 1-40.
- McQuaid, M. J., McNesby, K. L., Rice, B. M. and Chabalowski, C. F. (2002). Density Functional Theory Characterization of the Structure and Gas-Phase, Mid-Infrared Absorption Spectrum of 2-Azido-N,N-dimethylethanamine (DMAZ). *Journal of Molecular Structure (THEOCHEM)*, **587**: 199–218.

- McQuaid, M. J., Sun, H. and Rigby, D.(2004). Development and Validation of COMPASS Force Field Parameters for Molecules with Aliphatic Azide Chains. *Journal of Computational Chemistry*, **25**: 61–71
- Mee, A.J. (1971). *Physical Chemistry*, 6<sup>th</sup> edition, English Language Book Society & Heinemann Educational Books Ltd, London, p.583.
- Menger, F.M. and Sherrod, M. J. (1990). Origin of high predictive capabilities in transition-state modelling. *Journal of the American Chemical Society*, **112(22)**: 8071-8075.  
[DOI: 10.1021/ja00178a033](https://doi.org/10.1021/ja00178a033).
- Meyers, S. (2000). Use of neurotransmitter precursors for treatment of depression. *Alternative Medicine Review*, **5(1)**:64-71.
- Miller, A. and Solomon, P.H. (1999). *Writing Reaction Mechanisms in Organic Chemistry*. Elsevier Science and Technology Books, UK, pp.83, 113-124.
- Moller, C. and Plesset, M. S. (1934). Note on an Approximation Treatment for Many-Electron Systems. *Physical Review Letters, Physical Review, and Reviews of Modern Physics*, 46: 618. [DOI: http://dx.doi.org/10.1103/PhysRev.46.618](http://dx.doi.org/10.1103/PhysRev.46.618)
- Mondal, A. and Banerjee, R. (2009). Kinetics and mechanism of uncatalyzed oxidation of hydrazine with superoxide coordinated to cobalt(III). *Indian Journal of Chemistry, Section A*, **48A**: 645-649.
- Moore, J. W. and Pearson, R.G. (1980). *Kinetics and Mechanism*, 3rd edn., Wiley Interscience, New York, p.15-17, 31-57, 318, 455.
- Morelli, B. (1976) A kinetic experiment using a spring powered, stopped-flow apparatus. *Journal of Chemical Education*, **53**: 119-12.
- Morris, J.G. (1972). *Biologist's Physical Chemistry*, Edward Arnold Publishers Ltd., London, pp.165-193.
- Mota, A. J., de Cienfuegos, L. A., Robles, R., Perea-Buceta, J. E., Colacio, E., Vicente Timón, V. and Hernández-Laguna, A. (2010). DFT approach to reaction mechanisms through molecular complexes. The case of an organo-catalysed nucleosidation reaction. *Journal of Molecular Structure: THEOCHEM*, 944: 43–52.  
[doi:10.1016/j.theochem.2009.12.01](https://doi.org/10.1016/j.theochem.2009.12.01)
- Mshelia, M. S., Iyun, F., Uzairu, A. and Idris, S. (2010). Kinetics and mechanism of the oxidation of hydrazine dihydrochloride by aqueous iodine. *Journal of American Science*, **6(9)**: 293-296.
- Murrell, J. N. and Harget, A. J.(1972). *Semi-empirical self-consistent-field molecular orbital theory of molecules*, John Wiley & Sons, New York. In: Tennyson, J., Dinelli, B.M. and Polyansky, O. L. (1995). On the determination of potential energy surfaces of spectroscopic accuracy. *Journal of Molecular Structure*, **341**: 133-140.

- Murrell, J. N., Carter, S., Farantos, S. C., Huxley, P., and Varandas, A. J. C. (1984). *Molecular Potential Energy Functions*, Wiley, Chichester. In: Tennyson, J., Dinelli, B.M. and Polyansky, O.L. (1995). On the determination of potential energy surfaces of spectroscopic accuracy, *Journal of Molecular Structure*, **341**: 133-140.
- Norrby, P.O. (2000). Selectivity in asymmetric synthesis from QM-guided molecular mechanics, *Journal of Molecular Structure (Theochem)*, **506**: 9-16.
- Obiri, D., Flink, N., Maier, J., Neeb, A., Maddalo, D., Thiele, W., Menon, A., Stassen, M., Kulkarni, R. A., Garabedian, M., Barrios, A. M., and Cato, A. (2012) PEST-domain-enriched tyrosine phosphatase and glucocorticoids as regulators of anaphylaxis in mice, *Allergy*, **67**: 175-182.
- Ochterski, J. W. (2000). *Thermochemistry in Gaussian, Technical Support Information*, gaussian.com, Gaussian Inc, Pittsburgh, PA., pp.1-19.
- Odebunmi, E .O. and Owalude, S. O. (2005). Kinetics and mechanism of oxidation of sugars by Chromium (VI) in perchloric acid medium. *Journal Chemical Society of Nigeria*, **30(2)**: 187-191.
- Odebunmi, E. O. and Owalude, S.O. (2007). Kinetic and thermodynamic studies of glucose oxidase catalysed oxidation reaction of glucose. *Journal of Applied Sciences and Environmental Management*, **11(4)**: 95 – 100.
- Odebunmi, E. O. and Owalude, S. O. (2008). Kinetics and Mechanism of Oxidation of Some Simple Reducing Sugars by Permanganate Ion in Alkaline Medium. *Journal of Iranian Chemical Society*, **5 (4)**: 623-630.
- Ohnishi, S., Murata, M., Oikawa. S., Hiraku, Y. and Kawanishi, S. (2000). Copper-dependent DNA damage induced by hydrazobenzene, an azobenzene metabolite. *Free Radical Research*, **32(6)**: 469–478.
- Okeola, F.O., Odebunmi, E.O., and Olagoke, O.A. (2010). Comparative Study of Kinetics of Catalysed Oxidation of Glucose and Galactose by Hexacyanoferrate (III) Ion and Copper Sulphate in Alkaline Medium, *Advances in Environmental Biology*. **4(3)**: 451-455.
- Okiei, W., Ogunlesi, M., Azeez, L., Obakachi, V., Osunsanmi, M. and Nkenchor, G. (2008). The voltammetric and titrimetric determination of ascorbic acid levels in tropical fruit samples. *International Journal of Electrochemical Science*, **4**: 276-287.
- Olsen, P. T. and Jensen, F. (2003). Modelling chemical reactions for conformationally mobile systems with force field methods. *The Journal of Chemical Physics*, **118(8)**: 3523. <http://dx.doi.org/10.1063/1.1539033>
- Olsthoorn, A. J. J., Otsuki, T. and Duine, J. A. (1998). Negative cooperativity in the steady-state kinetics of sugar oxidation by soluble quinoprotein glucose dehydrogenase from *Acinetobacter calcoaceticus*. *European Journal of Biochemistry*, **255**: 255-261.
- Olusanya, S. O. and Odebunmi, E.O. (2011). A Comparative Study of Kinetics and Mechanism of Oxidation of Maltose and Lactose by Copper (II) Ion and

- Hexacyanoferrate (III) Ion in Alkaline Solution. *Pacific Journal of Science and Technology*.**12(2)**:328-333.
- Olusanya, S. O. and Odebunmi, E. O. (2013). Kinetics and mechanism of oxidation of sugars by alkaline solution of hexacyanoferrate (iii) ion in the presence of  $\text{Cr}^{3+}$  as catalyst. *Journal of Applied Sciences in Environmental Sanitation*, **8 (2)**: 119-124.
- Ostlund, N. S., Whiteside, R. A. and Hibbard, P. G. (1982). Computational Chemistry and Computer-Science, *Journal of Physical Chemistry*, **86**: 2190-2197.
- Pal, T., Jana, N. R. and Das, P. K. (1994). Kinetics Of Reduction of Silver(I) Gelatin Complex in Aqueous Alkaline-Solution. *Indian journal of chemistry. Sect. A: Inorganic, physical, theoretical & analytical*, **33(8)**: 760-762.
- Palmer, D.A. and Lietzke, M. H.(1982) . The equilibria and kinetics of iodine hydrolysis. *Radiochim Acta*, **31**: 37-44.
- Parr, R. G. and Yang, W. (eds.) (1989). *Density Functional Theory of Atoms and Molecules*. Oxford University Press, New York, pp.3,47-66, 334.
- Parry, B. L. (2001). The role of central serotonergic dysfunction in the aetiology of premenstrual dysphoric disorder: therapeutic implications. *CNS Drugs*,**15(4)**: 277-285.
- Patrick, L. (2008). Iodine: Deficiency and therapeutic considerations. *Alternative Medicine Review*, **13**:116-27.
- Pearce, E. N., Andersson, M. and Zimmermann, M. B.(2013). Global iodine nutrition: where do we stand in 2013? *Thyroid***23**: 523528.
- Perdew, J.P. and Schmidt, K. (2001). *Jacob's ladder of density functional approximations for the exchange-correlation energy*. In:Van Doren, V. (Ed), *Density Functional Theory and Its Application to Materials*, AIP Press, Melville, New York,**577**: pp. 1, 2, 26.
- Perdew, J.P. (1985). *What do the Kohn-Sham orbital energies mean? How do atoms dissociate?* in:Dreizler, R. M. and J. da Providência, J.(Eds.), *Density Functional Methods in Physics*, Plenum Press, New York, p. 265.
- Perdew, J.P. and Levy, M. (1997). Comment on "Significance of the highest occupied Kohn-Sham eigenvalue".*Physical Review*, **B 56(24)**: 16021. DOI:<http://dx.doi.org/10.1103/PhysRevB.56.16021>
- Perdew, J.P., Ruzsinszky, A., Tao, J., Staroverov, V. N., Scuseria, G. E. and Csonka, G. I. (2005). Prescription for the design and selection of density functional approximations: more constraint satisfaction with fewer fits. *Journal of Chemical Physics*, **123(6)**: 62201.
- Perolav, K. and Pedersen, B. (1994). Oxidation of L-Ascorbic Acid with Hydrogen Peroxide in Aqueous Solution.*Acta Chemica Scandinavica*.**48**: 646-651.

- Pigman, W. and Anet, E. F. L. J. (1972). *Mutarotations and actions of acids and bases*, In: Pigman, W. and Horton, D.,(Eds), *The carbohydrates Chemistry and biochemistry*, Academic Press, New York., volume 1A, p. 165.
- Poustie, V. J. and Wildgoose, J. (2010). Dietary interventions for phenylketonuria. *Cochrane Database of Systematic Reviews*, 2010, Issue 1. Art. No.: CD001304. DOI: 10.1002/14651858.CD001304. pub2
- Press, W. H., Flannery, B. P., Teukolsky, S. A. and Vetterling, W. T. (1992). "Minimization or Maximization of Functions." Ch. 10 in *Numerical Recipes in FORTRAN: The Art of Scientific Computing, 2nd ed.* Cambridge University Press, Cambridge, pp. 387-448.
- Raby, C., Lagorce, J. F., Jambutabsil, A. C., Buxeraud, J. and Catanzano, G. (2013). The Mechanism of Action of Synthetic Antithyroid Drugs: Iodine Complexation during Oxidation of Iodide. *Endocrinology*, **126(3)**: 1683-1688 .DOI: <http://dx.doi.org/10.1210/endo-126-3-1683>.
- Rahman, M. M., Rahman-Khan, M. M. and Hosain, M. M., (2007). Analysis of Vitamin C (ascorbic acid) Contents in Various Fruits and Vegetables by UV-spectrophotometry. *Bangladesh Journal of Scientific and Industrial Research*, 42(4), 417-424.
- Rahman-Khan, M.M., Rahman, M.M., Islam, M. S. and Begum, S. A. (2006). A simple UV- spectrophotometric method for the determination of vitamin C content in various fruits and vegetables at Sylhet area in Bangladesh. *Journal of Biological Sciences*, **6**, 388-392.
- Rahmawati, S. and Bundjali, B. (2009). *Prosiding Seminar Kimia Bersama UKM-ITB VIII* 9- 11 Jun **2009**.
- Rajanna, K. C., Reddy, K. N., UmeshKumar, U. and SaiPrakash, P. K. (1996). A kinetic study of electron transfer from L-Ascorbic acid to sodium perborate and potassium peroxydisulphate in aqueous acid and micellar media. *International Journal of Chemical Kinetics*, **28**: 153-164.
- Rangappa, K.S., Manjunathaswamy, H., Raghendra, M.P. and Gowda, D. C. (1998a). Oxidation of theose-series pentoses and hexoses by sodium N-Chloro-p- toluene sulfonamide, *Carbohydrate Research*, **307**, 253-262.
- Rangappa, K.S., Ranghendra, M.P., Mahadevappa, D.S. and Gowda, D. C. (1998b). Kinetics and mechanism of Oxidation of erythro-series pentoses and hexoses by N-Chloro-p-toluene sulfonamide. *Carbohydrate Research*, **306**: 57-67.
- Rao, K.V., Wara, R. and Thirupathi, M. (1995). Kinetics and Mechanism of Oxidation of Some Reducing Sugars by Diperoiodoargentate (III) in Alkaline Medium. *International Journal of Chemical Kinetics*. **27**:55-56.
- Rao, T. S. and Dalvi, P.S. (1990). Kinetics and mechanism of the rapid oxidation of hydrazine by iodine in weakly acidic solutions. *Proceeding of Indian national Science Academy*, **56(2)**: 153-160.

- Rao, T. S., Kale N. R. and Dalvi S. P. (1987). React. Kinetics and mechanism of the oxidation of L-ascorbic acid by 2,6-dichlorophenol-indophenol in aqueous solution, *Reaction Kinetics, Mechanisms and Catalysis*, **34(1)**: 179-184.
- Rick, S. W. and Stuart, S.J. (2002) In: Lipkowitz K. B., Boyd, D. B.(Eds.). *Reviews in Computational Chemistry*, Volume 18, Wiley-VCH, pp.89-146.
- Rizzo, R. C. and Jorgensen, W. L. (1999). OPLS All-Atom Model for Amines: Resolution of the Amine Hydration Problem. *Journal of American Chemical Society*, **121**: 4827-4836.
- Ryley, J. and Kajda, P. (1994). Vitamins in thermal processing, *Food Chemistry*, **49(2)**: 119-129,
- Sadlej, J.(1985). Semi-Empirical Methods of Quantum Chemistry, (Ellis Horwood Series in Chemistry), *Angewandte Chemie*, **98(10)**: 936-938.
- Santra, B., Michaelides, A. and Scheffler, M. (2007). On the accuracy of density-functional theory exchange-correlation functionals for H bonds in small water clusters: Benchmarks approaching the complete basis set limit. *Journal of Chemical Physics*, **127**: 184104. <http://dx.doi.org/10.1063/1.2790009>
- Schlegel, H.B.(1986). Potential energy curves using unrestricted Møller–Plesset perturbation theory with spin annihilation. *Journal of Chemical Physics*, **84**: 4530–4534.
- Schramm, V. L. (2005a). Enzymatic transition states and transition state analogues. *Current Opinion in Structural Biology*, **15**: 604-613.
- Schramm, V. L. (2005b). Enzymatic transition states: thermodynamics, dynamics and analogue design. *Archives of Biochemistry and Biophysics*, **433**: 13-26.
- Sengupta, K. K. and Sen, P. K. (1979). Kinetics of oxidation of hydrazinium ion by hexachloroiridate(V). *Inorganic Chemistry*, **18 (4)**: 979-982. DOI:10.1021/ic50194a019.
- Sengupta, K. K., Begum, B.A. and Pal, B.B. ((2009) In: Pushpalatha L., (2011). Kinetics and mechanism of oxidation of galactose and mannose by N-Bromonicotinamide (NBN). *Afinidad: Revista de química teórica y aplicada*, **68(551)**, 57-63.
- Sengupta, K. K., Begum, B. A. and Pal, B.B. (1999). Kinetics and mechanism of the oxidation of some aldoses, amino sugars and methylated sugars by tris(pyridine-2-carboxylato) Manganese(III) in weakly acidic medium. *Carbohydrate Research*, **315**:70-75.
- Sengupta, K.K., Begum, B.A. and Pal, B. (1998). Kinetic behavior and relative reactivities of some aldoses, amino sugars and methylated sugars towards platinum(IV) in alkaline medium, *Carbohydrate Research*, **309**: 303-310.
- Shaffer, A. A. and Wierschke, S. G. (1993). Comparison of computational methods applied to oxazole, thiazole, and other heterocyclic compounds. *Journal of Computational Chemistry*, **14**: 75-88.
- Shallangwa, G. A., Uzairu, A., Ajibola, V. O. and Abba, H. (2014a). MNDO and DFT Computational Study on the Mechanism of the Oxidation of 1,2-Diphenylhydrazine

by Iodine. *ISRN Physical Chemistry*, Vol. 2014, Article ID 592850, 8 pages.  
<http://dx.doi.org/10.1155/2014/592850>

- Shallangwa, G. A., Uzairu, A., Ajibola, V. O. and Abba, H. (2014 b). Computational study of the mechanism of the oxidation of ascorbic acid by iodine in the gas phase. *Biointerface research in applied chemistry*, **4(2)**:712-720.
- Shallangwa, G.A., Uzairu, A., Ajibola, V.O. and Abba, H. (2014c).DFT and PM3 Computational Studies of the Reaction Mechanism of the Oxidation of L-Tyrosine by Iodine in the Gas Phase. *Aceh International Journal of Science and Technology*, **3(2)**: 106-116. [Doi: http://dx.doi.org/10.13170/AIJST.0302.06](http://dx.doi.org/10.13170/AIJST.0302.06)
- Shallangwa, G.A., Uzairu, A., Ajibola, V.O., Abba, H., (2015). A Preliminary Computational Study of the Mechanism of Oxidation of D-Fructose by Iodine in Gas Phase, *Journal of Modern Chemistry and Chemical Technology*, **6(2)**: 41-49.  
<http://www.stmjournals.com>
- Singh, A.K., Chaurasir, N., Rehmani, S., Srivastava, J. and Singh, B. (2004b). Mechanism of ruthenium (III) catalysis of periodate oxidation of aldoses in aqueous alkaline medium. *Catalysis Letters*, **95**: 135-142.
- Singh, A.K., Rahmani, S., Singh, V.K., Srivastava, J. and Singh, B. (2006b). Mechanism of Pd(II) and Hg(II) co-catalysis in N-bromoacetamide oxidation of D-galactose and L-sorbose in perchloric acid: A Kinetic Study. *International Journal of Pure and Applied Chemistry*, **1**: 253-263.
- Singh, A.K., Rehmani, S., Singh, B., Singh, R. K. and Singh, M. (2004a). Mechanism of Ir (III) catalysed and Hg (II) co-catalyzed oxidation of reducing sugars by N-bromoacetamide in acidic medium. *Journal of Physical Organic Chemistry*, **17(3)**: 249-256.
- Singh, A. K., Srivastava, J., Rahmani, S. and Singh, V. (2006a). Pd(II) catalyzed and Hg(II) co-catalyzed oxidation of D-glucose and D-fructose by N-bromoacetamide in the presence of perchloric acid. *Carbohydrate Research*, **341(3)**: 397-409.
- Singh, H. S., Singh, B. and Singh, A. K. (1991). Mechanism of Oxidation of Reducing Sugars by Osmium Tetraoxide in Alkaline Medium by Stopped Flow Technique. *Carbohydrate Research*, **211 (2)**: 235-243.
- Singh, M.P, Singh, R.K., Singh, A.K. and Srivastava, A. (1980). Quinoxalines derived from D-glucose and O-phenylenediamine in acidic media. *Indian Journal of Chemistry*, **19A**, 547-549.
- Singh, M.P., Singh, A.K. and Trepathi, V. (1978). Non-catalyzed oxidation of sugars in alkaline medium in ammonical Ag(1) and Nessler's reagent. *The Journal of Physical Chemistry*, **82**,1222-1225,
- Singh, M.P., Singh, H.S., Tiwari, S.C., Gupta, K.C., Singh, A. K., Singh, V. P. and Singh, R.K. (1975). In organicoxidants such as Cu(II) in oxidation of sugars in alkaline media. *Indian Journal of Chemistry*, **13**: 819-822.

- Singh, U. C. and Kollman, P. A. (1984). An Approach to Computing Electrostatic Charges for Molecules. *Journal of Computational Chemistry*, **5**: 129-145.
- Singh, V., Singh, A.K., Singh, K. A., Gupta, N. and Singh, B. (2002). Kinetics and mechanism of Ru(III) and Hg(II) co-catalysed oxidation of D-galactose and D-ribose by N -bromoacetamide in perchloric acid. *Carbohydrate Research*, **337(4)**: 345-351.
- Sisler, H. H., Omietanski, G. M. and Rudner, B. (1957). The Chemistry of Quaternized Hydrazine Compounds. *Chemical Review*, **57(6)**: 1021–1047.
- Sitti, R. and Bunbun, B. (2009). Prosiding Seminar Kimia Bersama UKM-ITB VIII 9-11 Jun 2009.
- Smith, R. M. and Martell, A. E. (1976). *Critical stability constant*, Vol. 4. Plenum Press, New York. p. 43.
- Smith, S. J. and Sutcliffe, B. T. (1997). The development of Computational Chemistry in the United Kingdom. *Reviews in Computational Chemistry*, **70**: 271–316.
- Sousa, J. A., Silva, P. P., Machado, A. E. H., Reis, M. H. M., Romanielo, L. L. and Hori, C. E. (2013). Application of computational chemistry methods to obtain thermodynamic data for hydrogen production from liquefied petroleum gas. *Brazilian Journal of Chemical Engineering*, **30(1)**: 83 - 93
- Spartan (2003). Spartan User's Guide (2003), version 3.0, Wavefunction, Inc., 118401 Von Karman Ave., Suite 370 Irvine, CA 92612. [www.wavefun.com](http://www.wavefun.com)
- Spartan (2014). *Spartan'14 Topics*, Wave function Inc., 18401 Von Karman Ave., Suite 370 Irvine, CA 92612. [www.wavefun.com](http://www.wavefun.com)
- Springborg, M. (1997). *Density Functional Methods: Applications in Chemistry and Materials Science*, John Wiley & Sons, Ltd., Chichester, p. 233.
- Sridhar, S. K., Pandeya, S. N., Stable, J. P. and Ramesh, A. (2002). Anti Convulsant Activity of Hydrazones, Schiff and Mann Basis of Istatin Derivatives. *European Journal of Pharmaceutical Science*, **16(3)**: 129- 132. Doi: 1016/S0928-0987(02)00077-5.
- Stewart, J. J. P. (1986). Optimization of Parameters for Semi-Empirical Methods II- Applications, *Journal of Computational Chemistry*, **10(2)**: 221- 264.
- Stewart, J. J. P. (1990). 'Semiempirical Molecular Orbital Methods' in: Lipkowitz, K. B. and Boyd, D. B., (Eds.), *Reviews in Computational Chemistry*, Vol. 1, VCH: New York, p.45.
- Stewart, J. J. P. (2007). Optimization of parameters for semi empirical methods. V. Modification of NDDO approximations and application to 70 elements. *Journal of Molecular Modelling*, **13**: 1173-213.
- Sultan, S.M., Alzamil, I.Z., Al- Hajjaji, A.M., Al-Tamrah S. A. and Aziz Al-Rahman, A.M. (1985). A Kinetic Study on the Determination of Hydrazine by Iodine in Sulphuric Acid Media. *Journal of Chemical Society of Pakistan*. **7(2)**: 93-99.

- Swades, K. C. and Derek, R. L. (2003).Electricity generation by direct oxidation of glucose in mediator-less microbial fuel cells.*Nature Biotechnology LETTERS*, **21(10)**: 1229-1232.
- Szabo A. and Ostlund N. S. (1989). *Modern Quantum Chemistry: Introduction to Advanced Electronic Structure Theory*. McGraw-Hill, Inc.: New York, Pp.152-171.
- Szabo, A. and N. S. Ostlund, N.S. (1982). *Modern Quantum Chemistry: Introduction to Advanced Electronic Structure Theory*.Dover Press, USA, p. 14.
- Szajewski, R. P. and Whiteside, G. M. (1980). Rate Constants and Equilibrium Constants for Thiol-Disulfide Interchange Reactions involving Oxidized Glutathion. *Journal of the American Chemical Society*, **102(6)**: 2011-2026.
- Tang, Y., Sun, H., Jing Zhao, J., Liu, J.and Wang, R. (2013).Atmospheric chemistry of CF<sub>3</sub>O<sub>2</sub>: A theoretical study on mechanisms and pathways of the CF<sub>3</sub>O<sub>2</sub>+ I reaction. *Atmospheric Environment*, **65**: 164-170.  
<http://dx.doi.org/10.1016/j.atmosenv.2012.10.018>
- Tao, Z., Raffel, R. A., Souid, A. K. and Goodisman, J. (2009). Kinetic Studies on Enzyme-Catalyzed Reactions: Oxidation of Glucose, Decomposition of Hydrogen Peroxide and Their Combination. *Biophysical Journal*, **96**: 2977–2988.
- Thiel, W. (1998). Thermochemistry from Semi empirical Molecular Orbital Theory in: Irikura, K. K. and Frurip, D. J., (Eds.), *Computational Thermochemistry, ACS Symposium Series*, Vol. 677, American Chemical Society: Washington, DC, p.142.
- Thomas, E. L. and Aune, T. M. (1977). Peroxidase-catalyzed oxidation of protein sulfhydryls mediated by iodine. *Biochemistry*,**16 (16)**: 3581–3586. DOI: 10.1021/bi00635a013.
- Tiziani, S., Sussich, F. and Cesaroi, A. (2003). The use of periodate in the non-catalyzed oxidation of carbohydrate.*Carbohydrate Research*, **338**: 1083-1095.
- Tran, F., Laskowski, R., Blaha, P. and Schwarz,K. (2007). Performance on molecules, surfaces, and solids of the Wu-Cohen GGA exchange-correlation energy functional. *Physical Review. B* 75: 115131. DOI: <http://dx.doi.org/10.1103/PhysRevB.75.115131>
- Tro, N. J. (2010). *Principles of Chemistry: A Molecular Approach*. Pearson Education, Inc.,Upper Saddle, New Jersey, USA. Pp.147-152, 474-202, 514-544.
- Trouillas, P., Bergès, J. and Houée-Lévin, C. (2010).Toward understanding the protein oxidation processes: •OH addition on tyrosine, phenylalanine, or methionine? *International Journal of Quantum Chemistry*, **111(6)**: 1143-1151. DOI: 10.1002/qua.22556.
- Truong, T. N. Duncan, W. T. and Bell, R. L. (1996) in: Laird,B. B.,Ross,R. B. and Ziegler, T.(Eds.),*Chemical Applications of Density Functional Theory*, American Chemical Society, Washington, DC. pp. 85-104.
- Tumilty,L., Davison, G., Beckmann, M. and Thatcher, R. (2011). Oral tyrosine supplementation improves exercise capacity in the heat. *European Journal of Applied Physiology*,2011 Mar 25. [Epub ahead of print]

- Valdes, H., Klusak, V., Pitonak, M., Exner, O., Sary, I., Hobza, P. and Rulisek, L. (2008). Evaluation of the intramolecular basis set superposition error in the calculations of larger molecules: [n]helicenes and Phe-Gly-Phe tripeptide. *Journal of Computational Chemistry*, **29**(6): 861–870. DOI: 10.1002/jcc.20841
- Valeev, E.F. and Sherrill, C. D. (2003). The diagonal Born–Oppenheimer correction beyond the Hartree–Fock approximation. *The Journal of Chemical Physics*, **118**: 3921; <http://dx.doi.org/10.1063/1.1540626>
- vanSpronsen, F.J., vanRijn, M., Bekhof, J., Koch, R. and Smit, P.G. (2001). Phenylketonuria: tyrosine supplementation in phenylalanine-restricted diets. *The American Journal of Clinical Nutrition*. **73**(2): 153-157.
- Venkate, K. and Jaya, P. (1995). Kinetics and Mechanism of Oxidation of some Reducing Sugars by Diperoxidate Arsenate (III) in Alkaline Medium. *Transition Metal Chemistry*. **20**:344-346.
- Verma, K. K., Jain, A., Sahasrabuddhey, B., Gupta, K. and Mishra, S. (1996). Solid-phase extraction clean-up for determining ascorbic acid and dehydroascorbic acid by titration with 2,6-dichlorophenolindophenol. *Journal of AOAC International*, **79**:1236 -1243.
- Wanno, B. and Ruangpornvisuti, V. (2006). Structures of gas-phase nitrosamine-dimer isomers, their interconversions and energetics: A DFT study. *Journal of Molecular Structure (THEOCHEM)*, **775**: 113-120.
- Warshel, A. (1992). *Computer modeling of chemical reaction in enzymes and solutions*, Wiley, New York, USA. in: Aqvist, J and Fothegill, M. (1996). Computer Simulation of the Triosephosphate Isomerase Catalyzed Reaction. *The Journal of Biological Chemistry*, **271**: 10010- 10016.
- Warshel, A. and M. Levitt, M. (1976). Theoretical studies of enzymic reactions: Dielectric, electrostatic and steric stabilization of the carbonium ion in the reaction of lysozyme, *Journal of Molecular Biology*, **103**: 227-249.
- Webster, D. and Wildgoose, J. (2013). Tyrosine supplementation for phenylketonuria. *Cochrane Database of Systematic Reviews* 2013, Issue 6. Art. No.: CD001507. DOI:10.1002/14651858.CD001507.pub3
- Whalley, B. J. P., Evans, H. G. V. and Winkler, C. A. (1956). The oxidation of hydrazobenzene by ammonium persulphate in acetonitrile–water solution. *Canadian Journal of Chemistry*, **34**(9): 1154-1162.
- Widder, D. V. (1989). *Advanced calculus*, Dover Publications, New York, p. 128.
- Winget, P., Hawkins, G. D., Cramer, C. J. and Truhlar, D. G. (2000). Prediction of Vapor Pressures from Self-Solvation Free Energies Calculated by the SM5 Series of Universal Solvation Models. *Journal of Physical Chemistry*, **B104**: 4726-4734.
- World Health Organization (2002). Guidelines for Iodine Prophylaxis following Nuclear Accidents. Available at: [www.who.int/environmental\\_information/Information\\_resources/on\\_line\\_radiation.html](http://www.who.int/environmental_information/Information_resources/on_line_radiation.html). (Accessed 11 January 2002).

- Xiashi, Z. and Suqin, X. (2010). Determination of l-tyrosine by-cyclodextrin sensitized fluorescence quenching method. *Spectrochimica Acta*, **Part A77**: 566–571.
- Ya-Yin F., Rong-Xin, S., Hong-Wei S., Man-Xue, Y., Jie L., Zheng-Ming, L., Cheng-Ming, L. (2002). Mechanism analysis of catalytic hydrogenation of 3-anilino methylenedioxy-6-alkyl-5,6-dihydropyran-2,4-diones. *Journal of Molecular Structure (Theochem)* **578**: 71-78.
- Yeh, I. C. and Berkowitz, M. L. (1999). Ewald summation for systems with slab geometry. *The Journal of Chemical Physics*, **111(7)**: 3155. <http://dx.doi.org/10.1063/1.479582>
- Yen, P.M.(2001). Physiological and molecular basic of thyroid hormone action. *Physiological Reviews*, **81**: 1097-1142.
- Young, D. C. (2002). *Semi empirical Methods in Computational Chemistry: A Practical Guide for Applying Techniques to Real World Problems*, John Wiley & Sons, Inc., New York, USA. Doi:10.1002/0471220655.ch4
- Young, D. C. (2001). *Computational Chemistry: A Practical Guide for Applying Techniques to Real-World Problems*. John Wiley & Sons, Inc., New York, USA. Pp. 1-3, 9, 19, 32-39, 42-49, 67-71.
- Yusubova, M. S. and Zhdankin, V. V. (2015). Iodine catalysis: A green alternative to transition metals in organic chemistry and technology. *Resource-Efficient Technologies*, **1**: 49–67. <http://dx.doi.org/10.1016/j.reffit.2015.06.001>
- Zarkesh, R. A., Ziller, J. W. and Heyduk, A. F. (2008). Four-electron oxidative formation of aryl diazenes using a tantalum redox active ligand complex. *Angewandte Chemie International Edition*, **47(25)**: 4715–4718.
- Zdilla, M. J., Verma, A. K., Lee, S.C. (2008). Reactivity of a sterically hindered Fe(II) thiolate dimer with mines and hydrazines. *Inorganic Chemistry*, **47(23)**: 11382–11390.
- Zerner, M. (1991). Semi-empirical Molecular Orbital Methods in: Lipkowitz, K. B. and Boyd, D. B., (Eds.), *Reviews in Computational Chemistry*, Vol. 2, VCH: New York, P.313
- Zhang, J. and Hase, W. L. (2010). Electronic Structure Theory Study of the  $F + CH_3I \rightarrow FCH_3 + I$  Potential Energy Surface. *Journal of Physical Chemistry, Section A*, **114**: 9635–9643.
- Zhang, S., and Zhang, Z.-Y. (2007) PTP1B as a drug target: Recent developments in PTP1B inhibitor discovery, *Drug Discovery Today* **12**, 373-381.
- Zhao, Y. and Truhlar, D.G. (2008). The M06 suite of density functionals for main group thermochemistry, thermochemical kinetics, noncovalent interactions, excited states, and transition elements: two new functionals and systematic testing of four M06-class functionals and 12 other functionals. *Theoretical Chemistry Account*, **120(1-3)**: 215-241.

- Zhu, Q., Zhang, Y., Ying, Z., Wang, S., Wang, Z., Zhou, J. Cen. K. (2013). Kinetic and thermodynamic studies of the Bunsen reaction in the sulfureiodine thermochemical process. *International Journal of Hydrogen Energy*, **38**: 8617-8624. <http://dx.doi.org/10.1016/j.ijhydene.2013.04.110>
- Zimmermann, M. B. (2013). Iodine deficiency and excess in children: worldwide status in 2013. *Endocrine Practices*, **19**: 839–846.